



University
of Glasgow

Bordage, Simon (2013) *Organ specificity in the plant circadian clock*. PhD thesis.

<http://theses.gla.ac.uk/4387/>

Copyright and moral rights for this thesis are retained by the author

A copy can be downloaded for personal non-commercial research or study

This thesis cannot be reproduced or quoted extensively from without first obtaining permission in writing from the Author

The content must not be changed in any way or sold commercially in any format or medium without the formal permission of the Author

When referring to this work, full bibliographic details including the author, title, awarding institution and date of the thesis must be given

Organ specificity in the plant circadian clock

Simon Bordage

Submitted in fulfilment of the requirements for the Degree of
Doctor of Philosophy

Institute of Molecular, Cell and Systems Biology
College of Medicine, Veterinary and Life Sciences
University of Glasgow

June 2013

Abstract

Circadian clocks are endogenous oscillators that control many physiological processes and confer functional and adaptive advantages in various organisms. These molecular oscillators comprise several interlocked feedback loops at the gene expression level. In plants, the circadian clock was recently shown to be organ specific. The root clock seemed to involve only a morning loop whereas the shoot clock also includes an evening loop in a more complex structure. My work aimed at refining the differences and similarities between the shoot and root clocks, using a combination of experimental and theoretical approaches.

I developed an imaging method to obtain more data from the shoot and root clocks over time in various conditions. Some previous results were confirmed: the free running periods (FRPs) are longer in roots compared to shoots under constant light (LL). In addition, the amplitude of clock gene expression rhythms is lower in roots compared to shoots. However, the expression of several evening genes is circadian in roots, contrary to previous conclusions. This was confirmed with qPCR, and was observed in both light- and dark-grown roots. Yet light affects clock gene expression in roots, so an automatic covering system was designed to keep the roots in darkness and obtain data in more physiological conditions.

Clock genes behaved differently in shoots and light-grown roots that were in the same environmental conditions, and may be differentially affected by blue and red light. However shoot and root clocks were more similar under constant darkness (DD). My imaging and RT-qPCR data, together with new microarray results and preliminary studies on clock mutants suggest that shoot and root circadian systems may have a similar structure but different input pathways.

Entrainment is a fundamental property of circadian systems, which can be reset by cues such as light/dark (LD) cycles. I demonstrated that light can directly entrain the root clock in decapitated plants. The root clock could be entrained by a broad range of T cycles using low light intensity. In addition, rhythms were preferably entrained by low light than by any putative signal from shoots in experiments using conflicting LD cycles of different strengths. My results indicate that direct entrainment by LD cycles could be the main mechanism that synchronise the shoot and root clocks at constant temperature. This is physiologically relevant because dark-grown roots can perceive light channelled by the exposed tissues, in a fibre optic way. I also showed for the first time that clock and output genes could be rapidly entrained by temperature cycles in roots.

Several mathematical models of the shoot circadian clock were used to try and fit the root clock data by optimising some parameters. The best set of parameters gave a good qualitative fit to root data under LD, LL and DD. It reproduced the long FRP observed in roots under LL and captured the entrainment under LD with lower amplitude in roots. The parameters that were changed for these simulations were all related to light input, which supports the idea of similar clock structures in shoots and roots but with different input pathways. Together my results confirmed that the plant circadian clock is organ specific and suggest that it is organ autonomous.

Table of content

Abstract	3
List of tables	9
List of figures	11
Acknowledgments	13
Author's declaration	15
Abbreviations	17
1 General introduction	21
1.1 Why are biological rhythms important?	21
1.1.1 Biological oscillations are pervasive	21
1.1.2 Oscillations confer functional advantages	23
1.2 Circadian rhythms	24
1.2.1 The discovery of endogenous rhythms	24
1.2.2 Properties of circadian rhythms	25
1.2.3 Adaptive advantages conferred by the plant circadian clock	27
1.2.4 Some applications of circadian biology	28
1.3 Molecular basis of the plant circadian clock	30
1.3.1 Transcription – Translation Feedback Loops (TTFLs)	31
1.3.2 Other layers of regulation in the circadian clock	34
1.3.3 Connections between the clock and other networks	36
1.4 Entrainment of circadian oscillators	38
1.4.1 General concepts	38
1.4.2 Entrainment of the plant circadian clock by LD cycles	41
1.4.3 Entrainment of the plant circadian clock by non-photic signals	43
1.5 Modelling the plant circadian clock	44
1.5.1 The Locke et al models	45
1.5.2 The P2010 model	48
1.5.3 The P2012 model	50
1.6 From cell autonomous rhythms to organ specific clocks	52
1.7 Aims and outline of the work	56

2	Materials and Methods	59
2.1	Seeds	59
2.1.1	Seed stock	59
2.1.2	Seed surface sterilisation and stratification	60
2.2	Hydroponic system	60
2.2.1	Media	60
2.2.2	Seed sowing and plant transfer	61
2.2.3	Entraining conditions	62
2.2.4	Harvesting and sample storage	62
2.2.5	RNA extraction, DNase treatment and quality control	63
2.2.6	RT-qPCR	64
2.3	Imaging system	65
2.3.1	Media	65
2.3.2	Seed sowing, plant transfer and entrainment	66
2.3.3	Luciferase assay	66
2.4	Data analysis	67
2.4.1	BRASS analysis	67
2.4.2	ANOVA analysis	68
2.5	Modelling	68
2.5.1	Changing model parameters with Circadian Modelling (CM)	68
2.5.2	Global parameter optimization using Systems Biology Software Infrastructure (SBSI™)	69
2.5.3	Simulations with COPASI	74
3	Development of an imaging system to monitor gene expression over space and time	75
3.1	Introduction	75
3.1.1	The luciferase (LUC) reporter and its advantages for dynamic studies	75
3.1.2	Use of LUC to monitor gene expression in roots	76
3.2	Imaging simultaneously shoots and roots on vertical plates	77
3.3	Increasing the signal/noise (S/N) ratio	80
3.3.1	Increasing the root signal	80
3.3.2	Decreasing the noise	81
3.4	Comparison between time courses obtained with different lids and media	83
3.5	<i>TOC1:LUC</i> + activity is circadian in roots exposed to light	87

3.6	Keeping the roots in constant darkness	90
3.7	Conclusion.....	92
4	Direct effects of light on the root clock	95
4.1	Introduction	95
4.2	The expression of morning and evening clock genes are circadian in illuminated roots, with a longer FRP compared to shoots.....	96
4.3	Light directly affects the expression of clock genes in roots	99
4.4	Direct exposure to light affects clock gene transcript levels in roots.....	107
4.5	The FRP under DD is similar in shoot and root clocks.....	113
4.6	Both red and blue light can affect the root clock	118
4.7	Conclusion.....	123
5	Entrainment of the root circadian clock.....	127
5.1	Introduction	127
5.2	The clocks of shoots and illuminated roots are out of phase in LL and quickly resynchronised in LD cycles	128
5.3	The root clock can be entrained by direct perception of light.....	131
5.4	<i>GI</i> expression in roots is preferably entrained by direct perception of light than by any putative signal from shoots.....	136
5.5	Shoot and root clocks both have a broad range of entrainment but respond differently to T cycles.....	141
5.6	Shoot and root clocks respond differently to skeleton photoperiods	145
5.7	Entrainment of the root clock by temperature cycles.....	149
5.8	Conclusion.....	153
6	Effects of the <i>cca1/lhy</i> , <i>toc1</i> and <i>ztl</i> mutations on the root clock.....	157
6.1	Introduction	157
6.2	The <i>cca1/lhy</i> double mutant displays rhythmicity in roots, but with a shorter FRP than in shoots.....	158
6.3	The <i>toc1-4</i> mutation shortens the FRP in the root clock.....	160
6.4	The <i>ztl-105</i> mutation differentially affects <i>CCR2</i> expression in shoots and roots 163	
6.5	Conclusion.....	165

7	Modelling the root clock	169
7.1	Introduction.....	169
7.2	Changing the parameters g3, g4 and g6 of the L2006 model can simulate some aspect of the root clock in specific conditions	170
7.3	Changing only one parameter of the P2010 model (g5) can simulate many root clock data under LD, LL and DD	174
7.4	Low levels of light perceived by dark-grown roots is sufficient to explain the low amplitude and the long FRP under LL in the root clock.....	180
7.5	Entrainment of the root clock and longer FRPs in light-grown roots compared to shoots can be simulated after optimising P2012 model parameters	186
7.6	Differences in light inputs could explain most differences observed between shoot and root clocks under LD and LL	193
7.7	Conclusion	200
8	General discussion.....	203
8.1	Shoot and root circadian systems: same structure but different inputs?.....	203
8.1.1	Components	203
8.1.2	Wiring.....	206
8.1.3	Inputs	208
8.2	Plant circadian systems and their inputs at different levels of organisation	211
8.2.1	Intracellular networks and microenvironment.....	212
8.2.2	Tissue specificity in roots under constant light	213
8.2.3	Organ specificity and autonomy in different conditions	215
8.2.4	Plants in complex environments.....	219
8.2.5	Concluding remarks.....	220
	Appendix.....	223
	References.....	231

List of tables

Table 2.1: Nutrients and their final concentrations used in the hydroponic solution	61
Table 2.2: Primers used for PCR and qPCR	65
Table 5.1: Period estimates (h) of the time-courses presented in Figure 5.4	143
Table 5.2: Phases of peak expression in shoots and roots under T cycles	144
Table 6.1: FRPs of <i>CCR2</i> expression in roots and shoots of WT and mutants under LL ..	159
Table 7.1: Period estimates of simulated rhythms in shoots and “roots” under DD and LD using the L2006 model	173
Table 7.2: Period estimates of simulated rhythms in shoots and “roots” under DD, LL and LD using the P2010 model	179
Table 7.3: Optimal sets of parameters related to inhibition constants in roots	189
Table 7.4: Optimal set of “light-related parameters” for the root clock	195
Table 7.5: Period estimate of simulated rhythms in shoots and “roots” under LL and LD using the P2012 model	199

List of figures

Figure 1.1: Simplified version of a circadian system.....	27
Figure 1.2: A model representing the interlocked Transcriptional Translational Feedback Loops (TTFL) of the <i>Arabidopsis</i> circadian clock, and connections with modulators of physiological processes	33
Figure 1.3: Phase response curve for <i>Arabidopsis thaliana</i>	40
Figure 1.4: Diagrammatic representation for the last three ODE models of the <i>Arabidopsis</i> circadian clock	47
Figure 2.1: Two types of boxes used for the hydroponic cultures	61
Figure 3.1: Overview of the imaging system	78
Figure 3.2: Brief overview of the optimised imaging protocol, from sowing to imaging ...	81
Figure 3.3: Masking of the root signal by the shoot signal can be reduced by compartmentalising the plate	85
Figure 3.4: TOC1:LUC+ activity is circadian in roots exposed to light.....	88
Figure 3.5: <i>TOC1</i> rhythm in roots depends on light conditions.....	89
Figure 4.1: The expression of morning and evening clock genes is circadian in illuminated roots, with a longer FRP compared to shoots	97
Figure 4.2: Light directly affects the expression of clock genes in roots	101
Figure 4.3: Light directly affects the amplitudes of clock gene expression in roots in LD and LL, but not their FRP	104
Figure 4.4: Direct exposure to light affects clock gene transcript levels in roots.....	110
Figure 4.5: The expression of morning and evening genes free run in DD with similar FRP in shoots and roots.....	116
Figure 4.6: Transcript levels of morning and evening genes free run in DD with similar FRP in shoots and roots	118
Figure 4.7: Both blue and red light affect clock gene expression in root	120
Figure 4.8: Comparison of FRPs in shoots and roots in various conditions.....	122
Figure 5.1: the FRP is longer in roots compared to shoots in LL, but both organs are synchronised in diurnal conditions.....	131
Figure 5.2: LD cycles can directly entrain <i>GI</i> expression in roots.....	135
Figure 5.3: <i>GI</i> expression in roots is entrained by direct perception of light rather than any putative signal from shoots	139
Figure 5.4: <i>GI</i> expression can be entrained by a broad range of low amplitude LD cycles in both shoots and roots.....	143
Figure 5.5: The amplitude of <i>GI</i> expression rhythm resonates in both shoots and roots...	145
Figure 5.6: Shoot and root clock genes respond differently to skeleton photoperiods	146
Figure 5.7: Shoot and root clock genes can be entrained by temperature cycles.....	151
Figure 6.1: The <i>cca1-11/hy-21</i> double mutant displays rhythmicity in the root under LL	159
Figure 6.2: The <i>toc1-4</i> mutation shortens the FRP of <i>CCR2</i> expression in both light- and dark-grown roots under LL	161
Figure 6.3: The <i>ztl-105</i> mutation affects differently <i>CCR2</i> expression in shoots and roots	164

Figure 7.1: Simulations of <i>TOC1</i> and <i>LHY</i> mRNA levels in shoots and “roots” under DD using the L2006 model	172
Figure 7.3: Simulations of clock genes mRNA levels in shoots and “roots” under DD using the P2010 model	176
Figure 7.4: Simulations of clock genes mRNA levels in shoots and “roots” under LL using the P2010 model	177
Figure 7.5: Simulations of clock genes mRNA levels in shoots and “roots” under LD using the P2010 model	179
Figure 7.6: The P2012 model can reproduce Aschoff’s rules	181
Figure 7.7: Simulations of clock genes mRNA levels in shoots and “roots” under LL using the P2012 model with different light intensities.....	183
Figure 7.8: Simulations of clock genes mRNA levels in shoots and “roots” under LD using the P2012 model with different light intensities.....	186
Figure 7.9: Simulations of clock genes mRNA levels in shoots and “roots” under LL after modifying parameters related to inhibition constants.....	192
Figure 7.9: Simulations of clock genes mRNA levels in shoots, “dark-grown roots” and “light-grown roots” under LL after modifying parameters related to light inputs	196

Acknowledgments

First I would like to thank my supervisors, Hugh and Andrew, for giving me the opportunity to work on this project, and SULSA for the funding. Many thanks to Hugh who was my main supervisor and always had his door (and his mind) open. He has always been very supportive and encouraging. Thank you for all the time spent to correct this manuscript too. I also want to thank Andrew who provided precious advice and put me in contact with several people, especially experts in modelling.

Many thanks to the members of my supervisor's labs, especially here in Glasgow. Special thanks to Stuart for interesting discussions about my project and for corrections of some chapters. I'm also grateful to other people who have been working in the Bond lab: Jill who is one of the very few people who corrected my spoken English, Janet for her technical expertise, Allan for having organised many 5 a sides, and also past members who contributed to the good atmosphere in the lab.

I also want to thank people working in Edinburgh, particularly people who help me with modelling, especially Richard and his team from the SBSI (thanks for all the troubleshooting) and Alexandra for interesting discussions. Thank you to Karen and her lab too for kindly providing us with many seeds.

Thank you to my assessors for giving me advice during meetings. Special thanks to Richard and Bill for being very supportive, and also Gareth who dares to play football with youngsters. Many thanks to Julie for building the customised equipment I needed (using a real guillotine!), together with Nosrat, Alastair and Thom from the Bioelectronic unit.

I had the chance to supervise several very good students, all very motivated. Now it's my turn to acknowledge you guys. Thank you to Guillaume and Mike who carried out first trial experiments, Brian who repeated successfully one of them (presented in this thesis) and Ben for all his voluntary work in the lab and his friendliness.

It was a real pleasure to work in the Bower building, full of nice people, not only colleagues but also many good friends. Special thanks to Fab (for everything), Connie and Maya who are all good friends and also proofread some chapters. I have also enjoyed the company of many others, in the lab, in the pub and elsewhere. It was really fun to work and to go out with you guys.

And last but not least I would like to thank my friends and family. I wish I could see you more often. Thanks for everything!

Author's declaration

I declare that, except where explicit reference is made to the contribution of others, this dissertation is the result of my own work and has not been submitted for any other degree at the University of Glasgow or any other institution.

Simon Bordage

Abbreviations

[Ca²⁺]cyt: cytosolic free calcium concentration
APRR: Arabidopsis Pseudo Response Regulator
BS: Binary Slide
CAT3: CATALASE 3
CCA1: CIRCADIAN CLOCK ASSOCIATED 1
CCD: Coupled-charge device
CCR2: COLD CIRCADIAN RHYTHM RNA BINDING 2
CHE: CCA1 HIKING EXPEDITION
ChIP: Chromatin Immunoprecipitation
CHS: CHALCONE SYNTHASE
CM: Circadian Modelling
CO: CONSTANS
Col-0: Columbia
COP1: CONSTITUTIVE PHOTOMORPHOGENIC 1
CSBE: Centre for Systems Biology of Edinburgh
CT: Circadian Time
D: Dark
d: day
DD: Dark/Dark (constant darkness)
DEPC: Diethylpyrocarbonate
EC: Evening Complex
EDTA: Ethylenediaminetetraacetic acid
EE: Evening Element
EMSA: Electrophoretic Mobility Shift Assay
FFT: Fast Fourier Transform
FKF1: FLAVIN BINDING, KELCH REPEAT, F-BOX1
FRP: Free Running Period
GA: Genetic Algorithm
GI: GIGANTEA
GU: Glasgow University
HATS: High-Affinity Transport System
HC: Hot/Cold (temperature cycle)
L: Light
L2005a, L2005b and L2006 models: Locke *et al.* models
LD: Light Dark cycles; by default 12 h L, 12 h D
LED: Light-Emitting Diode
LHY: LATE ELONGATED HYPOCOTYL
LKP2: LOV KELCH PROTEIN 2
LL: Light/Light (constant light)
LUC: Luciferase
MOPS: 3-(N-morpholino)propanesulfonic acid
MS: Murashige and Skoog (growth medium)
MYB: Myeloblastosis
N: Nitrogen
NB: Nuclear Body
NI: Night Inhibitor
NLLS: Non Linear Least Square
NMD: Nonsense-mediated decay

NO₃⁻: Nitrate
NRT2.1: Nitrate Transporter 2.1
ODE: Ordinary Differential Equations
P2010 and P2012 models: Pokhilko *et al.* models
PC: Photon Counting modes
PGA: Parallelised Genetic Algorithm
PR1: Pathogenesis-Related protein 1
PRC: Phase Response Curve
PRR: Pseudo Response Regulator
qPCR : quantitative Polymerase Chain Reaction
R: Root
RT : Reverse Transcription
RVE1: REVEILLE1
S/N: Signal/Noise ratio
S: Shoot
SBML: Systems Biology Markup Language
SBSI: Systems Biology Software Infrastructure
SCN: Suprachiasmatic Nucleus
T cycle: cycle of period T
TBE: Tris/Borate/EDTA buffer
TF: Transcription Factors
TOC1: TIMING OF CHLOROPHYLL AB BINDING PROTEIN EXPRESSION 1
TTFL: Transcription Translation Feedback Loop
UBQ: UBIQUITIN
Ws: Wassilewskija
WT: Wild Type
ZTL: ZEITLUPE
 χ^2 : Chi-squared

1 General introduction

In biology, there may be only one constant: change! Some changes are not predictable and others are. When the changes in a variable recur with a similar pattern (a cycle) and systematic interval (period), they define a rhythm. Chronobiology is the study of rhythms in life. Biological rhythms are a fundamental property of all life and encompass a wide range of periods, from seconds (heart beats) to years (flowering). Life has evolved on a rotating planet, where some environmental changes are rhythmic and therefore predictable, especially the daily cycles of light and darkness (Koukkari and Sothorn, 2006a). The term circadian comes from the Latin words “*circa*” (about) and “*dies*” (day). Circadian rhythms are the subset of biological rhythms with a period of ~ 24 hours.

1.1 Why are biological rhythms important?

Rhythms are such an integral part of life that the absence or perturbation of specific oscillations (e.g. brain waves) in humans and other animals is used in the practice of medicine to distinguish between illness and good health. Life and death are defined by presence and absence of rhythms (Koukkari and Sothorn, 2006a).

1.1.1 *Biological oscillations are pervasive*

Biological oscillations are pervasive in three senses:

1) All major biological processes are represented. In animals, oscillations are involved in the acquisition, transfer and processing of information (e.g. neural oscillators), movement (oscillations in muscles), secretion (e.g. oscillations in the membrane potential of secretory cells such as pancreatic islet cells), reproduction (e.g. menstrual cycles), growth and development (e.g. periodic mitosis) (Rapp, 1987). Rhythms are involved in many biological processes in plants too: hormonal signalling (Robertson *et al.*, 2009), leaf movement (Harmer, 2009), solute transport (Haydon *et al.*, 2011), flowering (Andres and Coupland, 2012), growth in shoots and roots (Farre, 2012; Ruts *et al.*, 2012a), stomatal regulation (Lee, 2010), defence (Jander, 2012; Goodspeed *et al.*, 2012), *etc.* Just considering one type of oscillation, circadian rhythms, microarray data in the model plant

Arabidopsis thaliana suggest that about one third of the genes expressed are clock regulated (Harmer, 2009). If thermocycles and photocycles are also considered, 89% of *Arabidopsis* transcripts cycle in at least one condition, i.e. diurnal or constant conditions (Michael *et al.*, 2008). This reflects how pervasive 24 h rhythms are in plants.

2) Oscillations occur in a broad spectrum of chemical and biological systems spanning the most primitive to the most complex (Rapp, 1987). Several examples of rhythms have been given earlier in complex multicellular organisms (e.g. animal and plants). Circadian rhythms are also observed in much simpler eukaryotes. For instance *Ostreococcus tauri* is a green unicellular algae described as the smallest free-living eukaryote. Orthologs of plant specific genes, such as the core clock components *TOC1* and *CCA1*, are also involved in rhythmicity in *Ostreococcus* (Thommen *et al.*, 2012, and references cited therein). Circadian systems are also represented in other branches of life. For instance the filamentous fungus *Neurospora crassa* has served for decades as a model organism for uncovering the basic circadian physiology and molecular biology (Baker *et al.*, 2012). The production of conidia (spores) is an example of overt rhythm in this fungus. Biological rhythms are also found in some prokaryotes. *Synechococcus elongates* is a well-studied cyanobacterium that exhibits circadian rhythms. In this bacterium three genes are essential components of the clock: *kaiA*, *kaiB* and *kaiC*. Nakajima and colleagues were able to reconstitute the self-sustained oscillation of Kai phosphorylation in vitro by incubating KaiA KaiB and KaiC proteins and ATP (Nakajima *et al.*, 2005). This demonstrated that only a few components are sufficient to generate a circadian rhythm. The period of the KaiC phosphorylation measured in vitro was remarkably consistent with its period in vivo.

3) The periods can range from fractions of seconds to month or years. Circadian rhythms are probably the most studied rhythms in biology. However many other rhythms exist in life, with a very broad range of periods. The period of circadian rhythms are usually considered to be between 20 and 28 h. Rhythms with longer or shorter periods are called infradian or ultradian respectively. To give two extreme examples, thalamic sensory neurons in the monkey can fire rhythmically every 30 ms (Poggio and Viernstein, 1964) whereas some Chinese bamboos flower every 120 years (Janzen, 1976)! In between, many periods can be found in biological oscillation, notably circannual (e.g. bird migration), circatidal (e.g. crab activity), and of course circadian rhythms. These three subsets of

biological rhythms have natural synchronisers: physical rhythms generated by the rotations and revolutions of the earth and moon, namely seasons, tide and diurnal cycles.

1.1.2 Oscillations confer functional advantages

Temporal organisation is probably the most obvious advantage conferred by biological rhythms. Entrainment and synchronisation of biological rhythms keep natural processes in step with the demand of a periodic environment (Pittendrigh, 1993); the concept of entrainment will be detailed in section 1.4. Even in constant conditions key physiological pathways are temporally compartmentalised in *Arabidopsis* (Harmer *et al.*, 2000). The authors showed that under constant light (LL) photosynthesis genes peak near the middle of the subjective¹ day, whereas phenylpropanoid biosynthesis genes peak before subjective dawn. The latter are involved in the production of photoprotective pigments; the anticipation of dawn by their early production would probably be advantageous. The circadian clock can also coordinate key pathways in animals (Panda *et al.*, 2002).

The value of creating temporal order with oscillations is not always to ensure that two processes occur at the same time. The fixed phase angles introduced in periodic systems can also be used to separate incompatible processes (Rapp, 1987). For instance in cyanobacteria, nitrogen fixation requires nitrogenase, an enzyme that is inhibited by oxygen. Photosynthesis produces oxygen throughout the day, but nitrogen fixation is regulated by the clock so that it is maximal during the night. Therefore the same cell can perform two incompatible processes: photosynthesis during the day and nitrogen fixation during the night (Johnson *et al.*, 2011). More generally, stimuli of the same strength applied at different times of the day can result in responses of different intensities; this is known as “gating” (Hotta *et al.*, 2007). Gating of a signal may allow plants to better process and react to the wide range of environment signals they are constantly subjected to, such as light or cold temperature (Hotta *et al.*, 2007). Another example is the gating of cell division by the circadian clock in algae and in cyanobacteria. In these organisms cell division occurs during the night. The gating of this process may protect DNA from damaging UV radiation during DNA replication (Farre, 2012).

¹ The word “subjective” is used in constant conditions following entrainment. For instance in constant light (LL), the subjective night is the portion of the day that would have been dark if the entraining LD cycle had persisted

Endogenous rhythms offer the clear advantage of anticipatory preparation for predictably recurrent conditions (Pittendrigh, 1993). A striking example is the circatidal movement of *Euglena*, nicely described by John Palmer in his book “The Living Clock”. This unicellular protist can be found on river sides. *Euglena* anticipate the tide in and “bury themselves in the mud where they cannot be washed away. But when the tide recedes they ascend up and out of the mud to sit on the surface for some photosynthetic sunbathing” (Palmer, 2002).

Biological rhythms also confer adaptive advantages, and circadian biology can lead to practical applications, for instance in agriculture. These important aspects will be developed in the next section.

1.2 Circadian rhythms

1.2.1 *The discovery of endogenous rhythms*

Diurnal rhythms have been observed thousands of years ago, but it was not realised that they could be endogenous. Scientific literature on circadian rhythms began in 1729 and was related to plant leaf movement. The French astronomer de Mairan reported that the daily leaf movement of the sensitive heliotrope plant persisted in constant darkness, demonstrating their endogenous origin (de Mairan, 1729, cited in McClung, 2006). Strictly speaking it cannot be ruled out that the oscillations were driven by temperature changes, even though the experiments were carried out in a wine cellar! The endogenous origin was disputed, but de Candolle measured leaf movements more accurately and showed that they had a period of 22 to 23h in *Mimosa pudica* under constant conditions (de Candolle, 1832, cited in McClung, 2006). Until experiments on the fungus *Neurospora crassa* were conducted in space (Sulzman *et al.*, 1984), the fact that the period was not exactly 24 h was the best evidence that circadian rhythms were truly endogenous and not driven by some subtle and undetected geophysical cue associated with the rotation of the Earth on its axis.

The inheritability of circadian rhythms was already suggested in 1880 by Charles and Francis Darwin (McClung, 2006). Fifty years later, the inheritance of period length among progeny from crossed parents with distinct period lengths was first reported in *Phaseolus*: hybrids had period length intermediate between those of the parents (Bunning, 1932). Leaf movements are actually just one among many rhythms in plants, including germination,

growth, enzyme activity, gas exchange, photosynthetic activity, flower opening and fragrance emission (Cumming and Wagner, 1968). And plants belong to just one of the kingdoms possessing circadian rhythms. These appear almost ubiquitous in higher organisms (Harmer, 2009).

1.2.2 Properties of circadian rhythms

In contrast with other nycthemeral (or daily) rhythms, which also have a period of 24 h in diurnal conditions, circadian rhythms have other defining characteristics. They are endogenous and self-sustaining (McClung, 2006), so they persist under constant environmental conditions (such as constant light or dark, and constant temperature). In such conditions a circadian rhythm free runs, and is characterised by a Free Running Period (FRP). This FRP is usually not exactly 24 h, hence the term “circa”. A remarkable feature of circadian rhythms is their persistence: sustained rhythms could be observed for over two years in rodents under constant conditions (Pittendrigh, 1993). The same organism can have a different FRP depending on the experimental conditions; under constant light (LL) the FRP of a diurnal organism tends to decrease when the light intensity increases (Aschoff, 1960). This is known as “Aschoff’s rule”.

Another attribute of circadian rhythms is temperature compensation: the period remains relatively constant over a range of ambient temperatures (McClung, 2006). This characteristic allows the circadian system to keep accurate time even when ambient conditions are cold or hot. Chemical processes exhibit marked temperature dependence. For instance, the rate of a typical chemical reaction doubles with a 10°C increase in temperature ($Q_{10} = 2$). But Bunning observed a Q_{10} of only 1.2 for the period of leaf movement in *Phaseolus coccineus* (Bunning, 1931). This observation was extended to other plants and animals by the 1960s (Sweeney and Hastings, 1960), and the relative temperature insensitivity of the period is a striking feature of circadian rhythms.

Finally, circadian rhythms can be reset by environmental cues such as light and temperature (Harmer, 2009). Such cues are called zeitgebers, a German term meaning “time giver”. For instance a circadian rhythm with a FRP of 26 h under LL has a period of 24 h under normal Light/Dark (LD) or temperature cycles. Thus circadian rhythms can be entrained by the environment. The concept of entrainment will be developed in section 1.4.

Specific terminology is used to describe time in circadian biology (DeCoursey, 2004a). The time defined by the zeitgeber is commonly referred as “ZT” and usually starts at dawn (ZT0); in a cycle of 12 h light/12 h dark, the time of dusk would then be ZT12². However the circadian time (CT) is a subjective time: for an organism with a FRP of 26 h, each circadian hour would actually represent 26/24 h (i.e. ~ 1.1 h) in the international unit system. Other common terms in circadian biology are amplitude and phase. The amplitude is the extent of an oscillatory movement, usually measured from mean to extreme value (i.e. the difference between the mean value and the peak or the trough). The amplitude can also be defined as the difference between peak and trough. The phase is the instantaneous state of an oscillation within a period. It usually refers to the time of the peak (acrophase), relative to a reference which is often dawn or dusk. This phase relationship is more explicit in the term “phase angle”: the phase angle is the difference between identifiable phases (e.g. acrophase, or dawn) of two oscillations, and is expressed in hours or degrees of arc. For instance two 24 h rhythms which are in exact opposite phase have a phase angle of 12 h or π .

Circadian rhythms are not only seen at the whole organism level, such as change in behaviour; they are also found at the molecular level, with changes in gene expression and signalling molecules (Harmer, 2009). In several model organisms, circadian rhythms are generated by the interactions of rhythmically expressed genes that form positive and negative feedback loops (Dunlap, 1999). This central clock is a part of the circadian system that can be simplified as a core oscillator that generates rhythmic outputs via specific signalling pathways and can be reset by environmental cues such as light and temperature (Harmer, 2009). This is illustrated in figure 1.1. The circadian system could be considered at different scales, from the cellular to the organism level. In this thesis the expression “circadian system” will refer to the intracellular system, which can be described as a complex molecular network (see section 1.3).

² Note that ZT0 will occasionally refer to dusk in other chapters, e.g. when an experiment started at dusk

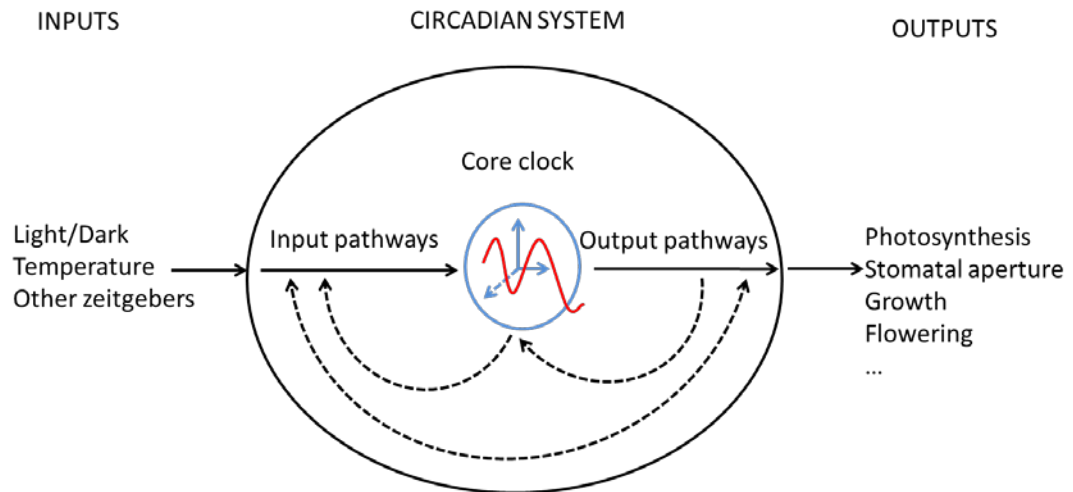


Figure 1.1: Simplified version of a circadian system

The circadian system includes the circadian (core) clock, but also input and output pathways. Zeitgebers such as Light/Dark and temperature cycles can reset the core clock via complex input pathways. In turn the circadian clock controls the expression of thousands of genes and physiological rhythms such as photosynthesis, stomatal and leaf movements, growth, flowering, fragrance emission *etc.* Solid black arrows represent the simplified linear pathway between inputs and outputs through the oscillator. Dotted arrows represent possible feedbacks and the complex network nature of the circadian system.

1.2.3 Adaptive advantages conferred by the plant circadian clock

The term adaptation is used in biology in two ways. Evolutionary adaptation refers to inherited features that enhance survival or reproduction of an organism. In contrast, physiological adaptation refers to the ability of an individual to adjust or acclimate to an environmental change (DeCoursey, 2004b). Evidence suggests that the plant circadian clock is adaptive in both senses: evolutionary and physiological. A few examples are given below.

In 2002 Green and colleagues showed that several circadian clock mutants had low-viability phenotypes. For instance CIRCADIAN CLOCK ASSOCIATED 1 (*CCA1*) is one of the key components of the circadian clock in *Arabidopsis*. Plants that overexpress *CCA1* lose the ability to anticipate the daily change in LD cycles. These *CCA1*-ox plants flowered

later and were less viable under very short day conditions than their wild-type (WT) counterpart (Green *et al.*, 2002). Later, Dodd and colleagues studied other circadian mutants, with shorter (~20 h) or longer (~ 28 h) FRP compared to the WT. They grew these plants under different T cycles, i.e. LD cycles with a period of T hours. Plants with a clock period matched to the environment (T20 or T28) had more chlorophyll, fixed more carbon, grew faster and survived better than plants with a circadian period differing from their environment (Dodd *et al.*, 2005). This illustrated the competitive advantage conferred by a circadian clock that resonates with the external environment. Another study confirmed the adaptive significance of the plant clock in terms of reproductive success (Yerushalmi *et al.*, 2011).

The circadian clock also contributes to physiological adaptation in plants. For instance the plant clock is involved in the adaptation of plant physiology to the change of seasons, with important implications in terms of reproduction and response to cold stress. In *Arabidopsis* flowering is accelerated in long days. This photoperiodic flowering is partly regulated by the circadian clock through the rhythmic expression of the clock gene *GIGANTEA* (*GI*). It is the coincidence between the circadian rhythms of *CONSTANS* (*CO*), *GI* and *FLAVIN BINDING, KELCH REPEAT, F-BOX1* (*FKF1*) and exposure to light under long days that determines whether the regulatory proteins such as *CO* are stabilised to promote flowering (Andres and Coupland, 2012). The circadian clock can also modulate cellular cold signalling networks, which would prepare the cell for the onset of winter (Eriksson and Webb, 2011). For instance the sensitivity to cold stimuli is gated by the clock. A conserved response to cold across plant species is the induction of *CBFs* (*C-REPEAT BINDING FACTORS*). The *CBFs* upregulate the expression of genes that increase the levels of cryoprotectants in the cell. *CBF* expression is upregulated by *CCA1* and *LHY*, two core clock genes. Freezing tolerance is reduced in the *cca1/lhy* double mutant compared to WT *Arabidopsis*. A similar effect is observed in poplar trees, where decreased expression of *LHY1* and *LHY2* reduces cold hardiness. In addition the circadian clock of poplar trees is involved in initiating growth cessation and dormancy (Eriksson and Webb, 2011).

1.2.4 Some applications of circadian biology

Clock genes identified in *Arabidopsis*, as described in the next section, are mostly conserved among angiosperms, suggesting that the clock mechanism may be conserved among plant species including important crops (Nakamichi, 2011). For instance orthologs

of *GI* have been identified in pea and in rice. As mentioned earlier, *GI* is involved in the photoperiod flowering in *Arabidopsis*, so homologs of *GI* might also play a role in the flowering of crops.

The control of flowering has an important impact on yield and has been a key trait in the domestication of crops (Zakhrabekova *et al.*, 2012). One example of an important crop is barley, and one of the cultivars of barley currently used in agriculture is Mari. This cultivar is an induced early flowering barley mutant and has been used for over 50 years to facilitate short season adaptation and further geographic range extension. The gene responsible for this key adaptive phenotype, *Mat-a*, was identified recently. Interestingly *Mat-a* is a homolog of the key clock gene *ELF3* (*EARLY FLOWERING 3*) in *Arabidopsis* (Zakhrabekova *et al.*, 2012; Faure *et al.*, 2012). The authors showed that *mat-a* mutations disturb the flowering pathway, leading to the early phenotype. The adaptation to different geographic regions and climatic conditions is a critical issue in times of global warming.

The role of the circadian clock in plant growth and defence against pathogens might also have applications in agriculture. Indeed the growth of the whole plant is severely affected by improper clock regulation in *Arabidopsis*, resulting not only in altered timing and capacity for growth but also aberrant development of shoot and root architecture (Ruts *et al.*, 2012b). The circadian clock also plays a role in plant immunity. Wang and colleagues recently discovered new defence genes in *Arabidopsis* that are under circadian control (Wang *et al.*, 2011a). This allows plants to anticipate possible infection at dawn when the pathogen normally disperse spores, and also time immune responses according to the perception of different pathogenic signals upon infection.

Circadian biology can have other applications in agriculture. At least 20 herbicides have been shown to display time of day-dependent effects upon plants (Koukkari and Sothorn, 2006c). Oscillations in the response of plants to herbicides have been attributed to many factors including the phases of other rhythms such as leaf movement, phloem transport, translocation of photosynthate and stomatal opening (Koukkari and Sothorn, 2006c). Rhythmicity in the response to herbicides was demonstrated for cotton seedlings under LD and constant conditions, suggesting the role of the circadian clock in this process (Rikin *et al.*, 1984). Miller and colleagues examined the influence of the time of the day when applying four different herbicides in the field. They found a circadian response to each

herbicide, even after adjusting for environmental conditions such as light, temperature and humidity that can affect the efficacy of a herbicide (Miller *et al.*, 2003). The authors concluded that the amplitudes in the response to these herbicides were large enough to consider the possible financial and environmental implications.

The concept that chemicals or other treatments are tolerated better at some times of the day than others is well known in medicine. Some treatments are given at a specific time of the day, and other treatments may soon be optimised so they are taken when they are more efficient and/or less toxic for the human body (Levi *et al.*, 2010). Circadian rhythms were first discovered in plants and now have potential applications in agriculture, but also in the practice of human medicine. Other discoveries in *Arabidopsis* may also have broader applications than in plant science or agriculture.

1.3 Molecular basis of the plant circadian clock

While overt circadian rhythms, such as leaf movement, were studied in plants much earlier than in other organisms, the molecular bases of the circadian clock were discovered later. Identification of circadian clock components began in the 1970s in several model organisms: *Drosophila*, *Chlamydomonas* and *Neurospora*. It was more than 10 years later that circadian rhythms were described at the molecular level in plants (Harmer, 2009). Although most of the molecular components of circadian systems are not evolutionarily conserved, the basic architecture of eukaryotic oscillators is similar: interlocked feedback loops between species-specific components that sustain robust rhythms (Nagel and Kay, 2012). In addition, similar layers of regulation apply to all circadian systems: transcriptional repressor and activator complexes, rhythmic transcript accumulation, rhythmic chromatin remodelling, regulation of cellular localization, phosphorylation, and proteasome-mediated degradation (Herrero and Davis, 2012).

In 1985 Kloppstech described a circadian rhythm in the abundance of three transcripts in pea, including the *LIGHT-HARVESTING CHLOROPHYLL A/B BINDING PROTEIN* (*LHCB*, or *CAB*). A few years later, Nagy *et al.* (1988) repeated and extended this experiment to wheat, where *CAB-1* transcription was under circadian control (Nagy *et al.*, 1988). It was soon established that in *Arabidopsis* the transcription rate and transcript

accumulation of *CAB* (Millar and Kay, 1991) and a number of other genes (McClung and Kay, 1994) were also under circadian control. *Arabidopsis* was emerging as a powerful system in which to combine forward genetic analysis with molecular gene cloning techniques (Somerville and Koornneef, 2002). Note that most of the results presented hereafter come from the study of *Arabidopsis thaliana*. The words “plant” and “*Arabidopsis*” will therefore refer to this plant species, unless stated otherwise.

CAB is an output gene, i.e. a gene whose expression is controlled by the clock. It has been often used to monitor the clock in *Arabidopsis*. Millar *et al.* (1992) demonstrated that a short fragment of the *CAB2* promoter could drive rhythmic transcription and mRNA accumulation of luciferase (*LUC*) mRNA detectable as rhythmic light emission from *Arabidopsis* seedlings bearing the *CAB:LUC* transgene. *LUC* catalyses the ATP-dependent oxidative decarboxylation of luciferin (sprayed on the plants) with a concomitant release of photons at 560 nm; this light emission can be quantified with a sensitive charge-coupled device (CCD) camera (Welsh and Kay, 2005).

1.3.1 Transcription – Translation Feedback Loops (TTFLs)

The development of the luciferase assay system permitted the first screen for *Arabidopsis* clock mutants. *Arabidopsis* seeds bearing the *CAB:LUC* transgene were mutagenised, and M2 seedlings were screened to yield the first plant clock mutant: *toc1* (*TIMING OF CAB EXPRESSION1*) (Millar *et al.*, 1995a). *TOC1* is also known as *PRR1*, a member of the Pseudo-Response Regulator family.

Another clock component, *CCA1* (*CIRCADIAN CLOCK-ASSOCIATED 1*), was initially identified as binding the *CAB2* promoter. Its overexpression causes arrhythmicity (Wang and Tobin, 1998), suggesting a role in the core clock. *LHY* (*LATE ELONGATED HYPOCOTYL*) is *CCA1*'s closest paralog in *Arabidopsis* (Carre and Kim, 2002). Both are morning-expressed MYB transcription factors, while *TOC1* is evening-expressed. *cca1* and *lhy* loss of function mutants confer a short period phenotype and have only residual rhythmicity, suggesting that they are core clock components that function redundantly (Alabadi *et al.*, 2002; Mizoguchi *et al.*, 2002). These three components formed the first loop proposed in the *Arabidopsis* clock (Alabadi *et al.*, 2001). *LHY* and *CCA1* negatively regulate *TOC1* expression by binding to its promoter. Conversely, *TOC1* appeared to augment the expression of *LHY* and *CCA1*, directly or indirectly.

Most of the clock components described in this section are shown in figure 1.2, and some of them are also presented in figure 1.4. Figure 1.2 illustrates the complexity of the clock machinery at the transcription-translation level; yet this model omits many levels of regulation (such as post-transcriptional modifications) for simplification. The models presented in figure 1.4 are simpler diagrammatic models, but they represent three versions of mathematical models that better explain the dynamics of the clock as a whole. These mathematical models, which progressively integrated more data and simulated more levels of regulation, will be presented in section 1.5.

The mechanism of TOC1 has remained unclear for almost a decade. In 2009 Pruneda-Paz *et al.* discovered that CHE (CCA1 HIKING EXPEDITION) repressed the activity of *CCA1*. In addition CHE and TOC1 physically interact, which established a molecular link between TOC1 and *CCA1* gene regulation. The authors suggested that TOC1 activates *CCA1* expression by antagonising its repression by CHE (Pruneda-Paz *et al.*, 2009). But in the last year, more evidence showed that TOC1 can directly bind DNA and repress the expression of genes such as *CCA1* (Gendron *et al.*, 2012; Huang *et al.*, 2012). In addition the repressor role of TOC1 allows more experimental data to be explained (Pokhilko *et al.*, 2012).

CCA1 and *LHY* seem to be mainly repressors of gene expression, but they can also act as activators (figure 1.2). For instance they form a morning loop with *PRR7* and *PRR9*: *CCA1* and *LHY* activate these *PRR*s which in turn repress the *MYB* transcription factors (Farre *et al.*, 2005; Nakamichi *et al.*, 2005; Salome and McClung, 2005a). *PRR9* has also been shown to participate in a positive feedback loop with *LIGHT-REGULATED WD1* (*LWD1*), a clock-associated protein involved in the regulation of period length and photoperiodic flowering (Wang *et al.*, 2011b). Two other *PRR* and *MYB* transcription factors form a negative feedback loop within the clock: *PRR5* and *RVE8* (*REVEILLE8*) (Rawat *et al.*, 2011).

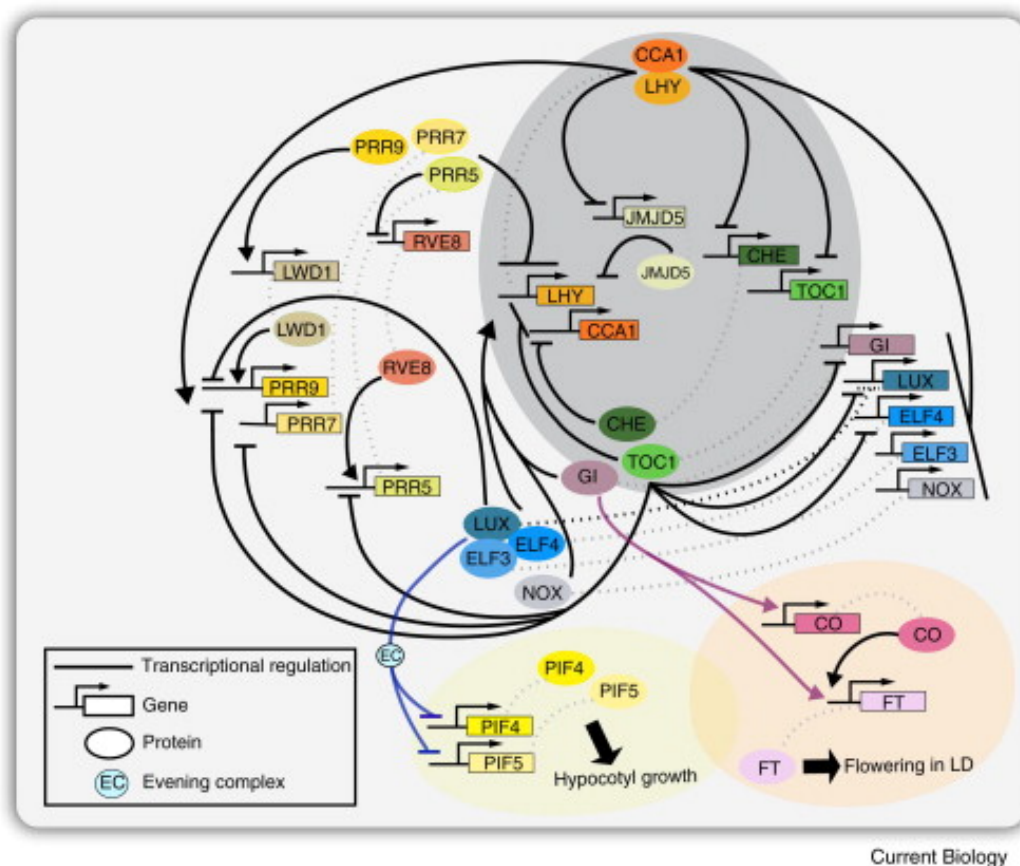


Figure 1.2: A model representing the interlocked Transcriptional Translational Feedback Loops (TTFL) of the *Arabidopsis* circadian clock, and connections with modulators of physiological processes

The central loop is shown in the darker grey background and consists of the two partially redundant MYB transcription factors CCA1 and LHY, and TOC1. CCA1/LHY form similar loops with CHE and with JMJD5. CCA1 and LHY act both as activators and repressors of clock gene expression. TOC1 has been recently revealed as a global repressor of clock gene expression. Some components of the clock network are not shown for simplification. Protein-protein interactions are only shown for LUX, ELF3 and ELF4 which form the Evening Complex (EC). The EC regulates hypocotyl growth by directly binding to the promoters of PIF4 and PIF5. Interaction between GI, CO and FT modulates photoperiodic flowering (LD = Long Days). Each gene/protein is represented by a distinct colour. Transcriptional regulations are represented by black lines. Dashed lines indicate the protein and gene associations. Arrows and horizontal lines represent activation and repression respectively. Molecular components are further described in text. The figure is from (Nagel and Kay, 2012).

An evening loop was proposed to be formed between *TOC1* and an unknown component *Y* that was thought to include *GI* (Locke *et al.*, 2005b; Locke *et al.*, 2006). *GI* was already known to be involved in the clock and in the control of photoperiodic flowering (Fowler *et al.*, 1999; Park *et al.*, 1999) but its position in the clock network was not clear yet. Later models distinguished *Y* and *GI* functions (Pokhilko *et al.*, 2010) and eventually replaced *Y* by other components. These include *ELF3* and *ELF4* (*EARLY FLOWERING 3* and *4*) and *LUX ARRHYTHMO* (*LUX*) (Pokhilko *et al.*, 2012). *LUX* and *ELF3* were proposed to bind to the *PRR9* promoter and repress its expression (Helfer *et al.*, 2011; Dixon *et al.*, 2011). Soon after Nusinow *et al.* (2011) showed that *LUX*, *ELF3* and *ELF4* proteins can interact and form the so-called Evening Complex (EC). *ELF3* and *ELF4* also form a complex with *NOX* (Latin for “night”) also known as *BOA* (*BROTHER OF LUX ARRHYTHMO*). *NOX* and *LUX* are homologs that are thought to be partially redundant (Adrian Troncoso-Ponce and Mas, 2012). *NOX* overexpression altered the rhythms of several clock genes, suggesting an important role of *NOX* within the core oscillator (Dai *et al.*, 2011).

Other components have been shown to modulate clock function such as *PRR3*, *TIC* (*TIME FOR COFFEE*) and *SRR1* (*SENSITIVITY TO RED LIGHT REDUCED*) and more recently *JMJD5*, a Jumonji C Domain-containing protein also known as *JMJ30* (Nagel and Kay, 2012). Jumonji C Domain-containing proteins appear to be involved in chromatin remodelling, acting as histone demethylases. They have been shown to modulate clock function in both plants and humans, suggesting that histone modification has evolved as an important mechanism of circadian systems (Lu and Tobin, 2011). Chromatin remodelling and other mechanisms of regulation will be further described in the next subsection.

1.3.2 Other layers of regulation in the circadian clock

Many biochemical mechanisms contribute to circadian regulation within the TTFL. These include chromatin remodelling, post-transcriptional and post-translational regulations, cellular localisation and protein complex formation. Some examples are given below.

Evidence in plant and animal systems has shown a link between dynamic change in chromatin structure and circadian regulation of gene expression (Adrian Troncoso-Ponce

and Mas, 2012). In *Arabidopsis* the induction of *TOC1* transcription and its repression by CCA1 were correlated with clock-controlled cycles of histone acetylation, favouring transcriptionally permissive or repressive chromatin structure depending on the circadian time (Perales and Mas, 2007). Therefore the transcription of a clock gene may depend on its promoter accessibility. Transcription can also be regulated by light. For instance *CCA1* transcription is induced by light (Yakir *et al.*, 2009). Once the mRNA is synthesised, its turnover is usually closely regulated (Staiger and Green, 2011). For *CCA1* mRNA, this turnover is also regulated by light: *CCA1* mRNA is relatively stable in the dark but has a short half-life in the light (Yakir *et al.*, 2007). The degradation of RNA can also depend on splicing variants. Unproductive isoforms with premature termination codons can be the substrate for Nonsense-mediated decay (NMD). More generally, alternative splicing can mediate clock responses to the environment in both plant and animals (Staiger and Green, 2011). This was recently shown in *Arabidopsis*, where extensive alternative splicing in clock genes was revealed in plants acclimated to different steady state temperatures or undergoing temperature transitions (James *et al.*, 2012).

Some mRNAs are then translated into functional proteins. Post-translational processes play critical roles in all circadian systems (McClung, 2011). One example is phosphorylation mediated by Casein Kinase 2 (CK2). This enzyme is one of the few evolutionarily conserved molecular components involved in the regulation of key clock genes. CK2 is found in the mammalian, *Drosophila*, *Neurospora* and *Arabidopsis* circadian systems (Nagel and Kay, 2012). In *Arabidopsis*, CK2 phosphorylates CCA1 and LHY, and this process is considered to be important for CCA1 function, specifically the DNA-binding properties and subsequent regulation of its targets within the oscillator. Protein stability and degradation also play an important role in the plant clock. For instance protein abundance of the blue-light photoreceptor and F-box protein ZEITLUPE (ZTL) is rhythmic although its mRNA is constitutively expressed. ZTL protein rhythmicity is conferred by a light-dependent interaction with GI and is necessary to sustain a normal circadian period by controlling the degradation of TOC1 (Kim *et al.*, 2007). TOC1 stability may also be dependent on cell type or tissue. Indeed, PRR3 expression appear to be restricted to the vasculature and may function to modulate TOC1 stability by hindering ZTL-dependent TOC1 degradation (Para *et al.*, 2007).

Dynamic subcellular distribution of clock components is at the core of eukaryotic circadian systems (Herrero and Davis, 2012). An example is the localisation of TOC1 protein: it is stabilised in the nucleus by interaction with PRR5. But the disruption of this interaction in weak alleles of *toc1* and *prr5* decreases the TOC1 nuclear pool and makes TOC1 susceptible for degradation mediated by ZTL in the cytoplasm (Wang *et al.*, 2010). In contrast, colocalisation of proteins can lead to the formation of functional complexes, such as the EC mentioned earlier. The activity of the EC might be modulated by the dynamics of ELF3 nuclear-cytoplasmic distribution (Herrero and Davis, 2012).

Therefore the circadian clock is a complex circuit made of multiple interlocked feedback loops regulated at many levels. Mathematical analysis has suggested that such complexity increases flexibility and enhances robust entrainment and temperature compensation (Rand *et al.*, 2006). Although the TTFLs are thought to be a central mechanism in various circadian systems, they are not always necessary to generate circadian rhythms. Indeed it was recently shown that non-transcriptional mechanisms are sufficient to sustain circadian rhythms in *Ostreococcus* and red blood cells (O'Neill and Reddy, 2011; O'Neill *et al.*, 2011a). Other mechanisms probably function in conjunction with TTFLs.

1.3.3 Connections between the clock and other networks

In diurnal and constant conditions, the clock can regulate the rhythmic expression of thousands of genes (Harmer *et al.*, 2000; Michael and McClung, 2003). Bioinformatics analysis revealed several motifs in the promoter regions of clock and output genes, associated with phase specific expression (Adams and Carre, 2011). These motifs include the morning and evening elements (ME and EE), and provide a mechanistic link between transcription factors, such as CCA1 and LHY, and clock-controlled genes. The mutation of such conserved sequences can alter rhythmicity; this was shown with the EE present in the *CCR2* (*COLD, CIRCADIAN RHYTHM, AND RNA BINDING 2*) promoter for example (Harmer *et al.*, 2000). *CCR2* is an output gene also known as *GRBP7* (GLYCINE-RICH RNA-BINDING PROTEIN 7). The EE is also implicated in the circadian regulation of the clock genes *TOC1*, *GI* and *ELF4* (Harmer and Kay, 2005).

The circadian clock is closely related to physiological processes such as growth and flowering. For instance the EC provides a link between the clock and the rhythmic growth of hypocotyls (figure 1.2): the EC directly binds to the promoters of the growth-related

transcription factors *PIF4* and *PIF5* (*PHYTOCHROME INTERACTING FACTORS*) (Nusinow *et al.*, 2011). The authors suggested that the EC has a key role in the circadian gating of hypocotyl growth in the early evening. A coordinated regulation by light and the clock explains the diurnal growth of hypocotyls (Nozue *et al.*, 2007). Photoperiodic flowering is another process that is coregulated by light and the clock. As mentioned in section 1.2.3, it is the coincidence between the circadian rhythms of CO, GI and FKF1 and exposure to light under long day that determines whether the regulatory proteins such as CO are stabilised to promote flowering (Andres and Coupland, 2012). Briefly, the light-dependent interaction between FKF1 and GI release the repression of *CO* mRNA transcription, allowing the translation of CO during long days. CO can then activate the transcription of *FT*, which is closely associated with flowering.

The circadian clock can also interact with many other networks, including responses to hormones (Robertson *et al.*, 2009), metabolic pathways (Kerwin *et al.*, 2011; Blasing *et al.*, 2005), cold signalling pathways (Eriksson and Webb, 2011), and solute transport (Dodd *et al.*, 2007; Haydon *et al.*, 2011). In addition, increasing evidence suggests that many signalling pathways can act as both inputs and outputs within the circadian network (Pruneda-Paz and Kay, 2010). For instance *CCA1* regulates expression of key genes involved in nitrogen assimilation; in turn, pulses of nitrogen can modify the phase of *CCA1* expression (Gutierrez *et al.*, 2008). Similarly, the abundance of calcium and cyclic adenosine diphosphate ribose (cADPR) is clock-regulated, and perturbation of these cycles alters circadian parameters (Dodd *et al.*, 2007).

Therefore, the circadian system is best described as a network. It acts as a signal integrator, interacting with many other signalling pathways to restrict plant responses to environmental stimuli to the most appropriate time of the day. In turn, these signalling pathways can feedback to affect clock functions (Harmer, 2009). The light-signalling pathway is one of these networks and its interaction with the clock is crucial for the proper entrainment of the circadian system.

1.4 Entrainment of circadian oscillators

As we have seen earlier, circadian rhythms do not always have a period of 24 h exactly. The FRP in constant conditions can be shorter or longer than 24 h. If the circadian system were not reset regularly, the endogenous rhythms would quickly lose synchrony with physical rhythms such as LD and temperature cycles. Consequently the clock could not provide an internal estimate of external environment time and would therefore lose its main function. In that context, entrainment is the most fundamental property of the clock to understand (Johnson *et al.*, 2003).

1.4.1 General concepts

Entrainment is not the equivalent of synchronisation. Synchronisation denotes the spontaneous expression of a common period by a population of coupled oscillators whereas entrainment is a special case of synchronisation in which it is possible to explicitly identify an oscillator that is driving another (Rapp, 1987). Certain authors consider that synchronisation also implies that the waveform of the driving rhythm coincides with the waveform of the driven rhythm (Johnson *et al.*, 2003). I will use in this thesis the more general definition of synchronisation mentioned above (1987). Entrainment also implies that a stable phase relationship is established between the entraining and entrained oscillations. In addition, after releasing the organism in constant conditions the entrained rhythm free runs with a phase determined by the zeitgeber cycle (Johnson *et al.*, 2003).

Most organisms live in a cyclic environment, with the possible exception of organisms dwelling in caves or deep in the ocean (Johnson *et al.*, 2003) and buried seeds (Millar, 2003). In nature, multiple environmental factors oscillate over the daily cycle, including light and darkness, temperature, humidity, food availability, and social cues. At least some of these factors can function as zeitgebers. The most consistent environmental time cue is the 24 h cycle of light and darkness (LD), and almost all circadian rhythms can be entrained to LD cycles (Johnson *et al.*, 2003). Temperature is another major zeitgeber, and other external factors such as feeding or sounds can also contribute to entrainment (Koukkari and Sothorn, 2006b).

Entrainment can occur by modulation of the period and/or phase of the biological rhythm so that its period conforms to the period of the environment. Light can influence both phase and period of circadian rhythms (Johnson *et al.*, 2003). Two different models have been proposed to explain circadian entrainment: the discrete model and the continuous model (Johnson *et al.*, 2004). The former focuses on the effects of environmental transitions such as dawn and dusk, and predict the entrainment on the basis of phase changes. The latter focuses on the importance of gradual changes in the environment and predicts the entrainment on the basis of period changes.

The entrainment behaviour of many organisms can be predicted by the discrete model, which uses the map of phase-dependent resetting called the Phase Response Curve (PRC) and the FRP to estimate entrainment characteristics. A PRC is a plot of phase shifts of a circadian rhythm as a function of the circadian phases at which the stimulus is given. One example of PRC for *Arabidopsis thaliana* is shown in figure 1.3. The observation of a PRC is universal for entrainment in all organisms, but the shape of the PRC varies greatly from one organism to the other (Johnson *et al.*, 2003). However, a characteristic feature of PRCs is that light has less phase resetting efficacy during the organism's subjective day than during its subjective night, as shown in figure 1.3. The shape of the PRC reflects the level of the state variables of the circadian system. The PRC can usually be broken down into three parts: phase advances, dead zone (during the subjective day) and phase delays. PRCs illustrate the fact that response to light (or other entraining stimuli) can be gated by the clock. Examples of gating at the molecular level are given in section 1.4.2.

The PRC only show the effect of a single stimulus on the phase, whereas entrainment results from regularly repeating perturbations (Roenneberg *et al.*, 2003). Nevertheless, if only two stimuli are given at appropriate times during each cycle, they can effectively act as a zeitgeber. For instance, most circadian clocks can entrain to skeleton photoperiods. A skeleton photoperiod is a LD cycle whose photophase consists only of brief photic stimulation at dawn and dusk (separated by a dark interval). In terms of entrainment of the clock, skeleton photoperiods mimic complete photoperiods quite well in some organisms and have provided a useful tool to chronobiologists (Johnson *et al.*, 2004). In *Arabidopsis* the shoot clock can be entrained by skeleton photoperiods (Millar, 2003) but at least 3 h of light per cycle was required to maintain normal plant development. An experiment

using skeleton photoperiods to investigate the entrainment of the clock in dark-grown roots will be presented in chapter 5.

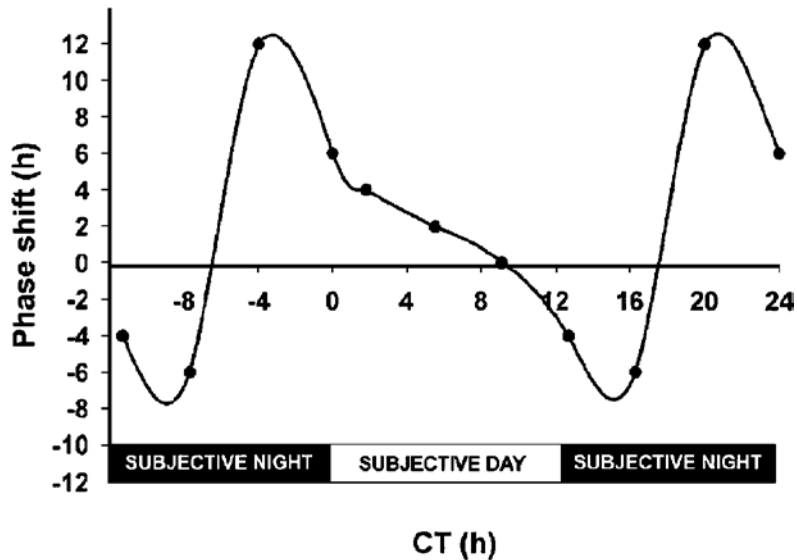


Figure 1.3: Phase response curve for *Arabidopsis thaliana*

Seedlings expressing a *CAB2:LUC* reporter were entrained for 6 days in LD cycles and then transferred to constant low fluence rate red light ($3 \mu\text{mol.m}^{-2}.\text{s}^{-1}$) for 5 days, during which the bioluminescence was monitored. At 4 h intervals after transfer to constant red light, successive batches of seedlings were given a light pulse (3 h of bright red light at $300 \mu\text{mol.m}^{-2}.\text{s}^{-1}$). The magnitudes of the resulting phase shifts were calculated as the difference between the mean phase of the rhythm in each batch of seedlings after the light pulse and the mean phase of the rhythm exhibited by control seedlings. Phase shifts are plotted against the circadian time (CT) of the pulse. Advances are plotted as positive values, and phase delays are plotted as negative values. From (Devlin and Kay, 2001)

Although circadian rhythms are entrained by cycles of 24 h in nature, they can also be entrained by cycles of different periods (T) in the laboratory. These non-24-h cycles are called “T cycles”. When an organism appears to entrain to several different T cycles with stable phase angles that are different and specific for each value of T, this is an excellent demonstration of entrainment (Johnson *et al.*, 2003). However, stable entrainment occurs within certain limits of T cycles. In *Arabidopsis*, rhythms were shown to be entrained by LD cycles in a range between T = 20 h and T = 32 h at least (Roden *et al.*, 2002). The

range of entrainment is the range of zeitgeber periods (T) to which an oscillator is able to entrain. This range depends partly on the type of oscillator: a rigid oscillator would have a narrow range of entrainment, whereas a weaker oscillator could be entrained by a broader range of T cycles (Abraham *et al.*, 2010). The range of entrainment also depends on the zeitgeber strength: the stronger the zeitgeber, the broader the range of entrainment. For instance Abraham *et al.* tested temperature cycles of various periods T on different clocks in mice³. They also used thermocycles with different amplitudes, from 1.5 to 8 °C changes in temperature. They showed that the supra chiasmatic nucleus (SCN) clock (considered as the master clock) in mice can entrain to T = 22 h Hot/Cold (HC) cycles with relatively strong zeitgeber (6 and 8 °C temperature variation) but not with weaker zeitgeber (1.5 °C and 4 °C temperature variation), whereas the lung clock can be entrained by any of these thermocycles. The lung clock is therefore more sensitive to temperature cycle entrainment than the SCN clock (Abraham *et al.*, 2010). T cycle experiments will be presented in chapter 5; they were used to compare entrainment properties of shoot and root clocks in *Arabidopsis*, using photocycles.

All entraining stimuli eventually alter the expression of some clock components, causing the necessary phase shift in the clock to synchronise the organism to the external cycle (Salome and McClung, 2005b). Light is the most studied zeitgeber in plants, so the rest of this section will mainly focus on the resetting of the clock by LD cycles. At the molecular level, this resetting is achieved through the modification of mRNA and/or protein and/or activity levels encoding one or more of the clock components.

1.4.2 Entrainment of the plant circadian clock by LD cycles

Plants can perceive light via photoreceptors. In *Arabidopsis* at least three families of photoreceptors are involved in the entrainment of the circadian clock: phytochromes (PHY), cryptochromes (CRY) and the blue light sensing LOV domain proteins.

These photoreceptors differ in their spectral and fluence sensitivity and in the response they trigger.

Phytochromes are red/far-red-light absorbing photoreceptors and in *Arabidopsis* there are 5 phytochromes, PHYA through PHYE. Amongst them PHYA and PHYB play the

³ The circadian clock is not necessarily the same in every cell; some organisms have different clocks in different organs. This will be discussed in section 6

predominant role in entrainment (Somers *et al.*, 1998a). In the dark PHYs are present in their inactive red-light-absorbing (Pr) form (Kozma-Bognar and Kaldi, 2008). After capturing a photon they are converted to the far-red-light-absorbing conformer (Pfr), which initiates downstream signalling events. The active Pfr form is converted to Pr by far red light. PHYA is the most sensitive and light-labile member of this family. PHY A can actually be activated by almost any wavelength of visible light, including blue light, but can be inactivated only by near infrared light. PHYB, D and E function redundantly as input photoreceptors in the high-fluence range of red light. The Pr forms are translocated to the nucleus where they form nuclear bodies (NB), which might represent multiprotein complexes in which PHYs interact with transcription factors (TFs) and other regulatory proteins to control the expression of light-induced genes (Kozma-Bognar and Kaldi, 2008).

The two other families are blue light photoreceptors (Christie and Briggs, 2001). The CRYs were first discovered in plants. They are also present in most eukaryotes and are implicated in the circadian clock of fruit fly and mouse. In insects as in plants, CRYs function as circadian photoreceptors that transduce blue light signals to the core oscillator, whereas the mammalian CRYs have essentially a light-independent function in the core feedback loop (Kozma-Bognar and Kaldi, 2008). Three LOV domain proteins are also involved in entrainment: ZTL, FKF1 and LKP2 (LOV KELCH PROTEIN 2) (Somers *et al.*, 2004; Schultz *et al.*, 2001; Nelson *et al.*, 2000). These three LOV domain proteins are believed to function by similar mechanisms and in a redundant fashion (Baudry *et al.*, 2010).

There are several mechanisms by which these photoreceptors transduce light signals to the clock. Some photoreceptors can directly interact with clock components. For instance ZTL interacts with GI in a blue-light dependent manner; this interaction confers rhythmicity to ZTL at the protein level although *ZTL* transcripts are expressed constitutively (Kim *et al.*, 2007). This interaction allows the accumulation of ZTL during the day and a rapid degradation of TOC1 at dusk through the F-box domain of ZTL (Mas *et al.*, 2003). A pulse of light after dusk would probably slow this degradation of TOC1, which might contribute to the phase delay observed in the PRC around dusk (figure 3.1).

Photoreceptors can also interact with light-signalling intermediates such as the PIFs. Following light perception PHYB translocates to the nucleus where it can interact with

PIFs which are bound to the promoters of light responsive genes including *CCA1* and *LHY* (Martinez-Garcia *et al.*, 2000). CONSTITUTIVELY PHOTOMORPHOGENIC 1 (COP1) is another light-signalling intermediate to the entrainment of the clock. COP1 interaction with the CRYs has been linked with the protein regulation of ELF3 and GI (Yu *et al.*, 2008).

Light can also regulate clock genes at the transcriptional level. As mentioned earlier, *CCA1* expression is induced by light whereas its mRNA is degraded under light (but is relatively stable in the dark). These two levels of regulation may be important to accurately entrain the circadian clock by allowing *CCA1* expression to peak at dawn (Yakir *et al.*, 2007). Light also activates the transcription of other clock genes, such as *LHY*, *PRR9* and *GI* (Salome and McClung, 2005b). In addition the translation of LHY can be upregulated by light, which would further increase the amplitude of LHY and contribute to the robustness of the clock (Kozma-Bognar and Kaldi, 2008; Kim *et al.*, 2003a).

These are a few examples that illustrate the complexity of light input pathways to the clock. Light can modulate the expression of several clock genes at many levels and at different time of the day. The response to light can be gated by the clock itself, since *PHYS* and *CRYs* transcription are clock regulated (Toth *et al.*, 2001; Hall *et al.*, 2001). A dark interval between each light cycle is also important for proper entrainment. In shoots the expression of thousands of genes can be entrained under LD cycles (Michael *et al.*, 2008).

1.4.3 Entrainment of the plant circadian clock by non-photic signals

Temperature is thought to be the second major zeitgeber in nature. The *Arabidopsis* clock can be entrained by temperature cycles of only 4 °C in amplitude, but the temperature-sensing mechanism is not known yet (McClung, 2011). Two clock components, *PPR7* and *PRR9*, appear to be necessary for entrainment within a certain range of temperature: the *prr7/prr9* double mutant cannot be entrained to 22/12 °C thermocycles (Salome and McClung, 2005a). Other plants can also entrain to temperature cycles with sometimes remarkable sensitivity: temperature steps as small as 0.5 °C can entrain the clock of the plant *Kalanchoe* (Rensing and Ruoff, 2002). The authors of this study argued that the efficacy of temperature as an entraining agent in nature - even in homeotherms - has been under-appreciated.

Microarray analysis revealed that thermocycles alone can drive at least half of all transcripts critical for synchronising internal processes such as the cell cycle and protein synthesis (Michael *et al.*, 2008). This study analysed transcriptome data of *Arabidopsis* plants grown under different environmental conditions, including photocycles. The rhythmic transcripts do not necessarily overlap between temperature and LD cycle conditions. An earlier study already showed that some genes respond preferably to thermocycles versus photocycles (e.g. *CAB2*) whereas others respond preferably to photocycles versus thermocycles (e.g. *CAT3*) (Michael *et al.*, 2003). This was demonstrated using conflicting zeitgebers: LD and temperature cycles were in antiphase so that light and dark cycles coincided with cold and hot cycles respectively. Other genes, such as *CCA1*, *LHY* and *TOC1*, can be entrained by thermocycles or photocycles and with the same phase of expression (Salome and McClung, 2005b). However these three core clock genes did not show acute induction or repression at temperature steps, suggesting that temperature might entrain the clock at the post-transcriptional level.

Factors other than light and temperature might contribute to the entrainment of the clock by modulating the expression of clock genes: hormones, including auxin, abscisic acid and cytokinin (Robertson *et al.*, 2009; Legnaioli *et al.*, 2009; Seung *et al.*, 2012), and solutes such as sucrose, nitrogen and calcium (Haydon *et al.*, 2011; Blasing *et al.*, 2005; Gutierrez *et al.*, 2008; Dodd *et al.*, 2007). For instance sucrose or other photosynthates are thought to entrain the clock of dark-grown roots under constant temperature (James *et al.*, 2008). In conclusion it is possible that several non-photoc mechanisms contribute to entrainment.

1.5 Modelling the plant circadian clock

There are many definitions for the word “model”, and even in a scientific context this word can have different meanings, from simple diagrams to complex equations. Indeed the diagram presented in figure 1.2 can be considered as a model. However, given the complexity of the circadian system introduced earlier, the dynamic behaviour of the clock would be hard to understand without mathematical models. There are many types of mathematical models, including Ordinary Differential Equations (ODE) models.

Compared to a diagrammatic model, an ODE model is a detailed translation of all the model's inherent steps into differential equations which describe the changes in all factors over time (Roenneberg *et al.*, 2008). Therefore mathematical models can incorporate detailed dynamics of sets of biochemical interactions. They have been used to summarise experimental data, to infer new relations from experimental data, guiding the researcher to new testable hypothesis and to find properties of the system that are hard to measure directly. If successful the model chosen should not only fit the existing data and but also give new biological insights on a system (Ay and Arnosti, 2011). Mathematical models present the opportunity to derive specific, sometimes non-intuitive, predictions and also to carry out critical testing. Simulations will reveal whether the mathematical model is capable of reproducing the observed phenomena (Beersma, 2005).

The rest of this section will focus on the ODE models of the plant circadian clock: the Locke *et al.* and the Pokhilko *et al.* models (Locke *et al.*, 2005a; Locke *et al.*, 2005b; Locke *et al.*, 2006; Pokhilko *et al.*, 2010; Pokhilko *et al.*, 2012). They will be referred hereafter as the L2005a, L2005b, L2006, P2010 and P2012 models respectively. Their differential equations represent biological events such as transcription, translation, protein transport and degradation. These models were mainly based on known genetic interactions, but also incorporated unknown components and tested new types of connexions. Michaelis-Menten kinetics was used to describe enzyme-mediated degradation of proteins, and Hill functions were used to describe activation and repression of transcription. The number of equations and parameters increased progressively, and more data were described and used to constrain parameters in newer versions of the clock models. *LHY* and *CCA1*, which have redundant functions, were always treated as a single component. The acute light response in activation of *PRR9*, *LHY/CCA1* and *GI* transcription was modelled using a light-sensing activator (protein P) which accumulates in darkness and is degraded in the light. The L2006, P2010 and P2012 models were used in this thesis to simulate clock gene expression in shoots and roots (chapter 7).

1.5.1 The Locke *et al* models

From the molecular loop identified in the *Arabidopsis* circadian clock (Alabadi *et al*, 2001), the first mathematical model was proposed in 2005 by Locke *et al.* A single feedback loop between *LHY/CCA1* and *TOC1* was sufficient to generate robust 24 h oscillations (Locke *et al.*, 2005a). It included a hypothetical component *X* as an

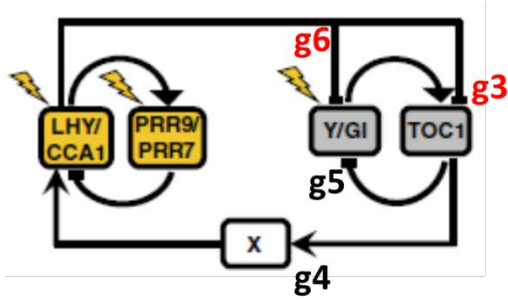
intermediate activator between *TOC1* and *LHY/CCA1* to simulate the ~12 h delay observed experimentally between *TOC1* expression and *LHY/CCA1* induction.

As for many biological systems, the data available for parameter fitting was noisy and varied. That is why a cost function was constructed to quantify the agreement between the model and key experimental features. The cost function was a sum of five terms that quantify the agreement between the model and qualitative experimental features: period in LD cycles, in DD cycles, phase, broadness of *LHY* mRNA peak and amplitude. This cost function, together with a global search of parameter space allowed identification of an optimal set of parameter values. A significant advantage of this approach is that it can show that a gene network is inconsistent with experimental data because its circuit is incorrect, not due to a poor choice of parameter values. Similar cost functions and global parameter optimisation were used for the L2005b and L2006 models.

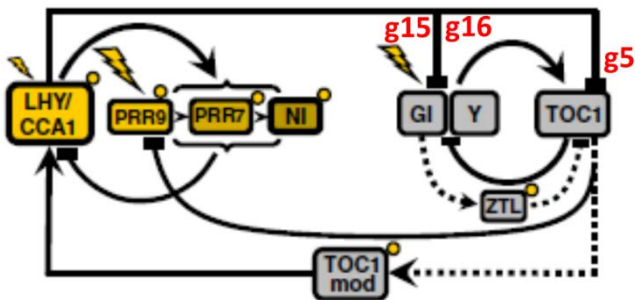
But the L2005a model failed to account for significant experimental data, such as rhythms observed in *cca1/lhy* plants. In 2005 other genes were known to play a role in the clock but they had not been located relative to the *LHY/CCA1* - *TOC1* loop. Therefore, an interlocked feedback loop network capable of oscillation in this double mutant was developed (Locke *et al.*, 2005b) and another hypothetical component (*Y*) was added. It activated *TOC1*, which in turn repressed *Y*, forming a second loop. This evening loop was retained in the L2006 model (figure 1.4.A). *TOC1* still activated *LHY* through *X*, and light input occurred via activation of *Y* and *LHY*. This model fitted not only the data specified in the parameter optimization, but also other experimental results.

To identify *Y*, transcript abundance of clock-affecting genes with peak mRNA levels in the evening in both wild type (WT) and *cca1/lhy* double mutant seedlings were analysed. *GI* mRNA levels fitted very well to the predicted *Y* profiles in WT and mutants. Moreover the *GI* promoter also includes an Evening Element (EE), the putative binding site for *LHY* acting as an inhibitor.

A. L2006



B. P2010



C. P2012

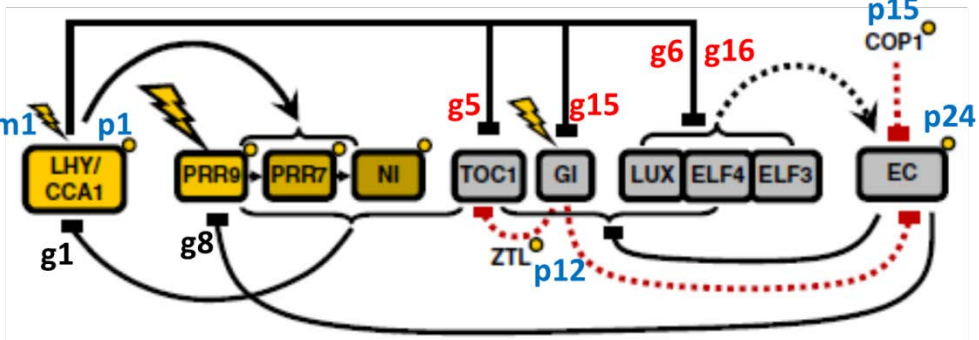


Figure 1.4: Diagrammatic representation for the last three ODE models of the *Arabidopsis* circadian clock

The main elements - especially genes (boxed), transcriptional regulation (solid lines) and the location of light inputs (flashes) are shown. Elements of the morning and evening loops are in yellow and grey boxes respectively. The locations of parameters that will be modified in chapter 7 are also shown: the parameters in red represent constants of inhibition by LHY/CCA1 (e.g. g16), the parameters in blue are some of the parameters directly related to light inputs (e.g. m1), and some other parameters are in black (e.g. g1).

- A. L2006 model (Locke *et al.*, 2006). X and Y are unknown components
 - B. P2010 model (Pokhilko *et al.*, 2010). Proteins are shown only for ZTL, LHY (LHYmod) and TOC1 modified (TOC1mod). Posttranslational regulation is shown by dashed arrows.
 - C. P2012 model (Pokhilko *et al.*, 2012). Proteins are shown only for the EC, ZTL and COP1. The EC protein complex is denoted by a dashed black line. Posttranslational regulation of TOC1 and EC by GI, ZTL and COP1 are shown by red dashed lines. Posttranslational regulation by light (or dark) is shown by small yellow circles.
- Diagrams adapted from Pokhilko *et al.* (2010 and 2012).

Importantly, mathematical models can produce quantitative predictions of dynamic processes that allow detailed experimental design. For instance, the acute light activation of *Y* in WT was predicted to be very transient (just after dawn), allowing targeting tissue sampling to the appropriate interval, whereas conventional sampling had obscured this induction of *GI*. The L2005b model highlighted the importance of *GI* as a component of light input to the clock.

A further study presented evidence that *GI* acts with *TOC1* in the feedback loop of the circadian clock (Locke *et al.*, 2006). This was an advance in systems biology because *GI* was identified as a candidate gene using experiments based directly on predictions from mathematical modelling. The L2006 model was extended to include a third loop between *PRR7/PRR9* and *CCA1/LHY* (figure 1.4.A). This three loop network consisted of morning and evening oscillators coupled intracellularly. It accounted for additional experimental data, especially the rhythmic *toc1* mutant allele, and allowed tracking of dawn and dusk. A very similar structure was proposed simultaneously by Zeilinger *et al.* (2006). The two models differ slightly in light induction of *Y* and *LHY/CCA1*, and in the details of the morning loop mechanism.

These models were not yet complete, as they did not incorporate known clock-affecting genes such as *PRR5*, *ELF4* and *LUX*. However, even incomplete mathematical models can be useful in providing a framework to understand the existing experimental results, in focusing future experimental work on key regulatory interactions that reveal the location of additional genes within the network and in informing the detailed design of these experiments (Locke *et al.*, 2006). The L2006 model was used to identify *GI* as a mediator for long-term response of the shoot clock to sucrose (Dalchau *et al.*, 2011).

1.5.2 The P2010 model

Although most of the L2006 model structure remained in the P2010 models, it was refined and other components and connections were added to this later version of the clock model (figure 1.4.B). Besides, some post transcriptional and post-translational regulations were integrated in the P2010 model. For instance, the unknown component *X* used in previous models was replaced by a modified *TOC1* protein, which represented a post-translational

modification or complex dependent on TOC1 protein, based on the fact that TOC1 can bind to protein complexes at the *CCA1* promoter (Pruneda-Paz *et al.*, 2009).

The other unknown component, *Y*, remained but it was distinguished from *GI*. Indeed *GI* did not perform all the function of *Y* (Locke *et al.*, 2005b). *Y* was still a direct activator of *TOC1* whereas *GI* became an indirect activator; the direct activation of *TOC1* by *GI* (partly represented by *Y* in the L2006 model) was removed because of the high levels of *TOC1* observed in *gi* mutants. In addition *ZTL* was explicitly added to the model. Indeed *ZTL* is necessary for the targeting of TOC1 protein degradation by the proteasome (Mas *et al.*, 2003). The model described the stabilisation of *ZTL* at the post-translational level by *GI* protein and the acceleration of TOC1 protein degradation by *ZTL* (Kim *et al.*, 2007). This caused an unexpected, indirect activation of TOC1 expression, consistent with the 2.5-fold increase of mean *TOC1:LUC* expression observed in *lhy/cca1* compared with *lhy/cca1/gi* (Locke *et al.*, 2006).

PRR9/7, also modelled as only one component in the L2006 model, was split into two components in the P2010 model: *PRR9* and *PRR7*. Another component was introduced in the “morning loop”: the night inhibitor (*NI*). This has an important function in controlling the phase of morning gene expression in the P2010 model. Experimentally, *PRR5* together with *PRR7* and *PRR9* is important for the regulation of *LHY* and *CCA1* (Farre *et al.*, 2005; Nakamichi *et al.*, 2005; Nakamichi *et al.*, 2010). New data on the *prr5/7* mutant showed a good match to the model, supporting the idea that *PRR5* is an essential part of the *NI*. The regulation of *LHY/CCA1* expression by a wave of inhibitors (*PRR9*, then *PRR7* and *NI/PRR5*) allowed dawn and dusk sensitivity, and the morning loop responded to changing photoperiod, contrary to the L2006 model.

An inhibition of *PRR9* expression by TOC1 was introduced because overexpression of TOC1 was shown to reduce *PRR9* mRNA to a negligible level (Matsushika *et al.*, 2002; Ito *et al.*, 2005). The model also matched the low level of *PRR9* in LL because the acute induction of *PRR9* at light-on does not occur in these conditions

Compared to previous models, some parameter values (35 out of 90) were constrained with experimental data. The remaining parameters were fitted to two types of data: the quantitative profiles of clock components, and values of FRPs in WT and mutants under

varying environmental conditions. Compared to previous models, the P2010 model matched more data in varying environments and mutants. In addition, the distinction between *PRR9*, *PRR7* and *NI/PRR5* and their modulation by light increased the flexibility of entrainment and the robustness of the present model to parameter changes compared with the L2006 model.

The P2010 model was used and modified by Guerriero and colleagues to introduce stochasticity in the model (Guerriero *et al.*, 2012). This allowed explanation of the dampening of rhythms observed experimentally in plants under LL.

1.5.3 The P2012 model

Compared to the other updates of the clock model, the P2012 model also kept some features of the previous versions but introduced more significant changes. The morning loop between *LHY/CCA1* and the *PRRs* has been maintained, and *LHY/CCA1* still represses evening genes in the P2012 model. As in the P2010 model, *PRR9* is repressed by an evening component, but this repression is now achieved by the Evening Complex (EC). The EC has been integrated in the model in accordance with recent experimental data. Three proteins form this complex: *ELF3*, *ELF4* and *LUX*. These were shown to form a complex and bind to the promoter of target genes (Nusinow *et al.*, 2011), including *PRR9* and *LUX* (Dixon *et al.*, 2011; Helfer *et al.*, 2011). *ELF3*, *ELF4* and *LUX* mutations caused striking, arrhythmic phenotypes (Hicks *et al.*, 1996; Covington *et al.*, 2001; Doyle *et al.*, 2002; Hazen *et al.*, 2005) so they were already suspected to operate in the clock machinery. But they were not integrated in previous models because their functions were unclear.

The post-translational regulation of *ELF3* by *COP1* (Yu *et al.*, 2008) was also added to the model. *ELF3* protein was also connected to *GI*, via the EC, based on experimental data (Yu *et al.*, 2008) and the assumption that *GI* can accelerate the destruction of the EC by bringing F box proteins into its vicinity. In turn, the EC was assumed to repress the expression of *GI* and the four other evening genes *TOC1*, *ELF3*, *ELF4* and *LUX*. This assumption was based on experimental data showing that the expression of the 5 evening genes was derepressed in *elf3*, *elf4* and *lux* mutants (Fowler *et al.*, 1999; Kikis *et al.*, 2005; Kolmos *et al.*, 2009; Dixon *et al.*, 2011; Helfer *et al.*, 2011).

Another significant modification compared to previous models was the connection between *TOC1* and *LHY/CCA1*. *TOC1* was previously thought to be an activator of these morning genes based on genetic data (Alabadi *et al.*, 2001). The role of *TOC1* as a repressor was already suggested in 2002 (Matsushika *et al.*, 2002). In addition, timeseries data on the *ztl* and *prr7/9* mutants were most consistent with *TOC1* being an inhibitor instead of an activator of *LHY* and *CCA1* (Pokhilko *et al.*, 2012). The authors also presented new data with *toc1* mutant and *TOC1-ox* plants that further supported the negative role of *TOC1* in regulation of *LHY/CCA1*. Moreover, two other papers showing that *TOC1* acts as a repressor were published a few months apart (Gendron *et al.*, 2012; Huang *et al.*, 2012).

The structure of the P2012 model includes the repressilator, i.e. the three inhibitor ring oscillator that was also recently found in the mammalian clock (Hogenesch and Ueda, 2011). In plants this repressilator includes the *EC*, *LHY/CCA1* and the *PRR* genes: in the late night the *EC* is inhibited by the rise of *LHY/CCA1*; these morning genes are then inhibited by the *PRRs* during the day, and the *PRRs* are inhibited by the *EC* in the early night. This new structure allows re-interpreting previous observations: for instance the previously suggested activation of *LHY* and *CCA1* by *EC* genes can now be explained by a double repression via the *PRRs*.

Multiple light inputs affect the kinetics of the system. Many of them were already present in the P2010 model. Others were added together with the *EC*: this complex is regulated by light through the light-regulation of *COP1*. The model provides an explanation for the different response to short light pulses at various times of the day (the PRC). Simulations with the P2012 suggest that the PRC is mostly determined by the acute light response in *LHY/CCA1* expression. Such activation results in phase delay or phase advance depending on the time the light pulse is given.

Compared to previous models, the P2012 model explains more experimental data from WT and mutant plants in various environmental conditions. But like any other model it has some limitations. For instance the identity of the “protein P” used to simulate the acute induction of several clock gene expression by light is still not known. Although the light intensity can be modulated for simulations, the model does not distinguish between different light qualities. Other inputs than light, such as temperature, are not included in the

model. More generally, other clock components and mechanisms of regulation need to be integrated. Finally it is assumed that the clock is identical in every cell of the plant, although increasing evidence suggests tissue and organ specificity. This last point is the object of the next section.

1.6 From cell autonomous rhythms to organ specific clocks

It has been generally assumed that all plant cells contain autonomous clocks (Harmer, 2009). Rhythms were recently observed at the cellular level in plants (Yakir *et al.*, 2011) and an intact plant is not necessary for rhythms to persist. For instance circadian gene expression could be observed in suspension cell cultures and calli (Nakamichi *et al.*, 2003; Sai and Johnson, 1999; Kim *et al.*, 2003b; Wilkins and Holowins, 1965) and in excised organs (Hall *et al.*, 2001; Thain *et al.*, 2002). Although rhythms have not been observed in isolated cells in plants yet, cell-autonomous rhythms are found in single cells from various branches of life, from the simplest to the most complex organisms. The clock in the cyanobacterium *Synechococcus* exerts a pervasive control over cellular processes including global gene expression and the regulation of nitrogen fixation so that it is maximal in the night phase (Johnson *et al.*, 2011). In *Ostreococcus tauri*, most of the biological processes appear to be rhythmically regulated at the transcriptional level (Pfeuty *et al.*, 2012). Persistent circadian rhythms can also be observed in single cells from mammals, such as fibroblasts (Nagoshi *et al.*, 2004) and in red blood cells (O'Neill and Reddy, 2011).

Although cell autonomous rhythms are found in various multicellular organisms, the complexity of circadian outputs is thought to be an emergent property of intercellular interactions in animals (Bell-Pedersen *et al.*, 2005). In mammals, a master clock is located in the SCN and synchronises the peripheral clocks of different organs (Richards and Gumz, 2012). Rhythms can also be observed in most if not all plant tissues. However, the intracellular clocks of different organs have been considered independent in plants. Thain *et al.* showed that the expression of the same gene (*CAB* or *CHS*) could be set at different phases in different organs and tissues of a single plant, by applying different LD treatments to restricted tissue areas in *Arabidopsis* and tobacco (Thain *et al.*, 2000).

In the same intact plant rhythms with different FRP can coexist under constant conditions, supporting the idea of autonomous and independent circadian systems in plant cells, but suggesting that these oscillators may differ between cells or tissues. Leaf movement rhythms have a longer FRP than rhythms in stomatal conductance, photosynthesis or expression of the *CAB2* gene (Millar *et al.*, 1995b; Somers *et al.*, 1998b). Stomatal conductance and carbon assimilation also have different FRP under LL (Dodd *et al.*, 2004). *CHS* expression is similar in epidermal tissues of shoots and light-grown roots, but its period differs from that of *CAB* expression in shoots under LL (Thain *et al.*, 2000; Thain *et al.*, 2002). As the different FRP mentioned above were observed in outputs that are primarily generated by different cell types, the variation may be due to different clock composition between cells rather than distinct clock mechanisms existing within a single cell. Several studies support this idea. *PRR3* is thought to modulate clock functions and is expressed most strongly in the vasculature (Para *et al.*, 2007). In *prp3* plants, genes with widespread expression patterns have a modest short period phenotype, whereas a stronger phenotype is seen for genes preferentially expressed in the vasculature. This supports the idea that *PRR3* acts primarily in that tissue (Para *et al.*, 2007). More recently, Yakir *et al.* monitored rhythms at the cellular level and showed that stomatal guard cells have a different FRP from surrounding epidermal and mesophyll leaf cells (Yakir *et al.*, 2011). However the authors showed that many clock genes were rhythmically expressed in guard-cell enriched extracts as well as in the whole leaf, although their expression profiles may be cell or tissue specific.

In many circadian mutants, multiple clock outputs are affected in a similar manner (Dodd *et al.*, 2004; Para *et al.*, 2007; Thain *et al.*, 2002; Hall *et al.*, 2002). This suggests that the clocks driving rhythmicity in diverse cell types are fundamentally similar, sharing many components but exhibiting some biochemical differences (Harmer, 2009). An example illustrating this idea is the differential effects of the *toc1* mutations on the rhythms of *CAB2* expression and cytosolic free calcium ($[Ca^{2+}]_{cyt}$) (Hotta *et al.*, 2008). The *toc1-2* mutation results in a truncated protein, whereas the mutant allele *toc1-1* leads to a full protein that has an amino acid change in the CCT domain (CONSTANS, CONSTANS-LIKE and TOC1). In the *toc1-2* mutant, the FRP of both *CAB2* expression and $[Ca^{2+}]_{cyt}$ were similar and shorter compared to the wild type, but the *toc1-1* mutation only affected the FRP of *CAB2*. The authors suggested that in the *toc1-1* mutant, the mutation on the CCT domain of TOC1 impaired its interaction with other proteins in a cell-specific

manner, resulting in a shorter FRP of *CAB2* expression in mesophyll and epidermis cells but without affecting the rhythms of $[Ca^{2+}]_{cyt}$ in other cell types.

Different output rhythms are also observed in different organs of animals, such as *Drosophila* and mammals, but the clock components are thought to be shared between the cells of the same organism (Allada and Chung, 2010; Richards and Gumz, 2012). In *Drosophila*, the same *PER*-based clock is found in peripheral and brain clocks, and can be directly synchronised to LD cycles in these various organs. The different rhythms observed in *Drosophila* may be due to tissue-specific control of circadian outputs (Allada and Chung, 2010). In mammals, tissues that are not exposed to light are entrained by other inputs, such as feeding cues, and display different rhythms compared to the SCN clock (Richards and Gumz, 2012). Similarly, the various rhythms observed in plants might be due to differences in input or output pathways within the circadian systems of different cells or tissues. For instance rhythmic output genes are differentially regulated by light and temperature cycles (Michael *et al.*, 2003; Michael *et al.*, 2008), but most if not all clock genes are rhythmic in both conditions (photo- and thermocycles). In the dark-grown roots of plants under LL, many less genes are rhythmic compared to shoots (James *et al.*, 2008). Nevertheless one would expect that at least the same clock genes are rhythmic in shoots and roots of WT plants.

Our laboratory has studied mature, hydroponically grown *Arabidopsis* plants and showed that clock gene expression differed markedly between roots and shoots (James *et al.*, 2008). In constant conditions, only the morning loop (*CCA1/LHY* and *PRR7/9*) was rhythmic in roots, and the period was longer in roots compared to shoots. Although *TOC1* transcripts oscillated in both shoots and roots under LD cycles, its rhythm was not detected at the mRNA level in roots under LL. A similar behaviour was observed for other evening genes implicated in the shoot clock: *GI*, *LUX*, *ELF3* and *ELF4*. In addition, TOC1 protein did not seem to oscillate in roots under LL, whereas the levels of LHY protein were rhythmic under the same conditions. Furthermore, the *toc1-10* mutation did not shorten the FRP of *LHY* mRNA in dark-grown roots, contrary to data for the shoots. This suggested that *TOC1* was not part of the root core clock.

In the shoot clock model *TOC1* and *GI* are repressed by LHY/CCA1 (Pokhilko *et al.*, 2012) and these repressions are thought to be mediated via binding of LHY and/or CCA1

to the EEs present in the promoters of *TOC1* and *GI*. Indeed EEs are necessary and sufficient to confer evening-phased circadian regulation, and CCA1 and LHY are likely to act as repressors via the EE (Harmer and Kay, 2005). However EE-binding complexes containing LHY could be detected in shoots but not in roots (James *et al.*, 2008). The authors suggested that the morning and evening loops found in the shoot clock are disengaged in the root clock because CCA1 and LHY would be unable to inhibit gene expression in roots. In addition microarray data showed that fewer genes display rhythmicity in roots than in shoots, 3.2% and 13.7% respectively. Notably for output genes regulated by EE and expressed both in shoots and roots, such as *CCR2* and *CHS*, the transcript abundance in LL was rhythmic only in shoots, not in roots (James *et al.*, 2008). Moreover the genes that were rhythmically expressed in roots had a longer FRP compared to shoots, consistent with the long FRP observed in the morning loop in roots. For instance *RVE1* and *RVE8* peaks of expression were delayed in roots relative to shoots, consistent with control by the root specific clock. Interestingly, one phosphoenolpyruvate carboxylase kinase gene (*PPCK*) in soybean is under robust circadian control in shoots but not in roots, and its promoter contains a sequence very similar to the EE found in *Arabidopsis* evening genes (Sullivan *et al.*, 2004).

However under LD conditions and constant temperature, transcript levels of most if not all clock genes oscillated in roots and were in phase with shoots in *Arabidopsis* (James *et al.*, 2008). In addition the abundances of LHY, CCA1 and TOC1 proteins closely followed the transcript abundances. The rhythms in dark-grown roots under LD and constant temperature were therefore thought to be synchronized by a signal from the shoots (James *et al.*, 2008). The authors reasoned that this signal might be related to photosynthesis, such as the diurnal fluctuations in the supply of carbohydrate to the roots. Indeed sugar metabolism strongly influences cycling gene expression (Blasing *et al.*, 2005). Addition of sucrose in the medium at dusk in LD resulted in an expression pattern like that observed in LL: it extended the next expression of *CCA1* and *PRR9* in roots but not in shoots, but it did not affect the expression of *TOC1* in roots (James *et al.*, 2008). Furthermore, DCMU, a specific inhibitor of photosynthetic electron transport, progressively disrupted operation of the root clock.

Therefore, the plant circadian clock appeared to be organ specific, but not organ autonomous (James *et al.*, 2008). The root clock seemed to be a simplified version of the

shoot clock, with only the morning loop running in dark-grown roots of WT plants. However, the expression of evening clock genes such as *TOC1* regained rhythmicity in the *prp7/9* double mutant under LL (James *et al.*, 2008), suggesting that the root clock may be more complex than a simple loop between *CCA1/LHY* and *PRR7/9*. The structure of the root clock had to be further investigated. In addition the mechanism of root clock entrainment remained unclear.

1.7 Aims and outline of the work

The general aim of my project was to add organ specificity to the plant circadian clock model. This work focused on the root circadian clock in *Arabidopsis thaliana*, its differences and similarities with the shoot clock, and the synchronisation of the two organs under diurnal conditions. Both experimental and theoretical approaches were used and focused on the transcriptional level of regulation.

In order to obtain more data of clock gene expression I developed an imaging system to monitor rhythms in both shoots and roots simultaneously. Similar systems already existed but with plants usually grown on media containing sucrose, and with their roots exposed to light. I optimised an automated protocol to image plants in more physiological conditions (chapter 3).

Our lab showed that the root clock was a simplified slave version of the shoot clock in *Arabidopsis*. They used mature plants grown in hydroponic solution in black boxes so the roots were kept in the dark (James *et al.*, 2008). One could wonder whether the differences observed between shoot and root clocks were simply due to the different light conditions experienced by these two organs. To address this question I used the same experimental set up as James and colleagues except that I exposed the roots to the same light conditions as shoots. I optimised a RT-qPCR protocol used in our lab, which allowed me to better compare the amplitudes of rhythms in shoots and roots as well as their periods. I performed similar experiments using imaging, i.e. with light-grown roots and dark-grown roots as a control. To investigate the possible effects of light on the root clock I illuminated the roots with either white light, or red and/or blue light; I also carried out experiments in constant

darkness. I compared the rhythms of several clock and output genes expression in both shoots and roots under these different light and dark conditions (chapter 4).

To investigate the entrainment of the root clock, plants were imaged under various light and dark conditions. These included LD 12/12 cycles preceding or following LL conditions, conflicting LD cycles, T cycles and skeleton photoperiods. Some plants were decapitated to study the entrainment of excised roots. The entrainment of the root clock by temperature cycles was also addressed (chapter 5).

Preliminary studies on the *cca/lhy* double mutant and the *toc1* and *ztl* single mutants were carried out. Together with other results, they could provide information on the role of these genes in the root clock, and the possible differences with the shoot clock (chapter 6).

In parallel with the experiments mentioned above, three mathematical models of the shoot clock were modified to fit the root clock data. The Circadian Modelling software was first used to simulate the qualitative differences between shoot and root clocks. Then global parameter optimisations were performed with the Systems Biology Software Infrastructure (SBSI). Simulations were then done with COPASI, using different sets of parameters in various conditions, and compared to clock gene expression profiles in roots (chapter 7).

Based on an increasing number of root data that I obtained in various conditions during my PhD, I progressively modified the most recent versions of the mathematical models in order to better understand the differences and similarities between shoot and root clocks.

2 Materials and Methods

The experimental data were obtained using two different methods, RT-qPCR or imaging. The protocols were specific for each method, from the media used to the data collection. A notable difference was the culture conditions: RT-qPCR data came from plants grown in hydroponic culture, whereas imaging data were obtained with plants grown on agar plates. The two methods will be referred as “hydroponic system” and “imaging system” hereafter. Both systems were optimised, from the plant growth conditions (including the media used) to the data analysis. The development of the imaging system is described in chapter 3, and only the optimised protocol is summarised in this chapter. The protocol for the hydroponic system and changes to the method used in the lab earlier (James *et al.*, 2008) are identified. Material and methods common to both systems are presented in sections 2.1 and 2.4. Finally the methods used for modelling are presented in section 2.5. All the chemicals were from Sigma unless stated otherwise.

2.1 Seeds

2.1.1 Seed stock

Different types of *Arabidopsis thaliana* were used depending on the systems. For the hydroponic system, the Col-0 Wild-Type (WT) was used, as in (James *et al.*, 2008).

For imaging experiments, several [*clock gene promoter*]:*LUC*⁺ (luciferase) fusions were used. They were in the Ws (Wassilewskija) Wild-Type (WT) background unless stated otherwise. The seeds with the following constructs were gifts from Andrew Millar and used in previous publications: *CCA1:LUC*⁺, *TOC1:LUC*⁺, *PRR9:LUC*⁺, *CCR2:LUC*⁺ and *CAT3:LUC*⁺

(Doyle *et al.*, 2002; Edwards *et al.*, 2010; Kim *et al.*, 2008; McWatters *et al.*, 2007). Seeds with the *GI:LUC*⁺ were also gifts from Andrew Millar. The *toc1-4* and *ztl-105* mutants with the *CCR2:LUC*⁺ construct were in Col-0 background and were gifts from Karen Halliday. The *cca1-11 lhy-21* double mutant with the *CCR2:LUC*⁺ construct was from the Nottingham *Arabidopsis* Stock Centre (reference N9809). Seeds with the *PRR7:LUC*⁺ and the *RVE1:LUC*⁺ construct were both in the Col-0 WT background; these seeds came from

Rob McClung's and Stacey Harmer's lab respectively (Rawat *et al.*, 2009; Salome and McClung, 2005a).

These seeds were first sown on soils with 0.2 g/L of Intercept (Bayer) and grown under LL and constant temperature (20°C) for bulking up. When plants started flowering the Arasystem (<http://www.arasystem.com/>) was used for each individual to avoid cross-fertilisation, seed contamination and spreading of seeds. Once the plants were dried the seeds were harvested and stored in darkness.

2.1.2 Seed surface sterilisation and stratification

Before starting any experiment seeds were surface sterilised. They were first washed with 70% ethanol for 1-2 min, and then sterilised for ~10 min with a solution containing 2-3% bleach and 0.1% tween 20. Finally they were rinsed 3 times with sterile water. After this surface sterilisation, the seeds were stratified for 2-4 days at 4 °C before sowing.

2.2 Hydroponic system

Initially the method of James *et al.* (2008) was used (section 4.2). Subsequently an optimised protocol was used for the other experiments presented in this thesis. The optimised protocol is presented below, and the differences (if any) with the previous protocol (James *et al.*, 2008) are in italics at the end of each subsection.

2.2.1 Media

The hydroponic solution contained the macro- and micronutrients presented in Table 2.1. Stock solutions were first prepared and autoclaved. These were then diluted in distilled water and the pH was adjusted to 5.7 with 1M NaOH. This solution was not autoclaved.

The same solution was used to prepare sterile solid medium used to grow plants for the first 10-12 days (cf. below). 0.7 % agar was added to the hydroponic solution described above, and then autoclaved before pouring in 1.5 mL eppendorf tubes.

Table 2.1: Nutrients and their final concentrations used in the hydroponic solution

Macronutrients	Final concentration (mM)	Micronutrients	Final concentration (μM)
KNO_3	1.25	CuSO_4	0.16
$\text{Ca}(\text{NO}_2)$	0.5	ZnSO_4	0.38
MgSO_4	0.5	MnSO_4	1.8
FeNaEDTA	0.0425	H_3BO_3	45
KH_2PO_4	0.625	$(\text{NH}_4)_6\text{Mo}_7\text{O}_{24}$	0.015
NaCl	2	CoCl_2	0.01

2.2.2 Seed sowing and plant transfer

Seeds were sown on 1.5 mL eppendorf tubes filled with solid medium (detailed above). The tips of these tubes were cut so that roots could later grow through. About 10 days after germination (before the roots reached the bottom of the tubes), plants were transferred to boxes containing the hydroponic solution. These boxes were covered with black tape to keep the roots in the dark, except for the experiment with light-grown roots where transparent boxes were used (figure 2.1). These boxes contained a hydroponic solution (table 2.1) that was replaced after ~ 10 days (i.e. about a week before harvesting).

**Figure 2.1: Two types of boxes used for the hydroponic cultures**

The black box (left) was used for dark-grown roots, and the transparent box (right) was used for light-grown roots. The same black lid was used for both boxes. It has 13 holes where 1.5 mL eppendorf tubes can be placed (each tube containing one plant). If less than 13 plants were used per box, the remaining holes were plugged with corks (as in the picture) or black tape. For light-grown roots extra lights were used at the bottom of the growth cabinet to have even light on shoots and roots.

Differences: The rubber corks shown in figure 2.1 were replaced by black tape. Every black box used was checked and retaped if necessary to make sure it was “light-tight”. This is because light (even at very low levels) turned out to have a significant effect on the root clock (see chapters 4 and 5). Note that boxes cannot be perfectly light-tight: some light can penetrate into the boxes at least through the eppendorf tubes (visible on the right-hand side box in figure 2.1).

2.2.3 Entraining conditions

All plants were first entrained in 12 h white light ($110\text{-}130 \mu\text{mol.m}^{-2}.\text{s}^{-1}$):12 h dark (referred as LD) for about 4 weeks. The growth cabinet was temperature and humidity controlled. The humidity was set at 60%. The temperature was constant until the end of harvesting (20 °C) except for the “temperature experiment” (see below).

Differences: There is some variability in the light intensity experience by any plant. However this variability was later reduced by not using the corners of the growth cabinet where the light intensity was lower.

2.2.4 Harvesting and sample storage

4 week old tissue (rosette leaves or roots) was harvested every 3 or 4 hours over 3 or 4 days depending on the experiment. During harvesting plants were released into LL or DD (usually after harvesting one last DL cycle). For the “temperature experiment” (section 5.7) the conditions of the cabinet were set to DD when harvesting started and the temperature alternated between 12 °C and 20 °C on a 12 hour cycle, 12 hours out of phase from the previous light dark cycle, i.e. the previous dawn became the new subjective dusk (transition from 20 to 12 °C).

For each time-point rosette leaves and roots were harvested separately. All the shoots/roots from the same box (8-10 plants per box unless stated otherwise, fig. 2.1) were pooled together, rapidly frozen in liquid nitrogen and stored at -80 °C. For the root tissue, most of the water (liquid medium) was removed in a few seconds with a tissue before freezing. To harvest time-points during dark cycles, a green safety light was used. All the samples were ground in liquid nitrogen and store at -80 °C before RNA extraction and quantification.

Differences: In James et al. (2008) plants were harvested about a week later, so they were close to flowering. No green safety light was used to harvest time-points during dark cycles (so plants were exposed to dim white light for a few seconds at each time-point).

2.2.5 RNA extraction, DNase treatment and quality control

RNA was extracted using the RNeasy Plant Mini kit (Qiagen). In this kit the RLT buffer was used by default. The purity of RNA was then estimated by spectrophotometry: the absorbance (A) at 230, 260 and 280 nm was measured. The A260/A280 and A260/A230 ratio were usually greater than 1.8 and 2 respectively, indicating a relatively pure RNA extract. If they were less than 1.7 and 1.9 respectively, the extraction was repeated a second time with the same RLT buffer and a third time if necessary but with the RLC buffer from the same Qiagen kit. Rarely the ratios were still not good enough after these three extractions. In that case the extracts were pooled together and purified by ethanol precipitation. RNA extracts were stored at -80 °C.

Each RNA extract was treated with DNase (Ambion DNA-free kit) according to the manufacturer's recommendation, except that the incubation time was increased to 50 min at 37 °C. After this treatment each sample was quantified again with a nanophotometer (GeneFlow). In most cases, the 260/280 and 260/230 ratios were unaltered; if not, the extraction was repeated.

The efficiency of the DNase treatment was checked by PCR and gel electrophoresis. For each sample a 1 µL aliquot was mixed with 1 µL actin primers (table 2.2), 3 µL DEPC (diethylpyrocarbonate) water and 5 µL GoTaq Hot Start Green Master Mix (Promega). Then a PCR was run for 35 cycles, each cycle consisting of 3 steps: denaturation at 94 °C, annealing at 55 °C and elongation at 72 °C. The PCR products were then run on a 0.5 x TBE/1.2% Agarose gel containing 3 µl EtBr (10mg/ml)/100 ml gel. A 100bp ladder (Promega G210A) was also used. The gel was run at 100V for 1 hour. Any sample that displayed a band at ~500 bp was still contaminated with DNA and therefore had to be treated again with the DNA-free kit.

Once the samples were DNA-free, a denaturing agarose gel electrophoresis was used to check the integrity of RNA preparations. The gel contained 1.3% agarose, 3.7%

formaldehyde and a MOPS buffer (3-(N-morpholino)propanesulfonic acid, 4.2 g/L, pH adjusted to 7 using NaOH). 1 µg of RNA was used, and a loading buffer with ethidium bromide (0.1 g/L) was added to each sample. The gel was run for 1 hour at 80V and then illuminated with UV light. The cytosolic 25 S and 18 S ribosomal RNAs usually appeared as discrete bands or peaks and in approximately 2:1 ratio. If not, the whole process of RNA extraction and quality control was repeated.

Differences: Previously RNA extracts were quantified only before the DNase treatment, and with a different spectrophotometer (Genquant, Amersham international). The efficiency of the DNase treatment was not systematically checked by PCR and gel electrophoresis. RNA quality gels were not carried out systematically.

2.2.6 RT-qPCR

After assuring the quality of each extract, their RNAs were reverse-transcribed using a cDNA synthesis kit with a Superscript™ II reverse transcriptase (Invitrogen). For each sample 1 µg of total RNA was used for the reverse transcription, and oligo dT was used as primer. The cDNA were then diluted 10 times with DEPC water.

The cDNA were then quantified by qPCR using the SyBr fluorophore (Brilliant SYBR Green III, Stratagene) and gene-specific primers (table 2.2). Reactions were conducted using at least one primer predicted to span an exon-intron boundary. The expression of *ISUI* was more constant over time courses and between organs compared to the expression of *UBIQUITIN (UBQ)*. Therefore *ISUI* served as a reference gene for the amounts of starting mRNAs. The reactions were conducted in the Mx3000P qPCR system (Agilent)

Differences: Previously the cDNA was synthesised with random hexamers. The fluorophore was SYBRI (Stratagene). Previous primers used to amplify GI were replaced by new ones giving a shorter amplicon. UBQ was replaced by ISUI as reference gene. Standards were not systematically used (i.e. not on each plate), so the absolute quantity of mRNA could not always be determined. Instead the quantifications were relative, e.g. calibrated to the maximum value in the time-course.

Table 2.2: Primers used for PCR and qPCR

The actin primers were used for simple PCR, to check for DNA contamination in RNA extracts. The other primers were used for qPCR. For genes marked * the primer labelled (1) were the ones that were first used, as in James *et al.* (2008), and then replaced by the primers labelled (2). The other primers were the same as in James *et al.* (2008).

Target	Forward	Reverse
Actin (PCR)	CTTACAATTTCCCGCTCTGC	GTTGGGATGAACCAGAAGGA
CCA1	ATCTGGTTATTAAGACTCGGAAGCC	GCCTCTTTCTCTACCTTGGAGAAAA
LHY	GAATTATTAGCTAAGGCAAGAAAGCC	GCCTCTTTCTCCAACCTTGTGAAGA
TOC1	GTGTTCTTATCAAGTGACTGCAGTG	CAAGTCCTAGCATGCGTCTTCTTC
PRR7	GTCTTTAAGTGCTTATCGAAAGGAGC	CACTACCACTAGAACTTTGGCATCT
PRR9	TGTTGAAGTGTATGCTGAGAGGTGC	ATCATCACGCAAAGTCAGTCTTCTC
CHS	CAGACAGGACATCGTGGTGGT	ACATGAGTGATCTTTGACTTGG
*GI (1)	GGTGTCACTACTGAGTGTGTTGTGATG	CAATGGCATAGTATCTATGAAACAAACG
*UBC (1)	TTAGAGATGCAGGCATCAAGAGCGC	CATATTTCTCCTGTCTTGAAATGAA
*GI (2)	CGGGCAACTGATGGAATGCTTG	TTGTTGCTGGTAGACGACACTTC
*ISU1 (2)	GCCATCGCTTCTTCATCTGTTGC	GTGGGAGAGAAAGATGCTTTGCG

The optimised RT-qPCR protocol described above was used for the experiments presented in sections 4.4 and 4.5, whereas the previous protocol (James *et al.*, 2008) was only used for the experiment presented in section 4.2. To summarise, several steps of the sample processing previously used were modified: plant tissue was harvested a week earlier, RNA extracts were quantified before and after DNase treatment, and their quality was then systematically checked, oligo dT was used as primers for the cDNA instead of random hexamers, SYBR I was replaced by SYBR III in the master mix for qRT-PCR and *ISU1* was used as a reference gene to normalise data. Overall this modified protocol reduced variability in our results.

2.3 Imaging system

2.3.1 Media

Two solid ½ MS media were used for the imaging experiments. First a liquid ½ MS medium was prepared from powder (Plant cell culture tested, Sigma) and its pH adjusted to 5.7 with 1M KOH. This solution was used to prepare two media: one with 1.2% agar and without charcoal, and the other one with 1.8% agar and 2% charcoal. The pH of the latter

had to be readjusted because charcoal acidifies the medium. The medium without charcoal is commonly used in plant biology, whereas the medium with charcoal was used to reduce light scattering. These media were then autoclaved 15 min. at 115 °C and poured on 120x120 mm square plates (Greiner). First 75 mL of ½ MS medium without charcoal was poured per plate. Once this medium was solidified, its upper part (~ 3 cm from the top of the plate) was removed and replaced by the medium containing charcoal. Figure 3.2 shows images of plates with and without charcoal. More generally the protocol for imaging experiments is the result of an optimisation process that is described in chapter 3.

2.3.2 Seed sowing, plant transfer and entrainment

Two rows of 10-12 transgenic seeds were sown per plate on medium without charcoal. Those plates contained about 50 mL of ½ MS medium with 1.2% agar (no sugar). About 10 days after germination, seedlings were transferred to new plates; usually 2 clusters of 3 plants were transferred per plate. These new plates contained the same medium except for the top part of the plate (in the shoot area) where 2% charcoal was added to darken the medium. For experiments with dark-grown roots, the plates and lids were partly covered with black tape, as shown in figure 3.2. Plants were then entrained in 12 h light ($80\text{-}100\ \mu\text{mol.m}^{-2}.\text{s}^{-1}$):12 h dark cycles (referred as LD) at 20 °C for 3-4 weeks from sowing to imaging.

2.3.3 Luciferase assay

Plates with 3-4 week old plants containing a *LUC* reporter gene were sprayed with 60 mM D-Luciferin (Promega) in 0.01% triton (300 μL per plate) and transferred to the dark imaging chamber. Plants with dark-grown roots were sprayed under low intensity green light. Each plate was put on the stand shown in figure 3.1 and the roots were kept in the dark by an automated covering system or exposed to light depending on the experiments. This dark room was set at a constant temperature (20 °C) and various light regimes depending on the experiment. Four block of blue and red LEDs could provide up to $20\ \mu\text{mol.m}^{-2}.\text{s}^{-1}$; by default the light intensity was set to $15\ \mu\text{mol.m}^{-2}.\text{s}^{-1}$ with equal amount of blue and red light.

The bioluminescence was detected over time by the Intensified CCD camera 225/18 (Photek) with a 16 mm lens. This camera, the LEDs and the covering system were

controlled by the same software (IFS32, Photek) so that the whole system was automated and synchronised: images could be captured in pitch dark, shoots and roots could be illuminated with LEDs between two images, but roots could also be covered during light cycles. Images were taken for 15 minutes every 1.5 – 3 h in photon counting mode, without any filter. The IFS32 software was used to process the data. The luminescence could be visualised spatially, as shown in figure 3.2. All the individual images of a time course were combined to get one image per plate and per experiment. This image, representing the total luminescence per plate recorded over the experiment, was used to divide the plate in distinct areas for either roots or shoots. This total luminescence allowed me to refine the area to be integrated, taking into account that the shoots moved over time and the roots could grow during the experiment. Raw data were then extracted and further analysed with Excel (Microsoft). The luminescence of each time-point was normalised with the average luminescence of the corresponding time-course over the last LD cycle, unless otherwise stated.

2.4 Data analysis

2.4.1 *BRASS analysis*

Time-course data from imaging and RT-qPCR experiments were analysed using Biological Rhythm Analysis Software System (BRASS) (www.millar.org). The whole time-courses were considered and the data from the first day in constant conditions were discarded from the analysis (because of possible transient effects), unless stated otherwise. The FFT-NLLS suite of programs was used to estimate periods between 15 and 35 h, considered to be within the circadian range. The same software was used to estimate phases, amplitudes and relative amplitude error (RAE). The RAE is defined as the ratio of the amplitude error to the most probable amplitude. It is used to assess individual rhythm robustness: values close to 0 indicate robust cycling and values at or near 1 indicate a rhythm with an error value as large as the amplitude itself, i.e. not statistically significant. The term “scored rhythmic” will refer to any rhythm detected by this BRASS analysis, regardless of the RAE.

2.4.2 ANOVA analysis

The analyses of variance (ANOVA) were carried out with Sigma plot 11.0 (Systat Software, Inc.), using the two-way analysis. Significance was determined by using the Holm-Sidak method for multiple pairwise comparisons.

2.5 Modelling

Some parameters of different mathematical models were modified in attempt to fit the root clock data. Software was used as detailed below.

2.5.1 Changing model parameters with Circadian Modelling (CM)

Circadian Modelling (CM) is a flexible, user-friendly software interface for running simulations. It was developed by Paul E. Brown and colleagues, and is available at <http://millar.bio.ed.ac.uk/>. Starting from the Locke *et al.* (2006) model, referred hereafter as L2006 model, the different biological parameters and light conditions can be easily changed.

In the L2006 model, *CCA1/LHY* and *PRR7/PRR9* are treated as single components labelled *LHY* and *APRR* respectively. 16 ODE (Ordinary Differential Equations) describe the dynamic expression of the core clock genes and their proteins. Three of them are shown below, representing the levels of *TOC1*, *X* and *Y (GI)* mRNA:

$$(1) \quad \frac{dc_T^{(m)}}{dt} = \left(\frac{n_2 c_Y^{(n)b}}{g_2^b + c_Y^{(n)b}} \right) \left(\frac{g_3^c}{g_3^c + c_L^{(n)c}} \right) - \frac{m_4 c_T^{(m)}}{k_4 + c_T^{(m)}}$$

$$(2) \quad \frac{dc_X^{(m)}}{dt} = \frac{n_3 c_T^{(n)d}}{g_4^d + c_T^{(n)d}} - \frac{m_9 c_X^{(m)}}{k_7 + c_X^{(m)}}$$

$$(3) \quad \frac{dc_Y^{(m)}}{dt} = \left(\Theta_{\text{light}}(t) q_2 c_P^{(n)} + \frac{(\Theta_{\text{light}}(t) n_4 + n_5) g_5^e}{g_5^e + c_T^{(n)e}} \right) \times \left(\frac{g_6^f}{g_6^f + c_L^{(n)f}} \right) - \frac{m_{12} c_Y^{(m)}}{k_{10} + c_Y^{(m)}}$$

These 3 equations contain the parameters g_3 , g_4 , g_5 and g_6 that were changed (see chapter 7, section 7.2). g_3 and g_6 are the inhibition constants for expression of *TOC1* and *GI*,

respectively, by LHY. g_4 is the activation constant for expression of X by TOC1. g_5 is the inhibition constant for expression of Y by TOC1. $C_i^{(j)}(t)$ is the cellular concentration of the products of the i th gene ($i = T, L, Y, X$ or P labels TOC1, LHY, Y, X or P); $j = m$ or n denotes that it is the corresponding mRNA or protein in the nucleus. $\alpha, a, b, c, d, e, f, g$ are Hill coefficients. n_j and g_j are transcription rates. m_j and k_j are degradation rates. $\Theta_{\text{light}}(t)$ are light activation terms.

The values of the parameters g_3, g_4, g_5 and g_6 were changed manually based on biological data and assumptions. Then simulations were run with these different set of parameters to try and fit the root data qualitatively. Many combinations of parameters were tried in different light conditions. The simulated time-courses of several clock gene mRNA were then compared to the root data.

2.5.2 Global parameter optimization using Systems Biology Software Infrastructure (SBSI™)

The Systems Biology Software Infrastructure (SBSI™) was used to optimize the parameters for the root clock with supercomputers in Edinburgh. This infrastructure is meant to automate the connection between data, models and analysis allowing the updating of large-scale data, models and analytical tools with greatly reduced overheads. SBSI™ includes algorithms for numerical simulation of complex models and for the indirect estimation of unknown parameter values by fitting to data, especially time series (<http://csbe.bio.ed.ac.uk/sbsi.php>). SBSIVisual, a desktop application, was used to access SBSINumerics in order to run parameter optimizations.

Optimization attempts to find the best possible parameter values for a biological model to reproduce a given set of experimental data. To configure an optimization, a model in SBML format and experimental data in SBSI data format must be provided (uploaded). The models used were the Locke *et al.* 2006, the Pokhilko *et al.* (2010 and 2012) models, referred hereafter as L2006, P2010 and P2012 respectively. Root clock data in DD and LL were converted into SBSI data format.

To configure the optimization process, several algorithms are available. The Parallelised Genetic Algorithm (PGA) was used. Genetic Algorithms (GAs) are search methods based on the principles of natural selection and genetics. GAs encode the decision variables of a

search problem into strings of alphabets which represent candidate solutions to the problem. The strings are referred to as chromosomes, the alphabets are genes and the values of genes are termed alleles. In this application, a chromosome would represent a candidate set of parameter values to be evaluated. GAs rely on a population of chromosomes, which undergo selection and mutation over a number of generations, where the evaluation function provides the selection force. The evolution proceeds through the following steps:

1. Initialization - an initial population of candidate solutions is generated by a set up phase.
2. Evaluation - the fitness values of candidate solutions are evaluated. Each candidate solution (or “allele”) gives a cost. This depends on the cost function chosen (see below).
3. Selection - the best solutions (those with lower costs) are propagated to the next generation.
4. Recombination/mutation - these two processes allow the creation of novel parameter sets which may be better than the parental sets.
5. The novel sets replace the original parental population.
6. Steps 2-5 are repeated until some terminating condition is reached (e.g. the target cost function value, or an absolute number of generations, is reached)

Several parameters can be configured in this process, for instance the population size, the number of generations and the mutation frequency.

Optimization proceeds using an objective or cost function to evaluate the goodness of fit of a particular parameter set. The FFT (Fast Fourier Transform) cost function evaluates the periodicity of oscillatory models. The target period is defined by the user. For the optimisation processes used in this thesis, the target period were chosen between 28 and 30 h (corresponding to FRPs of clock genes in roots under LL or DD with imaging). For example, if the data of *CCA1* mRNA are included in this process (note that one can use any data that are simulated by the model to constrain the optimisation), and if a set of parameters generated during this process gives a simulation with the exact target period (say 28 h), the corresponding cost would be 0. In this example, the further away from 28 h the simulated period is, the higher the cost. In most cases, the Chi-Squared (χ^2) cost function was also used: it evaluates the quantitative fit between simulation and experimental data.

The parameters to optimize and the constraints are configured by the user. Each optimisation process presented in this thesis started with the initial parameter values of the model used, except for the light (L) and dark (D) parameters: these were modified to simulate constant conditions (LL or DD) by setting their values to 0 or 1.

For the L2006 model, 4 parameters were optimised: g3, g4, g5 and g6. They appear in the 3 equations presented in the previous section. For each of them, the parameter space was searched for values between 0.001 and 1000 times their default value.

For the P2010 model, 3 parameters were optimised: g5, g15 and g16. g5 and g16 are the equivalents of the L2006 g3 and g6 parameters respectively, i.e. inhibition constants of *TOC1* and *Y* by LHY/CCA1. g15 is the inhibition constants of *GI* by LHY/CCA1. These 3 parameters appear in the 3 equations below:

$$(4) \quad \frac{dc_T^m}{dt} = \left(n_2 \frac{c_Y^d}{c_Y^d + g_4^d} + n_3 \right) \cdot \frac{g_5^e}{g_5^e + c_L^e} - m_5 c_T^m$$

$$(5) \quad \frac{dc_G^m}{dt} = L \cdot q_4 \cdot c_P + \frac{g_{14}^n}{g_{14}^n + c_T^n} \cdot \frac{g_{15}^o}{c_L^o + g_{15}^o} \cdot n_{12} L - m_{18} c_G^m$$

$$(6) \quad \frac{dc_Y^m}{dt} = L q_2 c_P + (n_5 L + n_6 D) \cdot \frac{g_7^s}{g_7^s + c_T^s} \cdot \frac{g_{16}^s}{g_{16}^s + c_L^s} - m_9 c_Y^m$$

c_i^m and c_i stand for dimensionless concentrations of mRNA and protein, respectively. Index “i” labels *TOC1* (T), *Y*, *LHY* (L) and *GI* (G).

d, e, n, o, s and g exponents are Hill coefficients

n_j and m_j are rates constants of transcription and degradation, respectively

g_j are Michaelis-Menten constants

q_j are the rate constant of acute (P-dependent) light activation of transcription

c_P is the concentration of protein P, a light-sensitive activator that accumulates in darkness and is quickly degraded by light

L and D represent Light and Dark (with values between 0 and 1 depending on the light conditions)

g5, g15 and g16 were allowed to change up to 100 fold (increase or decrease), starting from their default values.

For the P2012 model, 2 different sets of parameters were optimised. First a set of six Michaelis-Menten constants: g1, g5, g6, g8, g15 and g16. g5 and g15 are the equivalents of the L2006 g5 and g15 parameters respectively, i.e. inhibition constants of *TOC1* and *GI* by LHY/CCA1. The others are also constants of inhibition. They are presented in the equations below:

$$(7) \quad \frac{dc_L^m}{dt} = q_1 L c_P + n_1 \frac{g_1^a}{g_1^a + (c_{P9} + c_{P7} + c_{NI} + c_T)^a} - (m_1 L + m_2 D) \cdot c_L^m$$

$$(8) \quad \frac{dc_{P9}^m}{dt} = L \cdot q_3 \cdot c_P + \frac{g_8}{g_8 + c_{EC}} \left(n_4 + n_7 \cdot \frac{c_L^e}{g_9^e + c_L^e} \right) - m_{12} c_{P9}^m$$

$$(9) \quad \frac{dc_T^m}{dt} = n_2 \cdot \frac{g_4}{g_4 + c_{EC}} \cdot \frac{g_5^e}{g_5^e + c_L^e} - m_5 c_T^m$$

$$(10) \quad \frac{dc_{E4}^m}{dt} = n_{13} \cdot \frac{g_2}{g_2 + c_{EC}} \cdot \frac{g_6^e}{g_6^e + c_L^e} - m_{34} c_{E4}^m$$

$$(11) \quad \frac{dc_{E3}^m}{dt} = n_3 \frac{g_{16}^e}{g_{16}^e + c_L^e} - m_{26} c_{E3}^m$$

$$(12) \quad \frac{dc_G^m}{dt} = L q_2 c_P + n_{12} \frac{g_{14}}{g_{14} + c_{EC}} \cdot \frac{g_{15}^e}{g_{15}^e + c_L^e} - m_{18} c_G^m$$

Labels in these equations are similar to the labels in the P2010 model:

c_i^m and c_i stand for dimensionless concentrations of mRNA and protein, respectively. Index “i” labels LHY (L), PRR9 (P9), PRR7 (P7), the Night Inhibitor (NI), TOC1 (T), the Evening Complex (EC) and GI (G).

a and e exponents are Hill coefficients

n_j and m_j are rates constants of transcription and degradation, respectively

g_j are Michaelis-Menten constants

q_j are the rate constant of acute (P-dependent) light activation of transcription

c_P is the concentration of protein P, a light-sensitive activator that accumulates in darkness and is quickly degraded by light.

L and D represent Light and Dark, with values between 0 and 1 depending on the light conditions (e.g. under DD, L=0 and D=1)

Finally a set of 5 “light-related parameters” were optimised: m1, p1, p12, p15 and p24. They all appear in equations of the P2012 model together with the “L” parameter (they are multiplied by L). m1 is present in equation (7) above. p_j are constants of translation, protein modification, protein complex formation and translocation between nucleus and cytoplasm. They appear in the following equations:

$$(13) \quad \frac{dc_L}{dt} = (p_2 + p_1 L) \cdot c_L^m - m_3 c_L - p_3 \frac{c_L^e}{c_L^e + g_3^e}$$

$$(14) \quad \frac{dc_{COPIc}}{dt} = n_5 - p_6 c_{COPIc} - m_{27} c_{COPIc} (1 + p_{15} L)$$

$$(15) \quad \frac{dc_{COPIh}}{dt} = p_6 c_{COPIc} - n_6 L \cdot c_P \cdot c_{COPIh} - n_{14} c_{COPIh} - m_{27} c_{COPIh} (1 + p_{15} L)$$

$$(16) \quad \frac{dc_{EC}}{dt} = p_{26} c_{LUX} c_{E34} - m_{36} c_{EC} \cdot c_{COPIh} - m_{37} c_{EC} \cdot c_{COPId} - m_{32} c_{EC} (1 + p_{24} \cdot L \cdot \frac{c_{Gn_tot}^d}{g_7^d + c_{Gn_tot}^d})$$

$$(17) \quad \frac{dc_{ZTL}}{dt} = p_{14} - p_{12} L c_{ZTL} c_G + p_{13} c_{ZG} D - m_{20} c_{ZTL}$$

$$(18) \quad \frac{dc_{ZG}}{dt} = p_{12} L c_{ZTL} c_G - p_{13} c_{ZG} D - m_{21} c_{ZG}$$

$$(19) \quad \frac{dc_{Gc}}{dt} = p_{11} c_G^m - p_{12} L c_{ZTL} c_{Gc} + p_{13} c_{ZG} D - m_{19} c_{Gc} - p_{17} c_{E3c} c_{Gc} - p_{28} c_{Gc} + p_{29} c_{Gn}$$

More details about these equations and their parameters can be found in Pokhilko *et al.* (2012) and its supplements.

To optimise the 5 “light-related parameters” mentioned above, two optimisation algorithms were used: the PGA (described above) and the Particle Swarm Optimization (PSO). PSO is a computational method that optimizes a problem by iteratively trying to improve a candidate solution with regard to a given measure of quality (in this case it tries to reduce the cost). PSO optimizes a problem by having a population of candidate solutions, here

dubbed particles, and moving these particles around in the search-space according to simple mathematical formulae over the particle's position and velocity. Each particle's movement is influenced by its local best known position and is also guided toward the best known positions in the search-space, which are updated as better positions are found by other particles. This is expected to move the swarm toward the best solutions (http://en.wikipedia.org/wiki/Particle_swarm_optimization).

2.5.3 Simulations with COPASI

The name COPASI stands for COmplex PATHway Simulator. It is an open-source software application for creating and solving mathematical models and biological processes (<http://en.wikipedia.org/wiki/COPASI>). The version 4.8.35 was used for simulations, after changing manually some parameters of the P2012 model. Many “tasks” are available: they are different types of analysis that can be performed on a model. The two tasks used for this thesis were the “time-course simulation” and the “parameter scan”. Combined with the “time-course simulation”, the “parameter scan” allows rapid visualisation of the effects of a parameter change on a user-defined output (in our case, clock genes mRNA levels). Many more details can be found in the user manual available online (<http://www.copasi.org/>).

Several parameters were scanned with up to 100 fold changes from their initial values. For instance, a parameter p could be scanned between 0.1 and 1 in 0.1 increment. For each of these values (0.1, 0.2 ... 0.9 and 1), a time course of gene G expression could be visualised. When compared with the default values, the resulting simulations directly indicated for example whether a parameter has an influence on the FRP or amplitude.

In the P2012 model the parameter L is such as $L=1$ when light is present and 0 otherwise. The parameter D is by default $D=1-L$. When the parameter L was changed to x (e.g. $x=0.4$), the parameter D had to be changed to $D=x-L$ before running simulation in LD. This change allows D to have the value 0 during the dark cycles.

3 Development of an imaging system to monitor gene expression over space and time

3.1 Introduction

3.1.1 *The luciferase (LUC) reporter and its advantages for dynamic studies*

Gene expression studies have been greatly facilitated by the use of reporters such as β -glucuronidase (GUS), green fluorescent protein (GFP) and firefly luciferase (LUC). Reporter systems present advantages compared to the isolation and quantification of mRNA. The latter is laborious and destructive, and the spatial distribution of a specific mRNA within a tissue sample can be lost (de Ruijter *et al.*, 2003). On the other hand, methods using reporters can be non-destructive and automated.

The firefly LUC catalyses the oxidative decarboxylation of beetle luciferin using O_2 and Mg^{2+} -ATP as substrates. This reaction releases a photon at 562 nm. The use of firefly LUC as reporter of gene expression in plants was first demonstrated by Ow *et al.* (1986). These authors used X-ray films to detect the bioluminescence. Nowadays the photon production can be monitored over time by automated systems using a coupled-charge device (CCD) camera.

In 1992, Millar and colleagues used for the first time the firefly *LUC* gene as a reporter to monitor rhythmic gene expression in *Arabidopsis* (Millar *et al.*, 1992). It was the first time LUC was used to reveal the temporal regulation of transcription in a multicellular organism. LUC is inactivated after its reaction with luciferin. It makes a good reporter for promoter activity dynamics. For instance, Millar *et al.* (1992) used a *CAB:LUC* construct and could hardly detect any oscillation in LUC protein amount over time whereas the bioluminescence (reflecting the *CAB* promoter activity) was circadian. Since then, the *LUC* gene has been modified (*LUC+*) to increase the signal (de Ruijter *et al.*, 2003). LUC is targeted to the peroxisome whereas *LUC+* is cytosolic. This reporter has become a very common tool in circadian biology.

3.1.2 Use of *LUC* to monitor gene expression in roots

Although *LUC* is a very common reporter in shoots, it has not been often used to monitor gene expression in roots. This may be because there is less interest in this organ or just because roots are more difficult to image: the signal is usually lower compared to shoots and fewer plants can be monitored at a time.

In 2001, Toth *et al.* reported tissue-specific expression of photoreceptors using *LUC+*. All phytochrome (except *PHY C*) and cryptochrome promoters displayed circadian oscillations in shoots under constant conditions. Some images of whole seedlings showed the spatial expression pattern of these photoreceptors, but no time course of their expression in roots was reported (Toth *et al.*, 2001).

Thain and colleagues used *CHS:LUC* reporter to image different organs, including roots. But they had to image clusters of 15 plants (Thain *et al.*, 2000) or increase the light intensity up to $250 \mu\text{mol}\cdot\text{m}^{-2}\cdot\text{s}^{-1}$ (Thain *et al.*, 2002) in order to get enough signal from roots. Besides, they used 3% sucrose in the medium (as many researchers have been doing in our research field). In these conditions, the authors found that *CHS* was expressed rhythmically in the roots. However, *CHS* is not expressed in dark grown roots (James *et al.*, 2008).

LUC reporters have been used in other area of plant biology to study gene expression in roots, for instance in plant nutrition and plant-pathogen interactions. The nitrate transporter *NRT2.1* encodes a main component of the high-affinity transport system (HATS) for root uptake of NO_3^- , which plays a crucial role in N acquisition by crops. Its transcription is a major target of the systemic feedback repression exerted by high N status of the plant (Girin *et al.*, 2010b). These authors generated *NRT2.1:LUC* transgenic plants and showed different luminescence according to whether the plants were grown on medium with or without nitrate (expression was higher in the latter case). However, they did not follow *NRT2.1:LUC* activity over time, nor did they specify how many plants could be imaged at a time (presumably 6 seedlings at most).

Pathogenesis-related proteins, or PRs, are induced under specific pathological conditions (Van Loon, 1985). Santamaria and co-authors studied a *PRI*-like promoter activity (*AtPRBI*) and showed it was induced in an organ-specific manner. They could distinguish

leaves and roots, but also stems and flowers; in this case they apparently imaged at most one plant at a time (Figure 4 in Santamaria *et al.*, 2001). Like most other studies in roots, they did not follow LUC activity over time.

Many researchers add sucrose in their media. It allows plants to grow faster, and can increase the bioluminescence signal compared to medium without sugars. However, adding sucrose in the medium affects the root clock (James *et al.*, 2008) and also the shoot clock (Dalchau *et al.*, 2011). Therefore all my experiments were carried out without any sucrose in the media.

To summarise, similar methods using the LUC reporter gene have been used for decades, but mainly to image shoot luminescence. The use of the LUC reporter to monitor gene expression in roots has rarely been reported in the literature. When it has, the experimental conditions were not well documented (e.g. the number of plants or organs imaged simultaneously was not specified) or not physiological (e.g. sucrose in the medium or high light on the roots). In order to image simultaneously shoots and roots in more physiological conditions over time the standard protocol (usually used for seedlings or shoots, as described in (Hall and Brown, 2007)) needed significant adaptations, which will be described in this chapter. The optimised protocol that was used for further experiments is summarised in chapter 2 (“Materials and Methods”).

3.2 Imaging simultaneously shoots and roots on vertical plates

Our imaging system set up had to be adapted in order to image both shoots and roots simultaneously. We had access to a Photek ICCD225 photon-counting camera mounted in a light-tight box (Photek, UK). It was usually used to image plants grown on horizontal plates or pots, so the camera was mounted vertically. To image simultaneously shoots and roots, seeds have to be sown on top of vertical plates, so that the roots can grow down the plate, on the surface of the solid medium. To image these vertical plates, the whole system could have been rotated 90 degrees. But this was not possible given the space constraints. The light-tight box was too small to contain 6 vertical plates sitting on a new stand, a new set of red and blue LEDs and the automated covering system shown in Figure 3.1 and described later in this chapter. In addition, this box was not temperature controlled. It

would have to be open all the time for the temperature to be steady (the room is temperature controlled). Otherwise, the LEDs would have warmed up the whole box.

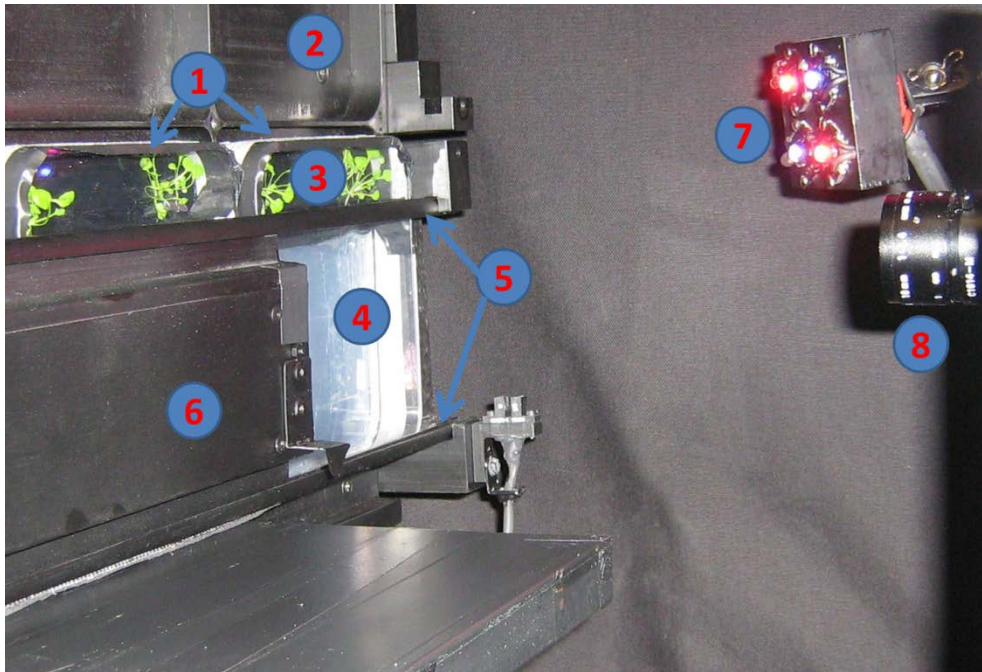


Figure 3.1: Overview of the imaging system

After spraying the plants with luciferin, the vertical plates (1) were placed on a stand (2) that could hold up to 6 plates (only 2 plates are shown here). Each plate was divided in two compartments: one for shoots (3) and one for roots (4). The plates were held by two rails (5). A black cover (6) could slide automatically between these two rails, and could keep the roots in darkness when the light was on. The light was provided by four blocks of blue and red LEDs; only one is shown here (7). These LEDs, the covering system and the camera (8) were all controlled by the same software (IFS32, Photek). The whole system was set up in a temperature-controlled dark room.

New stands for the plates and the camera, and another dark chamber had to be built. This was done in collaboration with the Glasgow University (GU) mechanical workshop. A LED system with both blue and red was designed in collaboration with the GU bioelectronics unit. The LEDs are controlled by the same software that controls the camera, i.e. IFS32 (Photek), switching the light on or off depending on the light regime required, but also ensuring that the light is off when capturing images.

Most components of the imaging system are shown in Figure 3.1. This new set up gave more space and therefore more flexibility to conduct different experiments. Indeed, one to six plates could be imaged at a time depending on the experiment. The relative positions of the plates, the camera and the LEDs could be easily adjusted (e.g. if the signal was high

enough, plants could be put further away from the camera so that up to six plates could be imaged at a time, as opposed to 1 plate if the signal was low). The room was temperature controlled (20 °C). The light intensity was set manually at the beginning of each experiment (equal amount of blue and red so that the irradiance was $15 \mu\text{mol.m}^{-2}.\text{s}^{-1}$, unless stated otherwise).

The final protocol can be found in chapter 2 section 2.2. It had to be optimised in order to image both shoots and roots simultaneously. However, the general procedure – from seed surface sterilisation to data analysis – has remained similar during this optimisation process. First, seeds were surface sterilised and stratified for 2-4 days at 4 °C. Then they were sown on vertical plates containing $\frac{1}{2}$ MS solid medium. Plants were entrained in LD (12/12) at 20 °C (white light, $80\text{-}100 \mu\text{mol.m}^{-2}.\text{s}^{-1}$). After 2-5 weeks the plates were sprayed with luciferin. They were then transferred to a dark chamber and imaged over time in different light conditions (e.g. LD followed by LL). The data were extracted with the IFS32 software (Photek) and analysed with the BRASS software.

The protocol was optimised using plants expressing the *CCA1:LUC+* fusion. This was chosen for several reasons. It was expected to be circadian in both shoots and roots. Its amplitude was high in shoots. Even though *CCA1* mRNA has a lower expression in roots compared to shoots (James *et al.*, 2008), its amplitude was high in roots too (hundreds of fold change between trough and peak). Moreover, the FRP of *CCA1* transcripts oscillations is longer in roots compared to shoots (James *et al.*, 2008). Therefore plants were imaged in LD followed by LL to check whether this period difference could be observed with imaging.

3.3 Increasing the signal/noise (S/N) ratio

With the *CCA1:LUC+* fusion, the root luminescence was much lower than the shoot luminescence. Therefore the relative noise was higher in roots. Other fusions used later also had a low S/N ratio in roots compared to shoots. Several ways of increasing this ratio were considered. This is detailed below.

3.3.1 Increasing the root signal

One reason for a lower root signal was simply that the amount of root tissue was small compared to shoot tissue. I therefore used older plants (4-5 weeks old) with bigger roots, and clustered (2-6 plants per cluster). To avoid the drying out of the medium and to make sure plants had enough nutrients, 10-12 days old seedlings were transferred to new plates with fresh medium (Figure 3.2 A and B); these plates were used for imaging.

Bigger plants contain more cells than smaller ones, and therefore consume more luciferin. I increased the concentration of luciferin sprayed on the plates. Spraying 300 μ L of luciferin 60 mM per plate and integrating the luminescence for 15 minutes every hour allowed me to detect signals from both shoots and roots for several days (imaging 4 plates at a time).

In preliminary experiments shoots and roots seemed to have the same FRP in constant light (data not shown). This was not consistent with the previous results from our lab (James *et al.*, 2008), where *CCA1* has a longer period in roots compared to shoots. Further studies showed this was an artefact. The noise was high and caused by the luminescence emitted by the shoots being reflected off the agar plate back to the camera (cf. next sub-section).

In the meantime our camera and software were upgraded. It allowed me to use another mode of the camera (Binary Slice or BS) in an automated manner. This mode of the camera was supposed to increase the S/N ratio. The signal was greatly amplified. This BS mode is discussed further later in the chapter.

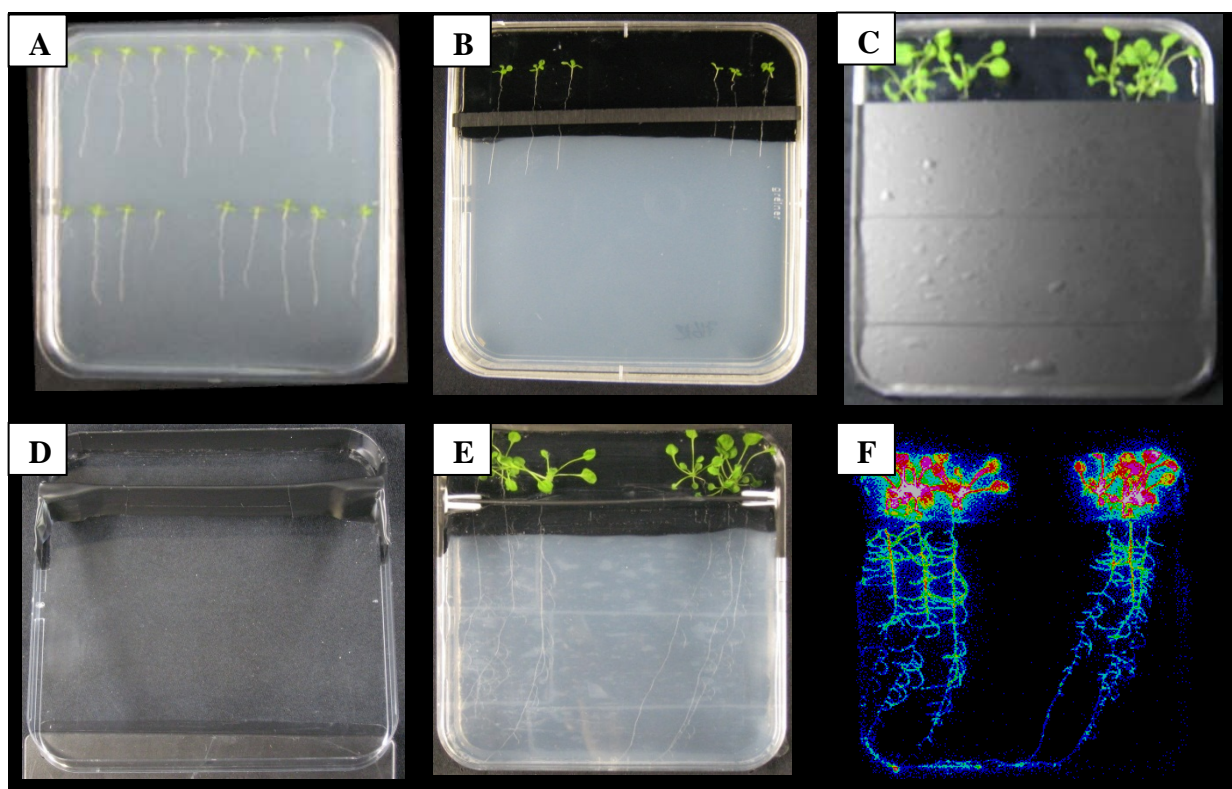


Figure 3.2: Brief overview of the optimised imaging protocol, from sowing to imaging

Seedlings were grown on 1/2 MS medium for 10-12 days (A) before being transferred on fresh 1/2 MS medium with charcoal on top (B). Roots were then either light- or dark-grown. In the latter case, a black acrylic bar was placed horizontally under the shoots (B) to minimise light leakage to the roots; to keep the roots in the dark, black tape was placed around the plate (C). After another 10-12 days of entrainment in LD (12/12) at 20° C, plants were ready for imaging (they were ~3 weeks old) (C). The original lid (with black tape as in C, or without if roots were light-grown) was removed. The plants were sprayed with luciferin (~6 μ mole per plant) and the new lid (D) was used to seal the plate. This new lid contained a black barrier and tape that distinguished two compartments (one for shoots and one for roots); this reduced light scattering between the two organs. An example of a bright field image and its corresponding luminescence is shown in E and F respectively.

3.3.2 Decreasing the noise

In the context of our imaging system noise can be divided into two categories: “electronic noise” and “optical noise”. The former is the noise intrinsic to the camera (dark current and readout noise for CCD cameras) and cannot be changed. The “optical noise” is the noise related to the “light pollution”. The photon counting camera being extremely sensitive to light, it is important to use it in a pitch dark chamber. But there is a source of light inherent to the technique used here: the photons emitted by the plants. Some of them are part of the signal to be measured. But others are noise, namely the chemiluminescence of the chlorophyll and the bioluminescence (produced by the luciferase) scattered from other

parts of the plant. The former can easily be discarded: it decreases exponentially over time after the light is off so discarding the first 2 minutes of darkness just after the light is off and before starting integrating the signal removes the chlorophyll chemiluminescence. The latter is the light scattering between two areas of interest (in this case between shoots and roots). The bioluminescence is much higher in the shoots compared to roots, at least for the *CCA1:LUC+* plants used in the optimisation experiments. This turned out to be true for most if not all the transgenic plants used later on. Therefore decreasing noise means in our case reducing this light scattering from shoots to roots.

To address this problem, Thain *et al.* (2000) added 1 % charcoal to their medium. But while this darkens the plates, it also seems to darken the plant's life: they did not grow well on media with charcoal. Therefore other "plate darkeners" were tested, but with no more success:

- black tape on the inside base of the plates: it reduced the reflection of light from the plants to the plastic and back to the camera. But again plants did not grow well. The remains of solvent or other compounds were probably toxic.
- black plastic or paper (with presumably less solvent or toxic compounds – if any at all were left after washing with ethanol 70%); but these materials being less dense than the medium, it was hard to keep them in the bottom of the plates until the agar solidified
- black food dye: as well as charcoal it can darken the whole medium, but plants could hardly grow on it.

These darkeners prevented the plants from growing normally and also seemed to reduce the signal from the roots, possibly due to reduced growth (and probably fewer cells). Another explanation could be a lower light scattering from root tissues to other root tissues. Actually this "noise" within the same organ is not a problem; it rather amplifies the signal since we are interested in the organ as a whole.

Preliminary experiments showed that it was important to reduce light scattering from shoots to roots. To achieve this, two compartments per plate were clearly distinguished: one for shoots and one for roots. To do so, a new lid was designed (Figure 3.2.D): it is made of the bottom part of a plate, with a card holders stuck on each side (at 2.5 cm from the top) and a plastic rectangle between the two. This rectangle defines the boundary between shoots and root compartments. The sides of the shoot compartment (sides of the

plate, card holder and plastic rectangle) were covered with black tape. Before using it for imaging, this new lid was washed with 70% ethanol and UV treated to prevent any contamination.

Because the bioluminescence from the shoots could also be scattered in a light medium, it was darkened with 2% of charcoal, but only for the shoot compartment. To do so, the plates were first poured with 1/2 MS without charcoal. Once solidified, the top part (up to 0.5 cm below the barrier, for overlapping) was removed and replaced by the medium with charcoal. The 10-12 days old plants were transferred to this plate with fresh media (with charcoal on top; Figure 3.2.B). These plants were entrained another 10-12 days before being sprayed and imaged.

Although adding charcoal in a medium seems absolutely straightforward, it initially gave some complications. The 1/2 MS medium contained 1.2 g/L of agar. Its pH was adjusted to 5.7 with KOH before autoclaving. When charcoal was added to this medium, the medium did not solidify properly after cooling down. It turned out the charcoal acidified the medium, and as a result the pH had to be readjusted to 5.7. Moreover, the solid medium with charcoal dried out faster than the basic medium (i.e. without charcoal). Adding more agar (1.8 g/L) in the medium containing charcoal limited this issue.

The effect of these adaptations on the S/N ratio were progressively tested with imaging. A representative experiment is detailed in the next section.

3.4 Comparison between time courses obtained with different lids and media

As described above, a number of parameters were modified in order to increase the S/N ratio. In the meantime, blue and red LEDs were designed and the camera and IFS32 software were upgraded. A key improvement seemed to be the division of the plate in two compartments (shoots and roots separated by a black barrier) and addition of charcoal in the medium (in the shoot compartment only). To test whether these modifications improved the S/N ratio in our final imaging system set up (with new LEDs, camera and

software), 5 weeks old plants were imaged for 4 days (1d LD and 3d LL) in 2 conditions: 1) with the new medium (with charcoal on top) and the new lid (with black barrier) or 2) without these adaptations. These conditions (and the corresponding plants or plates they are growing in) will be referred as 1 and 2 respectively.

Figure 3.3 A and B show an image of each plate (one per condition) and the area of integration for analysis of expression. Each plate was divided in 3 equal parts: shoots, top of the roots and bottom of the roots. Note that for condition 2 (Figure 3.3.B), the shoot area did not include all the shoots: some leaves could be found in the 2nd third of the plate (i.e. the middle part, labelled “R2 top”) because there was no barrier to hold them, unlike condition 1 (Figure 3.3.A). The corollary is that in condition 2 the top section of the roots (Figure 3.3.B) cannot be integrated as they are for the roots in condition 1: it is the only area that differs between the 2 conditions in terms of surface (and instead of being a rectangle, it is a polygon so it contains root tissue but no leaves). This observation already highlighted one advantage of the barrier: it could hold the shoots (which tended to fall down otherwise) and it allowed more of the root tissue to be imaged. Finally the bottom part had the same area in the 2 conditions.

The promoter activity in the shoots was similar in the two conditions, and this was also true for the promoter activity in the bottom section of the roots (Figure 3.3.C). Both shoots and roots had a sharp peak of *CCA1:LUC+* activity around the last dawn (ZT0); they were in phase. In LL *CCA1* continued to cycle in the roots but with a longer FRP compared to the shoots (Figure 3.3.C). The raw luminescence was clearly higher in condition 2 (Figure 3.3.B) compared to condition 1 (Figure 3.3.A) where charcoal and black tape reduced light scattering. Nevertheless the normalised data were very similar in both conditions, qualitatively and quantitatively (Figure 3.3.C). In LL, both shoot and root rhythms dampened, with broader peaks compared to LD, and a longer FRP in roots compared to shoots. The plots in condition 1 were almost superimposable with the plots in condition 2. Adding charcoal and black tape did not seem to make any difference as far as the lower part of the root is concerned.

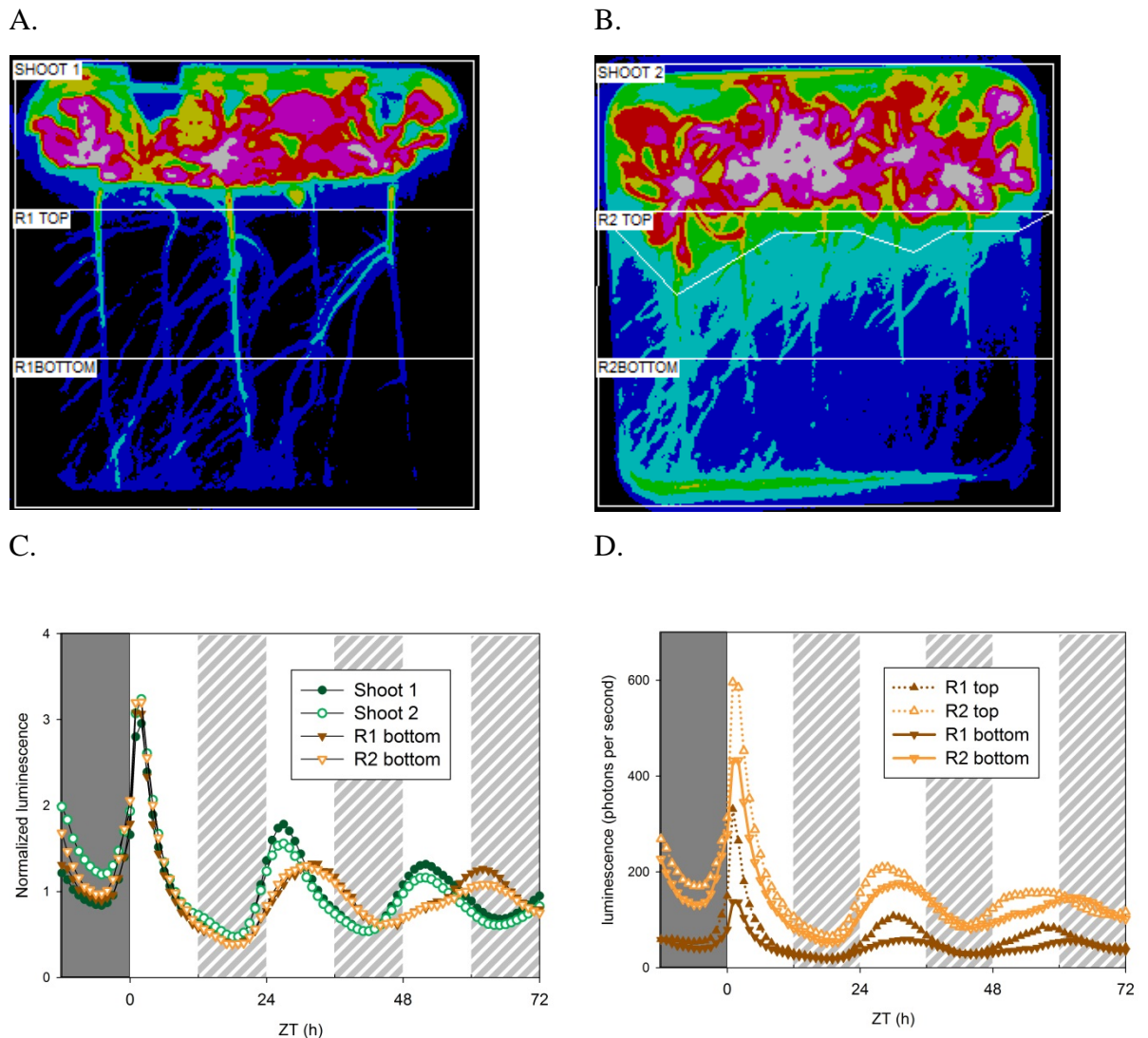


Figure 3.3: Masking of the root signal by the shoot signal can be reduced by compartmentalising the plate

Plants expressing *CCA1:LUC+* were all entrained 4-5 weeks in LD (12/12). Then *CCA1:LUC+* activity was monitored in shoots and roots under LL in two different conditions (i.e. two different media and lids): 1. With medium containing charcoal on top, and lid with black barrier. These distinguish two compartments described in text and in Figure 2 B-D; 2. Without this compartmentalisation. A and B show images obtained in condition 1 and 2 respectively, with 3 areas of integration per plate: shoots, top and bottom of the roots (labelled “shootX”, “RXtop” and “RXbottom” respectively, X = 1 or 2 labels the condition). These images were obtained after adding up all the frames (or time-points) of the corresponding time-courses (i.e. they represent the total luminescence for each condition). C shows normalised data from the shoots and the bottom section of the roots. Each time-point was normalised with the mean luminescence of the corresponding time-course. D show raw data from the two sections (top and bottom) of roots. Shoots are represented by green lines and circles, roots are represented by orange or brown lines and triangles. White and hatched bars represent light (days and subjective nights respectively), the dark bar represent the last night. ZT0 = last dawn

However, the difference between the 2 conditions becomes clear once the upper part of the roots is considered. First, a halo of light can be observed all around the shoots in condition 2 (Figure 3.3 B) to a much greater extent compared to condition 1 (Figure 3.3 A). Given the much stronger signal in shoots compared to roots, the part of this halo of light that is in the “R2 TOP” area is expected to contain a significant amount of signal from the shoots (scattered in the root area), masking the root signal at least partly. This is indeed observed in Figure 3.3.D, which shows that after the first subjective dawn (ZT24), “R2 TOP” peaked earlier than any other root area analysed here; its phase was then closer to the corresponding shoot phase (shoot 2, Figure 3.3.C). At least part of the signal must have come from the shoot 2. In addition, after the second subjective dawn (ZT48) “R2 TOP” started rising earlier than the other root areas, before reaching a plateau. Again, the bioluminescence integrated here must have been a sum of shoot and root signals: this could explain the observed earlier rise (like shoots) and later fall (like roots) with a plateau in between, resulting in a broad peak.

Peaks of the other root areas analysed were broad too, yet their phase was more delayed compared to shoots. The total amount of photon per time point and area analysed was higher in plate 2 compared to plate 1 (Figure 3.3.D). This was consistent with a higher level of noise in that plate (light scattering from shoot 2 to the roots). In general noise was not obvious when looking at individual images. However Figure 3.3 A and B are images obtained after adding all the images of the time course. This allowed me to refine the area to be integrated, and to take account of the fact that the shoots move over time and the roots can grow during the experiment.

In terms of FRP, no clear difference could be observed between the two conditions. The BRASS software was used to analyse the rhythms in LL (between ZT0 and ZT72) presented in Figure 3.3. Shoots 1 and 2 had a FRP of 25.4 h and 25.8 h respectively. All the roots (top and bottom, 1 and 2) had a FRP close to 30h (+/- 1 h). Because this experiment was not repeated in the exact same way, no statistical analysis could be done between the two conditions. However, it is important to note that plants were about 5 week old: they had therefore more root tissue than younger plants, but they were also close to flowering. The amount of tissue must have produced a higher signal compared to the

younger plants imaged in previous trials (where the FRP in roots was much closer to the FRP in shoots). When the signal is high enough, the noise becomes less significant, as would be the case in near-flowering plants. However I avoided the study of flowering plants since their physiological state would be markedly different compared to younger plants, and their clock might work differently compared to younger plants.

Therefore 3-4 week old plants were used for further experiments, as shown in Figure 3.2. Their amount of root tissue was high enough for the luminescence to be detected and distinguished from the shoot signal (i.e. the S/N ratio was high enough). It also allowed to image up to 6 plates simultaneously, with 2 clusters of 2 or 3 plants per plate. Therefore more data could be produced faster. This will be presented in the next sections and chapters.

In conclusion, with black tape and charcoal on top of the plate:

- two compartments were clearly distinguished (one for shoots, one for roots)
- light scattering between these two compartments was reduced
- the barrier between shoots and roots was also useful to hold the shoots and therefore integrate a bigger area for roots (e.g. “R1TOP” vs. “R2TOP” in Figure 3.3.A and B).

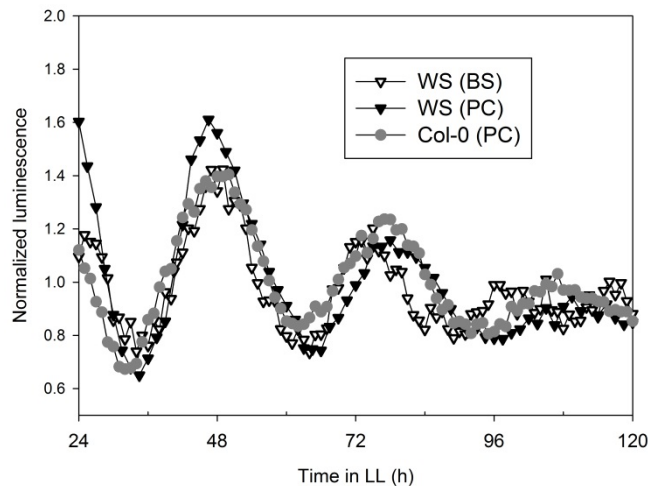
With this imaging set up, previous RT-qPCR results (James *et al.*, 2008) were qualitatively reproduced (Figure 3.3.C): in LD, the expression of CCA1 was synchronised in shoots and roots, but in LL these two organs were out of phase.

3.5 *TOC1:LUC+* activity is circadian in roots exposed to light

The set up including a new lid and charcoal on top of the medium as described above was used to image plants with the *TOC1:LUC+* reporter (Figure 3.4). The time-courses represent three independent experiments with different combinations of the following parameters: ecotype (Ws or Col-0) and mode of the camera (Binary Slice [BS] or Photon Counting [PC]). In all cases, the first day of LL was discarded and the promoter activity was rhythmic in roots for several subsequent days. The activity of *TOC1* promoter was circadian in roots (as well as shoots) in both Ws and Col-0 backgrounds.

Figure 3.4: *TOC1:LUC+* activity is circadian in roots exposed to light

Plants carrying the *TOC1:LUC+* fusion were entrained in LD for 4 weeks and then imaged in constant light (time 0 = last dawn). The first day in LL was discarded. The ecotypes were *Ws* or *Col-0* and 2 modes of the camera were used: BS (Binary Slice) or PC (Photon Counting). Each time course represents the luminescence of a cluster of 5-6 whole roots. Data were normalised with the average luminescence of the corresponding time course.



The comparison of BS and PC modes showed that although BS mode increased the signal, it also increased the noise so the S/N ratio was not improved. In addition, it gave a lower resolution, and was less quantitative than the PC mode (which gives 1 count per photon). Therefore the PC mode was used by default in all other experiments.

Figure 3.4 shows clearly that the *TOC1* promoter activity was circadian in roots of *Col-0* and *Ws*. This was in apparent contrast to previous results which showed *TOC1* transcript abundance was not clearly rhythmic in roots (James *et al.*, 2008).

The different results obtained with RT-qPCR and imaging are not necessarily contradictory. Imaging data give us information about the promoter activity, whereas the RT-qPCR results mentioned above quantify the accumulated mRNAs. The mRNA degradation is not taken into account in the former case, and possible splicing effects are not considered in the latter case. Alternative splicing is widespread in plants and plays a regulatory role in the circadian clock (James *et al.*, 2012). Therefore the transcript abundance need not exactly reflect promoter strength. However, there is another major difference between the two protocols: the RT-qPCR results were obtained with dark grown roots, whereas the plants used for imaging were entirely exposed to light. Light is a key environmental signal for plants, regulating gene expression and development (Neff *et al.*, 2000). I therefore tested the influence of light on the root clock directly.

Two plates with 6 *TOC1:LUC+* plants in each were imaged simultaneously (Figure 3.5). For one plate, roots were kept in darkness all the time (using a manual cover all the time

except during imaging) whereas for the other one, roots were exposed to light. In both cases, the expression profiles were very similar in shoots and consistent with the literature:

- in LD they have a sharp peak around dusk but also a small peak after dawn;
- in LL, they free run with smoother peaks and they become damped over time.

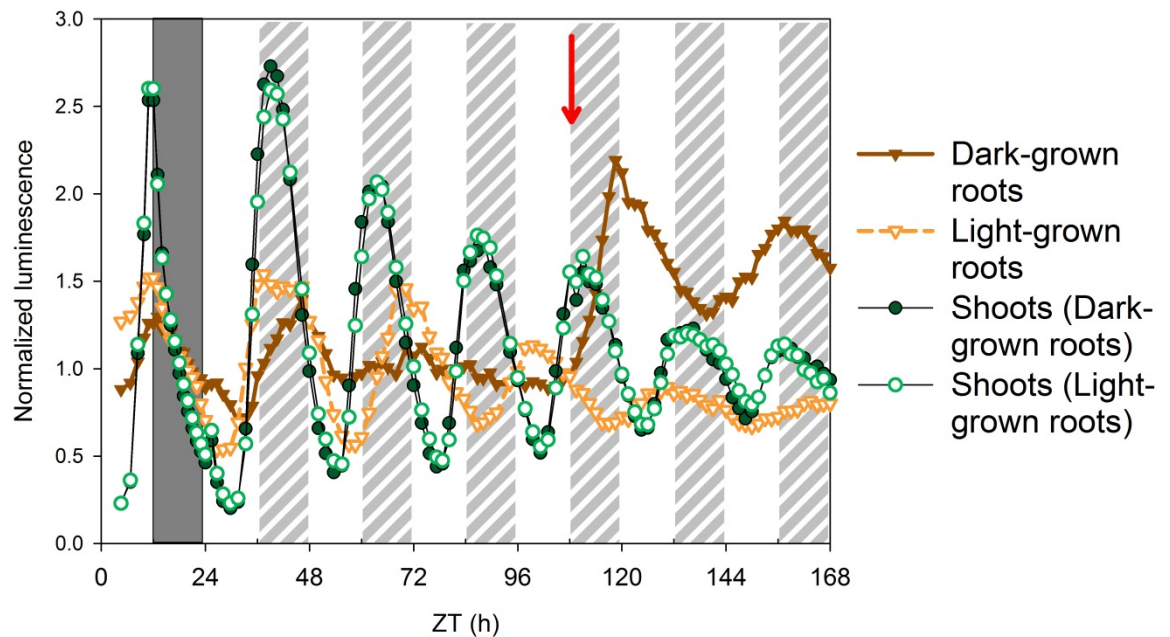


Figure 3.5: *TOC1* rhythm in roots depends on light conditions

Two plates with plants carrying the *TOC1:LUC+* fusion were entrained in LD for 4 weeks and then imaged for 1 day in DL followed by 6 days in LL. For one plate, roots were covered until the 4th day in LL (ZT108) when they were uncovered (represented by the red arrow). The other plants had roots exposed to light all the time. For each organ in each condition (light- or dark-grown roots) the data were normalized with the average of the corresponding time-course until ZT108. Shoots are represented by green lines and circles, roots are represented by orange or brown lines and triangles. White and hatched bars represent light (days and subjective nights respectively), the dark bar represent the last night.

Shoots and roots were rhythmic and in phase in LD. Roots were still rhythmic during the first day of LL in both cases (exposed to light or not), and roots exposed to light peaked earlier and with a higher amplitude than roots kept in the dark (Figure 3.5).

In LL the expression of *TOC1* in roots depended on whether this organ was exposed to light or not. Illuminated roots had a higher level of luminescence and *TOC1* maintains rhythmicity for over 5 days. The absolute levels of luminescence in roots kept in the dark

were on average 3.4 times lower than those in the light (note that the data presented in Figure 3.5 were mean normalised), and rhythmicity was not detected after two days.

After 108 hours (at subjective dusk), the cover was removed so that all roots were exposed to the light. The luminescence of roots previously covered increased rapidly and regained rhythmicity. The absolute luminescence was comparable to the one of roots always exposed to the light. It is important to bear in mind that all luminescence values were normalised with the average value of the corresponding 108 h time-course (i.e. the period before uncovering the roots, Figure 3.5). We cannot easily compare the root profiles of the 2 plates (previously covered or not) after ZT108. For instance they have different phase and period, which could be influenced by the time the roots were uncovered and the total amount of light they had received (which is obviously much less for the roots that were uncovered).

Thus the experiments showed that light can directly affect TOC1 expression in roots. This “direct” effect of light on the root clock will be further investigated and confirmed in the next chapter. It is well known that light induce the expression of some clock genes in shoot. It is also thought to have an indirect effect on clock gene expression roots, possibly through photosynthates (James *et al.*, 2008). But a more direct effect of light on the root clock may well mask some clock mechanisms in the roots grown in physiological conditions (they are supposed to be in the dark), for instance its entrainment by shoot signals. To investigate this systematically, our imaging system had to be adapted so that roots could be covered automatically whenever desired.

3.6 Keeping the roots in constant darkness

Roots are usually in a dark environment so it is more relevant to study directly the root clock in this more physiological condition. An automatic covering system for the roots was therefore designed with the help of the GU bioelectronic unit and mechanical workshop. This system allowed me to cover the roots when the light was on for the shoots, and uncover them automatically to measure the bioluminescence of both shoots and roots.

The “prototype” covering system allowed me to cover the roots for half of the plates imaged (i.e. the bottom row, see Figure 3.1). To validate this new covering system, the

previous experiment (Figure 3.5) was repeated: using *TOC1:LUC+* as a reporter gene, plants with roots covered or exposed to light were imaged over time. The data were compared to the ones obtained previously with a “manual cover” (Figure 3.6). The results were very similar, especially when roots were uncovered: *TOC1* was then rhythmic in LD and LL. When roots were covered, the absolute level of *TOC1* expression was low and not clearly rhythmic. Nevertheless results were qualitatively confirmed:

- shoots and roots were synchronised in LD conditions (note that shoot data were not shown in Figure 3.6)
- roots were still rhythmic in LL when roots are exposed to light
- roots seemed to regain rhythmicity in LL when roots previously covered were exposed to light.

Therefore the prototype was extended to allow the coverage of all the plates (top and bottom row presented in Figure 3.1) used for imaging.

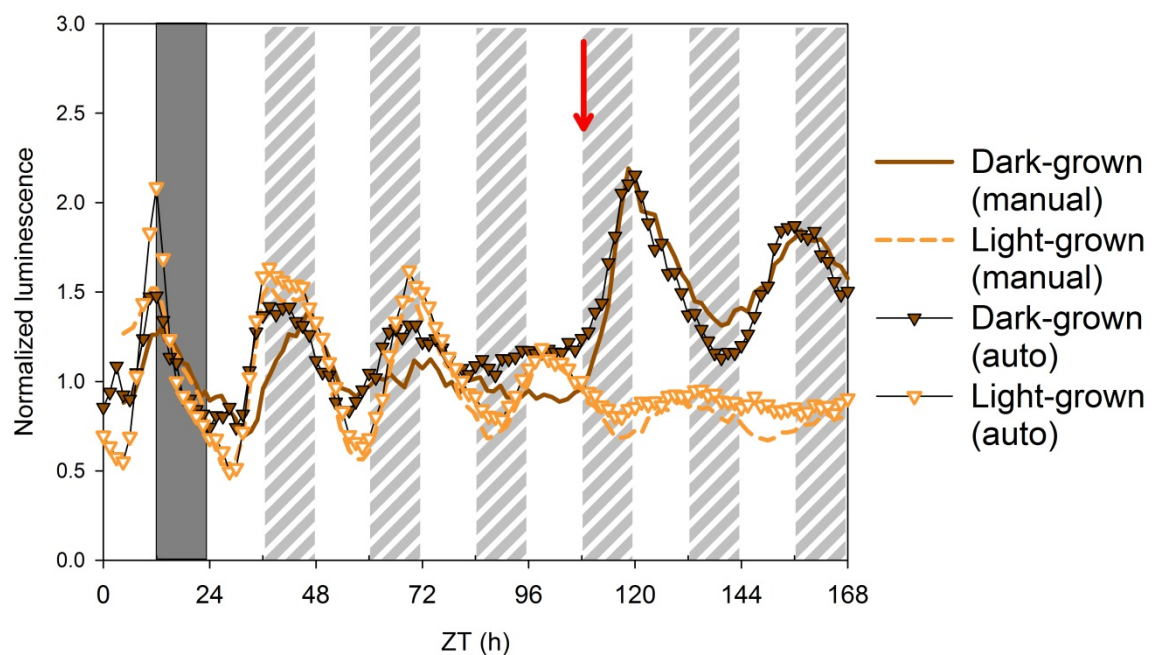


Figure 3.6: Validation of the new covering system for the roots.

Comparison of results obtained with manual and automatic covering of the roots. In both cases plants with a *TOC1:LUC+* reporter were entrained in LD cycles for 4 weeks, and then imaged for 1 day in LD followed by 6 days in LL. Triangles are data obtained with manual cover, smoother lines (without symbols) are data obtained with the automatic covering system. Orange dashed lines and open triangles represents data from roots always exposed to light; brown line and closed triangles represents data from roots kept in darkness until ZT108 when they were uncovered (represented by the red arrow). Data were normalised with their mean luminescence over the last 24 h in LD. Grey bars: dark cycles, white and hatched bars: light cycles (day and subjective days respectively).

Covered roots might express *TOC1* rhythmically in LL too but with lower amplitude. That could explain why its rhythm is not always detected. It would also be consistent with its (regain of) rhythmicity when roots are exposed to light (or uncovered). Using *CCR2:LUC+* reporter in the *toc1* mutant background, the role of TOC1 in the root clock will be further investigated in chapter 6.

3.7 Conclusion

Monitoring the activity of a promoter in the roots with the luciferase reporter gene has been described in different areas of plant biology. However, this method has rarely been used to follow gene expression over time and space, e.g. in different organs. When organ-specificity was shown in that way, it was not clear how many plants were imaged at a time (Thain *et al.*, 2002; Santamaria *et al.*, 2001), probably a few organs or seedlings only. This is in contrast with the monitoring of gene expression in shoots where hundreds of seedlings can be imaged at the same time (Southern and Millar, 2005). One reason for this huge difference in the number of organs imaged simultaneously is the low signal in roots. To increase the root signal, Thain and colleagues (2002) used clusters of plants and high light intensity. They also used sucrose in the growth medium, but later sucrose was shown to affect clock gene expression in shoots and roots (Dalchau *et al.*, 2011; James *et al.*, 2008). Therefore I did not use any sugar in the media. To increase the root signal I used clusters of organs but from older plants. Most experiments presented in the following chapters were done with 3-4 weeks old plants.

Older plants mean bigger shoots and therefore more signal from this organ. This resulted in higher noise for the roots, the light emitted by shoots being scattered in every directions. Using a specific lid divides our plates in two distinct compartments (one for shoots and one for roots, with a black barrier in between) and adding charcoal in the medium of the top part (shoot compartment) greatly reduces this light scattering (Figures 3.2 and 3.3). This was particularly useful when the signal/noise ratio was low in roots. In addition, using two compartments allowed keeping the roots in constant darkness. Depending on the strength of the promoter and its induction, the imaging protocol allowed me to image up to 24 individual plants (shoots and roots) at a time, and even more with fusion such as 35S:LUC (35S being highly expressed constitutively).

Light can affect genes expression in the roots (*cf.* next chapter) so my protocol kept this organ in constant darkness, with an automated covering system during imaging. Using such a system over a few days without exposing the roots to light has not been reported as far as I know. It is the first time this imaging method was used in physiological conditions (no sugar in the medium, no light on the roots) to monitor different gene expression in shoots and root over time.

My optimised protocol for imaging the root luminescence is summarised in chapter 2. It is significantly longer than protocols usually used for seedlings. Much more media (with or without charcoal) and plates needed to be prepared: only 2 clusters of 3 plants were usually imaged per plate. The plants needed to be transferred half way through: this allowed me to keep the medium fresh and to add some charcoal on the top of vertical plates. But it also increased the risk of contamination: this was rarely an issue but it increased the time of preparation in sterile conditions. Finally, to keep the roots in the dark the roots had to be covered, then sprayed with luciferin under dim green light. The protocol was more time-consuming at the beginning, when the roots needed to be covered manually between each image. But the next chapter will show that light could affect the root clock.

The promoter activity of *CCA1* was synchronised in shoots and roots under LD cycles. In LL, shoots and roots were out of phase, with a longer FRP in roots (Figure 3.3). This was qualitatively consistent with the previous study (James *et al.*, 2008). The method was further validated with other promoter of morning genes (chapters 4 and 5), and allowed me to obtain more data and faster compared to RT-qPCR: longer time-courses and higher temporal resolution. In addition, the imaging method is non-destructive: the same organs can be monitored over time, which reduces the biological variability of the results. The technical variability is probably also reduced compared to the experiment using RT-qPCR, because the latter necessitate many steps and each of them could add in some variability, from harvesting to data analysis through RNA extraction and cDNA synthesis. However, this chapter showed some discrepancies between imaging and RT-qPCR data for *TOC1* expression. These discrepancies will be investigated in chapter 4.

4 Direct effects of light on the root clock

4.1 Introduction

James *et al.* (2008) showed that the root clock mechanism differs markedly from that of the shoot clock. In these experiments roots were kept in the dark. Light is such an important factor in circadian biology (and in life more generally) that one can wonder whether it is the parameter responsible for the differences observed between shoot and root clocks. Are shoot and root clocks different just because the roots are virtually in constant darkness? Or are there more fundamental differences between the mechanisms of these two clocks?

As we have seen in the previous chapter, it would be much easier to use light-grown roots for imaging. Not only would it not require any customised equipment, such as the automatic covering system presented in the previous chapter, roots exposed to light can give a higher signal compared to dark-grown roots: this has been shown for *TOCI:LUC+* in the previous chapter and will be detailed for other constructs in this chapter. Therefore, if light did not have any significant direct effect on the root clock (i.e. if light only increases the signal but without affecting the clock mechanism), we would probably leave the roots exposed to light.

Etiolated seedlings (which have never seen the light) entrained by temperature cycles display much less rhythmicity compared to seedlings entrained by LD cycles (Wenden *et al.*, 2011). For instance, a *TOCI* rhythm was not detected in these dark grown seedlings. Besides, the FRP of *CCA1* was longer than 24 h in these etiolated seedlings. Interestingly this is qualitatively similar to the rhythms of dark-grown roots in James *et al.* study (2008): in constant conditions, *TOCI* was arrhythmic and *CCA1* had a FRP longer than 24 h (and longer than light-grown shoots). However, etiolated seedlings were entrained by temperature before release to constant temperature (and DD) in the study of Wenden *et al.* (2011), whereas James *et al.* (2008) kept the roots in the dark and constant temperature.

The clock of dark grown roots, as well as the etiolated seedling clock, has a 24 h period in diurnal cycles (LD and constant temperature for the former, DD and temperature cycles for

the latter). Since roots were dark-grown in James *et al.* (2008), it was thought that a rhythmic signal from shoots could couple the shoot and root clocks in diurnal conditions. Whatever this signal is, it is most likely different from direct absorbance of light in LD cycles which entrain the shoot clock. Similarly, etiolated seedlings were entrained by a non-photic zeitgeber. Can the different light inputs alone explain the different mechanisms between these circadian systems, especially between shoot and root clocks?

To address this question, plants were grown in two different light conditions: with the roots illuminated in the same way as the shoots (light-grown roots), or kept in darkness (dark-grown roots). Time-courses in LD followed by LL were analysed using RT-qPCR and imaging.

4.2 The expression of morning and evening clock genes are circadian in illuminated roots, with a longer FRP compared to shoots

To investigate the possible effects of light on the root clock, plants were grown in the same conditions as in James *et al.* (2008) except that roots were light-grown. Briefly, *Arabidopsis thaliana* (Col-0) wild type plants were grown in hydroponic culture. The black boxes used previously to keep the roots in darkness (James *et al.*, 2008) were replaced by transparent boxes and additional lights were placed underneath to ensure that shoots and roots received comparable light (Figure 2.1). After four to five weeks of entrainment in LD (12/12), plants were harvested over 4 days (one diurnal cycle followed by 3 days of LL) and mRNA was quantified by RT-qPCR (Figure 4.1).

In the diurnal cycle, morning and evening gene expression were synchronised in shoots and illuminated roots. Profiles in shoots and roots were very similar for “morning genes” (these include *PRR7* that peaks during the first half of the day, Figure 4.1.A). There were more differences between shoots and roots for evening genes (Figure 4.1.B), especially for *GI*: shoots had a small *GI* peak at dawn and a much higher peak before dusk, consistent with the literature (Locke *et al.*, 2006), whereas in roots *GI* rose continuously from dawn and peaked earlier than shoots. It resulted in a broader peak for *GI* in roots compared to shoots, already observed with dark-grown roots in James *et al.* (2008).

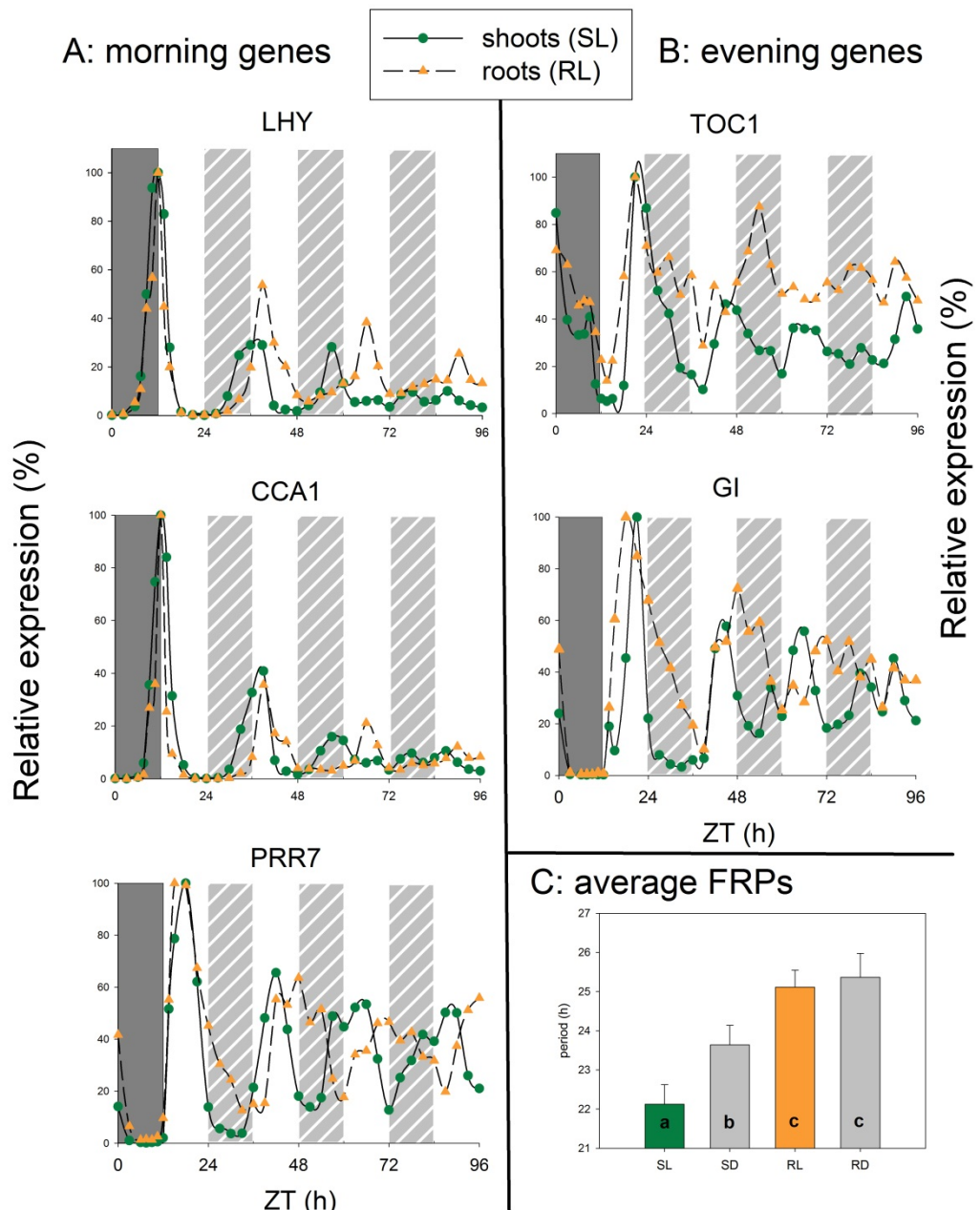


Figure 4.1: The expression of morning and evening clock genes is circadian in illuminated roots, with a longer FRP compared to shoots

Plants were grown in hydroponic culture with their roots in transparent boxes so that roots were exposed to the same light/dark conditions as shoots (i.e. “light-grown roots”). Plants were entrained 4-5 weeks in LD before release in LL. A and B: relative expression of “morning” (*LHY*, *CCA1* and *PRR7*; Figure A) and “evening” (*TOC1* and *GI*; Figure B) clock genes in shoots and roots; mRNA levels were normalised to *UBQ* and calibrated to the highest value of the corresponding time-course (highest peak value = 100%). White and hatched bars represent light (days and subjective nights respectively), dark bars represent nights. C. Average Free Running Periods (FRPs) of shoots (S) and root (R) “morning” and “evening” gene expression. Individual FRP were estimated from data presented in A and B respectively, using BRASS. Their averages (labelled L for Light-grown roots) are compared to the corresponding averages from James et al, 2008 (labelled D for Dark-grown roots). Because the evening genes were not circadian in dark-grown roots, only morning genes FRP were averaged for roots (RD and RL). Different letters on the bars indicate significantly different groups; e.g. shoots (SL and SD) and roots (RL and RD) FRPs were significantly different ($P < 0.001$) but RL and RD FRPs were not ($P = 0.558$) according to a 2 ways ANOVA test.

In LL, the morning loop of illuminated roots ran with a longer FRP compared to shoots, and the average FRP of “morning genes” was not significantly different from the James *et al.* (2008) study (Figure 4.1.A&C, and Table 4.1). The average FRP of genes in shoots with light-grown roots (SL) was shorter compared to that in shoots with dark-grown roots (SD) (Figure 4.1.C and Table 4.1.); these FRPs (SL and SD) were significantly different ($P=0.001$), which was consistent with Aschoff’s rules (Aschoff, 1960); indeed the overall light irradiance in our conditions was actually higher than in James *et al.* (2008) due to the additional light illuminating roots. Nevertheless, light had no significant effect on the FRP of morning genes in the roots.

Surprisingly the evening genes were rhythmic under LL in illuminated roots (Figure 4.1. B and C, and Table 4.1), which was not previously observed in dark-grown roots (James *et al.*, 2008). The FRP of *GI* in roots was similar to the average FRP of morning genes in this organ (Table 4.1); however, the FRP of *TOC1* was a few hours longer than other clock genes in roots (Table 4.1.).

Table 4.1: FRP of clock gene expression in shoots and roots under LL

A. Plants with Light-grown roots (L). Individual FRPs for “morning” and “evening” gene expression were estimated from data presented in Figure 4.1.A and 4.1.B respectively, using BRASS. These FRP were then averaged for “morning” genes, “evening” genes or both (labelled “all” in last column).

B. Plants with Dark-grown roots (D). Corresponding FRPs for shoots with dark-grown roots from James *et al.* (2008).

		<i>LHY</i>	<i>CCA1</i>	<i>PRR7</i>	<i>TOC1</i>	<i>GI</i>	<i>morning</i>	<i>evening</i>	<i>all</i>
A.Light-grown roots (L)	Shoots (SL)	22.11	22.39	22.17	22.65	21.32	22.22	21.99	22.13
	Roots (RL)	24.67	25.15	25.53	29.5	26.24	25.12	27.87	26.22
B.Dark-grown roots (D)	Shoots (SD)	23.3	23.3	23.9	23.3	24.4	23.5	23.85	23.64
	Roots (RD)	25.9	25.5	24.7	ND	ND	25.37	ND	25.37

Overall, these results show that differences observed between shoot and root clocks are not solely due to different light conditions. It suggests that these two clocks have fundamental differences, at least different FRP in LL. However light seems to directly affect clock gene

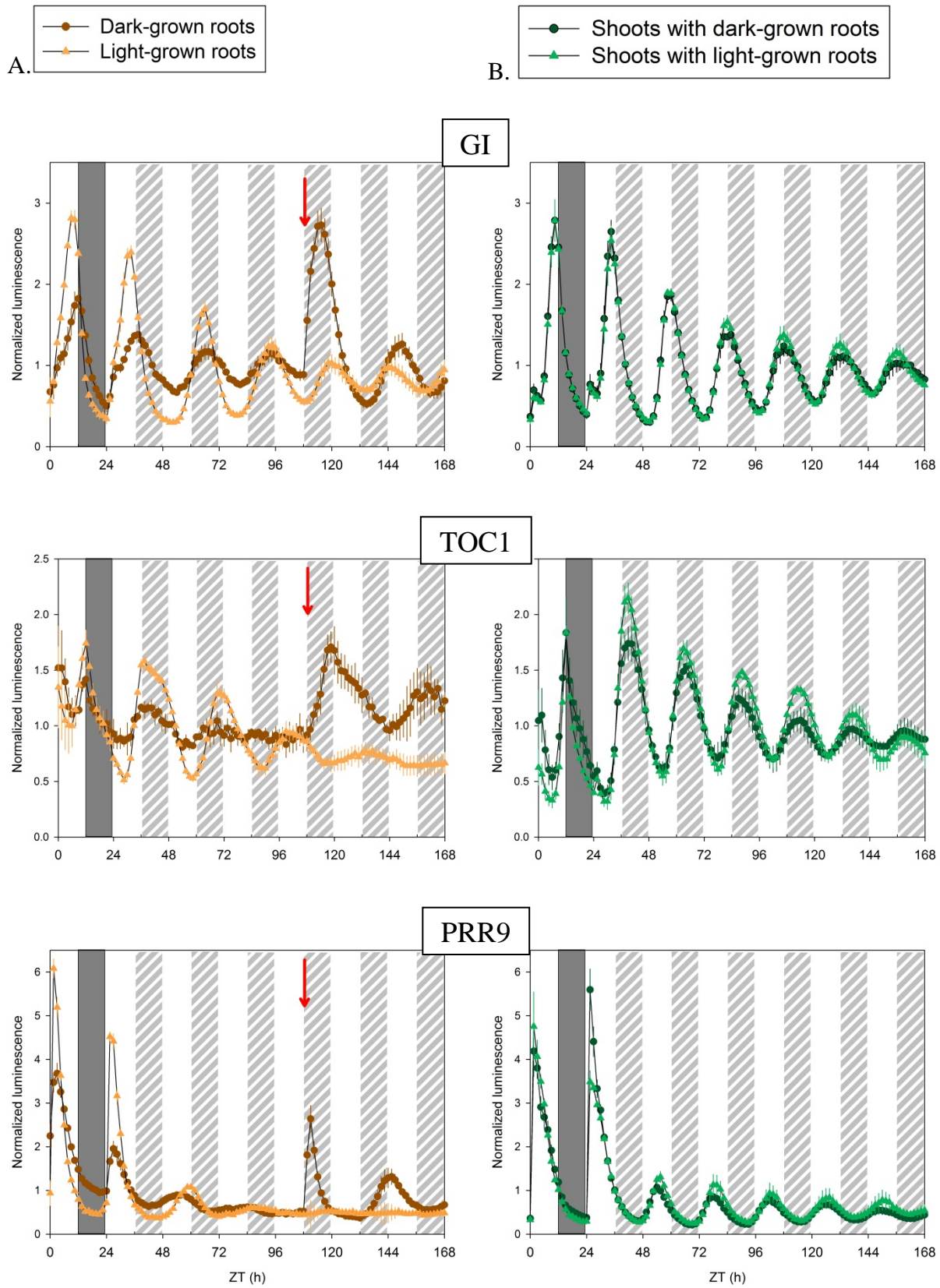
expression in roots, such as entraining evening clock genes. In this section only one set of RT-qPCR data was presented (Figure 4.1). But light effects were also observed using imaging: *TOC1:LUC+* activity free ran when roots were illuminated, and exposing dark grown roots to light had a direct effect on *TOC1* expression (section 3.5). In the latter case, it seemed that *TOC1* regained rhythmicity in roots once they were illuminated. Does light entrain the evening clock genes in roots? Or does it just reveal existing low amplitude rhythms that were previously not detected in dark-grown roots? To answer this question, similar experiments were done using our imaging method. Results are presented in the next section.

4.3 Light directly affects the expression of clock genes in roots

The previous section showed that direct exposure to light may affect clock gene expression in roots.

The experiment presented in section 3.5 was repeated with *TOC1:LUC+* plants. The same experiment was also carried out with other constructs: *CCA1-*, *CCR2-*, *GI-* and *PRR9:LUC+* in *Ws*. Briefly, plants were entrained for 3-4 weeks in LD (12/12) under white light with roots exposed to light or not (light- or dark-grown). For each construct, two sets of plants were then imaged simultaneously under LD and LL (a combination of blue and red light, see method in section 2.3): one with dark-grown roots and another one with light-grown roots (Figure 4.2).

Organ specificity in the plant circadian clock



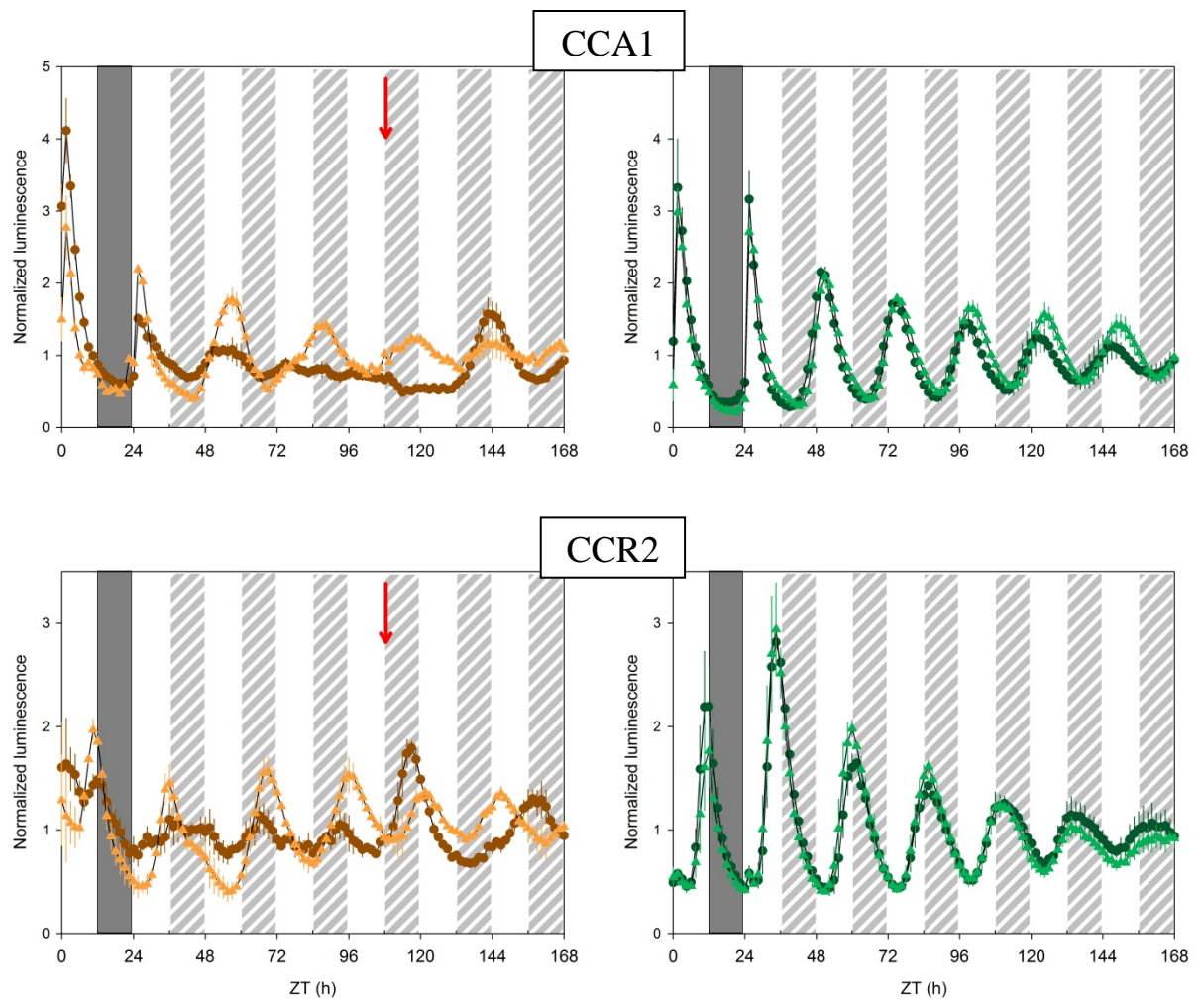


Figure 4.2: Light directly affects the expression of clock genes in roots

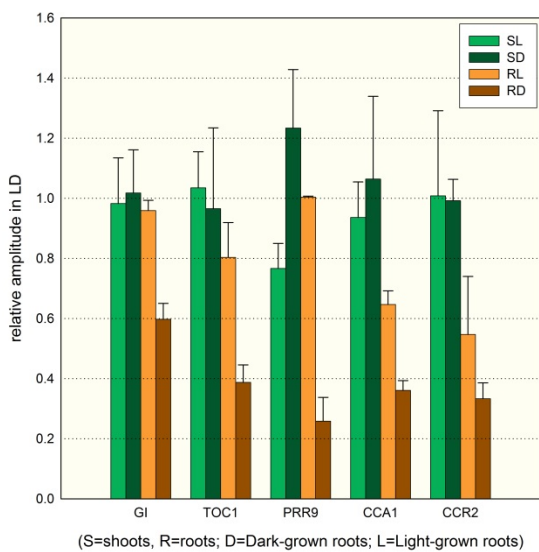
Plants were entrained for 3-4 weeks in LD (12/12) before release in LL. For half of the plants, roots were light-grown (i.e. exposed to the same light/dark conditions as shoots); for the other half roots were dark-grown. The promoter activities of *GI*, *TOC1*, *PRR9*, *CCA1* and *CCR2* were monitored in roots (A) and shoots (B) over the last day in LD (ZT0 = dawn) and in LL. From ZT108 (red arrows), dark-grown roots were exposed to light (i.e. put in the same conditions as shoots and light-grown roots). For each organ in each condition (light- or dark-grown roots) the data were normalized with the average of the corresponding time-course until ZT108. Bars in the backgrounds represent days or subjective days (white bars), night (dark grey bars) and subjective night (hatched bars). Error bars are SEM for 3 clusters of 2-6 plants (organs) from 2 independent experiments.

Whether roots were light- or dark grown, shoots had very similar profiles as expected (the shoots themselves were in the same conditions) (Figure 4.2.B). Shoot data were consistent with the literature: in LD, *TOC1* and *GI* had sharp peaks around dusk but also a small peak after dawn; *CCA1* and *PRR9* peaked around dawn; in LL, they all free ran with smoother peaks than in LD and the amplitude decreased over time. Note that the dawn peaks of *TOC1* and *GI* could be observed by using RT-qPCR (Figure 4.1) because an extra time-point was harvested 1.5 hours after dawn; plants for RT-qPCR were usually harvested

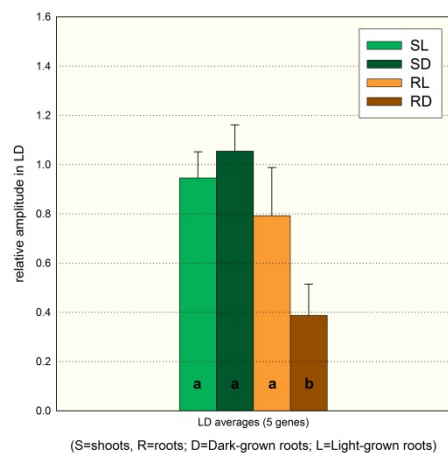
every 3-4 h, whereas imaging gave us a greater temporal resolution. For each construct, shoots of plants with dark-grown and light-grown roots were grown and imaged in the same conditions (e.g. at the same light intensity). In this case clock genes have the same FRP in shoots, whether roots are light- or dark-grown. This indicates that the differences observed previously in the FRPs of clock genes in shoots (Figure 4.1 and Table 4.1) were probably due to differences in light intensity between experiments.

But the expression of clock genes in roots differs significantly whether roots were light- or dark-grown. In LD, clock gene expressions were synchronized in shoots and roots (dark- or light-grown). The amplitudes were significantly lower in dark-grown roots compared to shoots and compared to light-grown roots (Figure 4.2 and 4.3.A&B). In addition, the relative amplitudes were not significantly different in light-grown roots compared to shoots (Figure 4.3.B). Whether roots were light- or dark-grown, phases were similar in shoots and roots for each gene (Figure 4.2) except *GI*: it peaked earlier in light-grown roots compared to dark-grown roots (Figure 4.2.A).

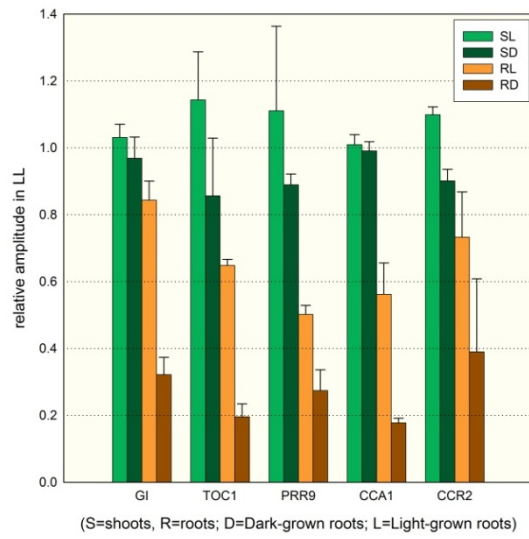
A.



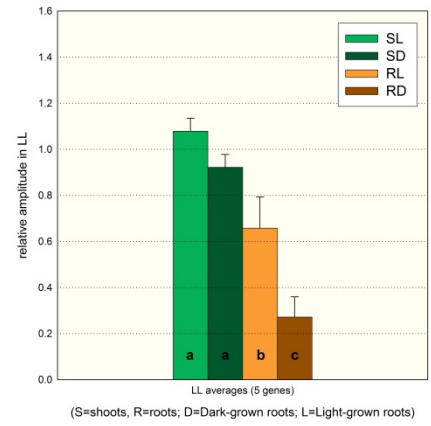
B.



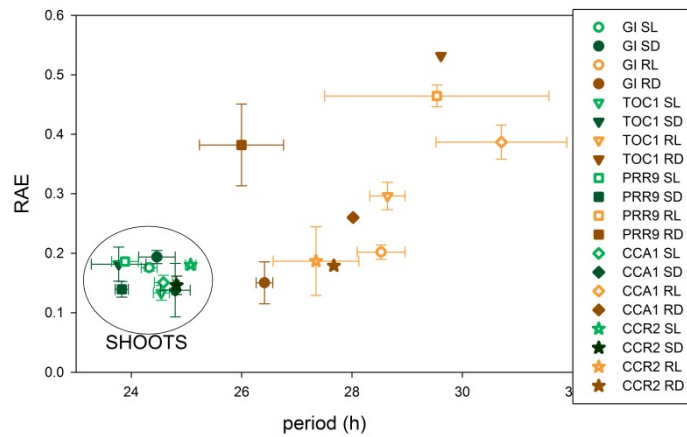
C.



D.



E.



F.

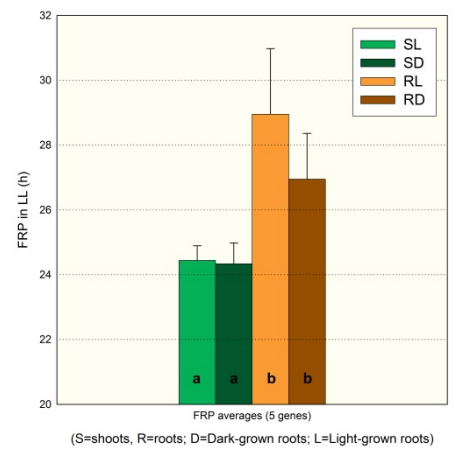


Figure 4.3: Light directly affects the amplitudes of clock gene expression in roots in LD and LL, but not their FRP

All data from Figure 4.2 were used to estimate amplitudes and periods of clock and output genes in Shoots (S) and Roots (R) with Light-grown (L) or Dark-grown (D) roots.

A, B: Relative amplitudes under LD. For each individual time-course used for Figure 4.2, the raw amplitude was estimated as the difference between peak and trough values during the last DL cycle (ZT12-36, Figure 4.2). This raw amplitude was normalised to the average amplitude in shoots (i.e. average of 6 values from SL and SD). The normalised amplitudes were then averaged for each gene and in each condition (i.e. SL, SD, RL and RD) (A). The mean values presented in A were then averaged for each condition, i.e. SL, SD, RL and RD (B).

C, D: Relative amplitudes under LL. For each individual time-course used for Figure 4.2, the raw amplitude was estimated with BRASS between ZT48 and ZT108. This raw amplitude was normalised as in A (C). The normalised amplitudes were then averaged as in B (D).

Error bars are standard deviations for 2-3 clusters of 2-6 plants (organs) (A-D).

E, F: Circadian period estimates using BRASS. Each individual time-course presented in Figure 4.2 was analysed between ZT48 and ZT108, i.e. before the dark-grown roots were exposed to light. The average periods and RAE are presented for each gene and in each condition (E). Error bars are SEM for 2-3 clusters of 2-6 plants (organs). A few time-courses from dark-grown roots (*TOC1*, *CCA1* and *CCR2*) were not considered rhythmic; hence there are no error bars for these 3 data points. The values presented in E were then averaged for each condition, i.e. SL, SD, RL and RD (F). Different letters on the bars indicate significantly different groups ($P < 0.001$) according to 2 ways ANOVA tests (B, D, F).

In LL morning as well as evening genes were always rhythmic in roots when roots were exposed to light. This confirmed the previous observation about *GI* and *TOC1* expression being rhythmic in light-grown roots (Figure 3.5 and 4.1). In dark-grown roots with shoots under LL, all genes studied here were scored rhythmic in at least one set of data (Figure 4.2 and 4.3). For instance *TOC1* and *CCR2*, i.e. two evening genes that were thought to be arrhythmic in dark-grown roots (James et al, 2008) were scored rhythmic at least once out of three replicates (Figure 4.3.E). Note that all the plants were in the Ws background. The same experiment was done with *TOC1:LUC+* in Col-0 background and gave very similar results (data not shown): the rhythm could be detected in dark-grown roots. *GI* was always scored rhythmic in light- and dark-grown roots. In addition the FRPs were similar for morning and evening genes in roots, which indicates they could be part of the same oscillator (i.e. morning and evening loops may not be uncoupled in LL). However the FRPs were more variable in roots compared to shoots. The average FRP tended to be higher in light-grown roots compared to dark-grown roots (Figure 4.3.F), but this was not highly significant ($P = 0.044$). But the average FRPs were significantly higher in both light-grown and dark-grown roots compared to shoots (Figure 4.3.E&F, $P < 0.001$), which is consistent with all our previous results obtained with imaging and RT-qPCR.

The relative amplitudes of clock genes were lower in dark-grown roots compared to light grown roots in LL (Figure 4.3.C), and more generally the amplitudes in the roots were

lower than in the shoots (Figure 4.3.D). To confirm the direct effect of light on levels of gene expression in roots, dark-grown roots were illuminated (uncovered) after 3 days in LL: the root covers were removed from ZT108 so that all roots were exposed to the same light as shoots (from the red arrow in Figure 4.2.A). Plants were then imaged for another 3 days in LL. *TOC1* and *GI* expression in roots previously covered went up very quickly and peaked 9-12h later (at ZT117-120, Figure 4.2.). Their absolute luminescence reached levels comparable to the one of light-grown roots (cf. Figure A.1 in Appendix). All luminescence values presented in Figure 4.2 were normalised against the mean value of the corresponding 108 h time-course (i.e. period before illuminating dark-grown roots); this allowed us to compare gene expression profiles in light- and dark grown root, for instance their amplitudes (Figure 4.3). But the absolute levels of luminescence in roots kept in dark were much lower than those in the light (cf. Figure A.1 in Appendix).

The difference in gene expression between light- and dark-grown roots was also obvious for *PRR9*, *CCA1* and *CCR2* (Figure 4.2.A). The amplitudes of these genes were higher in light-grown roots compared to dark-grown roots (Figure 4.3.C). After the cover was removed (from ZT108, indicated by red arrow in Figure 4.2.A), the expression increased in dark-grown roots. For *CCR2* this was qualitatively similar to *GI* and *TOC1*: the expression in roots previously covered went up quickly and peaked ~9-12 h later (ZT117-120, Figure 4.2.). For morning genes this was different: *PRR9* peaked sharply 3 h after the cover was removed in dark-grown roots, and *CCA1* peaked only about 36 h later (Figure 4.2). These interesting results suggested that the effect of light on gene expression in roots was gated by the clock.

In conclusion, some previous results were confirmed: the root clock has a longer FRP in LL compared to the shoot clock, whether roots were exposed to light or not. But the expression of most if not all clock genes in roots was directly affected by light. The extent of these effects depended on genes and possibly on the time of exposure; indeed the effect of light on gene expression seemed to be gated by the clock. Overall, direct exposure to light increased expression levels and amplitudes of clock genes in roots; it might also advance the phases of some clock genes in roots, but this was only observed for *GI* in LD. These new data not only confirmed a direct effect of light on clock gene expression in roots, they also showed that the expression of evening gene is circadian in dark grown roots too. This is in contrast with previous RT-qPCR results (James *et al.*, 2008) where *GI*

and TOC1 were thought to be arrhythmic. It is possible that low amplitude rhythms of GI and TOC1 in dark-grown roots were not detected at the mRNA level by RT-qPCR in previous work. Are these genes really arrhythmic at the transcript level, or are their rhythms just harder to detect because of variability? This question will be addressed in the next section.

4.4 Direct exposure to light affects clock gene transcript levels in roots

The previous two sections showed that light can directly affect clock gene expression in roots. But these RT-qPCR and imaging data raised other questions:

- 1) are *GI* and *TOC1* transcript levels actually circadian in dark-grown roots?
- 2) does light increase clock gene amplitude in roots at the transcript level?

If both answers are positive, this would explain why *GI* and *TOC1* rhythms are more easily detected in light-grown roots compared to dark-grown roots. And if these evening genes are circadian in dark-grown roots, they presumably play a role in the root core clock as they do in the shoots.

To address these questions, the experiment described in section 4.2 with light-grown roots was repeated in a slightly different way. The results are presented along with controls, i.e. plants with dark-grown roots; these were harvested every 4 h, whereas plants with light-grown roots were harvested every 3 h as before. The differences between experiments presented in section 4.2 and in this section are detailed in chapter 2. To summarise, several steps of the method previously used to process the samples were modified:

- Plant organs (shoots and roots) were harvested a week earlier to make sure no plant was about to flower by the end of the experiment;
- RNA extracts were quantified before and after DNase treatment (this treatment can degrade some RNA), and their quality was then systematically checked;
- oligo dT was used as the primer for the cDNA synthesis instead of random hexamers;
- SYBR I was replaced by SYBR III in the master mix for RT-qPCR;
- *ISUI* was used as a reference gene to normalise data instead of *UBQ*.

Overall this modified protocol reduced the variability of data points. It was therefore adopted by the laboratory.

Figure 4.4 and Table 4.2 show the results obtained for plants with light- or dark-grown roots. In both conditions, transcript profiles are very similar in shoots (Figure 4.4.A). Shoots with light- or dark-grown roots are labelled SL and SD respectively. The averages of SL and SD FRPs in LL were not significantly different ($P=0.328$, Figure 4.4.D),

contrary to the results presented in section 4.2 where slight differences in light conditions between experiments gave different FRPs for SL and SD (Figure 4.1). The FRPs in SLs are consistent with previous results (~22 h) and less variable compared to FRPs in SDs where the FRPs are ~22 h for morning genes, but ~24h for evening genes FRPs (Table 4.2). However this experiment needs to be repeated before any firm conclusion can be drawn.

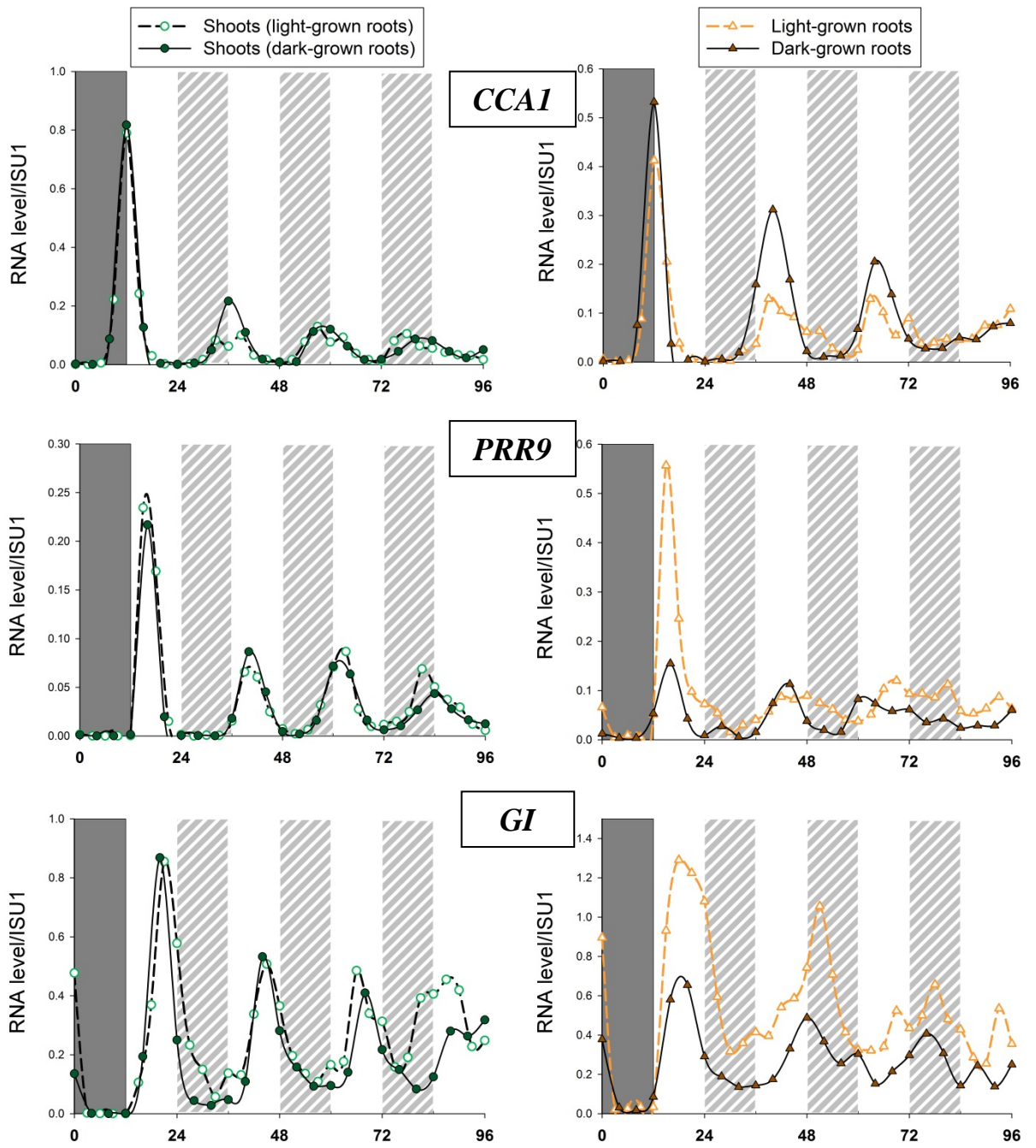
The amplitude for *PRR9* in SL was similar to that in SD; the same was true for *GI* (Table 4.2). But *TOC1* and *CCA1* amplitudes showed more differences between these sets of data (i.e. between SL and SD). For *CCA1*, this may be due to only one time-point: at ZT36 (Figure 4.4 top left), the level of *CCA1* RNA seems abnormally low in the shoots with light-grown roots compared to the control, whereas the rest of the time course is almost the same in both conditions. There might have been something wrong with this sample (which should have been repeated), and the low level when a peak was expected could explain a reduced amplitude. Overall shoot transcript profiles were very similar in both conditions.

On the other hand, transcript profiles differed markedly in roots whether they were exposed to light or not (light- or dark-grown roots, labelled RL and RD respectively). Overall, transcript levels were higher in RL compared to RD except for *CCA1* (Figure 4.4). The lower levels in *CCA1* when roots were exposed to light (compared to dark-grown roots) were consistent with the work of Yakir and colleagues: *CCA1* RNA was more stable in the dark than under light (Yakir *et al.*, 2007). Although *PRR9* levels were similar in both conditions under LL, its peak in LD was much higher in RL compared to RD (Figure 4.4.B), which was consistent with the imaging data (section 4.3). It was even higher than in shoots. Surprisingly no rhythm of *PRR9* transcript levels in dark-grown roots was detected under LL here (Table 4.2) so the amplitude cannot be compared between RD and RL in constant conditions.

In LD the amplitudes were significantly lower in dark-grown roots compared to shoots for all genes, but the amplitudes in light-grown roots were much more variable: light affected differentially gene expression in roots (Figure 4.4.B&C). For instance *PRR9* expression was more induced in light-grown roots compared to dark-grown roots and shoots, but *CCA1* amplitude seemed to be lower in light-grown roots compared to dark-grown roots.

A. SHOOTS

B. ROOTS



Organ specificity in the plant circadian clock

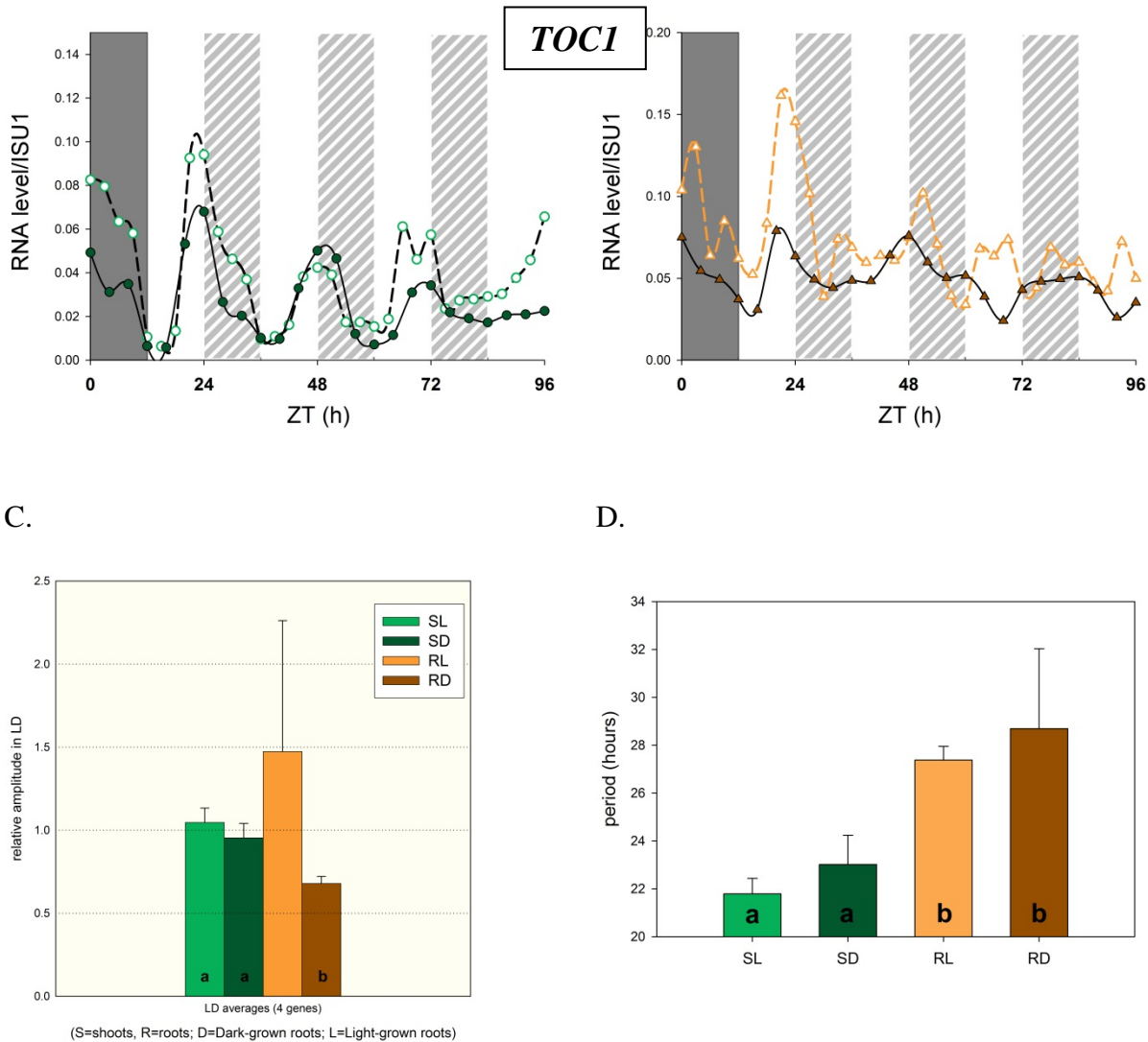


Figure 4.4: Direct exposure to light affects clock gene transcript levels in roots

Plants were grown in hydroponic culture with their roots in transparent or dark boxes (for light- and dark grown roots respectively). Plants were entrained 4 weeks in LD before release in LL.

A and B: Transcript levels of *CCA1*, *PRR9*, *GI* and *TOC1* in shoots (A) and roots (B) for plants with light-grown roots (i.e. exposed to the same light/dark conditions as shoots) or with dark grown roots; mRNA levels are normalised to *ISU1*. White and hatched bars represent light (days and subjective nights respectively), dark bars represent nights.

Data from A and B were used to estimate amplitudes and periods of clock genes in Shoots (S) and Roots (R) with Light-grown (L) or Dark-grown (D) roots.

C: Relative amplitudes under LD. For each individual time-course in A and B, the raw amplitude was estimated as the difference between peak and trough values during the last DL cycle (ZT0-24). This raw amplitude was normalised to the average amplitude in shoots (i.e. average of 2 values from SL and SD). The normalised amplitudes were then averaged for each condition (i.e. SL, SD, RL and RD). Different letters on the bars indicate significantly different groups ($P < 0.001$) according to a one way ANOVA test; RL was not considered in this analysis.

D. Average Free Running Period (FRP) of shoots (S) and roots (R) clock gene expression for plants with light-grown (L) or dark-grown (D) roots. Individual FRP were estimated from data presented in A and B, using BRASS. Different letters on the bars indicate significantly different groups ($P < 0.001$) according to a 2 way ANOVA test. The controls (plants with dark-grown roots) were from Sullivan *et al.* (unpublished)

In both LD and LL *GI* and *TOC1* transcript levels were higher in RL compared to RD (Figure 4.4.B), and *GI* had a higher amplitude in RL compared to RD (Figure 4.4 and Table 4.2). Indeed *GI* RNA levels were rhythmic in both RL and RD under LL, which was consistent with imaging data (section 4.3). And although *TOC1* was not scored rhythmic in RL for this set of data (contrary to section 4.2 where it was), *TOC1* was rhythmic in RD under LL! Again this is only one set of data, but it is consistent with other results: *TOC1* and *GI* promoter activities are circadian in light-grown roots, but also dark-grown roots and they are circadian in shoots. Their rhythms may not always be detected in dark-grown roots because of a lower signal/noise ratio; for instance, the *GI* mRNA amplitude is almost doubled when roots are exposed to light (RL) compared to control (RD) (Table 4.2), which makes the rhythm easier to detect when roots are exposed to light.

Although transcript profiles differed markedly in roots whether they were exposed to light or not, their average FRP was similar in both conditions. There was no significant difference between RL and RD average FRPs ($P < 0.001$, Figure 4.4.C). It confirmed the previous RT-qPCR results (section 4.2).

Table 4.2: FRP and amplitudes of clock gene transcript levels in shoots and roots under LL

Values are estimates from all data presented in Figure 4.4 using BRASS. L = Light-grown roots, D = Dark-grown roots, L/D = ratio of L and D amplitudes. "Average" represents the averages of clock genes scored rhythmic. ND; Not Determined (i.e. not scored rhythmic)

		FRP (LL)		Amplitude (LL)		
		L	D	L	D	L/D
SHOOTS (S)	<i>CCA1</i>	21.91	21.99	0.04	0.06	0.66
	<i>PRR9</i>	21.53	21.96	0.03	0.03	1.05
	<i>GI</i>	21.09	23.85	0.16	0.15	1.11
	<i>TOC1</i>	22.63	24.28	0.02	0.02	1.27
	<i>average</i>	21.79	23.02			
ROOTS (R)	<i>CCA1</i>	27.03	25.70	0.04	0.09	0.41
	<i>PRR9</i>	28.04	ND	0.03	ND	ND
	<i>GI</i>	27.08	28.09	0.21	0.11	1.86
	<i>TOC1</i>	ND	32.29	ND	0.01	ND

	<i>average</i>	27.38	28.69	
--	----------------	--------------	--------------	--

In conclusion, most results of previous sections (4.2 and 4.3) were confirmed qualitatively: shoot and root clocks have differences in FRP and amplitudes, and light can affect the root clock. Direct exposure to light did not seem to affect the FRP in roots: clock genes had a similar FRP in light- and dark-grown roots, and these FRP were longer compared to the FRP in shoots. There were some quantitative differences with previous RT-qPCR results: although FRP in shoots were similar to the values presented in section 4.2, more differences could be observed in roots. This might be due to greater variability in roots, where the expression was usually lower compared to shoots. The RT-qPCR experiments should be repeated several times in the same conditions. However, taken together the results presented in sections 4.2 – 4.4 are qualitatively consistent.

Light increased expression levels and amplitudes of several clock genes in roots. Notably the amplitude of *GI* was higher under LD and LL when roots were exposed to light than in dark-grown roots, and the peak of *PRR9* in LD was higher in light-grown roots compared to dark-grown roots and shoots. This is consistent with shoot data where both *GI* and *PRR9* are known to be induced by light, with *PRR9* expression being particularly induced after dawn but quickly dampened under LL in seedlings (Pokhilko *et al.*, 2012). In LD the amplitudes were lower in dark-grown roots compared to shoots: this is in agreement with imaging data (section 4.3) and it was missed in previous studies and in section 4.2 due to different methods of analysis.

Our improved RT-qPCR protocol allowed us to detect *GI* and *TOC1* rhythms in dark-grown roots. This was in contrast with a previous study (James *et al.*, 2008). Therefore shoot and root clocks seem to be more similar than previously thought:

- They may share many components; not only morning genes (*CCA1*, *LHY*, *PRR9* and *PRR7*) but probably some evening genes too (*GI*, *TOC1* and possibly *LUX* and *ELF4*). In fact a recent microarray⁴ showed that *LUX* and *ELF4* were rhythmic in dark-grown roots

⁴ *LUX* and *ELF4* were arrhythmic in roots under LL in the first microarray (James *et al.*, 2008). The second microarray mentioned here was done in similar conditions but Agilent chips were used (instead of Affymetrix chips), and plants were ~1 week younger and only harvested every 4 h (instead of 3 h).

under LL (Sullivan *et al.*, unpublished). The role of some of these genes as root clock components will be further investigated in chapter 6.

- Some clock genes, such as *GI* and *PRR9*, can be induced by light in roots, as well as in shoots. Whether light can actually reset the root clock will be clarified in the next chapter.

Shoot and dark-grown root clocks have significantly different FRP under LL, but their entrainment conditions also differ before release in LL. Different entrainment “histories” could affect the FRP (Aschoff, 1960). If differences between shoot and dark-grown root clocks were caused only by these different inputs and entrainment conditions (i.e. different light conditions), one could expect these two clocks to be even more similar under DD. This will be investigated in the next section.

4.5 The FRP under DD is similar in shoot and root clocks

Under DD the shoot clock had a longer FRP than under LL (Millar *et al.*, 1995b; James *et al.*, 2008). However the root clock FRP did not change much between LL and DD (James *et al.*, 2008). Since the latter experiment was only done once, it is not clear whether results in roots were significantly different between LL and DD conditions. These data suggested that the shoot FRP might be similar (if not longer) compared to the root FRP under DD. The following experiments were carried out to investigate the clock in DD more thoroughly.

Plants expressing different reporters were entrained as usual (4 weeks of LD (12/12) cycle on ½ MS medium without sucrose) before release in DD and imaging. Plants expressed a [clock gene promoter]:LUC+ fusion with one of the following promoters: *CCA1*, *PRR9*, *PRR7* or *GI*. Experiments were replicated three to four times. Results are presented in Figure 4.5.

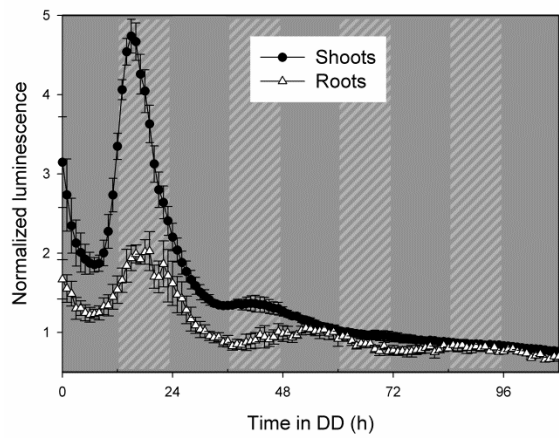
Shoot rhythms dampened very quickly and had very low amplitude after a few days in DD (Figure 4.5 A-D). This was consistent with Dalchau *et al.* (2011): without exogenous sucrose, they could detect rhythmicity in shoots under DD but with lower amplitude (if any rhythm at all) compared to media without sucrose. Surprisingly rhythms seemed to be more sustained in roots (Figure 4.5 A-D).

If the whole time-courses in DD presented in Figure 4.5 were considered when analysing rhythms with BRASS, most time-courses in shoots were scored arrhythmic (Figure A.2 in appendix). The arrhythmicity could be due to quick dampening of a rhythm. But this quick dampening in shoots might have been an artefact of the method: the luciferin-luciferase reaction requires ATP, which presumably declines the longer the plant is in the dark.

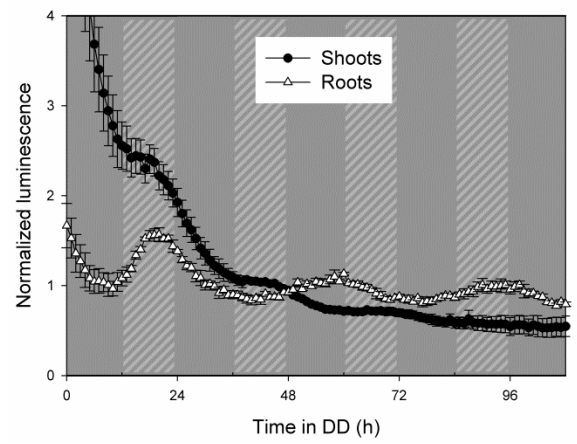
To be able to detect rhythms in both shoots (where oscillations dampened very quickly) and roots for at least two consecutive cycles, the BRASS analysis was performed with the “all windows” mode. Each window was set at 72 h, with an increment of 6 h from ZT0 (last dusk, start of DD). In other words, BRASS algorithms tried to detect rhythmicity from ZT0 to ZT72, then ZT6 to ZT78, *etc.* until ZT36 to ZT108. Then if several windows gave a rhythm for a certain gene, the software automatically chose the window that gave the lowest RAE. In this less stringent way of analysis, more datasets were scored rhythmic and RAE values were lower.

Results presented in Figure 4.5 E and F show the FRP was more variable (both between replicates and between promoters) in shoots compared to roots. Variability in the seedling FRP under DD was also shown for *CAB* expression (Millar *et al.*, 1995b): its FRP was much more variable in DD compared to LL. Interestingly the rhythms seemed more robust in roots under DD (Figure 4.5). Overall the average FRPs of shoots and root gene expression were not significantly different ($P=0.038$ according to a t-test). However, the periods seemed shorter in shoots compared to roots when considering the whole time-course (Figure A.4 in appendix). These experiments under DD should be repeated to determine whether FRPs are significantly different in shoots and roots when comparing the same time windows. Given the very low signals under DD compared to LL (cf examples of row data in Figure A.3, appendix) plants may then have to be imaged one at a time (i.e. closer to the camera) to increase the signal/noise ratio. *TOC1* rhythms were detected neither in roots nor in shoots, possibly because the signal was too low in our conditions. All the other genes studied were scored circadian at least once in both organs, including *GI* in roots (Figure 4.5.E). This was in contrast with previous data of the root clock in DD (James *et al.*, 2008); this experiment in DD using RT-qPCR was therefore repeated and is presented in Figure 4.6.

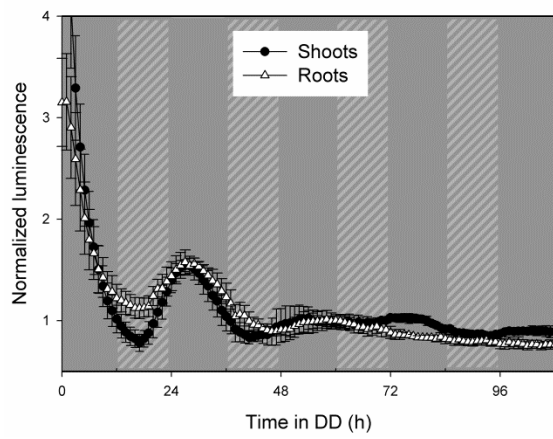
A. *CCA1*



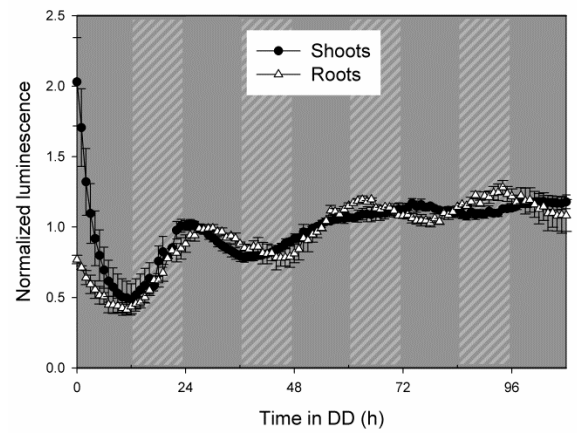
B. *PRR9*



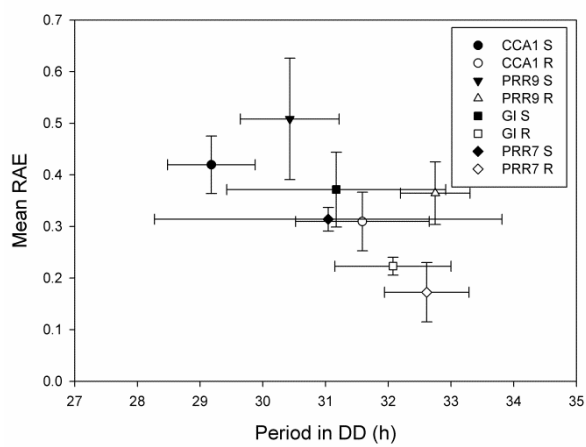
C. *GI*



D. *PRR7*



E.



F.

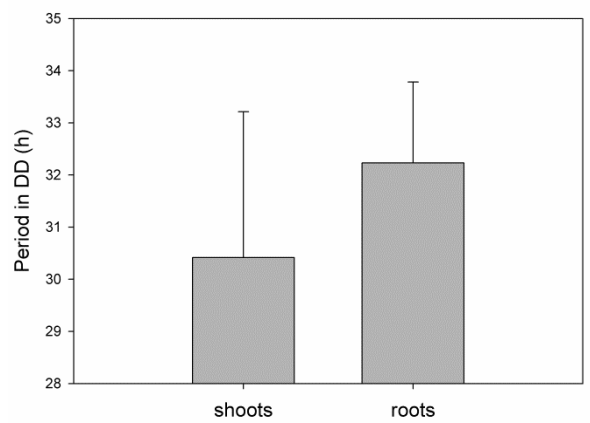


Figure 4.5: The expression of morning and evening genes free run in DD with similar FRP in shoots and roots

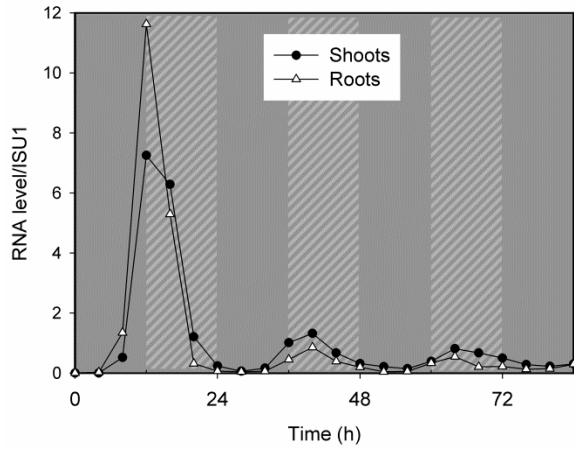
Plants were entrained for 4 weeks in LD (12/12) before release in DD. All the roots were dark-grown. A-D: Luminescence of *CCA1:LUC+*, *GI:LUC+*, *PRR7:LUC+* and *PRR9:LUC+* over 4 days in DD in roots (open symbols) and shoots (closed symbols). Data are averages of 2-4 independent experiments. The data are normalized with the mean value of the corresponding time-course. Error bars are SEM for 2-4 clusters of 3-6 plants (organs) from independent experiments. Hatched bars represent subjective days, dark bars represent subjective nights. E: Circadian period estimates of data presented in A-D using BRASS for roots and shoots. F. Average Free Running Period (FRP) of shoots and root gene expression; individual gene FRPs were from E. The differences between shoot and root FRP averages is not highly significant ($P=0.038$) according to a t-test. Time 0 (=ZT0) is the last dusk before DD

The same experiment as in section 4.4 (with dark-grown roots) but with release in DD instead of LL was carried out by Stuart Sullivan and Janet Laird. Results are presented in Figure 4.6. It confirmed that not only morning genes (such as *CCA1*, *LHY* and *PRR9*) but also *GI* and *TOC1* are circadian under DD (Figure 4.6 A-E). But at the transcript level, rhythms dampened less in shoots compared to previous imaging data. And in this case it was in the roots that amplitudes were lower and FRPs more variable (Figure 4.6). Besides, FRPs were shorter in shoots and roots compared to imaging results (Figure 4.5).

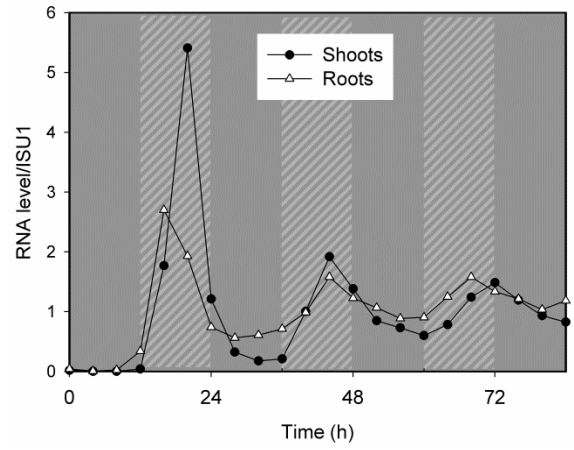
These quantitative differences between Figure 4.5 and 4.6 could be partly due to different techniques used, but also differences in experimental conditions: plants grown in hydroponic cultures (Figure 4.6.) were entrained with higher (white) light intensity until release to DD, whereas plants grown on plates (Figure 4.5.) were entrained with lower (blue and red) light intensity a day before release to DD. As mentioned earlier, the history of the organism under entrainment can influence the FRP, this is known as aftereffect (Johnson *et al.*, 2004). Interestingly the expression profiles of most genes differed mostly during the first day in DD between shoots and roots, i.e. when the very recent history of each organ was significantly different: the shoots were under LD whereas the roots were dark-grown. This was true with both imaging and hydroponic systems (Figure 4.5 and 4.6 respectively).

Nevertheless, both experiments gave similar results qualitatively: most if not all clock genes studied were circadian in shoots and roots under DD and their average FRPs were similar in both organs. These results suggest again that differences between shoot and root clocks may be due to different inputs.

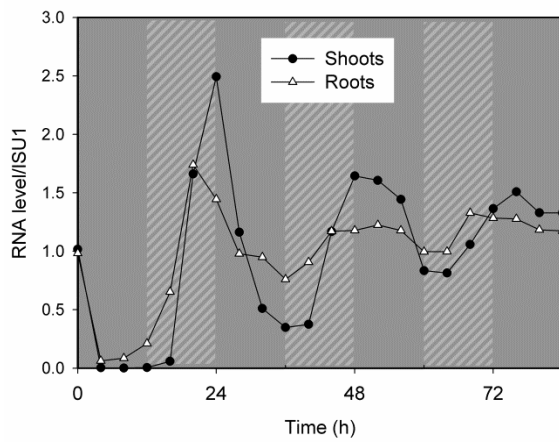
A. *CCA1*



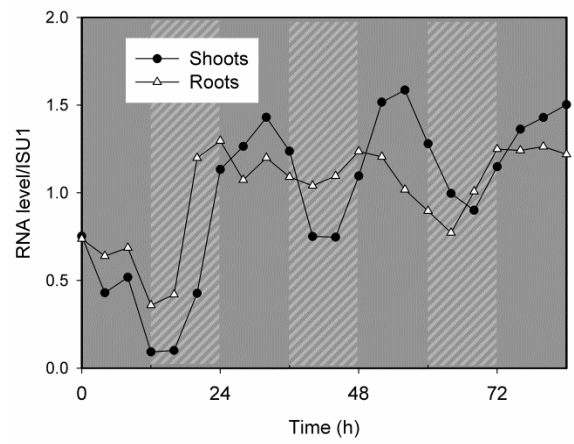
B. *PRR9*



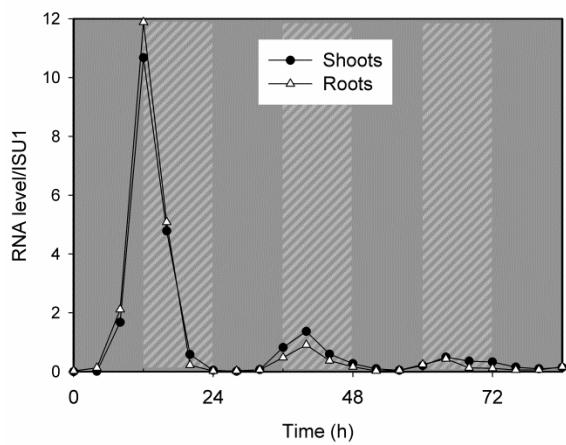
C. *GI*



D. *TOC1*



E. *LHY*



F. Average periods

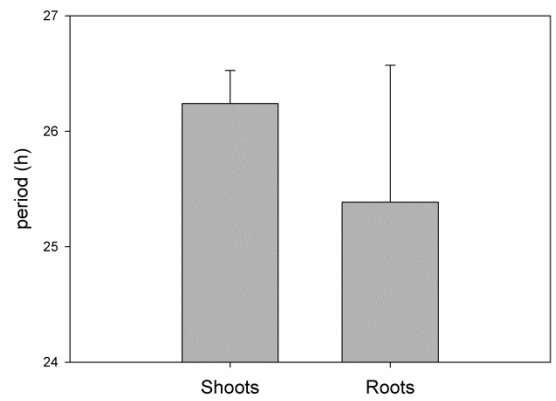


Figure 4.6: Transcript levels of morning and evening genes free run in DD with similar FRP in shoots and roots

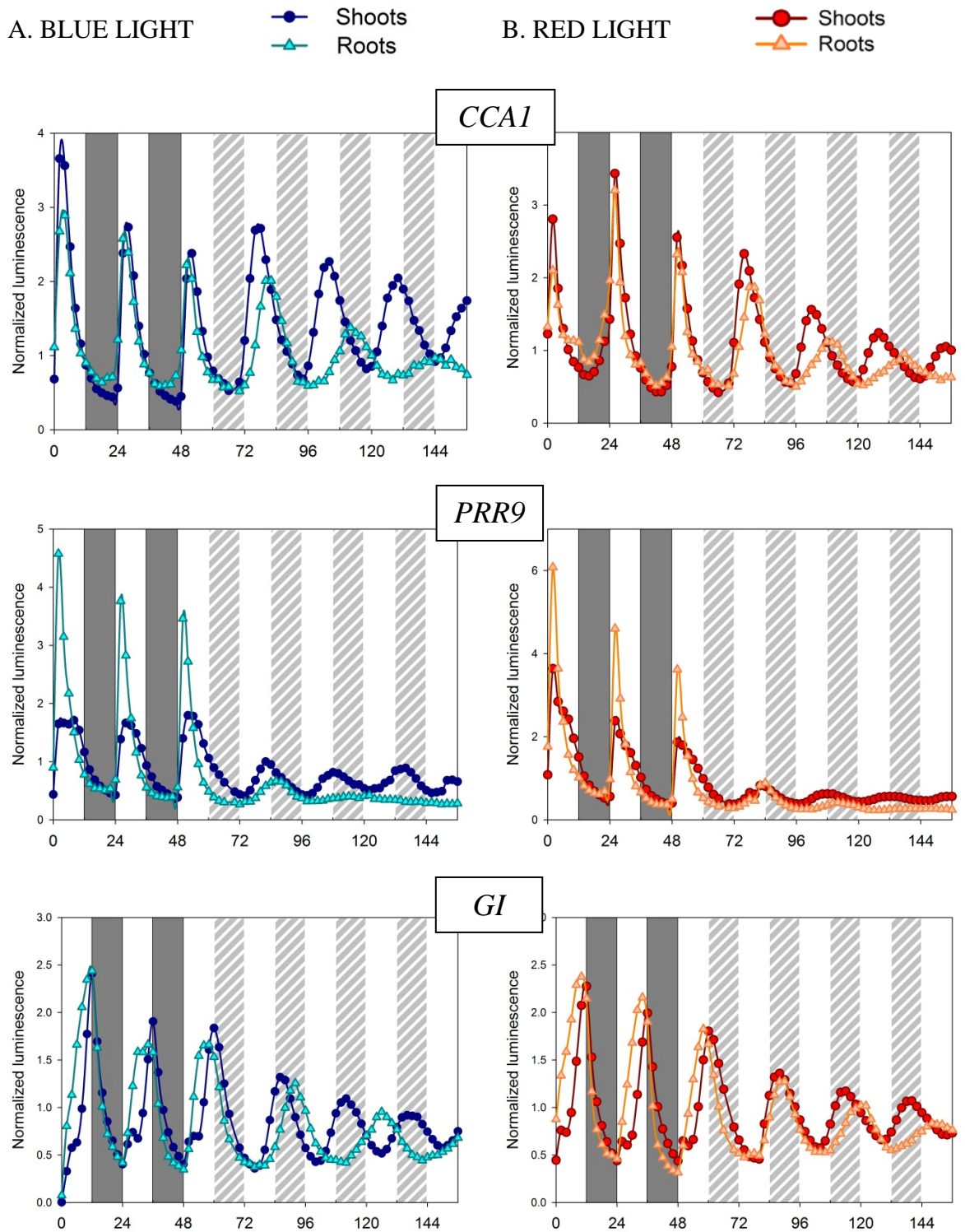
Plants were grown in hydroponic culture with dark-grown roots. Plants were entrained 4 weeks in LD before release in DD. A-E: mRNA levels of *CCA1* (A), *PRR9* (B), *GI* (C), *TOC1* (D) and *LHY* (E) in shoots and roots; mRNA levels are normalised to *ISU1*. Hatched bars represent subjective days; dark bars represent nights (last night and subjective nights). F. Average Free Running Period (FRP) of shoots and root gene expression; individual FRPs were estimated from data presented in A-E, using BRASS. The difference between shoot and root average FRPs is not significant ($P=0.106$) according to a t-test. Data from Sullivan *et al.* (unpublished). Time 0 (=ZT0) is the last dusk before DD

4.6 Both red and blue light can affect the root clock

The clock of dark-grown roots was thought to be indirectly entrained by light, possibly via photosynthate rhythms (James *et al.*, 2008). But in natural conditions, light (especially red and far-red) can actually penetrate through the soil (Tester and Morris, 1987). Even in our soil-free experimental conditions, roots were probably not grown in pitch dark: there could be some light leakage that could reach the roots via the eppendorf tubes going through the black lids, as suggested in Figure 2.1.

The effects of light were studied in this chapter by using combinations of different wavelengths: ~ 460 nm and ~645 nm for blue and red lights (imaging experiments), and the whole visible spectrum for white light (RT-qPCR experiments). Different light qualities can have different effects on the circadian clock. For instance ZTL is a photoreceptor that control *TOC1* stability in a blue light regulated manner (Kim *et al.*, 2007; Mas *et al.*, 2003). The results presented so far were qualitatively similar with either white light or blue and red light: the FRP was longer in roots (dark- and light-grown) compared to shoots, and light could directly affect clock gene in roots.

To investigate whether both blue and red light can affect the root clock, I used imaging. Plants were grown as in section 4.3 with light-grown roots. Briefly, plants were entrained for 3-4 weeks in LD (12/12) under white light with roots exposed to light. For each construct, plants were then imaged 2 days in LD and 4 days in LL (blue or red light) (Figure 4.7).



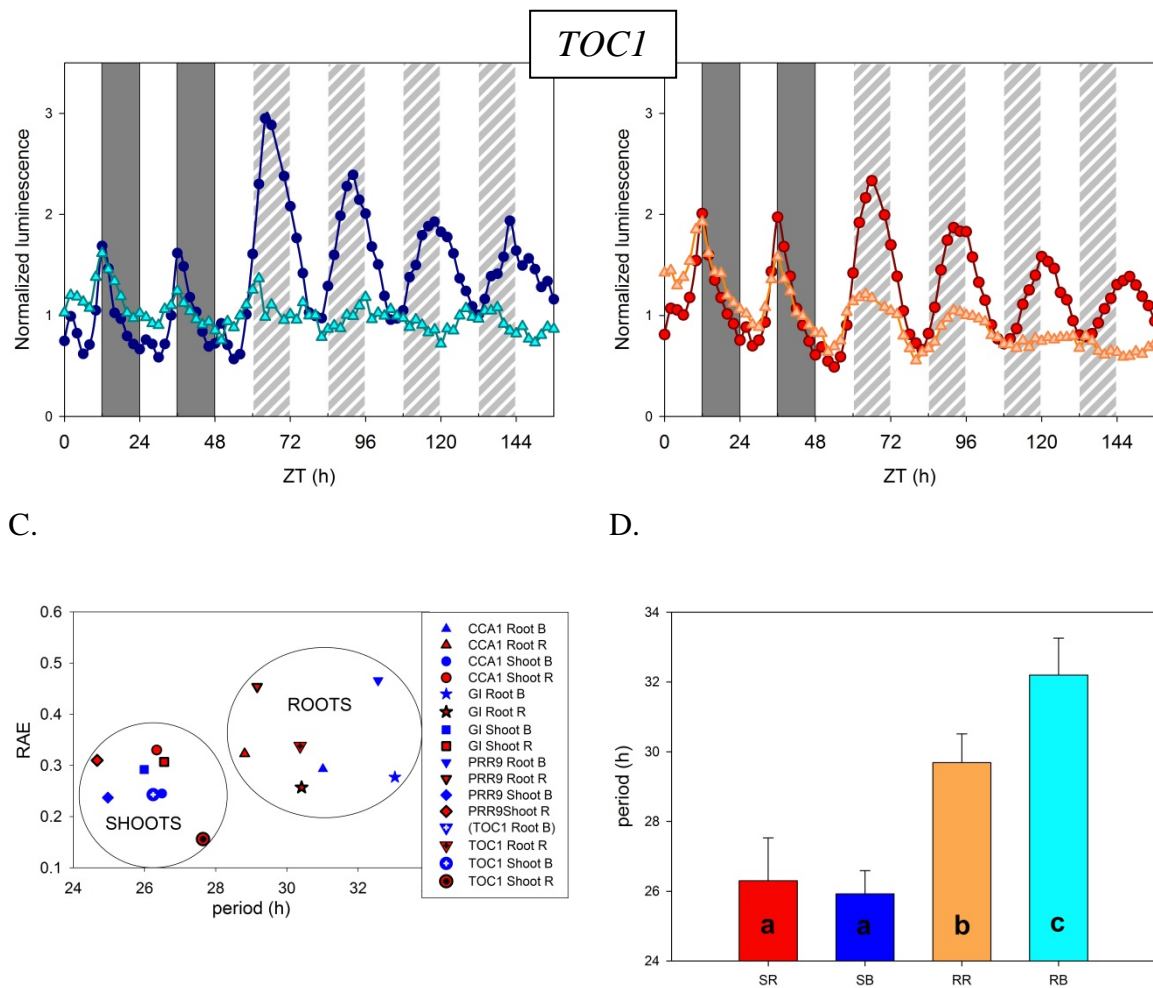


Figure 4.7: Both blue and red light affect clock gene expression in root

Plants were entrained in white LD cycles for 4 weeks, and then imaged for 2 days in LD followed by 4 days in LL, using either blue or red LEDs over these 6 days. Roots were light-grown all the time. A and B: promoter activity of *CCA1*, *PRR9*, *GI* and *TOC1* under blue light (A) or red light (B). Darker colours and circles: shoots; lighter colours and triangles: roots (dark and light blue: blue light; red and orange: red light). Data were normalised with their mean luminescence over the last 24h in LD. Grey bars: dark cycles, white and hatched bars: light cycles (day and subjective days respectively). Data are average luminescence of 1 cluster of 3-6 plants from 1 experiment. C. Circadian period estimates under LL of all time-courses (all genes in shoots and roots) presented in A and B using BRASS. D. Average FRP of shoots (S) and roots (R) clock gene expression for plants under blue (B) or red (R) light. Individual FRP were from fig. C. Different letters on the bars indicate significantly different groups; e.g. shoots (SR and SB) and roots (RR and RB) FRPs are significantly different ($P < 0.001$) and RR and RB FRPs are significantly different too ($P < 0.01$) according to a 2 ways ANOVA test

As for a combination of blue and red light or white light, each of these two wavelengths (blue or red light) could entrain most (if not all) clock genes studied here in roots (Figure 4.7). All rhythms were synchronized between shoots and roots under LD, and FRPs were significantly longer in roots compared to shoots in LL ($P < 0.001$, Figure 4.5 D). There was possibly one exception: *TOC1* was not scored rhythmic in roots under constant blue light; but the signal was very low so it is possible that this precluded detection of oscillations. A

rhythm of ~17 h period could actually be detected, but with a RAE of ~1, i.e. it is not considered rhythmic; this might reveal a 34 h period biphasic rhythm (for instance, the *TOC1* rhythm is biphasic under LD).

The effects of blue or red light on clock gene profiles and amplitude in roots were similar to the effects of a combination of blue and red light. When roots were exposed to light (blue and/or red), *CCA1* and *GI* amplitudes were similar in shoots and roots (under both LD and LL). *PRR9* peaks in LD were higher and sharper in roots compared to shoots. The peak of *GI* in LD was broader and earlier in roots compared to shoots (Figure 4.7 A and B).

There was no significant difference between shoot average FRPs under blue or red light (i.e. between SR and SB in Figure 4.5.D; $P=0.544$). However the root average FRP under blue light was significantly higher than the root average FRP under red light ($P<0.01$, Figure 4.7.D). For both blue and red light, the average FRPs are longer in roots compared to shoots.

Figure 4.8 recapitulates all shoot and root FRPs under LL (with light-grown roots) and DD (with dark-grown roots) obtained in this chapter with imaging. All these periods were used together for a 2 way ANOVA test. This analysis confirmed that for each LL conditions (red, blue, or red and blue light) the FRP is longer in roots compared to shoots.

It also showed that different light qualities had different effects on shoot and root clock FRPs, as detailed below.

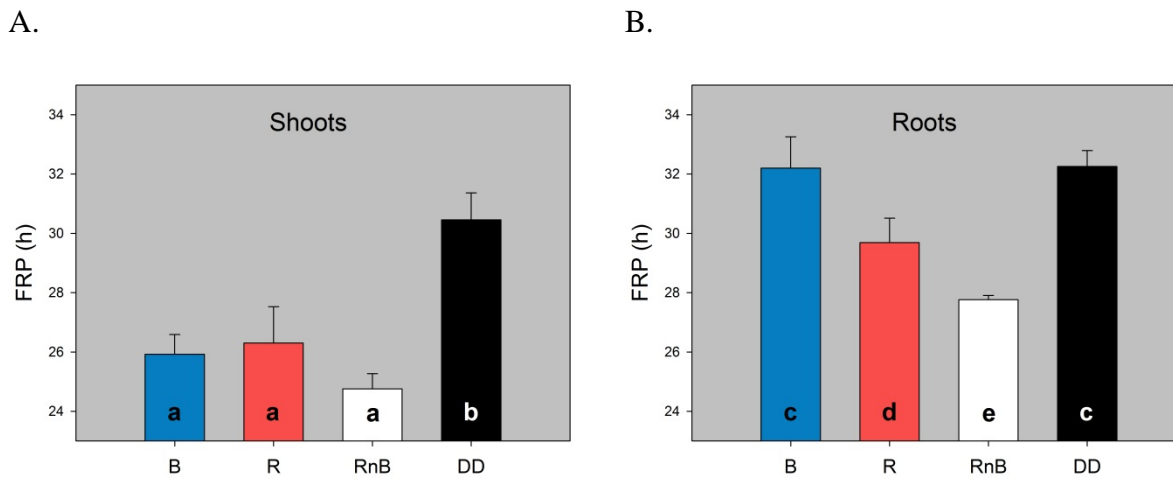


Figure 4.8: Comparison of FRPs in shoots and roots in various conditions

Average FRP of shoots (A) and roots (B) clock gene expression for plants under constant light (blue (B), red (R) or red and blue (RnB) light) or constant dark (DD). Individual FRP were from Figure 4.3 (light-grown roots), 4.5 and 4.7. Different letters on the bars indicate significantly different groups; e.g. all roots FRPs are significantly different in LL (under blue, red and red and blue light), and significantly different from the shoot FRPs in LL ($P < 0.001$) but root FRP are not significantly different between Blue LL and DD ($P = 0.929$) according to a 2 way ANOVA test.

Shoot FRPs were on average longer (~ 26 h) under blue or red light compared to their average FRP under blue and red light (~ 25 h); but the differences were not highly significant ($P > 0.02$, Figure 4.8.A). This was consistent with Aschoff's rules: indeed the light intensity was halved in this "blue or red experiment" compared to the "blue and red experiments" of section 4.3. In both experiments, each wavelength gave a $7-8 \mu\text{mol}\cdot\text{m}^{-2}\cdot\text{s}^{-1}$ irradiance, i.e. $\sim 15 \mu\text{mol}\cdot\text{m}^{-2}\cdot\text{s}^{-1}$ when blue and red were combined. Therefore lower light intensity increased FRP in shoots as expected. In addition, the shoot FRP was significantly higher in DD compared to any LL conditions ($P < 0.001$, Figure 4.8.A).

On the contrary, different light qualities had different effects on the root clock FRP (Figure 4.8.B). Red as well as red and blue light both significantly shortened the root clock FRP compared to DD ($P < 0.001$) but to a lesser extent compared to their effect on the shoot clock FRP. Besides, a combination of red and blue shortened the root clock FRP more compared to red or blue light separately ($P < 0.001$); again this was consistent with Aschoff's rules (the total intensity was doubled in red and blue light condition). But there

was also a significant difference between blue and red light ($P=0.001$), and blue light did not shorten the root clock FRP compared to DD ($P=0.929$).

In conclusion, both blue and red light seemed to have similar effects on the clock gene amplitudes: clock genes had a similar profile under red, blue, and red and blue light. But red light may have a greater effect in shortening the root FRP. It is important to note that the experiments presented in this section have only been carried out once. Although their results are consistent with previous data, they should be repeated before drawing any firm conclusions. It would be particularly interesting to further investigate the possible distinct effects of blue and red light on the root clock.

4.7 Conclusion

The main question addressed in this chapter was: is the root clock different from the shoot clock just because the roots are virtually in constant darkness, whereas the shoots are exposed to light and dark? The answer is no. There are differences between shoot and root circadian systems. Otherwise, clock genes would have more similar profiles in shoots and light-grown roots. But they do not: the FRP are significantly longer in roots compared to shoots in LL. This was demonstrated with imaging and RT-qPCR experiments, and in different conditions with the same light on shoots and roots: blue, red or white light (Figure 4.1.C, 4.3 E&F, 4.4.D, 4.7 C&D, Table 4.1 & 4.2).

There were quantitative differences between imaging and RT-qPCR data in terms of FRP. The period estimates in shoots under LL were higher for imaging data compared to RT-qPCR data. But this was likely due to the lower light intensities used for imaging and is consistent with Aschoff's rules. These rules apply to diverse organisms including plants, at least for shoots. For instance Somers and colleagues showed that with either blue or red constant light, the lower the intensity, the longer the FRP of *CAB* expression in *Arabidopsis* (Somers *et al.*, 2004). But Aschoff's rules have not been tested in roots yet, and I did not aim to do this (otherwise I would have used a range of light intensities with the same light quality). Although different intensities were used in this chapter, the light quality varied as well. In the diverse light conditions used here (red and/or blue, white

light) the FRP in roots were variable but without any clear trend. Nevertheless the FRP were always higher in roots compared to shoots.

Another key difference between shoot and root clock gene expression is their amplitude in LD. The amplitudes of all the clock genes studied in this chapter were lower in dark-grown roots compared to shoots. This was first revealed with imaging (Figure 4.3.A&B), and then confirmed with RT-qPCR (Figure 4.4.C). However the amplitudes of clock promoter activities were always higher in light-grown roots compared to dark-grown roots, getting closer to the amplitudes in shoots. For instance the amplitudes were not significantly different in shoots and light-grown roots under LD with imaging (Figure 4.3.B). This similarity between shoots and light-grown roots under LD was not observed at the mRNA level: light affected differentially the relative amplitudes of clock genes in light-grown roots compared to shoots. For instance the amplitudes of *CCA1* and *PRR9* were respectively lower and higher in light-grown roots compared to shoots.

Differences in amplitudes were also observed in LL between light- and dark-grown roots (Figure 4.2.B, 4.3 and 4.5). Light could differentially affect clock gene expression in roots. The most striking examples were when dark-grown roots under LL were suddenly exposed to light: their expression increased greatly, especially for evening genes (Figure 4.2.B). However this induction by light was not the same for all genes and seemed to be gated by the clock. The amplitudes of clock genes in roots exposed to light were also more variable at the mRNA level compared to dark-grown roots: they seemed to be increased only for evening genes whereas they were decreased for morning genes. On the other hand, the relative amplitudes in dark-grown roots compared to shoots were more stable and lower, which made some rhythms harder to detect.

However this chapter also revealed similarities between the shoot and root clocks. Many components of the shoot clock are also circadian in the roots at the transcript level. This includes evening genes such as *GI* and *TOC1* that were previously thought to be arrhythmic in dark-grown roots. Their rhythmicity in various conditions (LD, LL and DD) could be detected here with the imaging system I developed, and also with an improved protocol for RT-qPCR experiments. However *TOC1* rhythms were usually weak and not always detected in roots: this does not necessarily mean that *TOC1* was arrhythmic in some cases; indeed a low amplitude rhythm can be missed depending on the variability and the

method used. This highlights the interest in using different techniques and different conditions. To illustrate this point, let us go back to the example of *GI* rhythm in roots. It was first detected by RT-qPCR when this organ was exposed to light. This was confirmed with imaging in similar conditions (i.e. with light-grown roots). Using imaging revealed that *GI* promoter activity was also circadian in dark-grown roots, in LD, LL and DD. *GI* rhythmicity was therefore questioned at the mRNA levels, and an improved RT-qPCR protocol finally revealed *GI* rhythms in dark-grown roots under LL and DD, at the transcript level. In the end, *GI* was scored rhythmic in every condition and with both methods. Although rhythms were weaker for *TOCI* compared to *GI*, they could be detected at least once in each condition, i.e. in LD and LL with light- and dark-grown roots, and also in DD. Taken together, the results presented in this chapter suggest that the root clock contains evening genes too, as the shoot clock does.

Interestingly both morning and evening genes were rhythmic in roots under DD, and with a similar FRP than in shoots (Figure 4.5 and 4.6). The rhythms dampened quickly in this condition, they were more variable and not always detected. Nevertheless, the similarities between shoot and root clocks under DD suggest that the differences observed between their mechanism in LD and LL might be explained by different light input pathways in these two organs. Indeed different input pathways feeding the clocks of shoots and light-grown roots could result in different gene expression in each organ, which in turn could give different FRPs under LL. For instance roots under constant blue light had a similar FRP than roots under DD, whereas constant red light shortened the FRP of roots. On the contrary, both blue and red light shorten the FRP in shoots compared to DD. These results presented in section 4.6 indicate that blue and red light may have differential effects on shoot and root clocks.

More generally light can differentially regulate gene expression in different organs of *Arabidopsis* and rice, including roots (Jiao *et al.*, 2007). Roots can express photoreceptors whether they are light-grown on plates (Toth *et al.*, 2001) or dark-grown in hydroponic culture (Sullivan *et al.*, unpublished). Some phytochromes and cryptochromes are even circadian regulated in roots. In addition, some photoreceptors can be functional in this organ: for instance root-localised phytochromes can play a role in root elongation and sensitivity to jasmonic acid (Costigan *et al.*, 2011). Therefore the study of light effects in the roots is relevant physiologically.

However roots usually grow in the dark. That is why our imaging system was adapted to keep roots in darkness. In natural conditions, light can penetrate through the soil (Tester and Morris, 1987) but the intensity reaching the roots are usually much lower compared to the shoots. And in natural conditions, most plants grow under LD cycles. Therefore the effects of light were further studied by using different light intensities and under diurnal conditions, as described in the next chapter.

5 Entrainment of the root circadian clock

5.1 Introduction

As we have seen in the general introduction, most organisms have an internal clock that allows them to anticipate rhythmic changes such as LD and temperature cycles. To be synchronised with these environmental rhythms, the circadian clocks are reset by external cues. The main zeitgebers for plants and other organisms are light and temperature. In shoots, the clocks of different tissues that were completely out of phase under LL were resynchronised within a few days after transfer to LD cycles (Wenden *et al.*, 2012). One can wonder whether such a rapid resynchronisation could also occur between shoot and root tissues.

It is not clear which mechanisms entrain the root clock. When *Arabidopsis* plants were grown at constant temperature and with their roots in dark boxes, the root clock was still entrained under LD cycles (James *et al.*, 2008). How could dark-grown roots at constant temperature be entrained? Experiments using sucrose or DCMU (a specific inhibitor of photosynthesis) suggested that the root clock could be entrained by light indirectly, e.g. via photosynthate (James *et al.*, 2008). These experiments used plants grown in hydroponic culture and RT-qPCR to quantify their clock gene expression over time. In this chapter I further investigated the entrainment of the root clock using imaging and RT-qPCR.

The previous chapter showed that exposure of the roots to “high” light intensity can have a strong effect on clock gene expression in this organ. Could lower light levels have a significant effect on the root clock too? Small amounts of light can penetrate through the soil (Tester and Morris, 1987), and photoreceptors are expressed in dark-grown roots (Sullivan *et al.*, unpublished). Therefore direct entrainment of the root clock by LD cycles might be relevant physiologically. Such entrainment has been shown previously but with light-grown roots (Thain *et al.*, 2000). The authors exposed shoots and roots to opposite LD cycles and observed that the expression of CHS was in antiphase in shoots and roots. In these experiments shoots and roots were exposed to the same white light ($250 \mu\text{mol.m}^{-2}.\text{s}^{-1}$). This indicated that the root clock could be directly entrained by LD cycles, and also suggested that the clocks of different tissues may not be coupled. However, roots are

usually not exposed to high light intensity, which may have masked any coupling in the experiments of Thain *et al.* I also used conflicting LD cycles to consider the possible coupling between shoot and root clocks, but by exposing dark-grown roots to lower light intensities.

The sensitivity of an oscillator to an entraining signal can be studied by using T cycles of different zeitgeber strength (Abraham *et al.*, 2010). The shoot clock can be entrained by photocycles of different periods (T), in a range between T = 20 h and T = 32 h at least (Roden *et al.*, 2002), but the light intensity used was $80 \mu\text{mol.m}^{-2}.\text{s}^{-1}$ in this study. I have tested a broader range of T cycles with lower light intensity to explore the sensitivity of shoot and root clocks to LD cycles.

The shoot clock is particularly sensitive to the light/dark transitions at dawn and dusk since it can be entrained by skeleton photoperiods (Millar, 2003). Pokhilko *et al.* used skeleton photoperiods to test their predicted regulation of *LHY/CCA* by its inhibitors (Pokhilko *et al.*, 2010). In that case theoretical work – updating of the mathematical model – preceded validation by experiments. Here the experiments were carried out before modelling. I asked whether the root clock could be entrained by skeleton photoperiods because this could provide further information about the clock mechanism and might also reveal additional differences between shoots and roots.

This chapter focuses mainly on entrainment by LD cycles, but also considers entrainment by temperature cycles. Indeed thermocycles seem an obvious zeitgeber for dark-grown roots in a natural environment.

5.2 The clocks of shoots and illuminated roots are out of phase in LL and quickly resynchronised in LD cycles

In chapters 3 and 4 the shoot and root clocks were investigated under constant conditions following entrainment in LD cycles. To test whether the shoot and root clocks would be re-entrained after several days in LL, clock gene expression was monitored over several days in LD cycles both before and after a period in LL.

The results presented in Figure 5.1 confirm that shoot and root clocks have different FRPs in LL (Figure 5.1 A-D) and also show that both clocks can be very quickly resynchronised

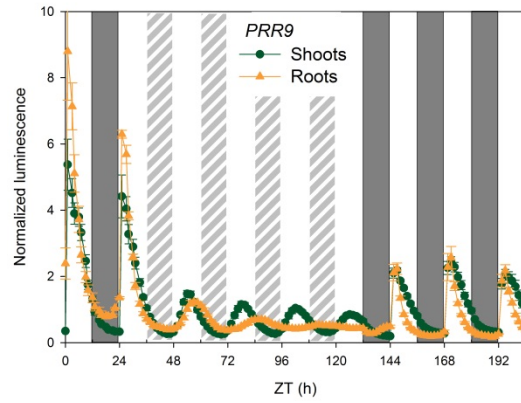
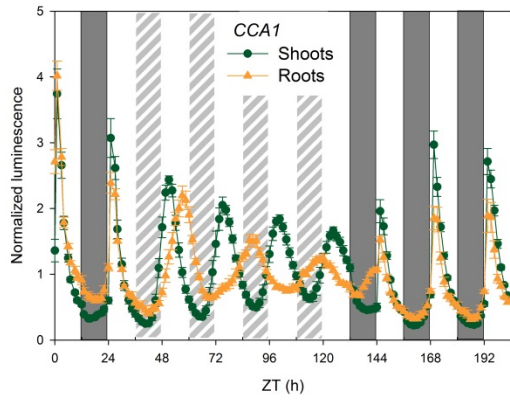
under LD conditions (Figure 5.1 A-C, E). After only one dark period (ZT 132-144), shoot and root clocks that were desynchronised under the preceding LL were in phase again (Figure 5.1 A-C).

Interestingly morning and evening genes seemed to react in different ways: *TOC1* and *GI* expression decreased abruptly from ZT132 (i.e. as soon as the first dark cycle following LL started), whereas *CCA1* and *PRR9* profiles changed dramatically only 12h later: they were greatly induced after ZT144 (i.e. at the first dark to light transition following the LL period). This transient LD cycle (ZT132-156) had a very similar effect on evening genes in both shoots and roots. However, it seemed to affect morning and evening genes differently: *CCA1* and *PRR9* become synchronised in shoots and roots only after the DL transition (from ZT144). It indicates that morning genes may be reset at dawn rather than dusk, whereas evening genes might be reset at dusk (and possibly at dawn too).

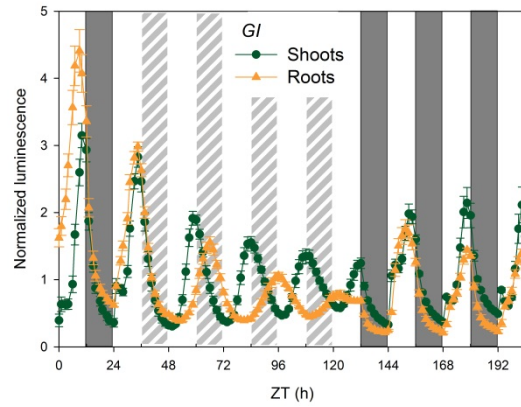
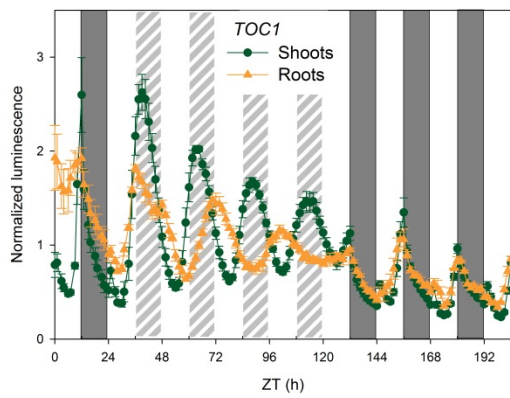
Similar results were obtained with output genes (Figure 5.1.C). Shoots and roots were in phase in LD cycles, but roots had a longer FRP in LL compared to shoots. After the LL period, *CCR2* behaved like the other evening genes: its resetting seemed to be stronger at dusk than dawn. Interestingly *CAT3* (*CATALASE3*), which peaks in the middle of the day, seemed to be strongly reset at both dawn and dusk. However this could be a masking effect: the promoter of *CAT3* seemed to be most active during the light period in both organs.

Thus this experiment confirmed previous conclusions, including that *TOC1* is rhythmic in light-grown roots. It also showed that roots and shoots could be rapidly re-synchronised in LD cycles. It may take a few more days for the shoots to adopt a stable phase angle with the LD cycles following LL. This would be consistent with published results (Wenden *et al.*, 2012), where a full resynchronisation of shoot tissues were observed within 2-4 days, and would explain why rhythms in the shoots were different from 24 h (Figure 5.1.E). The roots and shoots were exposed to the same LD conditions. The entrainment of the root clock by these LD cycles could be either direct or indirect. Each of these possible mechanisms was investigated and the results are presented in the following sections.

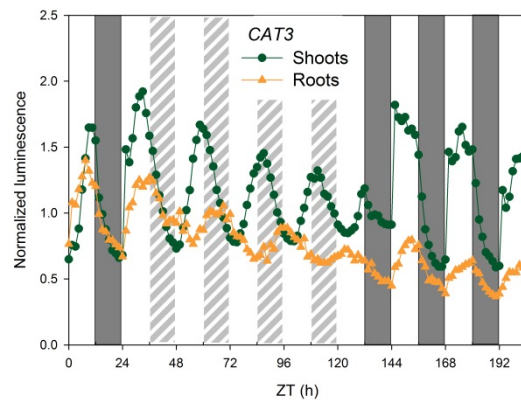
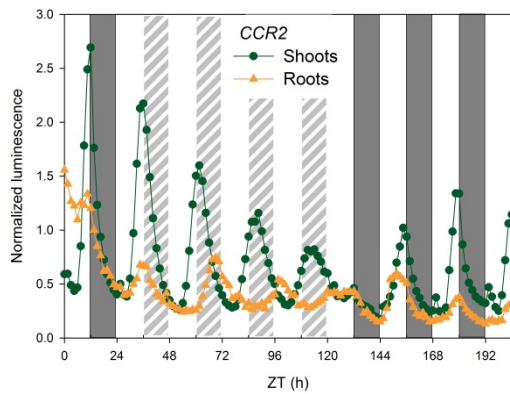
A. Morning genes



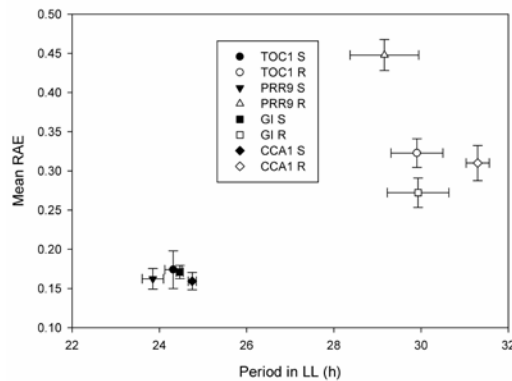
B. Evening genes



C. Output genes



D.



E.

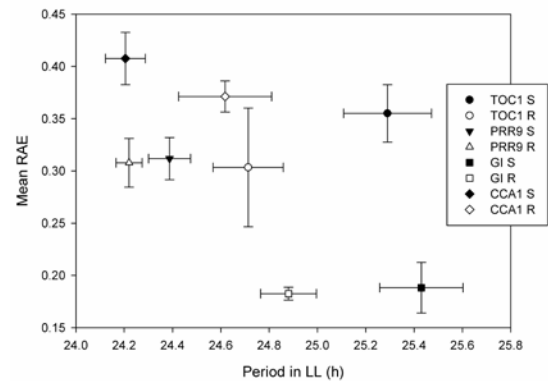


Figure 5.1: the FRP is longer in roots compared to shoots in LL, but both organs are synchronised in diurnal conditions

Plants with different LUC+ reporter were entrained for 3-4 weeks in LD (white light) before imaging (blue and red light); roots were all light-grown (i.e. exposed to the same light/dark conditions as shoots). Plants were then imaged for 24 h in LD before release in LL and re-entrainment in LD.

A-C: Bioluminescence over time of shoots and roots for morning genes (A: *CCA1* and *PRR9*), evening genes (B: *TOC1* and *GI*) and output genes (C: *CCR2* and *CAT3*). Experiments for A and B were repeated at least twice, whereas C is a single experiment.

Green lines and circles represent shoots; orange lines and triangles represent roots. Bars in the backgrounds represent days or subjective days (white bars), night (dark grey bars) and subjective night (hatched bars). Error bars are SEM for 2-3 clusters of 3-6 plants/organs (from 2-3 independent experiments).

D and E: Circadian period estimates for *CCA1*, *PRR9*, *TOC1* and *GI* promoter activities (S = shoots, black symbols; R = roots, white symbols) in LL (D) and LD (E) using BRASS. The first day of LL and LD were discarded for this analysis.

5.3 The root clock can be entrained by direct perception of light

The previous section showed that the clock of light-grown roots is entrained by LD cycles. This entrainment could be achieved by direct exposure to light or indirectly through a rhythmic signal from shoots. To rule out this possible indirect effect in the case of light-grown roots, and ask whether light can directly entrain the root clock, some plants were decapitated.

Plants with the *GI:LUC+* reporter gene were used. Roots were either light- or dark-grown; a bright field image and the corresponding luminescence are shown in Figure 5.2.A and B. Plants were first entrained in LD cycles for 3.5 weeks, and then imaged for 13 days: 4 days in LD, 4 days in LL and another 5 days in LD. Half of the plants were decapitated at ZT24 (before dawn). Results are presented in Figure 5.2.

GI expression profiles were almost superimposable in shoots with light- or dark-grown roots (Figure 5.2.D) as expected (indeed the shoots were all in the same light conditions, whereas the roots were not). Rhythms under LD cycles had a 24 h period, but the FRP was longer in LL (Figure 5.2 D, G, H). This is consistent with previous results (Figure 5.1 and previous chapter) and could be considered as an internal control.

Figure 5.2.C shows the result of decapitation for plants with light-grown roots. *GI* behaved as expected in the control roots: it had a 24 h rhythm under LD cycles (Figure 5.2 C, G) but a longer FRP in LL (~30 h; Figure 5.2 C, H), which is consistent with previous results (Figure 5.1 and previous chapter). Interestingly the *GI* expression profile was similar in the roots of decapitated plants, although levels of expression were lower in decapitated plants compared to the controls. This might be due to lower energy levels in these roots that are deprived of their shoots. Nonetheless, the periods of *GI* expression were also 24 h under LD and longer under LL in decapitated plants. Therefore *GI* expression can be entrained by direct exposure to light in roots.

The results were very similar for dark-grown roots (Figure 5.2.E). In this case plants were under the same conditions as before (Figure 5.2.C) except that the roots were always kept in the dark, i.e. roots were effectively in DD. For the control (non-decapitated) these dark-grown roots had a 24 h rhythm in diurnal conditions (Figure 5.2 E and G). This is consistent with previous RT-qPCR data and was thought to be the result of indirect entrainment via shoots which are directly exposed to LD cycles (James *et al.*, 2008). The decapitated plants maintained a 24 h rhythm in “LD” (ZT24-96) as well (Figure 5.2 E and G). This is surprising because they were expected to free run (with a FRP>24 h) as under DD (Figure 5.2.F). The decapitated plants with dark-grown roots also free ran in LL with an FRP longer than 24 h (ZT96-208 in Figure 5.2.E and Figure 5.2.H). These dark-grown roots that were decapitated were therefore entrained, which was unexpected.

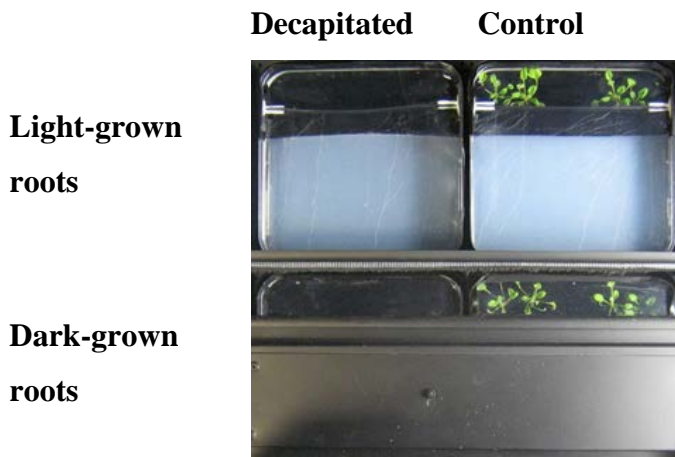
There are at least two possible explanations of these data. First it is possible there was some light leakage from the shoot compartment of the plate to the root compartment. Second some root tissue remained in the shoot compartment after decapitation; its luminescence can be seen in Figure 5.2.B. This tissue could have conducted light to the rest of the roots via light piping: indeed plant tissue can act as a fibre optic (Sun et al, 2003).

To try to distinguish between these two explanations, the same experiment as in Figure 5.2.E was repeated in a slightly different way: no root tissue was left in the shoot compartment, so that if any entrainment were still observed under LD, it could only be due to light leakage. The results were very similar to the one presented in Figure 5.2.E: the decapitated dark-grown roots had a 24 h period under LD and a longer FRP under LL (data not shown). This was surprising because our imaging protocol was designed so that roots are kept in darkness. Adding charcoal in the medium and using a customised lid (Figure 3.2) must reduce light leakage from the shoot compartment of the plate to the root compartment to a minimum level. However this set up cannot be perfectly light-tight: some light is probably channelled by the front of the lid, from top (this is the only part of the lid that cannot be covered if the shoots need to be exposed to light) to bottom.

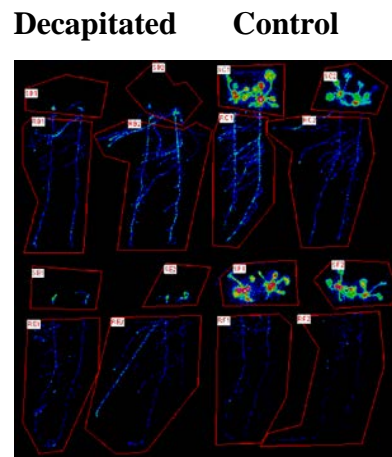
To make sure that light leakage could not be directly from the LEDs to the root compartment, the experiment presented in Figure 5.2.E was repeated in the same way except that black tape was put around the shoot compartment. In this case the dark-grown roots free ran from the moment they were decapitated: the results were the same as in Figure 5.2.F (i.e. under DD), although the imaging room was under LD for 3 days (as in Figure 5.2.E). This confirmed that the covering system for roots is light-tight. It does not distinguish between light piping and light leakage from the shoot to the root compartment. In either case, the root clock must be extremely sensitive to light.

The same experiment as in Figure 5.2 was done with *CCR2:LUC+* as a reporter, and the results were qualitatively similar to *GI* (cf. Figure A.4 in Appendix). Decapitated roots had a 24 h rhythm during LD cycles, whether roots were light- or dark-grown (Figure A.4 A&C 2 in Appendix). After one day in LL the signal of decapitated roots was very low. However the signal increased again in light-grown roots when the plants were retransferred to LD cycles, and their rhythm were close to 24 h. In DD the signal of decapitated roots was too low to be detected.

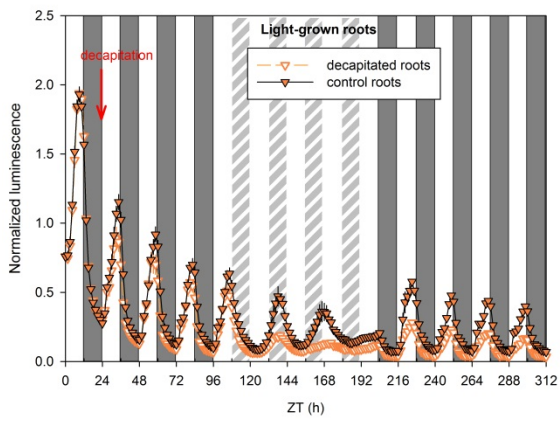
A.



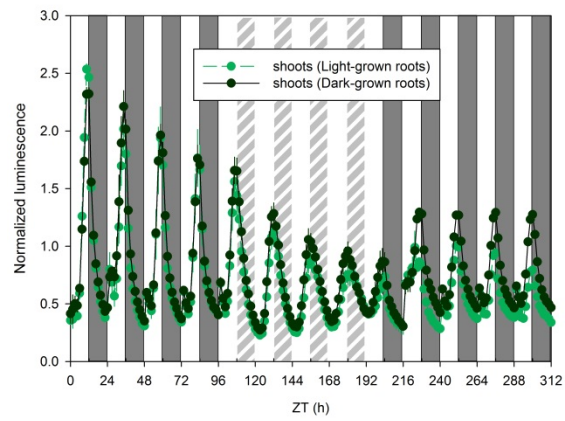
B.



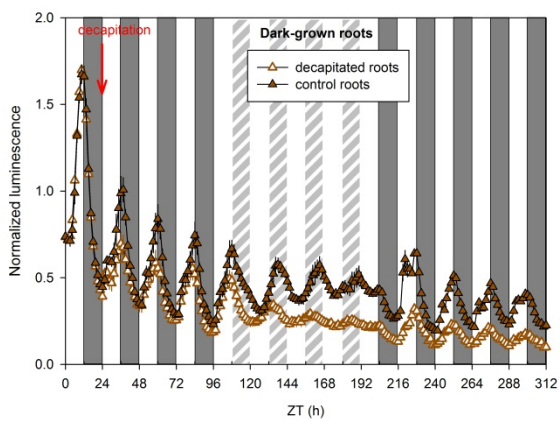
C.



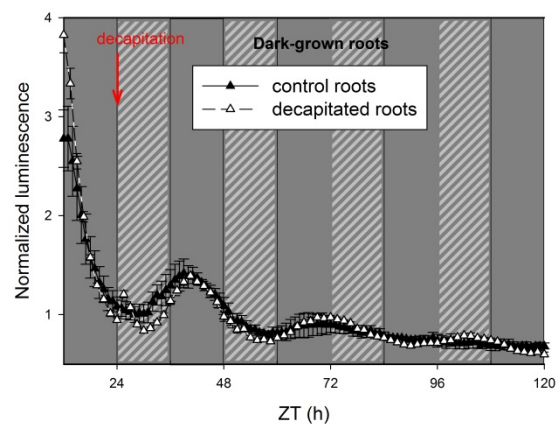
D.



E.



F.



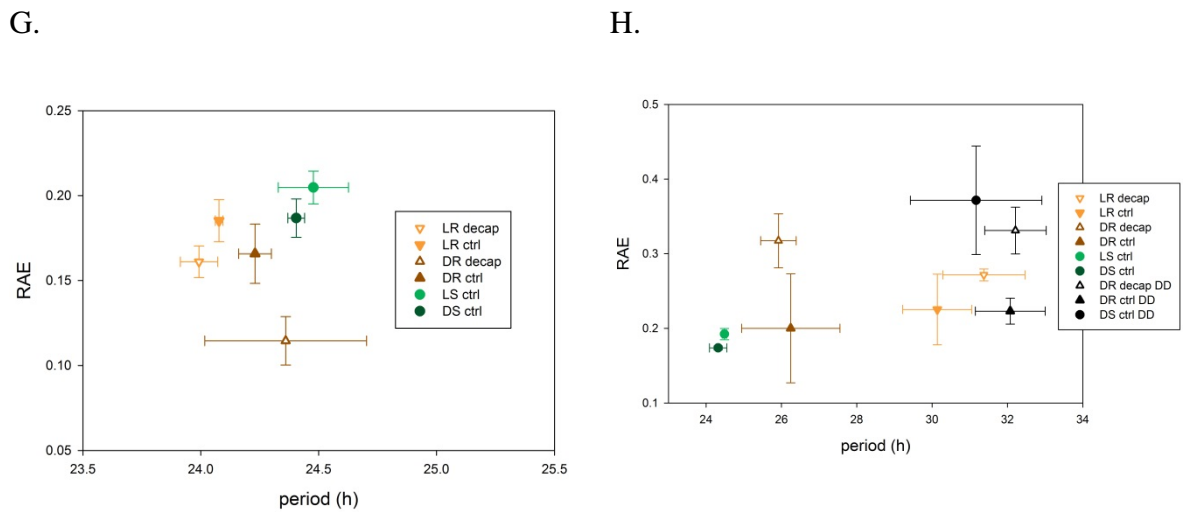


Figure 5.2: LD cycles can directly entrain *GI* expression in roots

Plants with the *GI:LUC+* reporter were entrained 3.5 weeks in LD (white light) before imaging (blue and red light); roots were light- or dark-grown. Plants were imaged for 24h in LD. Then half of them were decapitated before dawn (at ZT24, indicated by the red arrows).

A and B: bright image of 4 plates with 2 clusters of 2 plants in each (A) and corresponding luminescence (B) after decapitation; the plants were decapitated (left-hand sides) or not (right-hand sides) and their roots were light-grown (top plates) or dark-grown (bottom plates).

After half of the shoots were removed at ZT24 (decapitation), all the plants were either transferred to LD and LL cycles (C-E) or to DD (F).

C-F: Bioluminescence over time of light-grown roots (C), shoots (D) and dark-grown roots (E, F). Grey bar represents D cycles, white and light grey hatched bars represent L and subjective L respectively, and dark grey hatched bars represent subjective nights. Data were normalised with the mean luminescence of the first LD cycle (before decapitation, C-E) or with the mean luminescence of the time-course in DD (F). The time course for shoots was not displayed in F for clarity. Error bars are SEM for 4 clusters of 2-3 plants (organs) from 3 independent experiments, except for the last 3.5 LD cycles (following the LL period) where only 1 cluster were imaged.

G and H: Circadian period estimates of data presented in C-F in LD (G) and constant conditions (H : LL or DD) using BRASS for roots and shoots

Symbols and colours used in Figure C-F are the same as in Figure G and H for clarity. Shoots and roots are represented by circles and triangles respectively. For each graph the lighter colours represents organs of plants with light-grown roots, whereas darker colours represents organs of plants with dark-grown roots. The open symbols represent decapitated plants.

The results presented in this section strongly suggest that light can act as a direct zeitgeber for the root clock. It does not rule out the possible existence of other zeitgebers, such as photosynthates. This raises the question: if both light and photosynthates can entrain the root clock, which one is the stronger zeitgeber?

5.4 *GI* expression in roots is preferably entrained by direct perception of light than by any putative signal from shoots

The previous section demonstrated that the root clock can be directly entrained by LD cycles, using decapitated plants. In intact plants, the root clock might also be indirectly entrained by LD cycles, e.g. via photosynthate rhythms (James *et al.*, 2008). If these two mechanisms (i.e. direct *and* indirect entrainment by LD cycle) coexist in the root circadian system, which one is the main zeitgeber? To address this question, roots and shoots were exposed to conflicting LD cycles with varying light intensities.

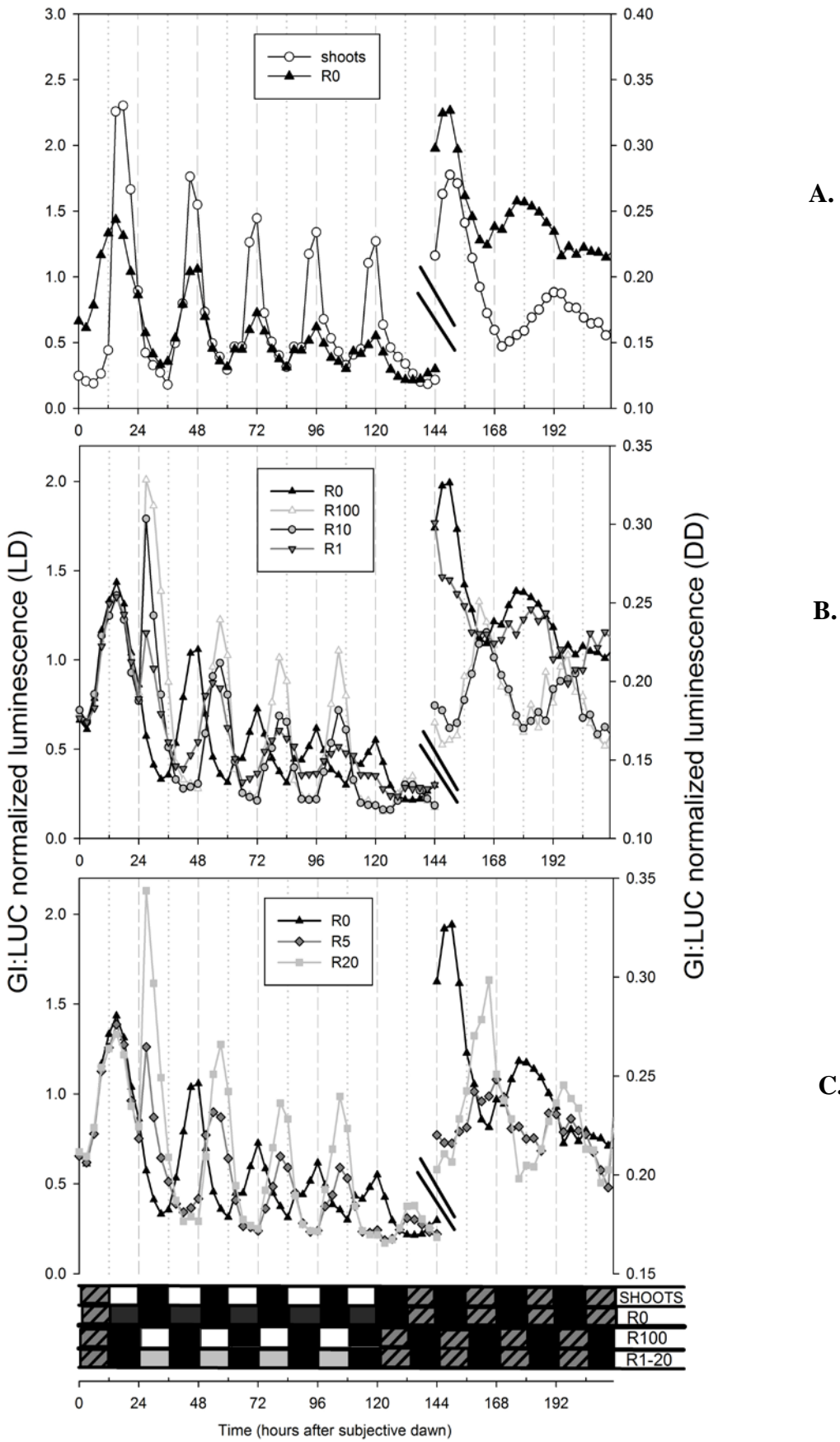
Plants with dark-grown roots and carrying the *GI:LUC+* reporter were entrained in LD cycles before imaging. After spraying them at dusk with luciferin, they were subjected to 24 h of darkness. Shoots and roots were then exposed to LD cycles exactly in antiphase and finally allowed to run free in DD (Figure 5.3). Shoots were exposed to light at $20 \mu\text{mol.m}^{-2}.\text{s}^{-1}$ while roots were exposed to intensities between 0.2 and $20 \mu\text{mol.m}^{-2}.\text{s}^{-1}$ (except a control for which roots were kept in the dark, labelled R0). These roots were exposed to 1, 5, 10, 20 or 100% of the light illuminating shoots; they were therefore labelled R1, R5, R10, R20 and R100 respectively.

Shoots and dark-grown roots (R0) behaved in a very similar way (Figure 5.3.A). As soon as illumination started during the first invert cycle (i.e. from ZT12) *GI* expression increased in both organs and peaked 3-6 h after this new dawn. It then decreased and rose again the next day, reaching a maximum 3 h before dusk (ZT45). After these two transient cycles (ZT12-60) both organs were clearly entrained to the new LD cycles. *GI* expression adopted a stable phase angle during the next three LD cycles (ZT60-132), with a peak at dusk in both organs. The period under LD was ~ 24 h in shoots and R0 (Figure 5.3.D). After release in DD, *GI* free ran with a longer period in both organs (Figure 5.3.D). Thus *GI* can be rapidly re-entrained by LD cycles that were in antiphase with previous LD cycles (during entrainment before imaging). This is true for both shoots and dark-grown roots (R0), which was not surprising given that shoots and roots are known to be in phase under LD cycles.

The amplitudes of shoots and dark-grown roots were also rapidly stabilised: they decreased the first two days and were almost unchanged the last three days under LD (Figure 5.3.A). The decrease in amplitude might be due to the perturbation caused by the inversion of LD cycles. Another possible explanation might be the different light intensity used for these invert cycles: plants were entrained for 3 weeks in LD at $\sim 100 \mu\text{mol.m}^{-2}.\text{s}^{-1}$ and then for 5 days in LD at $\sim 20 \mu\text{mol.m}^{-2}.\text{s}^{-1}$. Amplitudes were always lower in roots compared to shoots (Figure 5.3).

During the first day of imaging (ZT0-24), the *GI* expression profile was very similar in all the roots (Figure 5.3.B&C). This was expected because all the roots had been in the same conditions (i.e. dark-grown) until then. However, as soon as roots were exposed to light, *GI* cycled in antiphase compared to the control roots. The phase of *GI* expression progressively shifted to the new “root dusk” (represented by dotted lines in Figure 5.3.A-C). A transient could be observed the first day (ZT24-48), as it was observed in shoots (ZT12-36, described in previous paragraph): *GI* peaked ~ 3 h after the first “new dawn” (ZT27). *GI* rhythms quickly seemed to adopt a stable phase angle during the next three LD cycles (ZT48-120, Figure 5.3.B&C), with a peak ~ 3 h before dusk for all the roots exposed to $1 \mu\text{mol.m}^{-2}.\text{s}^{-1}$ or more. There was one exception in terms of phase: the roots exposed to the lowest light intensity ($0.2 \mu\text{mol.m}^{-2}.\text{s}^{-1}$) peaked earlier than the other roots, at least during the second LD cycle (ZT54, Figure 5.3.B).

The period under LD was ~ 24 h in all roots exposed to $2 \mu\text{mol.m}^{-2}.\text{s}^{-1}$ or more (Figure 5.3.D). After release in DD, *GI* free ran with a longer period in these roots. Thus *GI* can be rapidly entrained in roots by LD cycles that were in antiphase with LD cycles experienced by shoots. The phase of *GI* expression in DD was determined by the LD cycle the organ was directly exposed to: this is obvious between ZT120 and ZT168 when roots that were exposed to light free ran in antiphase compared to shoots and control roots (Figure 5.3.B&C).



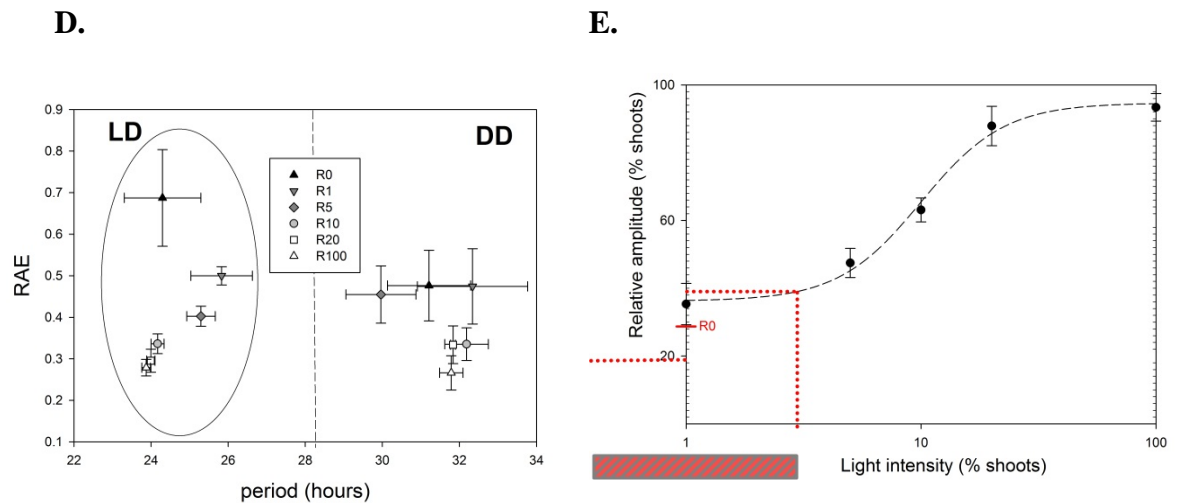


Figure 5.3: *GI* expression in roots is entrained by direct perception of light rather than any putative signal from shoots

Plants with the *GI:LUC+* reporter were entrained 3 weeks in LD with dark-grown roots before imaging. Plants were then transferred one day in DD (1 D cycle followed by 1 subjective D cycle); imaging started at this subjective dawn (time 0). Shoots and roots were then exposed to LD cycles in antiphase, except for the controls. Shoots and roots (R0) controls were entrained in phase, but shoots were exposed to LD cycles that were in antiphase with the LD cycles experienced before imaging, and R0 were kept in the dark. All shoots were exposed to $20 \mu\text{mol}\cdot\text{m}^{-2}\cdot\text{s}^{-1}$ light (= 100%). The roots R1, R5, R10, R20 and R100 were exposed to 1, 5, 10, 20 and 100% of the light intensity that shoots were exposed to. After these antiphase LD cycles (4 cycles for roots, 5 for shoots), plants were released into DD.

A-C: Bioluminescence over time of shoots and control roots (A), and roots exposed to antiphase LD cycles (B and C); the control root time-course (R0) is shown on the 3 graphs for comparison. Note the 2 different Y axis scales. White bars represents L cycles on the shoots and on the roots R100 (100% of the light intensity), grey bars represent L cycles (with x % of the light intensity, x = 1, 5, 10 or 20) on roots R1, 5, 10 and R20 respectively, black and hatched bars represents D and subjective D cycles respectively. Data were normalised with the mean luminescence of the first 24 h of imaging, i.e. before roots were exposed to light (all plants were in the same conditions during these 24 h). The data points represent averages of at least 3 replicates (from 2-3 independent experiments). Although the SEMs were low they were not displayed on Figure A-C for clarity.

D: Circadian period estimates of root data presented in A-C in LD and DD using BRASS. The last 3 days in LD and day 2-4 in DD were considered for this analysis.

E: relative amplitudes of roots exposed to light as a function of light intensity (1- 100% of the light on shoots). The amplitudes were estimated by BRASS for the last 3 cycles in LD (as in D) and normalised with the average of the shoots amplitude (estimated in the same way, = 100%). Error bars are SEM for 2-4 clusters of 2-3 plants/organs. The relative amplitude of R0 is shown on the y axis (average = 29%, SD = 10%); by extrapolation the light intensity that might be perceived by R0 via light piping from shoots is represented by the grey and red dashed bar (i.e. less than 3% of the light intensity on shoots)

Although *GI* did not have a 24 h period under LD in the roots exposed to lower light intensities (0.2 and $1 \mu\text{mol}\cdot\text{m}^{-2}\cdot\text{s}^{-1}$, i.e. R1 and R5), it was rhythmic in both LD and DD conditions (Figure 5.3.D). In DD the FRP and the phases of *GI* in R5 were similar to the ones observed in the other roots (exposed to higher light); *GI* free ran in antiphase in R5

compared to R0 (Figure 5.3.C). The phase of *GI* in R1 under DD was less clear and possibly determined by the extra L cycle on the corresponding shoots (Figure 5.3.B). But the periods for both R1 and R5 in LD cycles were 25-26 h, not 24 h; very similar periods were estimated with both BRASS and COSOPT, another commonly used software for rhythm analysis. This was possibly because the phase angles were not stabilised yet after the four LD cycles on roots. For instance Figure 5.4.B shows that it is only during the last two LD cycles on roots (ZT72-108) that R1 peaked ~3 h before dusk, i.e. like the other roots exposed to higher light. Before that, the phase of *GI* in R1 progressively shifted towards dusk. A similar but less obvious observation could be made for R5. However there could be a more intriguing explanation. Interestingly the periods under LD of R1 and R5 were ~ 25-26 h. This matches with the FRP of *GI* in dark-grown roots under LL (Figure 5.2). It is possible that ~ 1-5% of the light perceived by the shoots was channelled down the roots. If this was the case, R1 and R5 were virtually under LL (during the LD period), which would explain why they were maybe not entrained in “LD”. One way to test these ideas (phase angle stabilisation VS. free running) would be to repeat the experiment and run it longer under invert LD cycles.

In the roots, the amplitudes tended to be stabilised after one or two transient cycles in LD (Figure 5.3.B&C). The interval between ZT48 and ZT120 was used to estimate both the periods (described above) and the amplitudes in roots with BRASS (Figure 5.3.E). There is clear positive correlation between the amplitudes of *GI* in roots and the light intensity this organ was exposed to. Interestingly this correlation could be well fitted with a Hill equation (dashed line in Figure 5.3.E). This might indicate some cooperativity in the mechanism of *GI* induction by light. In addition, the amplitude of *GI* in R0 was close to its amplitude in R1. Using the Hill equation (from the regression in Figure 5.3.E) to determine the light intensity possibly perceived by dark-grown roots (R0) would result in a broad range of values below ~3%. This range of values would be consistent with the fraction of light that could be channelled from shoots to roots (Sun *et al.*, 2005).

To summarise, *GI* rhythms in roots were preferably entrained by the light they were directly exposed to rather than a putative entraining signal from their shoots. This was the case even when the light intensity of the LD cycles illuminating roots was much lower than that of the LD cycles illuminating shoots. In addition, the shoots were exposed to one more light cycle compared to the roots (ZT108-120); yet the roots then free ran in DD with a

phase determined by the LD cycle they had been directly exposed to. Therefore light seems to be a stronger zeitgeber for the root clock than any putative signal from the shoots at constant temperature.

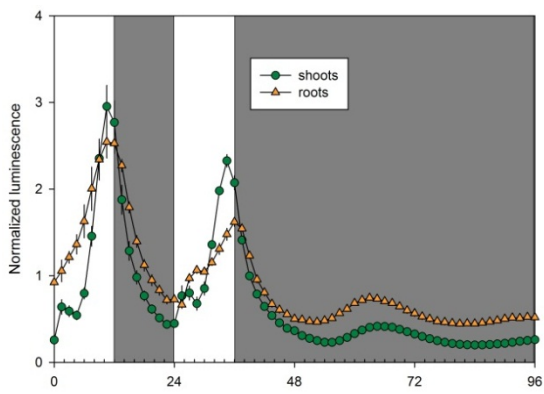
5.5 Shoot and root clocks both have a broad range of entrainment but respond differently to T cycles

The previous sections show that the root clock – at least *GI* – can be directly entrained by LD cycles with very low light intensity. Is the root clock more sensitive to light than the shoot clock in terms of entrainment? If so, Herzog and colleagues' work suggests that the root clock should have a broader range of entrainment compared to the shoot clock (Abraham *et al.*, 2010). I decided to ask whether both shoot and root clocks could entrain to weak zeitgebers, and if so, how broad is the range of entrainment in each case.

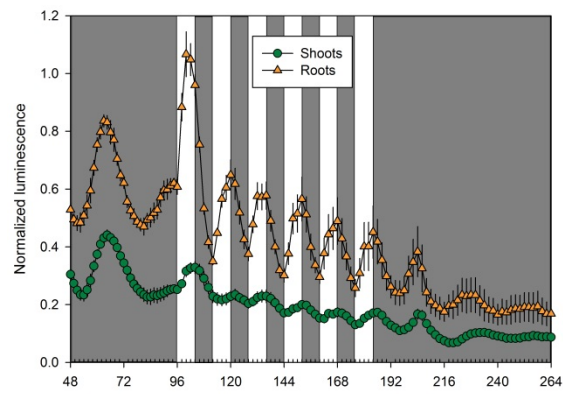
T cycle experiments were carried out with low light intensity ($0.15 \mu\text{mol.m}^{-2}.\text{s}^{-1}$, Figure 5.4). *GI:LUC* was used as the reporter. Plants with dark-grown roots were entrained for 3 weeks in LD 12/12 (white light, $\sim 100 \mu\text{mol.m}^{-2}.\text{s}^{-1}$) as usual. They were then sprayed with luciferin and imaged over time. First they were all entrained for another 2 days in LD 12/12 (blue and red light, $15 \mu\text{mol.m}^{-2}.\text{s}^{-1}$) and released in DD for 2 days (Figure 5.4.A). These LD cycles were used as a control and to normalise the whole time-courses. Figure 5.4.A shows that results were very reproducible during this period. After these 4 days of imaging plants were transferred to different T cycles but at low light intensity (blue and red light, $0.15 \mu\text{mol.m}^{-2}.\text{s}^{-1}$) and finally released into DD (Figure 5.4.B-F). The following periods were used for T cycles: 16, 24, 28, 32 and 40 hours in Figure B-F respectively (the photoperiod being half of each cycle, e.g. LD 8/8 for T16 cycles).

Surprisingly *GI* was entrained in both shoots and roots by all of these T cycles during the LD periods (Figure 5.4.B-F and Table 5.1). The periods of *GI* in both organs matched the periods of the corresponding T cycles very well under LD (Table 5.1). Moreover *GI* was quickly synchronised with the “new LD cycles”: it took only 1 or 2 T cycles before the rhythms stabilised in both shoots and roots (Figure 5.4.B-F); the damping observed during these first T cycles may be due to the very low light intensity used in these experiments. Free-running rhythms of *GI* were detectable in DD after the T cycles in all cases except for shoots after the T24 and T40 cycles (Table 5.1).

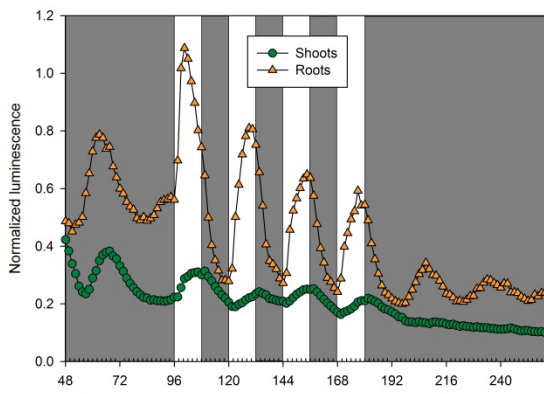
A. LD(12/12)DD averages



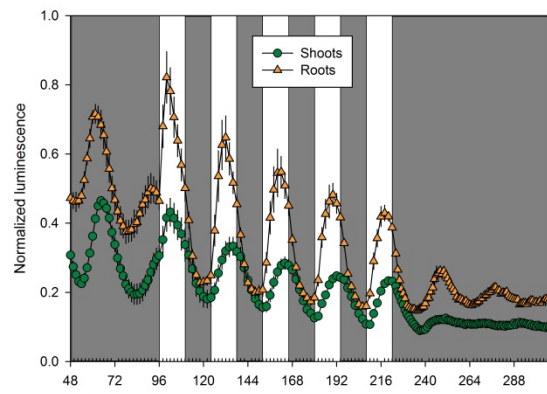
B. T16



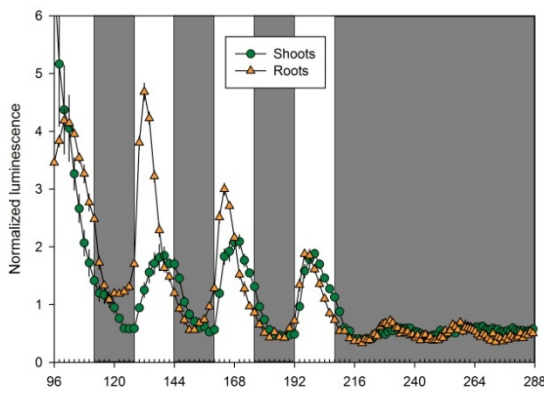
C. T24



D. T28



E. T32



F. T40

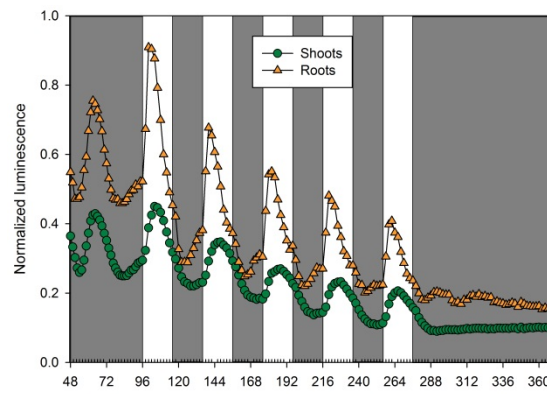


Figure 5.4: *GI* expression can be entrained by a broad range of low amplitude LD cycles in both shoots and roots

Plants with the *GI:LUC+* reporter were entrained 3 weeks in LD 12/12 (white light) before imaging started. They were entrained another 2 days in LD 12/12 (blue and red light $15 \mu\text{mol.m}^{-2}.\text{s}^{-1}$) and released 2 days in DD (A) before transfer to different T cycles (blue and red light $0.15 \mu\text{mol.m}^{-2}.\text{s}^{-1}$) and release in DD (B-F).

A. The first 4 days (L12/D12- DD) of the time-courses presented in B, C, D, F (different T cycles) were averaged for shoots and roots

B, C, D, F: The 2 days of DD presented in A are shown for each T cycle experiment, followed by low amplitude LD cycles (B, C, D, F: T = 8/8, 12/12, 14/14 and 20/20 LD cycles respectively) and release in DD. Row data from each time-course were normalised with the mean luminescence of the corresponding LD 12/12 last cycle. Normalised data are averages of 2-4 clusters of 2-3 plants from 1 or 2 independent experiments.

E: Other T cycle experiment but with LD 16/16 cycles and without imaging before the T cycles started. These time-courses were normalised with the mean luminescence over the last T cycle (from ZT192 to ZT224). See text for more details.

There was no clear correlation between FRPs under DD and the periods of the preceding T cycles. Nevertheless, the FRP in roots increased with T between 16h and 28h (with FRPs of about 26, 28 and 30 h for T=16, 24 and 28 h respectively) but it decreased afterwards (Table 5.1). The opposite trend was observed in shoots but since free-running rhythms were only detectable in 3 of the 5 T cycle datasets it is difficult to draw any conclusions.

Table 5.1: Period estimates (h) of the time-courses presented in Figure 5.4

The last 3 T cycles and the first 3 days in DD (72 h from the first subjective dawn) were used to estimate the period in LD and DD respectively, using BRASS.

	T16		T24		T28		T32		T40	
	LD	DD								
Shoots	16.12	27.41	23.81	ND	28.28	21.57	30.7	28.59	39.76	ND
Roots	16.23	26.1	24.05	28.56	28.25	30.19	32.25	28.85	40.04	28.49

An obvious difference between shoots and roots under the different T cycles was the phase of *GI* expression. Figure 5.4 shows that for each T cycle, *GI* peaked earlier in roots compared to shoots. It took both organs only one or two transient cycles to adopt a stable phase relationship to the zeitgeber cycle. This phase angle depends on T for each organ (Table 5.2), which indicates a real entrainment of *GI* by LD cycles.

In addition, the waveforms were different in the two organs, especially under LD 20/20 cycles: the *GI* peak was asymmetric in roots but not in shoots. More generally, peaks were sharper in roots. These differences between shoot and roots in terms of phases and expression profiles clearly suggest different regulation of *GI* in these organs.

Table 5.2: Phases of peak expression in shoots and roots under T cycles

The last 3 T cycles of the time-courses presented in Figure 5.4 were used to estimate the phases of *GI* expression in shoots (S) and roots (R) under LD using BRASS. The average phases of peak expression and their SEM are presented in 2 ways: in terms of hours after dawn (upper part) or in terms of Circadian Time (CT, lower part; the values presented in the upper part were multiplied by 24 and divided by T)

		T16		T24		T28		T32		T40	
		Phase	<i>SEM</i>								
hours	S	7.77	0.39	13.24	0.50	12.81	0.47	13.26	0.75	13.94	0.54
	R	6.10	1.08	9.89	0.54	9.88	0.60	5.10	0.30	8.33	0.50
CT	S	11.65	0.59	13.24	0.50	10.98	0.40	9.95	0.56	8.36	0.32
	R	9.14	1.62	9.89	0.54	8.47	0.51	3.83	0.23	5.00	0.30

Another obvious difference between *GI* rhythms in shoots and roots under T cycles is their amplitude: they were higher in roots under all these low LD cycles. But in both shoots and roots, the amplitude depends on T, with a peak at T32 (Figure 5.5). This indicates that both shoot and root clocks can resonate, at a surprisingly high value for T (32 h), which is actually very close to the FRPs in shoots and roots under DD in my conditions (Chapter 4, Figure 4.5). Regardless of the resonance frequency, it would suggest that both clocks are “weak” (Abraham *et al.*, 2010) or flexible, as opposed to rigid oscillators which are more robust (their amplitude varies little with T).

In conclusion *GI* could be entrained by a weak zeitgeber (low amplitude LD cycles) in a broad range of T cycle in both shoot and root clocks. This suggests that both clocks are very sensitive to entrainment by LD cycles. The fact that *GI* resonates more in shoots than in roots at T32 (Figure 5.5) suggest that the shoot clock might be even more sensitive to light than the root clock and would be a weaker oscillator according to Abraham *et al.* (2010). Nevertheless the root clock seems sensitive enough to be entrained by very low light intensity, which is consistent with other results presented in this chapter.

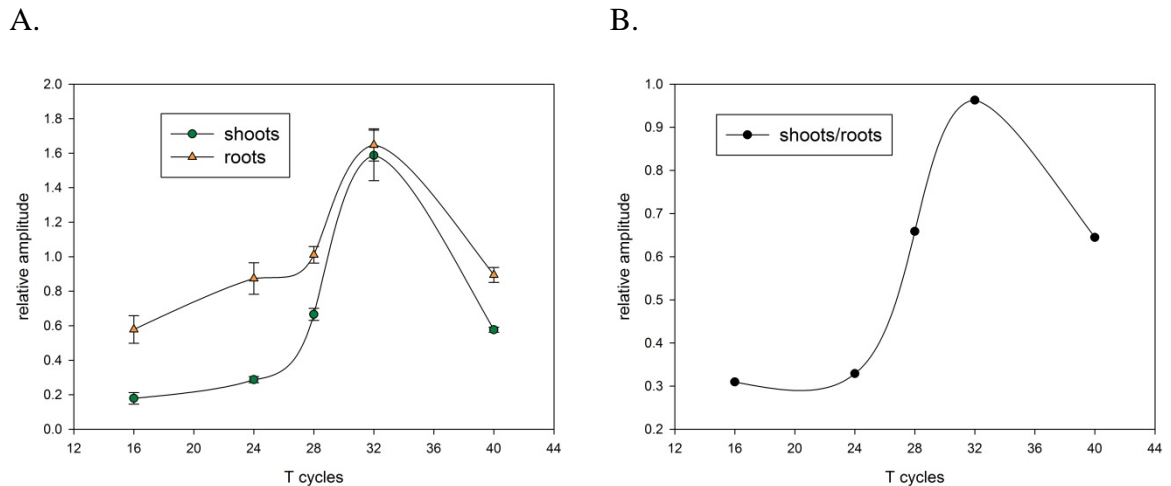


Figure 5.5: The amplitude of *GI* expression rhythm resonates in both shoots and roots

The amplitudes of *GI* expression rhythms under different T cycles were estimated from the data presented in Figure 5.4. Since the different T cycle experiments presented in Figure 5.4 were done in slightly different ways (e.g. there was no data before the T cycles started in the T32 experiment), the data were renormalized in order to compare amplitudes between the different T cycles. All the time courses for the different T cycle experiments were renormalized with the average luminescence over their 4th T cycle (i.e. last common cycle for all experiment) to be comparable. Then the amplitudes of these 4th T cycles were plotted. Data are averages of 2 clusters of 2-3 plants from the same experiment. Bars represent SEM.

A. Shoot and root resonance curves

B. Ratio between shoot and root amplitudes (i.e. data from A).

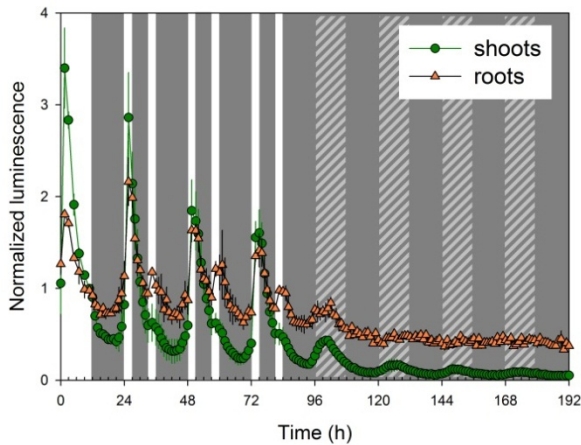
5.6 Shoot and root clocks respond differently to skeleton photoperiods

Since dark-grown roots can perceive light, they can presumably recognise the transitions between light and dark under diurnal conditions. Previous sections strongly suggest that the root clock can be directly entrained by low light/dark cycles. The light/dark transitions at dawn and dusk are sufficient to entrain the shoot clock (Millar, 2003). Can such skeleton photoperiods entrain the clock of dark-grown roots too?

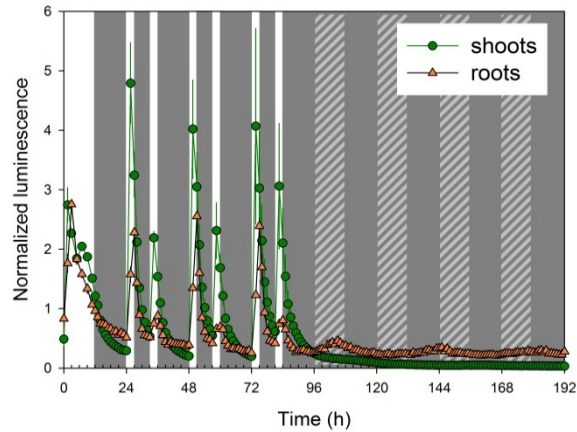
The response of shoots and roots to skeleton photoperiods were tested experimentally by measuring the bioluminescence of the *CCA1*-, *PRR9*-, *PRR7*- and *GI:LUC* reporter genes. Plants expressing these reporters were entrained as usual (4 weeks of LD 12/12 cycle on ½ MS medium without sucrose). They were then imaged over the last day in LD 12/12 before

transfer to skeleton photoperiod for 3 days and finally released in DD. Roots were kept in the dark all the time. Results are presented in Figure 5.6.

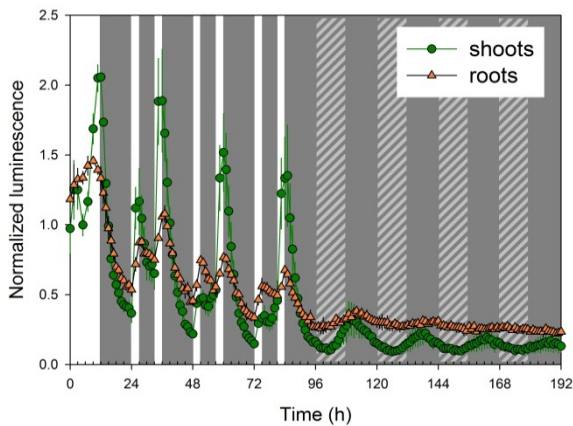
A. *CCA1*



B. *PRR9*



C. *GI*



D. *PRR7*

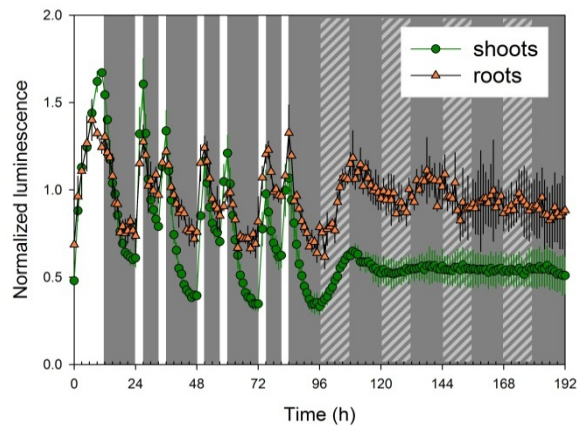


Figure 5.6: Shoot and root clock genes respond differently to skeleton photoperiods

Plants were entrained in LD (12L:12D) for 3 weeks, then imaged a last day in 12L:12D (from ZT0) before transfer to skeleton entrainment for 3 days and release in DD (from ZT96). Each skeleton photoperiod consist of two 3 h light pulses, one starting at dawn and the other one finishing at dusk (3L:6D:3L:12D), from ZT24 to ZT96.

A-D: Normalised luminescence from *CCA1*-, *PRR9*-, *GI*- and *PRR7:LUC* plants respectively. White bars represent light periods; black and hatched bars represent dark periods. The luminescence was normalised to the mean luminescence over the last 12L:12D period for each organ. Data were averages of 2-3 clusters of 1-3 plants from 1 experiment. Bars correspond to SEM.

During the skeleton photoperiods, the expression of clock genes was differentially regulated in shoots and roots. In shoots, the profiles of *CCA1* and *PRR9* were consistent with published data (Pokhilko *et al.*, 2010). The peaks were higher at dawn compared to

dusk, especially for *CCA1* with only a shoulder at dusk (Figure 5.6.A). *PRR9* also peaked at dusk but with a lower level compared to dawn (Figure 5.6.B), which was also predicted and observed experimentally by Pokhilko and colleagues. Interestingly, this trend was inverted in roots, where the *PRR9* peak at dusk was much lower compared to its dawn peak, whereas the *CCA1* peak at dawn was not much higher than its dusk peak (Figure 5.6.A&B). The difference between shoots and roots was even more pronounced for *GI* under skeleton photoperiods: in shoots *GI* only peaked at dusk with a shoulder at dawn, whereas *GI* peaked at dawn and dusk in roots with a similar level of expression (Figure 5.6.C). This profile was similar to the *PRR7* profile in both shoots and roots: *PRR7* peaked to similar levels at dawn and dusk (Figure 5.6.D).

These different responses to skeleton photoperiods observed between shoots and roots reveal different regulation of genes by light and by the clock in the two organs. Possible explanations are speculative at this stage but could provide the basis for further experiments. In shoots, the shoulder of *CCA1* at dusk – as opposed to its high peak at dawn – could be explained by *CCA1/LHY* repression by a wave of inhibitors that are mainly expressed from the afternoon until the night (*PRR9*, *PRR7* and the Night Inhibitor (NI) constitute this wave). The relatively higher peak of *CCA1* at dusk (compared to dawn) observed in roots compared to shoots (Figure 5.6.A) suggest less repression of *CCA1* in roots at dusk. This could be due to lower levels of clock gene expression in dark-grown roots compared to shoots (chapter 4); the lower levels of *PRR9* and *PRR7* in roots would repress *CCA1/LHY* less compared to shoots. In addition *PRR5* is a good candidate for NI (Pokhilko *et al.*, 2010) but was arrhythmic in roots (Sullivan *et al.*, unpublished). Its levels of expression at dawn and dusk were similar and therefore it might not inhibit *CCA1/LHY* at dusk any more than at dawn. These interpretations are based on the P2010 model, but are still valid with the P2012 model where the same wave of inhibitors (together with *TOC1*) inhibits *CCA1/LHY*. Besides, *TOC1* acts later in the evening and in the night in the P2012 model. Furthermore, *TOC1* protein seemed to be lower in roots compared to shoots (James *et al.*, 2008). Altogether, results presented in Figure 5.6.A are consistent with the published results mentioned above and other root data (chapter 4).

The differences between shoot and root responses to skeleton photoperiods were more striking for *PRR9* and *GI*. In roots *PRR9* had much smaller peak at dusk compared to dawn (Figure 5.6.B), and *GI* peaked at similar levels at dawn and dusk (Figure 5.6.C). But considering the P2010 model these observations could be consistent with previous root

data. In diurnal cycles *TOC1* mRNA had a broader peak in roots compared to shoots, its level rising already in mid-afternoon (James *et al.*, 2008); that could explain more repression of *PRR9* during the 3h before dusk in roots under skeleton photoperiods. Considering the P2012 model, data presented in Figure 5.6.B suggest there is more repression of *PRR9* by the EC around dusk in roots compared to shoots. The EC might peak earlier or have more inhibitory effects in roots. Data in diurnal cycles (e.g. Figure 5.6.B) already suggested differential regulation of *PRR9* in shoots and roots: the peak was sharper in root, consistent with more repression than in shoots at the end of the day.

GI data in roots under skeleton photoperiods suggest it is similarly regulated during the 3h after dawn and before dusk. The peak at dawn – as opposed to the shoulder observed in shoots - is consistent with the observation that LHY-containing EE-binding complexes could not be detected in roots (James *et al.*, 2008). Therefore *GI* would be less (if at all) inhibited by morning genes around dawn. This is also consistent with imaging data (Figure 5.6.C, previous sections and chapter 4): in diurnal conditions *GI* levels increase in roots from dawn to dusk, without a dawn peak whereas in shoots, an acute light activation of *GI* expression followed by its inhibition by CCA1/LHY results in a sharp dawn peak of *GI*. Although *GI* peaked at dawn and dusk in roots under skeleton photoperiods, it free ran in DD with only its dusk peak (Figure 5.6.C).

PRR7 had a similar profile in both shoots and roots under skeleton photoperiods: it had the same peak at dawn and dusk, although the amplitude was lower in roots compared to shoots. After release in DD the relative levels were higher in roots compared to shoots (Figure 5.6.D) but rhythmic in both organs (Table 5.3).

After release in DD, the rhythms seemed to be more sustained in shoots for *CCA1* and *GI*, but more sustained in roots for *PRR9* and *PRR7* (Figure 5.6). Nonetheless it suggests that skeleton photoperiods are sufficient to entrain the root clock as well as the shoot clock.

Note that the averages represent 2-3 clusters of 1-3 plants imaged at the same time (in other words this experiment has only been done once). This experiment should be repeated before drawing any firm conclusion about the data in DD. Nevertheless, the same pattern observed for each gene/organ over 3 consecutive days (under skeleton photoperiod) could be considered as a triplicate. These data are therefore more reliable than the following data under DD

In conclusion, the different responses of clock gene expression to skeleton photoperiods in shoots and roots may reflect different clock mechanisms in these two organs. The main differences were observed for *PRR9* and *GI*. The former is probably more repressed at the end of the day and the later less repressed at the beginning of the day, in roots compared to shoots. A lower repression of *GI* in roots would be consistent with the lack of CCA1/LHY binding to EE in this organ. However the mechanism of *PRR9* repression in roots is not known and should be further investigated.

5.7 Entrainment of the root clock by temperature cycles

Most of my initial work was focused on the effects of light on the root clock. It showed that the clock of dark-grown roots can be entrained by direct perception of light. This could be relevant physiologically and indeed could be the main mechanism of entrainment at steady temperatures. But in natural conditions, temperature changes daily in a rhythmic manner (with some random fluctuations). Temperature is one of the main zeitgebers for circadian clocks in general. Given that much of the root network is underground, in close to full darkness, I decided to test whether the root clock can be entrained by temperature cycles using RT-qPCR.

In this experiment, plants were entrained 4 weeks in LD cycles and constant temperature (20 °C) before starting harvesting (ZT0). Then the growth cabinets were set to DD and temperature cycles (12 h at 12 °C followed by 12 h at 20 °C) during the 3 days of harvesting. It is important to note that the zeitgeber phase was inverted: the “subjective dawn” at ZT0 corresponds to the start of the cold cycle (which would be a “new subjective dusk”). Figure 5.7.A&B clearly illustrated this phase shift: *CCA1* and *RVE1* are morning genes that usually peak around dawn. On the first day of harvesting both shoots and roots peaked a few hours after the first “subjective dawn” (ZT0). However their next peak appears only 36 hours later, i.e. at the “new subjective dawn”. The mRNA levels in both shoots and roots even anticipated this transition between the cold cycle (new subjective night) and the warm cycle (new subjective day): they started rising before ZT36, and they peaked again 24 h later. This is exactly what would happen in LD cycle: they would rise before dawn. Therefore *CCA1* and *RVE1* expression seemed to be entrained by temperature cycles.

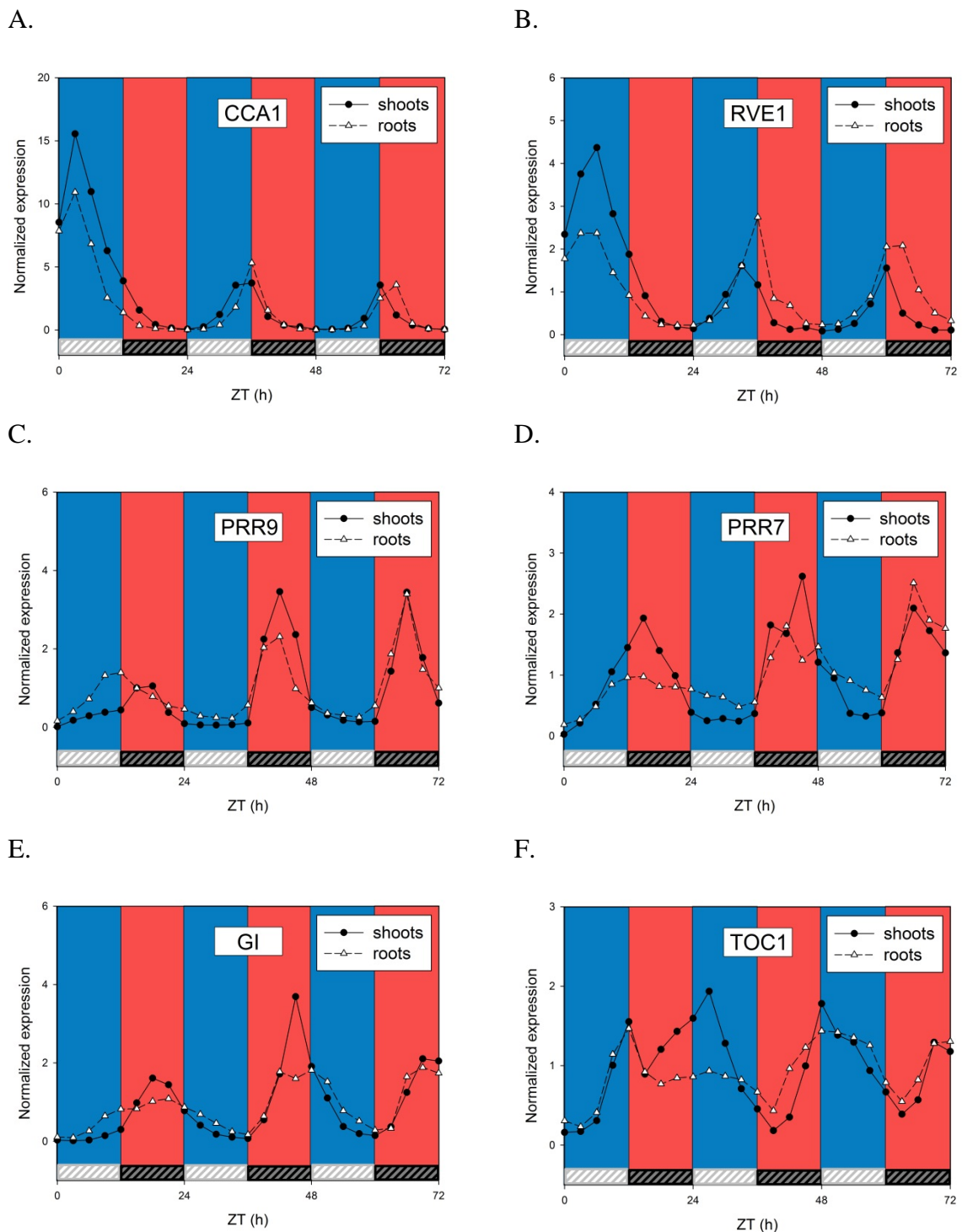


Figure 5.7: Shoot and root clock genes can be entrained by temperature cycles

Plants were entrained in LD 12/12 and constant temperature for four weeks. At ZT0 they were transferred to DD and temperature cycles (12/20 °C). The blue and red bars represent 12 and 20 °C respectively, and the light and dark hatched bar represent the subjective light and dark cycles respectively (i.e. LD cycles experienced before DD and temperature cycles).

A-F: Transcript levels of *CCA1*, *RVE1*, *PRR9*, *PRR7*, *GI* and *TOC1* respectively. The data were normalized twice: first with UBQ and then with the mean value of these data (normalised with UBQ) over the last two days. This experiment was processed by Brian McDade.

LHY expression was very similar to *CCA1* (results not shown). *RVE1* is known to be induced by *LHY* protein and the expression of this downstream gene matches that of the new phase shown by the clock genes. This is indirect evidence that the levels of *LHY* protein reflect the observed shift in its mRNA levels, resulting in a rhythmic activation of *RVE1* expression.

PRR7 and *PRR9* are thought to be involved in temperature entrainment of the shoot clock (Salome and McClung, 2005a). Interestingly, their phase of expression started shifting to the new zeitgeber phase during the first temperature cycle in both shoots and roots (ZT0-24, Figure 5.7.C&D). As for *CCA1* and *RVE1*, the mRNA levels of these *PRRs* were synchronised with the new zeitgeber after only 2 – 3 days of temperature cycles.

The expression profile of *GI* was similar to that of *PRR7/9* (Figure 5.7.E). For *TOC1*, the transition from one phase to another seems more complex (Figure 5.7.F). However the last 2 days show us similar results: shoots and roots were in phase and peaked at the expected “time of the day” based on the temperature cycle (i.e. around the “new dusk” for *TOC1* and *GI*). Some differences between shoots and roots were evident on the second day but less so on the third one. It is likely the circadian system needs more than 48 hours to reach a steady state after such a big change in light and temperature conditions.

A longer time-course and extra time-points would be helpful to estimate the rhythm characteristics (e.g. phases and periods) and possibly show us more differences between shoots and roots. For instance, the phases of *CCA1* and *RVE1* expression seems to be delayed in roots compared to shoots (Figure 5.7.A&B). However, temperature changed more slowly in the hydroponic medium than in the air (Sullivan *et al.*, unpublished), which would explain the phase delays between shoots and roots.

This experiment was done before *ISUI* was chosen as a new reference gene for RT-qPCR. We previously used *UBQ* as a reference gene for our time-courses. There is no universal reference gene for RT-qPCR, and depending on the conditions, one gene may be better than another. In the particular conditions used in this experiment, the level of *UBQ* was quite variable over the time-course and between the two different organs. It was actually more variable during the first 24 hours, which may be due to the huge change in the

conditions: from LD cycle we switched directly to DD and temperature cycles with opposite phases (the cold cycle corresponding to the previous light cycle). Ideally we should use a reference gene that is stably expressed over the whole time-course, in both shoots and roots. But such a gene has not yet been found for these specific conditions. However the *UBQ* levels were more stable the last 2 days of our experiment. I therefore normalized the data twice: first with *UBQ* (as usual), and a second normalization with the mean value of these data (normalised with *UBQ*) over the last two days. This allows us to compare relative levels of expression in both shoots and roots (e.g. relative amplitudes).

Even better, a good reference gene would fulfil the same condition (described above), but also be stable in LL and temperature cycle. We planned to do the same experiment as discussed above, but setting LL instead of DD during the temperature cycles. We processed most of the samples but lost one day because of technical issues. Nevertheless, the preliminary results (not shown) indicated that temperature cycles also drive the root clock in LL.

To determine whether the rhythms observed in roots after temperature cycles are truly circadian, we need another experiment. Plants should be entrained for several days by temperature cycles, and then released to constant conditions (light and temperature). Circadian genes would still be expressed rhythmically in those constant conditions.

5.8 Conclusion

This chapter showed that the root clock can be entrained by both LD and temperature cycles. The entrainment by LD cycles at constant temperature seems to be mainly related to direct perception of light by the roots, rather than an indirect signal from the shoots as it was thought before (James *et al.*, 2008). This is true whether roots are directly exposed to LD cycles, or kept in darkness. In fact dark-grown roots can perceive light channelled by upper tissues exposed to light (Sun *et al.*, 2005). Although this piped light is probably much lower than light directly perceived upper tissues, it must be sufficient to entrain dark-grown roots. This was demonstrated after decapitating plants.

By “direct entrainment” I mean that LD is probably the “direct pacemaker” for the root clock, i.e. there would be no “intermediate” oscillator(s) between the LD cycles and the

central clock in roots. This is in contrast with previous work that suggested the entraining effects of light and dark would be “indirect” (James *et al.*, 2008); for instance LD cycles could entrain a metabolic oscillator (e.g. sugar levels) that would in turn entrain the root clock. This hypothesis has not been ruled out, but there is now more evidence for a direct entrainment of the root clock by LD cycles at constant temperature. This is summarised below. Note that the effects of light on the clock are not so “direct”, as mentioned in the general introduction. There are many ways by which light could contribute to the entrainment of the clock, for instance by direct interaction of photoreceptors with clock proteins, by activation of transcription or translation, *etc.*

The surprising results from the “decapitation experiment” raised other questions: if very low light levels can directly entrain the root clock, is it a stronger zeitgeber than a putative rhythmic signal from shoots? And is the root clock more sensitive to LD cycles compared to the shoot clock? The answer to the first question is probably yes, to a certain extent. For instance LD cycles with an “amplitude” of only $2 \mu\text{mol.m}^{-2}.\text{s}^{-1}$ could entrain *GI* in roots even though the shoots were exposed to LD cycle with much higher amplitude ($20 \mu\text{mol.m}^{-2}.\text{s}^{-1}$) and in antiphase with the LD cycles experience by the roots. Other studies with different organisms also used conflicting phasing of zeitgebers, namely LD and temperature cycles. The clock was either entrained by LD or temperature cycles depending on the relative strength of each zeitgeber (Liu *et al.*, 1998; Johnson *et al.*, 2004). In our case, even with only 0.2 or $1 \mu\text{mol.m}^{-2}.\text{s}^{-1}$ of light on the roots *GI* expression peaked during the second half of the “root day”, and then free ran with a phase determined by these “root LD cycles” (Figure 5.3). If a zeitgeber from shoots (e.g. photosynthates) was strong enough, it would have entrained *GI* in the roots so that it peaked during the second half of the “shoot day” (i.e. when roots were in the dark). This was not the case. However, *GI* did not seem properly entrained in R1 and R5 (Figure 5.3.C&D): the periods in LD cycles were 25-26 h, not 24 h. Either the phase angles were not stabilised yet after the four LD cycles on roots or *GI* free ran because the roots might have been virtually in LL (due to light piping from the shoots). This would need more experiments to be clarified. Nevertheless, the results presented in this chapter support the idea that plant clocks from different tissues and organs are probably not coupled, or very weakly.

Because light levels are most likely decreasing when transmitted down the roots (e.g. by absorption and diffraction), the root tips would be exposed to very low levels of light – if

any at all. It means that roots must be either extremely sensitive to light, or the root clock must be entrained by (an) other pacemaker(s). The T cycle experiments showed that both root and shoot clocks seem to be very sensitive to weak zeitgebers, namely LD cycles of different periods with very low light intensity ($0.15 \mu\text{mol.m}^{-2}.\text{s}^{-1}$). In both organs *GI* could be entrained by a very broad range of T cycles (from 16 to 40 h at least), which demonstrate how sensitive to entrainment by LD the plant clocks are. When dark-grown roots were decapitated but still entrained by LD cycles (Figure 5.2), the amount of light reaching the roots was possibly less than $0.15 \mu\text{mol.m}^{-2}.\text{s}^{-1}$. It is possible that other mechanisms of entrainment coexist in the root: for instance the LD cycles perceived by the top of the roots might be translated to other rhythmic signals that would in turn entrain the other parts of the roots. For instance a light-induced intercellular signalling, as suggested by Bischoff *et al.* (1997) cannot be excluded.

Most if not all the experiments presented in this chapter showed that root and shoot clocks behave differently under entraining conditions, although the zeitgebers were the same for both organs. The differences became evident during the entrainment by T cycles and by skeleton photoperiods. In the latter case, *GI* and *PRR9* responses to skeleton photoperiods were clearly different between shoots and roots, whereas *CCA1* and *PRR7* profiles were more similar in both organs. These differences reveal different mechanisms in each organ, and could be due to different regulation by the clock, by light, or both. For instance *GI* had very similar peaks at dawn and dusk in roots, contrary to the shoots where *GI* peaked mainly at dusk. This might be due to masking effects in roots: 3 hours of light had almost the same effect at dawn and at dusk in roots. However the much smaller peak of *GI* in shoots at dawn is explained by *CCA1/LHY* inhibition of *GI* in the current model (Pokhilko *et al.*, 2012). This inhibition may not occur in roots, because *CCA1/LHY* may not bind *EE* in roots (James *et al.*, 2008). This possibility will be explored using modelling in chapter 7.

Finally the root clock was shown to be entrained by temperature cycle for the first time. The phases of clock genes shifted in one or two days from the phases dictated by the previous LD cycles to the new phases of temperature cycles (in antiphase compared to the previous LD cycles). The phase angle under temperature cycles seemed to be rapidly stabilised, but the time-course was too short to confirm this for all genes. In addition, the plants were not released in constant conditions afterwards: a free run would be needed to confirm that the root clock was truly entrained. In the meantime such experiments were carried out in the lab: they confirmed that temperature can really entrain the root clock, as

expected. Although low levels of light can directly entrain the root clock, temperature seems to be a more obvious zeitgeber for dark-grown roots in natural conditions.

6 Effects of the *cca1/lhy*, *toc1* and *ztl* mutations on the root clock

6.1 Introduction

The data presented in this chapter come from experiments that have not been repeated yet. These preliminary results could therefore be informative but not conclusive. When I started my PhD the root clock was thought to be a simplified version of the shoot clock; only the “morning loop” seemed to be circadian under LL (James *et al.*, 2008). In the models at that time (Locke *et al.*, 2006; Zeilinger *et al.*, 2006), *LHY/CCA1* and *PRR7/9* formed this morning loop. In these mathematical models the morning loop was coupled with the evening loop via connections with *LHY/CCA1* (Figure 1.4.A). A prediction was that the *prp7/9* mutation should have stopped the root clock. But contrary to this, in the *prp7/9* double mutant, *TOC1* transcripts regained rhythmicity in roots under LL (James *et al.*, 2008). One explanation for this unexpected rhythmicity was that in roots, disengagement of the morning and evening loops would require *PRR7* and/or *PRR9*. The current model of the clock is more complex than the L2006 model (Pokhilko *et al.*, 2012) but it still includes a morning loop between the *PRRs* and *LHY/CCA1*. If this is the only loop present in the root clock mechanism, the *cca1-11/lhy-21* double mutation should then stop the root clock. The effects of this double mutation were therefore tested experimentally.

The previous chapters suggest that shoot and root clocks may share the same components, including evening genes. Yet these two clocks behave differently, especially under LL. Therefore some of the clock components may play different roles in shoots and roots. If so, mutations of such components should affect shoot and root clocks differently. Earlier studies showed that the *toc1-10* mutation did not affect the root clock; at least it did not seem to shorten the root clock FRP under LL, although the same mutation did shorten the FRP in the clock of mature shoots (James *et al.*, 2008). Previous chapters showed that *TOC1* expression is actually rhythmic in roots under LD, LL and DD, at least at the mRNA levels. But this does not necessarily mean that *TOC1* is part of the core mechanism in roots, even though *TOC1* is a core clock gene in shoots. For instance *TOC1* might be an output in roots, which could reconcile the results mentioned above: *TOC1* could be circadian in roots but its mutation would not have any effect on the root clock, at least not

on the FRP under LL. This idea was tested with imaging by monitoring the *CCR2:LUC+* activity in the *toc1-4* mutant.

Finally, the effect of the *ztl-105* mutation was explored. This mutation lengthens the FRP of clock genes in shoots (Baudry *et al.*, 2010; Somers *et al.*, 2004). But in WT plants clock genes already have a longer FRP in roots compared to shoots. Is ZTL functional in roots? If not, it could explain why the FRP under LL is longer in roots compared to shoots.

6.2 The *cca1/lhy* double mutant displays rhythmicity in roots, but with a shorter FRP than in shoots

Does the *cca1-11/lhy-21* double mutation stop the root clock? To answer this question, 5 week old plants carrying the *CCR2:LUC+* reporter in the *cca1-11/lhy-21* double mutant background were imaged for 5 days in LL (Figure 6.1). This double mutant has a clear growth phenotype: shoots and roots are smaller and the plants flower earlier compared to the WT. Therefore plants were already flowering when imaging started. But the signal from dark-grown roots of younger (and smaller) plants was too low to be monitored. The following results should be considered with caution, the plants being in a different developmental stage (reproductive stage) compared to other studies presented in this thesis.

Under LD, the phase of *CCR2* was advanced in the *cca1-11/lhy-21* double mutant compared to the WT, in both shoots and roots (Figure 6.1). The levels of luminescence were relatively high in roots during the first few hours of imaging, making the dusk peak of *CCR2* in the double mutant hard to distinguish (Figure 6.1). This is probably because more luciferase accumulated in these old plants than in the younger plants I usually image. Although plants were sprayed with luciferin at least 12 h before imaging started, it may have taken longer for all the accumulated luciferase to be inactivated.

The FRP of *CCR2* in shoots under LL was shorter in the double mutant compared to the WT (19.17 h and 25.02 h respectively, Table 6.1), consistent with previously published work (Locke *et al.*, 2005b). In roots, the *CCR2* rhythm persisted the first 3 days under LL in the double mutant, and its FRP was also shorter compared to the WT (22.48 h and 28.06 h respectively, Table 6.1); these period estimates only considered the LL period between ZT24 and ZT96 because *CCR2* was arrhythmic the last 2 days in LL. Note that the rhythm

of *CCR2* was rapidly dampened in the roots of the double mutant, but interestingly *CCR2* rhythm damped less in roots than in shoots in the double mutant (Figure 6.1).

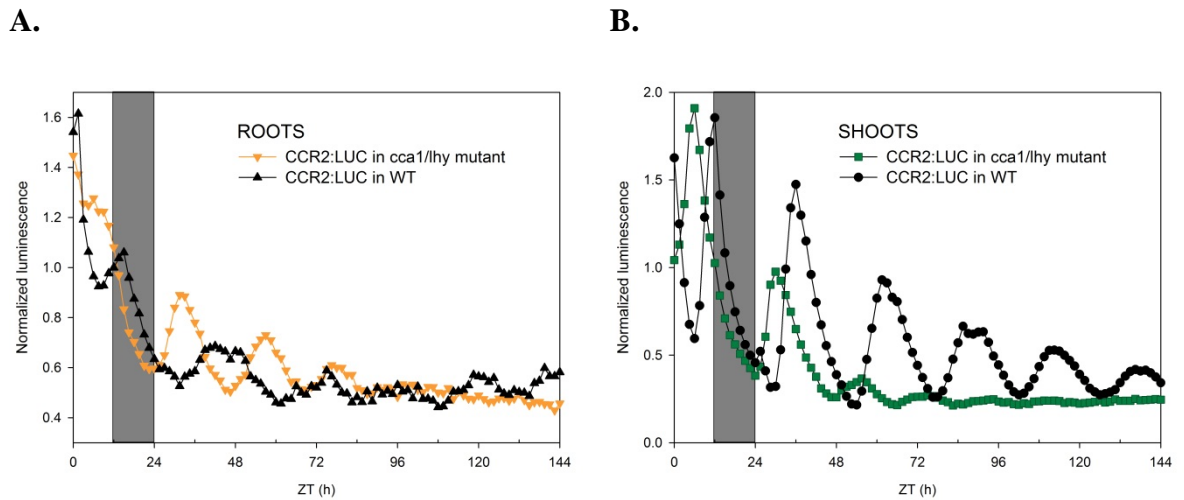


Figure 6.1: The *cca1-11/lhy-21* double mutant displays rhythmicity in the root under LL

All the plants were in the WS background. WT and *cca1-11/lhy-21* double mutant plants carrying the *CCR2:LUC+* reporter were entrained for 5 weeks in LD cycles before imaging. They were then entrained a last day in LD before release in LL for 5 days. Roots were dark-grown.

A and B: Luminescence of *CCR2:LUC+* in roots (A) and shoots (B) over time. Each time-course was normalised to the mean over the last LD cycle. Data were from 1 cluster of 5-6 plants. The dark grey bars in the backgrounds represent the last night before release in LL.

This experiment should be repeated to test how significant the differences between FRPs are, and it should be repeated with younger (non-flowering) plants. Nevertheless it already indicates that the root clock involves probably more than just a morning loop.

Table 6.1: FRPs of *CCR2* expression in roots and shoots of WT and mutants under LL

The periods were estimated from the data presented in figures 6.1, 6.2 and 6.3. The time-courses between ZT48 and ZT144 were considered (i.e. all the period in LL except the first 24 h), except for dark-grown roots of *cca1-11/lhy-21* and *toc1-4* mutant (periods marked with *): the time-courses between ZT24 and ZT96 were considered because rhythms were too dampened afterwards. ND: Not Determined, because the experiments were not done.

shoots		dark-grown roots		light-grown roots	
mutant	WT	mutant	WT	mutant	WT

<i>cca1/lhy-21</i> vs. WT	19.17	25.02	22.48*	28.06*	ND	ND
<i>toc1-4</i> vs. WT	21.41	25.75	25.62*	29.72*	23.45	27.47
<i>ztl</i> vs. WT	29.85	24.50	30.69	28.47	ND	ND

6.3 The *toc1-4* mutation shortens the FRP in the root clock

To investigate whether TOC1 actually plays a role in the root clock or not, the *toc1* mutant was studied. Plants expressing the *CCR2: LUC+* reporter in the *toc1-4* mutant or in the WT were entrained in LD for 3-4 weeks. They were then imaged one day in LD followed by 5 days in LL (Figure 6.2). The roots were light- or dark-grown to see if the possible role of TOC1 in the root clock depends on light conditions.

Under LD, the profiles of *CCR2* expression were almost identical in shoots of WT and mutant, with the same time of peak expression (Figure 6.2.B). *CCR2* also peaked at the same time in roots of WT and mutant (Figure 6.2.A). However the phase of *CCR2* was advanced a few hours in light-grown roots compared to dark-grown roots.

In LL, the FRP was shorter in the *toc1-4* mutant compared to the WT in shoots (21.41 h and 25.75 h respectively, Table 6.1), consistent with previous results (Millar *et al.*, 1995a). In roots, *CCR2* free ran too and its FRP was ~ 4 h shorter in the *toc1-4* mutant compared to the WT whether roots were light- or dark-grown (Figure 6.2 and Table 6.1). However rhythms dampened rapidly to a low and arrhythmic level in dark-grown roots of the *toc1-4* mutant (Figure 6.2.A). Therefore only the first 3 days of LL were considered for the period analysis (i.e. ZT24-96, Figure 6.2.A).

The FRP of *CCR2* in the roots of the *toc1-4* mutant was shorter when roots were exposed to light compared to dark-grown roots (23.45 h and 25.62 h respectively, Table 6.1), but plants with dark-grown roots started flowering during the experiment, which might have affected rhythms in roots.

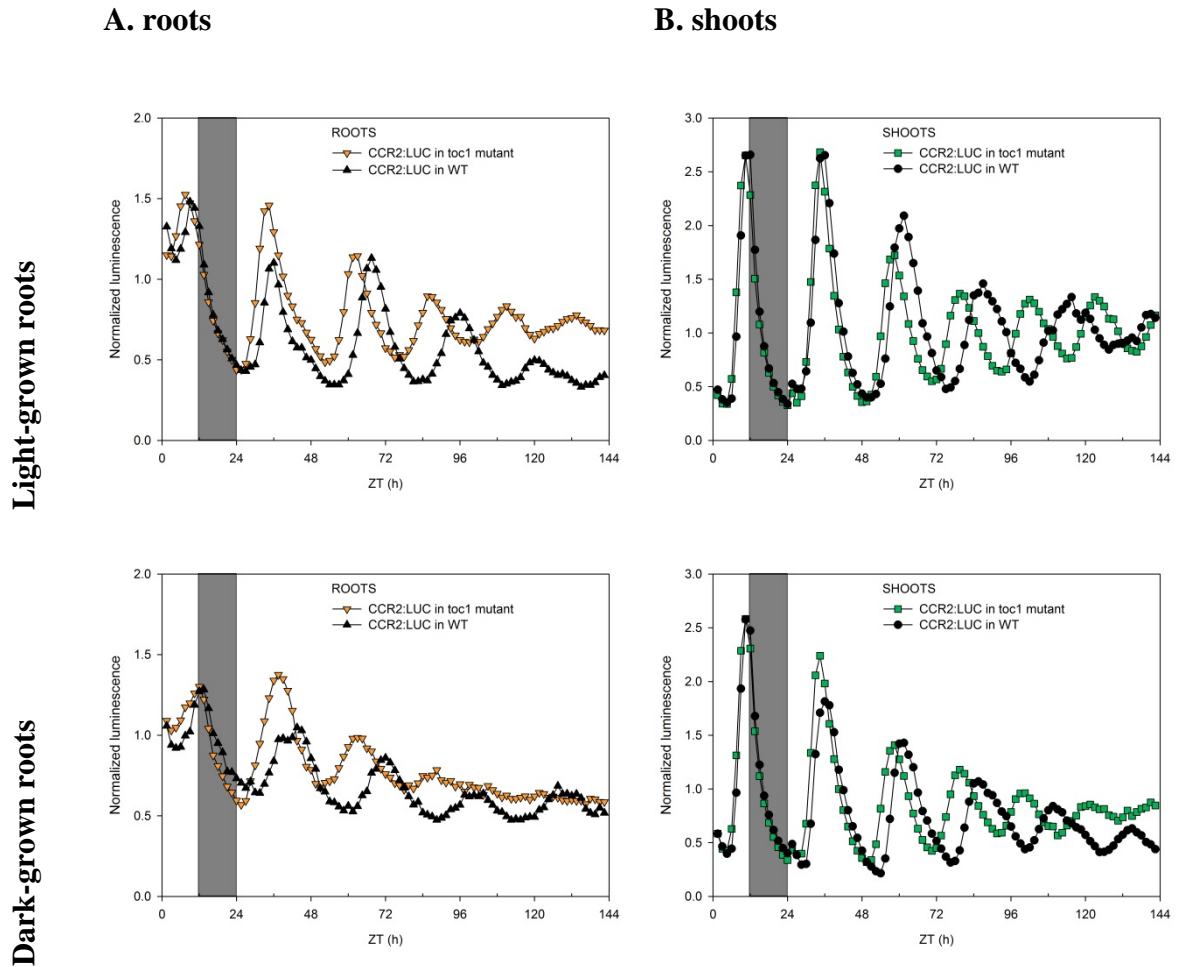


Figure 6.2: The *toc1-4* mutation shortens the FRP of *CCR2* expression in both light- and dark-grown roots under LL

WT and *toc1-4* mutant plants (both in the Ws background) carrying the *CCR2:LUC+* reporter were entrained for 3-4 weeks in LD cycles before imaging. They were then entrained a last day in LD before release in LL for 5 days. Roots were either light- or dark-grown (top and bottom row respectively).

A and B: Luminescence of *CCR2:LUC+* in roots (A) and shoots (B) over time. Each time-course was normalised to the mean over the last LD cycle. Data were from 1 cluster of 3-6 plants. The dark grey bars in the backgrounds represent the last night before release in LL.

In conclusion, the data from light-grown roots are consistent with the data from shoots, in the sense that the *toc1-4* mutation shortened the FRP of the mutant in both organs compared to the WT. The results were qualitatively similar when roots were dark-grown, although the rhythms dampened rapidly. In any case the experiments should be repeated, especially the one with dark-grown roots that should be done with non-flowering plants.

Nevertheless, the preliminary results presented in this section indicate that *TOC1* is possibly a core clock gene in roots.

6.4 The *ztl-105* mutation differentially affects *CCR2* expression in shoots and roots

If *ZTL* is a component of the root clock, its mutation should affect the FRP of clock-controlled genes in this organ. *CCR2* is such an output gene: its expression is rhythmic under LL in roots of the WT (figure 6.1 and 6.2). Plants expressing the *CCR2: LUC+* reporter in the *ztl -105* mutant or in the WT were entrained in LD for 4 weeks. They were then imaged one day in LD followed by 5 days in LL (Figure 6.3). The roots were dark-grown.

Under LD, the profiles of *CCR2* expression were almost identical in shoots of WT and mutant, with notably the same time of peak expression (Figure 6.3.B). *CCR2* also peaked at the same time in roots of WT and mutant (Figure 6.3.A), and *CCR2* peaked at dusk in both organs (Figure 6.3.A-C).

The FRP of *CCR2* was longer in the *ztl -105* mutant compared to WT, in both shoots and roots (Figure 6.3 and Table 6.1). However the difference between mutant and WT was much more pronounced in shoots than in roots (Figure 6.3.D). The FRP in shoots was about 6 h longer in the *ztl -105* mutant compared to the WT. This is consistent with published data (Baudry *et al.*, 2010; Somers *et al.*, 2004). The difference between FRP in WT and mutant was much less in roots (~ 2 h, Figure 6.3.D and Table 6.1), although it seemed longer the first 3 days in LL (Figure 6.3.A). Indeed there were at least 35 h between the two first peaks of *CCR2* in the roots of the mutant in LL but the time between the subsequent peaks was reduced, hence a FRP estimate of 30.69 (Table 6.1). There was therefore a phase shift in LL for the expression of *CCR2* in the roots of the *ztl -105* mutant, which was then in antiphase with shoots (Figure 6.3.C, ZT72-144).

Interestingly the FRP was very similar in shoots and roots of the *ztl -105* mutant (~30h, Figure 6.3.D and Table 6.1). This experiment needs to be repeated to see whether differences in FRP are significant or not, between shoots and roots and between WT and mutant. Considering these four conditions (shoots and roots in WT and mutant) with future

replicates, an ANOVA analysis might then reveal that only the FRP of shoots in WT is significantly different from the three other FRPs. If this speculation is correct it would suggest that ZTL is not functional in roots.

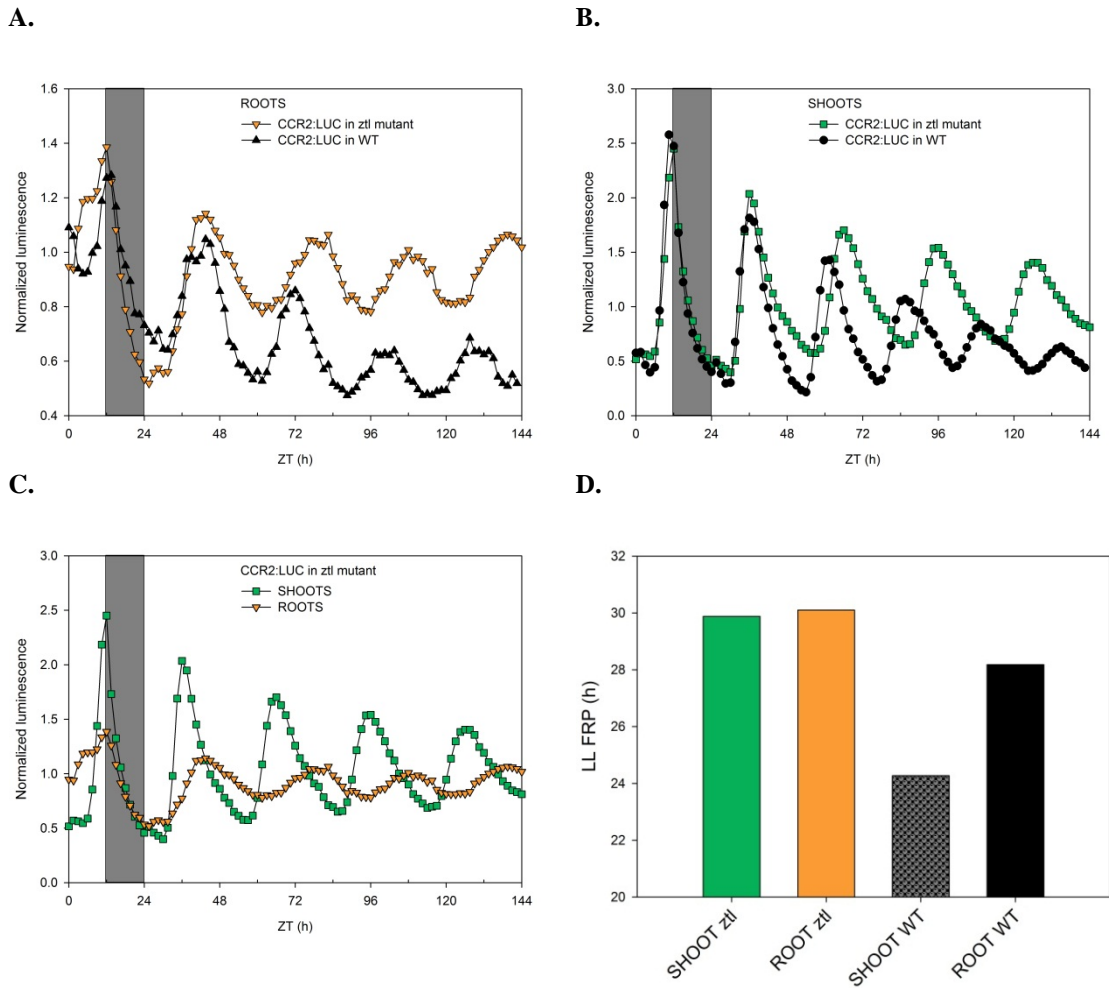


Figure 6.3: The *ztl-105* mutation affects differently *CCR2* expression in shoots and roots

WT and *ztl* mutant plants carrying the *CCR2:LUC+* reporter were entrained for 4 weeks in LD cycles before imaging. They were then entrained a last day in LD before release in LL for 5 days. Roots were dark-grown.

A-C: Luminescence of *CCR2:LUC+* in roots (A) and shoots (B) for WT and *ztl-105* mutant. Shoots and roots of the mutant were replotted together in C. The dark grey bars in the backgrounds represent the last night before release in LL. Data were from 1 cluster of 3-6 plants.

D: FRPs in LL of data presented in A-C. Circadian period were estimated using BRASS for roots and shoots in WT and mutant; their values are also presented in Table 6.1.

6.5 Conclusion

The mutants studied in this chapter are known to be clock mutants in shoots, but apart from the *toc1* mutant they had not been studied in roots before. The single mutations of *TOC1* and *ZTL*, and the double mutation of *CCA1* and *LHY* had qualitatively similar effects on the expression of *CCR2* in both shoots and roots. In LL the *toc1-4* and *cca1-11/lhy-21* mutations shortened the FRP in shoots and roots compared to the WT, whereas the *ztl-105* mutation lengthened the FRP in both organs.

In LD, the profiles of *CCR2* expression, including its dusk phase, were very similar in WT, *toc1-4* and *ztl-105* mutants but different in the *cca1-11/lhy-21* double mutant, where the phase was advanced. This was true for both shoots and roots. The amplitudes were lower in roots compared to shoots in the three mutants, as it is the case in WT.

In LL, the amplitudes were in general lower in roots compared to shoots in WT and mutants, with the possible exception of the *cca1-11/lhy-21* double mutant where *CCR2* damped quickly in LL to relatively flat levels in both organs. For all mutants the lower amplitude of clock genes in dark-grown roots compared to shoots is comparable with the data in WT presented in this chapter and in the previous ones.

In the *cca1-11/lhy-21* double mutant, the amplitude in LL seemed to dampen more in shoots compare to roots, but this may be an artefact. In fact the plants were older and flowering, and the mechanism of the clock might depend on the developmental stage. This is probably the case in humans where chronotype is age-dependent (Roenneberg *et al.*, 2007). Therefore these results should be taken carefully, as well as the data from dark-grown roots in the *toc1-4* mutant because the plants were starting to flower. More generally, all the results presented in this chapter are only indicative because the experiments were only done once.

The FRP of *CCR2* was clearly shorter in light-grown roots of the *toc1-4* mutant than in that of the WT. This is consistent with the effects of *toc1* mutation on the shoot clock. But it is

in contrast with a previous study (James *et al.*, 2008) where the *toc1-10* mutation did not seem to have any effect on the root FRP in LL. However James and colleagues studied dark-grown roots. When the roots were dark-grown for my imaging experiment, the effect of the *toc1-4* mutation was clearer: it shortened the FRP of *CCR2*. In addition, James and colleagues used the *toc1-10* mutant whereas the plants I imaged were in the *toc1-4* mutant background. Mutations at different loci of *ztl* result in different FRP under LL, e.g. ~25 h and ~ 28 h for the *ztl-21* and *ztl-31* mutants respectively (Kevei *et al.*, 2006). Similarly, different *toc1* alleles might have different effects on the root clock. The effect of the mutation may also depend on the presence or absence of light on the roots. However, *TOC1* was shown to be rhythmic in light- and dark-grown roots in most conditions (Chapters 3-5), and it is a core clock gene in shoots. Taken together with the preliminary data of *toc1-4* mutant in roots (section 6.2), this indicates that *TOC1* might be a key player in the root clock too.

The experiment with the *ztl-105* mutant was also done once. However, the FRP in shoots and roots of the mutant were very similar (~ 30 h) and only 2 h longer than the FRP in roots of the WT. In contrast, the FRP in the shoots of the WT were 4-6 h shorter, i.e. ~ 24 h as previously published (Somers *et al.*, 2004).

If these results are reproducible, they could suggest that ZTL may be less effective in roots compared to shoots. Indeed in shoots the enhanced stabilisation of ZTL by GI under blue light seems to contribute to normal clock function (Kim *et al.*, 2007). In dark-grown roots there must be less blue light, if any at all (Sun *et al.*, 2005; Tester and Morris, 1987). ZTL would therefore be less stable in dark-grown roots, assuming this mechanism is similar in both organs. This might contribute to the longer FRP observed in the roots of WT plants, as is observed in the shoots of *ztl* mutant (Mas *et al.*, 2003). ZTL functions need to be further investigated in roots, at different levels (e.g. mRNA and protein) and under different conditions (e.g. blue or red light).

7 Modelling the root clock

7.1 Introduction

All the mathematical models of the plant circadian clock published so far - between 2005 and 2012 - have been based on seedling data. These are mainly imaging data and are very similar to our data from mature shoots⁵. However it was shown in 2008 that the circadian clock differs in shoots and roots (James *et al.*, 2008). Therefore the general aim of the work in this chapter was to refine the plant circadian clock model, adding some organ specificity.

The root clock was first thought to be a simplified slave version of the shoot clock (James *et al.*, 2008). Although most if not all the clock genes found in shoots were also rhythmic in roots under diurnal conditions, only the morning loop was running in the roots under constant conditions, and with a longer FRP compared to shoots. Thus my initial aim was to model these differences: the longer FRP of morning genes, the arrhythmia of evening genes under LL or DD, and also a synchronisation mechanism between the two organs under LD. In 2008 the latest versions of the plant circadian model were the Zeilinger *et al.* (2006) and the Locke *et al.* (2006) models, the latter being referred as the L2006 model hereafter. Some parameters of the L2006 model were modified in an attempt to simulate the behaviour of the root clock (section 7.2).

During the last few years, more root clock data have been acquired in different conditions. It turned out that the evening loop is actually circadian in roots too (under LL and DD); this was easier to detect with imaging than with RT-qPCR. Nevertheless these data confirmed that the shoot and root clocks have different FRPs under LL. In the meantime, two updated versions of plant circadian clock models were published (Pokhilko *et al.*, 2010; Pokhilko *et al.*, 2012) and will be referred as the P2010 and P2012 models hereafter. Both models were used and some of their parameters changed in attempt to fit the more recent root data (sections 7.3-7.6).

⁵ Seedling data are mostly – if not only – shoot data. Similarities with data from mature shoots were therefore expected, although our plants are a few weeks older than seedlings

Later experiments showed that the clock of dark-grown roots, which can perceive some light channelled from the exposed tissues, can be directly entrained by LD cycles. Therefore the equations and parameters modelling light and dark inputs to the clock in the latest model (P2012) may be appropriate for a model of the root clock too. Some of these “light-related parameters” were optimised in order to fit more root data (section 7.6).

In this chapter simulations with default parameters of published models will be referred as shoots and be represented by solid green lines. Simulations with other parameters (attempting to fit the behaviour of the root clock) will be referred as “roots” and represented by dashed or dotted lines. For simplification, all the simulations presented in this chapter were done with the same (default) initial states. All these are simulations of mRNA levels for different clock genes.

7.2 Changing the parameters g3, g4 and g6 of the L2006 model can simulate some aspect of the root clock in specific conditions

In 2008 one of the latest versions of the plant circadian clock model was the L2006 model. Some of its parameters were changed to attempt to fit the root clock data qualitatively. The first simulations were run with Circadian Modelling (CM), a user friendly software where the different biological parameters and light conditions can be easily changed. As for other mathematical models the L2006 model is based on seedling data. Could the parameters of this model be modified to fit the behaviour of the root clock? At that time our knowledge about the root clock was the one published by James *et al.* (2008). The main differences between root and shoot (or seedling) clocks were that:

- only the morning loop oscillated under LL in dark-grown roots
- the period of this oscillations was about 2 h longer than that of the 3-loop clock in shoots.

To simulate the dark environment of the roots, the light terms in the differential equations had to be removed. When all light inputs in the equations were removed the three loops remained rhythmic with a period close to 24 h (Table 7.1). This simulated FRP in DD did actually not match experimental data. Therefore other parameters had to be changed. For the following simulations the default set of parameters in constant darkness was used as a

starting point; then a few parameter values were changed based on biological data and assumptions as detailed below.

Experimentally, no EE-binding complex containing LHY could be detected in roots and therefore LHY/CCA1 may not be able to inhibit gene expression in this organ (James *et al.*, 2008). To simulate this behaviour, the values of two parameters were changed: g_3 and g_6 (cf. Figure 1.4.A and equations 1 and 3 in section 2.5). The bigger these values, the lower CCA1/LHY inhibition of *TOC1* and *Y* mRNA synthesis respectively. Several combinations of parameters that reduced *TOC1* amplitude were tried, e.g. in setting g_3 and g_6 to 1000-fold their default value (Figure 7.1). The mean expression level of *TOC1* was then higher, but expression was still rhythmic with a shorter period. In increasing g_3 and g_6 less (20 times), *TOC1* expression remained high and still oscillated with a lower amplitude (Figure 7.1.A). Besides, *LHY* had a slightly longer period with these sets of parameters (g_3 and g_6 increased 20 or 1000 times) compared to the default value representing the shoots (Figure 7.1.B and Table 7.1). However, the FRP should be even longer (~25.4 h on average for dark-grown roots under LL according to James *et al.*, 2008). Many other combinations of these two parameters were used for simulation, but without fitting the root data better (simulations not shown).

Then the observed effects of the *prr7/9* double mutant were considered: in the roots of this mutant, the evening loop surprisingly regained rhythmicity (James *et al.*, 2008). The PRR7 and PRR9 proteins are actually related to TOC1 (also known as PRR1). Hence biochemically two plausible explanations of the *prr7/9* mutant would be that in roots PRR7 and PRR9 might either compete with or enhance the function of TOC1. In the L2006 model, this could be simulated by changing the values of g_4 and g_5 (cf. Figure 1.4.A and equations 2 and 3 in section 2.5). Many combinations for these 2 parameters were used together with different combinations of g_3 and g_6 to run other simulations. Some of these new parameter sets affected the morning loop period or gave a lower amplitude for *TOC1*. One example is shown in Figure 7.1 C&D, where changing g_3 , g_4 and g_6 simultaneously gave not only a higher level for *TOC1* mRNA (Figure 7.1.C) with lower and more variable amplitude (hence its rhythmicity might have not been detected by RNA quantification), but also a 2 h longer FRP for the morning loop (Figure 7.1.D and Table 7.1). This set of parameters, with g_3 and g_6 increased 20 fold and g_4 decreased 100 fold, is the one that best fitted the root data qualitatively. It will be referred as 20(g_3g_6)0.01 g_4 . For instance,

the FRP for APRR (representing PRR7 and PRR9) mRNA is also longer with $20(g3g6)0.01g4$ compared to the default value (Table 7.1).

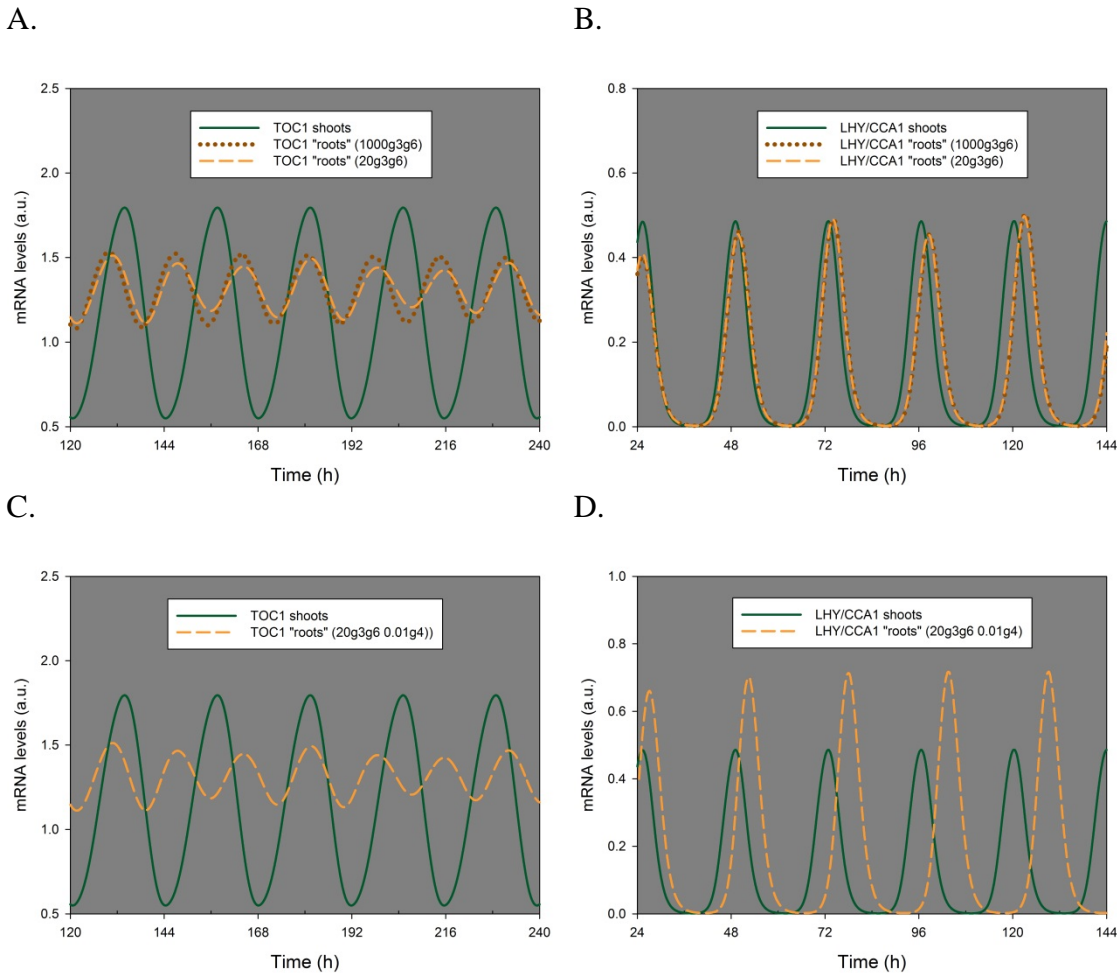


Figure 7.1: Simulations of *TOC1* and *LHY* mRNA levels in shoots and “roots” under DD using the L2006 model

The simulations with default parameters of the L2006 model represent seedling data in DD and are labelled shoots (green solid lines). The other simulations attempt to fit the root clock data obtained with dark-grown roots in LL (James *et al.*, 2008); they are labelled “roots” (orange dashes or brown dots)

A and B: Simulations with the “1000(g3g6)” and “20(g3g6)” sets of parameters. The default set of parameters of the L2006 models were used, except g3 and g6 (both increased 1000 or 20 fold respectively) to simulate the LHY and CCA1 lack of binding to EE. Simulations under DD for *TOC1* (A) and *LHY* (B) mRNA levels.

C and D: Same as A and B respectively but with g3 and g6 increased 20 fold, and g4 decreased 100 fold (labelled “20(g3g6)0.01g4”).

The “optimised” set of parameter (20(g3g6)0.01g4) was then used to run simulations in LD (Figure A.5 in appendix).. Interestingly, the period of clock genes in “roots” was then close to 24 h, especially for *TOC1* (Table 7.1).

Table 7.1: Period estimates of simulated rhythms in shoots and “roots” under DD and LD using the L2006 model

The periods of simulated rhythms from Figure 7.1 and 7.2 were estimated with CM. The default values are from the L2006 model and represent shoots. A few parameter values were then changed: g3 and g6 increased 20 fold (labelled “20(g3g6)”) and g4 decreased 100 fold (labelled “0.01g4”). With the CM software the periods were estimated in two ways: time (h) between two consecutive peaks or trough. Both estimates gave very similar results; they were then averaged over the time courses presented in Figure 7.1 and 7.2. ND= Not Determined (i.e. considered arrhythmic).

mRNA	DD			LD	
	shoots	“roots” 20(g3g6)	“roots” 20(g3g6)0.01g4	shoots	“roots” 20(g3g6)0.01g4
LHY	23.75	24.37	25.74	24.00	24.56
TOC1	23.75	17.11	15.79	24.00	24.10
Y	23.75	17.09	16.46	ND	ND
APRR	23.75	24.37	25.64	24.00	24.36

Since the roots were dark-grown, it was unlikely that the root clock data could be simulated in LD (or LL) using the same input-related terms in the equations (e.g. the light parameter “L”), at least not the same parameter values⁶. However, some inputs for the root clock could be indirectly related to LD cycles such as rhythmic levels of sugars (James *et al.*, 2008). Therefore it might be possible to keep the same equations as in the L2006 model but modify the light-related parameter values to fit the root data. Since many terms of the model are related to light it would have been very time-consuming to optimise them manually with CM. A more global and automated approach to optimize parameters for the root clock was preferable. That is why the Systems Biology Software Infrastructure (SBSI) was used in the next sections. Nonetheless, the main features of the root clock could be fitted qualitatively in specific conditions: longer FRP for the morning genes, and high relative levels of *TOC1* with low amplitude, whose rhythms could have been missed experimentally by RNA quantification due to variability and sampling frequency. This suggested that the framework of the L2006 model might also be applicable to roots.

⁶ it was later found that light can directly entrain the root clock, but the level of light perceived by dark-grown roots would then be lower

7.3 Changing only one parameter of the P2010 model (g5) can simulate many root clock data under LD, LL and DD

The Systems Biology Software Infrastructure (SBSI) allowed me to search a broader space of parameters compared to CM, in an automated way. Once the model and the data to be fitted were chosen, the optimisation process could be configured with SBSI Visual. The main steps of the process to be configured are the optimisation algorithm, the parameters to optimise and the cost function(s). The latter evaluates the goodness of fit of a particular parameter set. See section 2.5 for more details.

A first parameter optimisation was run using the L2006 model and root data in DD (from Figure 4.5). The same parameters as in previous section (using CM) were chosen for the optimisation process, i.e. g3, g4, g5 and g6. The Parallelised Genetic Algorithms (PGA) and the Fast Fourier Transform (FFT) cost function (with a target of 30 h) were used. Some of the “optimised” parameter sets gave a longer FRP for all clock genes (over 30 h) and lower amplitudes, which was consistent with our root data from imaging experiments (simulations not shown). For instance an increase in g3, g4 and g5 values (about 6-, 75- and 3-fold respectively) together with a decrease in g6 (161-fold) gave such a long period. But these parameters could not predict root data in LD and in LL. Besides, an updated version of the plant circadian clock model had been published in the meantime (Pokhilko *et al.*, 2010). Therefore this newer model (P2010) was used for further optimisation jobs to try and fit the root data.

Although many equations and parameters differed between the L2006 and P2010 models, the overall structure of these two models were comparable: a morning and an evening loop were connected by a central loop between *LHY/CCA1* and *TOC1*. In the P2010 model, *CCA1* and *LHY* were modelled as one component that will be referred as *LHY/CCA1*. This morning component repressed not only *TOC1* but also *GI* and *Y* (as it did in the L2006 model), which is represented by the parameters g5, g15 and g16 respectively in the P2010 model (cf. Figure 1.4.B and equations 4-6 in section 2.5). Therefore these parameters were changed for the same reasons that g3 and g6 were changed (cf. previous section): the experimental data suggested that *CCA1* and *LHY* were unable to inhibit gene expression in roots (James *et al.*, 2008).

Starting from the P2010 default parameters and allowing up to 100 fold increase or decrease for g_5 , g_{15} and g_{16} , these parameters were optimised to fit the root data. The PGA optimisation algorithm and the FFT cost function were used to get a longer FRP in roots based on our root data for *CCA1:LUC+* and *PRR7:LUC+* in DD (from Figure 4.5). The Chi-squared (χ^2) cost function was also used so that the actual data could be fitted (not just the 30 h period used as a target for the FFT cost function). These two cost functions were not weighted. Four thousands generations were used for this optimisation process and the last few hundreds did not decrease the cost further so the process was stopped.

The optimal parameter sets had about 50 fold increase of g_5 but only 8% increase of g_{16} and no change of g_{15} . Interestingly these parameters increased although they were also allowed to decrease; this was consistent with a lack of binding to EE observed in roots. This set gave a slightly longer FRP compared to the default set of parameters in DD (data not shown). Given the robustness of the model, 8% change in one value did not have much effect on the clock (cf. next paragraph). Then further simulations were run with only one value changed: g_5 increased 50 fold (but no change in g_{15} and g_{16}); this will be referred as the 50 g_5 set. Figure 7.3, 7.4 and 7.5 show these simulations for different clock genes in DD, LL and LD respectively.

Indeed changing only one parameter of the P2010 model (i.e. g_5 increased 50 fold) gave the same longer FRP in DD as the optimised set of parameter mentioned above (Figure 7.3). This period was only 0.2 h longer than with the default set (Table 7.2). However the same period was also reached for the other clock genes (e.g. *TOC1* and *PRR9*) not used in the optimisation process, consistent with the period values of *CCA1* and *PRR7* (used for optimisation, Table 7.2). It was also consistent with our more recent data in DD, where a *TOC1* rhythm could be detected at the mRNA level (Figure 4.6). In DD the simulated levels of *GI* dropped to 0 in less than 12 h with both parameter sets (default and 50 g_5). This was probably a weakness of the P2010 model since *GI* is rhythmic in DD in both shoots and roots experimentally (Figure 4.5 and 4.6). However *Y* mRNA levels were rhythmic in DD and were qualitatively similar to the levels of *GI* in DD. Presumably the P2010 model could give satisfactory fits in DD even though *GI* was zero because *GI* function in DD was provided by *Y*.

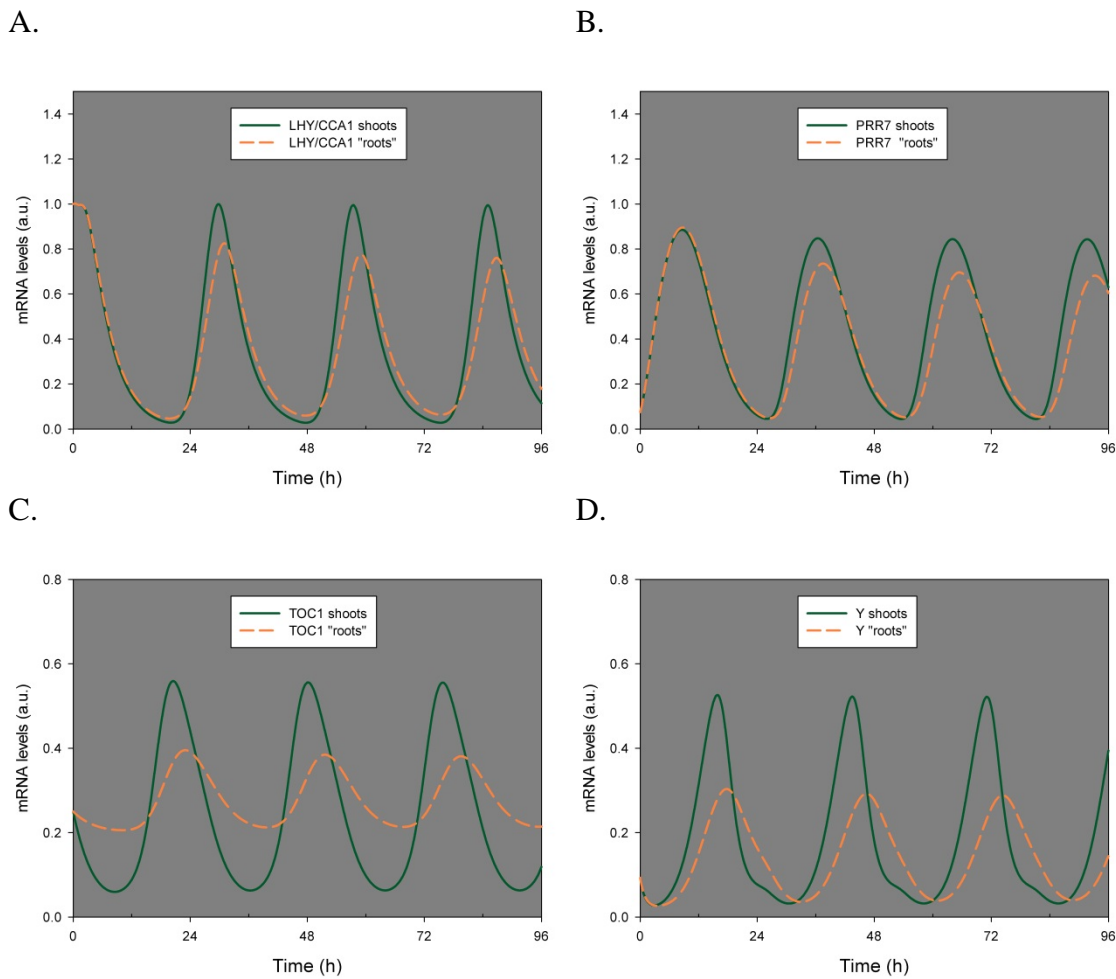


Figure 7.2: Simulations of clock genes mRNA levels in shoots and “roots” under DD using the P2010 model

The simulations with default parameters of the P2010 model represent shoot data. The other simulations (labelled “roots”) derive from a set of parameter attempting to fit the root clock data in DD (see text for details): it is the same set of parameters as shoots except g_5 that was increased 50 fold.

A, B, C and D: *LHY/CCA1*, *PRR7*, *TOC1* and *Y* mRNA levels respectively.

Interestingly, the 50 g_5 set gave a significantly longer FRP in LL compared to the default set, although this was not constrained in the optimisation process (Figure 7.4). The FRP was on average 1.5 h longer (Table 7.2) which was almost the difference observed between the FRP of shoot and root clocks in LL (James *et al.*, 2008). These attempts to simulate the root clock involved the same light inputs as in the P2010 model of the shoot clock. This was not realistic for dark-grown roots (e.g. James *et al.*, 2008) but might be realistic for

light-grown roots as in chapter 4 and 5. In the latter case, the FRP was also longer in roots compared to shoots, so the simulations with the 50g5 set matched qualitatively these data. As for DD (previous paragraph), the simulations in LL gave almost the same FRP for the expression of different clock genes except for *GI* whose period was shorter than other genes in LL. Yet the 50g5 set gave a longer period for *GI* compared to the default set of parameters (Table 7.2).

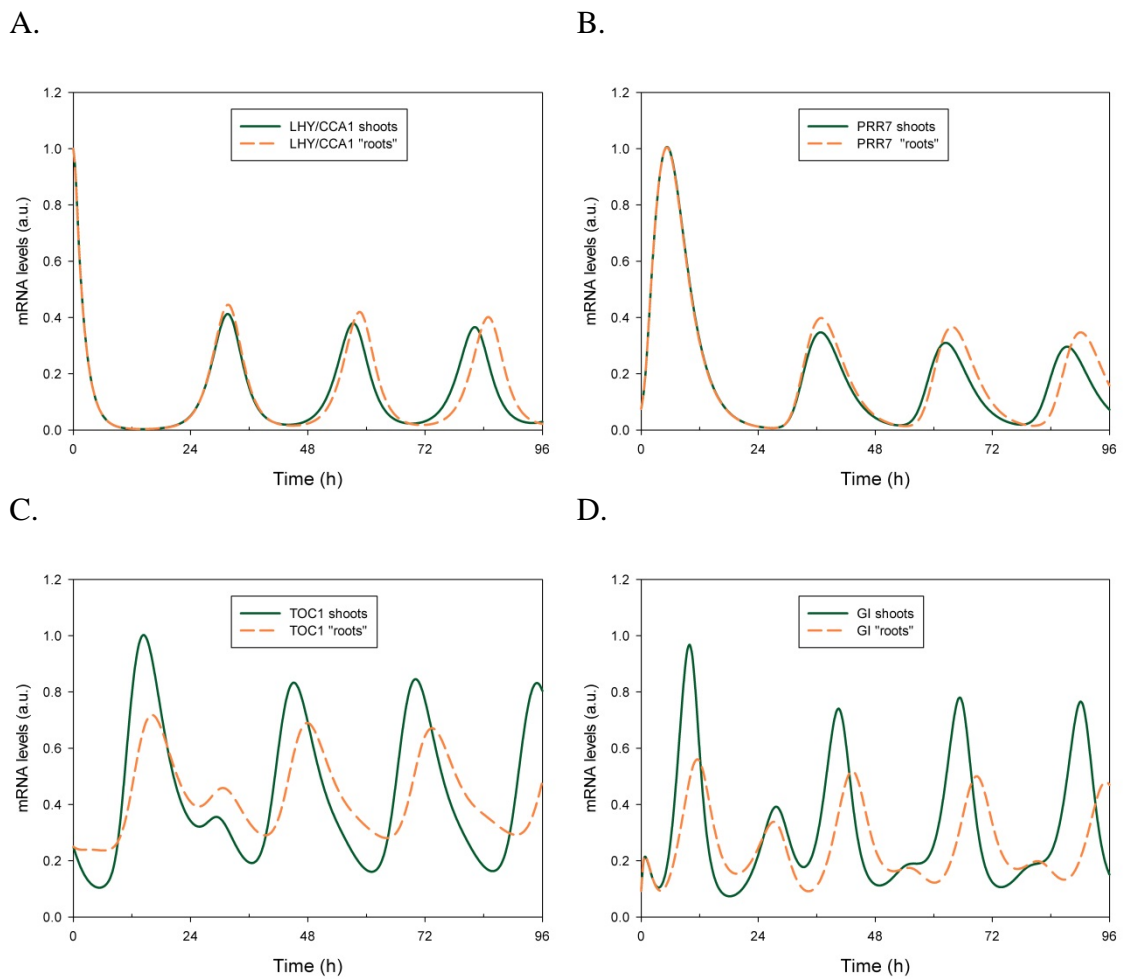


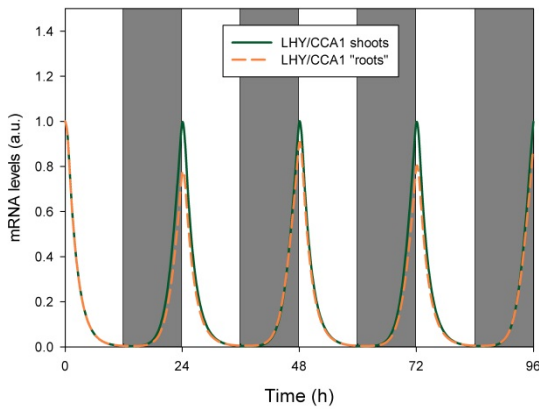
Figure 7.3: Simulations of clock genes mRNA levels in shoots and “roots” under LL using the P2010 model

The simulations with default parameters of the P2010 model represent shoot data. The other simulations (labelled “roots”) derive from a set of parameter attempting to fit the root clock data in DD (see text for details) but used in LL here: it is the same set of parameters as shoots except g_5 that was increased 50 fold.

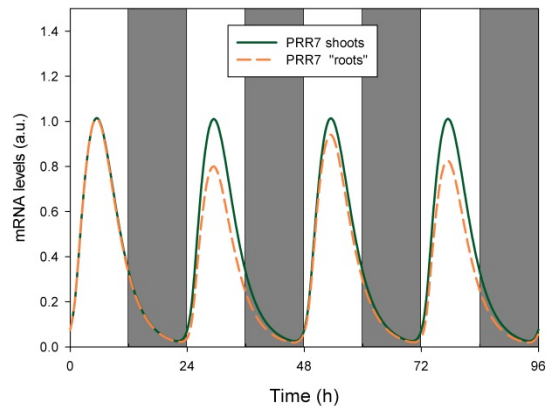
A, B, C and D: *LHY/CCA1*, *PRR7*, *TOC1* and *GI* mRNA levels respectively.

Finally the same set of parameter (50g5) was used for simulations in LD and compared with default values (Figure 7.5 and Table 7.2). As in LL, the amplitude of *TOC1* was lower in “roots” (50g5 set) compared to the shoots (default set of parameters); again this was consistent with experiments. The periods were almost the same for most if not all genes in shoots and “roots”. The period was slightly lower than 24 h for *PRR7* but with both sets of parameters (Table 7.2). Overall the period obtained with the 50g5 set in LD were much closer to 24 h compared to the corresponding simulations of the previous section (Table 7.1). In addition the phases in LD were the same in shoots and “roots”. Therefore this new set of parameters (50g5) captured one fundamental property of circadian clocks: entrainment. Overall the 50g5 set of parameter fitted the root data much better than any other “optimised set” found so far in this chapter.

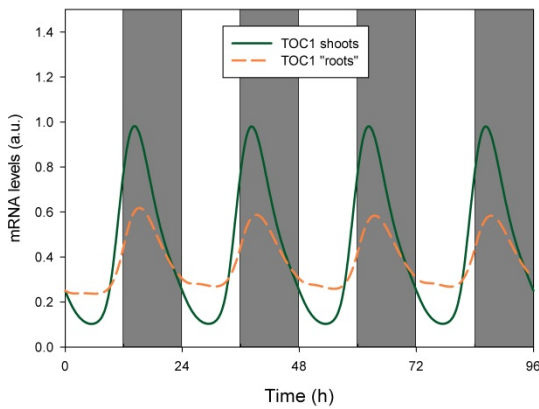
A.



B.



C.



D.

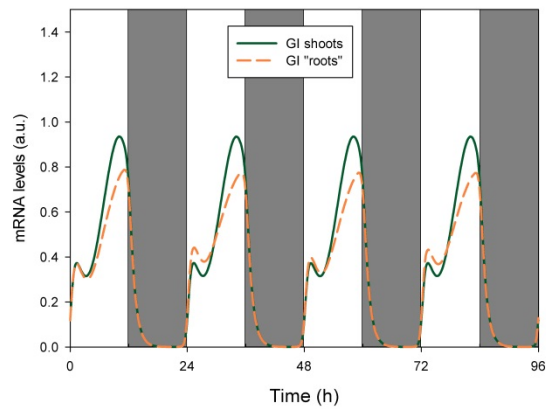


Figure 7.4: Simulations of clock genes mRNA levels in shoots and “roots” under LD using the P2010 model

The simulations with default parameters of the P2010 model represent shoot data. The other simulations (labelled “roots”) derive from a set of parameter attempting to fit the root clock data in DD (see text for details) but used in LD here: it is the same set of parameters as shoots except *g5* that was increased 50 fold.

A, B, C and D: *LHY/CCA1*, *PRR7*, *TOC1* and *GI* mRNA levels respectively.

Thus changing only a one parameter of the P2010 model could provide a qualitative fit to several aspects of the root data: a longer free-running period in LL but synchronization with the shoot clock in LD. In DD, the simulations gave similar FRPs for both shoots and root clocks. This was consistent with our more recent data, using imaging and RT-qPCR (Figure 4.5 and 4.6). However, the behaviour of *GI* under DD could not be simulated accurately with this model (P2010). More generally, an updated version of the shoot clock model (P2012) could integrate more shoot data. Therefore the P2012 model was used to simulate the root clock in the next sections.

Table 7.2: Period estimates of simulated rhythms in shoots and “roots” under DD, LL and LD using the P2010 model

The periods of simulated rhythms from Figure 7.3, 7.4 and 7.5 were estimated with BRASS (in hours); the periods for different mRNA were then averaged for each time course; SD: Standard Deviation. ND= Not Determined (i.e. considered arrhythmic). The default values are from the P2010 model and are labelled shoots. The other parameter set is the same except *g5* increased 50 fold (labelled “roots”).

	DD		LL		LD	
mRNA	shoots	“roots”	shoots	“roots”	shoots	“roots”
LHY	27.56	27.77	25.09	26.42	24.01	23.98
TOC1	27.59	27.86	25.00	26.22	24.01	24.02
GI	ND	ND	24.00	25.81	24.01	24.06
PRR7	27.66	27.80	25.07	26.56	23.89	23.86
PRR9	27.64	27.78	25.15	26.60	24.02	24.02
average	27.61	27.80	24.86	26.32	23.99	23.99
SD	0.05	0.04	0.48	0.32	0.05	0.08

7.4 Low levels of light perceived by dark-grown roots is sufficient to explain the low amplitude and the long FRP under LL in the root clock

By the time the most recent model was published (Pokhilko *et al.*, 2012) - referred as P2012 hereafter, more root clock data had been produced in different conditions: in LD, LL and DD with light- or dark-grown roots. Evening genes such as *TOC1* and *GI* are actually circadian in dark-grown roots (chapters 4 and 5). In addition, other experiments showed that light can directly entrain the root clock (chapter 5). Therefore the current mathematical models – including their light-related terms- could be used with more confidence to simulate the root clock. In fact, light directly perceived by the roots (e.g. via piping or leakage) is probably a stronger zeitgeber than indirect effects of light (e.g. via photosynthates), at least at constant temperature. The very same equations as in the P2012 model but with a different set of parameters might be able to simulate the root data. The question is: which parameters are organ-specific?

Now the main differences between the shoot and root clocks are:

- a longer FRP in roots under LL
- a lower amplitude in roots under LD

Considering that dark-grown roots must perceive lower light levels compared to shoots during light cycles, this lower light should give a longer FRP in roots under LL according to Aschoff's rules. In addition, the expression of several clock genes is acutely induced by light (e.g. *PRR9* and *GI*). Therefore lower light levels perceived by dark-grown roots might also explain lower amplitudes in roots compared to shoots. Can the P2012 reproduce these features when levels of light inputs are modified? To test this, the "light parameter" (L) value was decreased. However, how much light the roots can perceive is not known, so a range of values between 0.1 and 1 was tested (1 being the default value in light cycles).

Simulations were done with COPASI. The "parameter scan" task allows running quick simulations with a user-defined range of one or more parameters. In this case, the L parameter was scanned between L=0.2 and L=1 (here with 5 intervals of 0.2), and "outputs" such as clock gene expressions over time were visualised for each of these values of L (Figure 7.6). The scan was run in LL to check whether the P2012 model can reproduce the Aschoff's rules. Figure 7.6 shows that for *LHY/CCA1* and *GI* simulations, the lower the light, the longer the FRP under LL. This was also true for other clock genes

(not shown). Therefore the P2012 model can reproduce Aschoff's rules. But if L value is too low (e.g. 0.2), clock genes levels dampens quickly and FRPs are too long.

Note that L does not necessarily represent the light intensity, at least not on a linear scale. The P2012 is such that $L=1$ when light is present and 0 otherwise⁷. For instance, the default value of 1 might represent a light intensity of 50-100 $\mu\text{mol.m}^{-2}.\text{s}^{-1}$ (i.e. an order of magnitude usually used to produce data feeding the model), but a value of 0.2 does not represent a fifth of this intensity (10-20 $\mu\text{mol.m}^{-2}.\text{s}^{-1}$). Otherwise the simulation with $L=0.2$ should give a much shorter FRP (it is over 30 h in Figure 7.6); for instance the shoot FRP under 10-20 $\mu\text{mol.m}^{-2}.\text{s}^{-1}$ is less than 26 h (previous chapters and Somers *et al.*, 1998). Anyway, since Aschoff's rules were apparently not used to constraint the P2012 model (Pokhilko *et al.*, 2012), it is interesting that this model can reproduce these rules at all.

A. LHY/CCA1

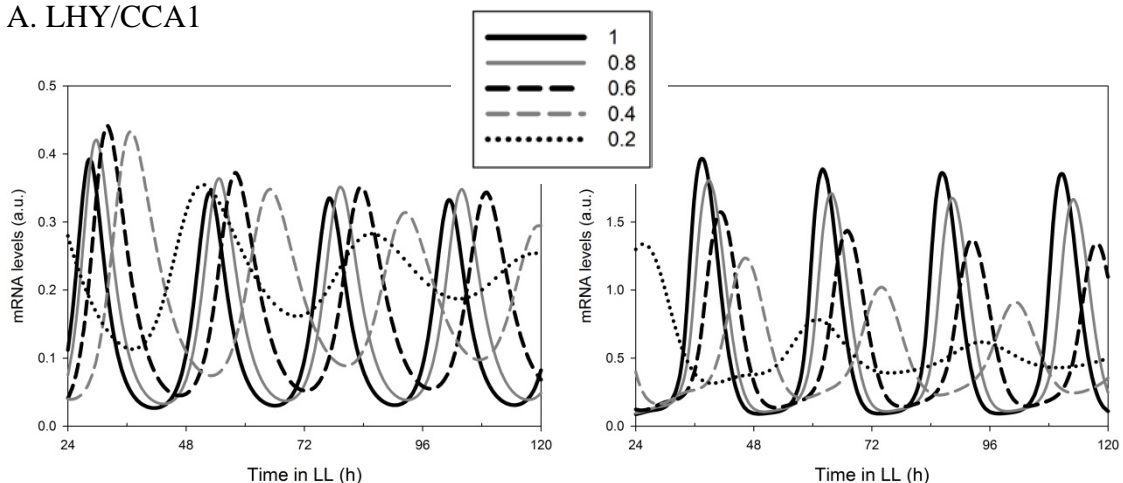


Figure 7.5: The P2012 model can reproduce Aschoff's rules

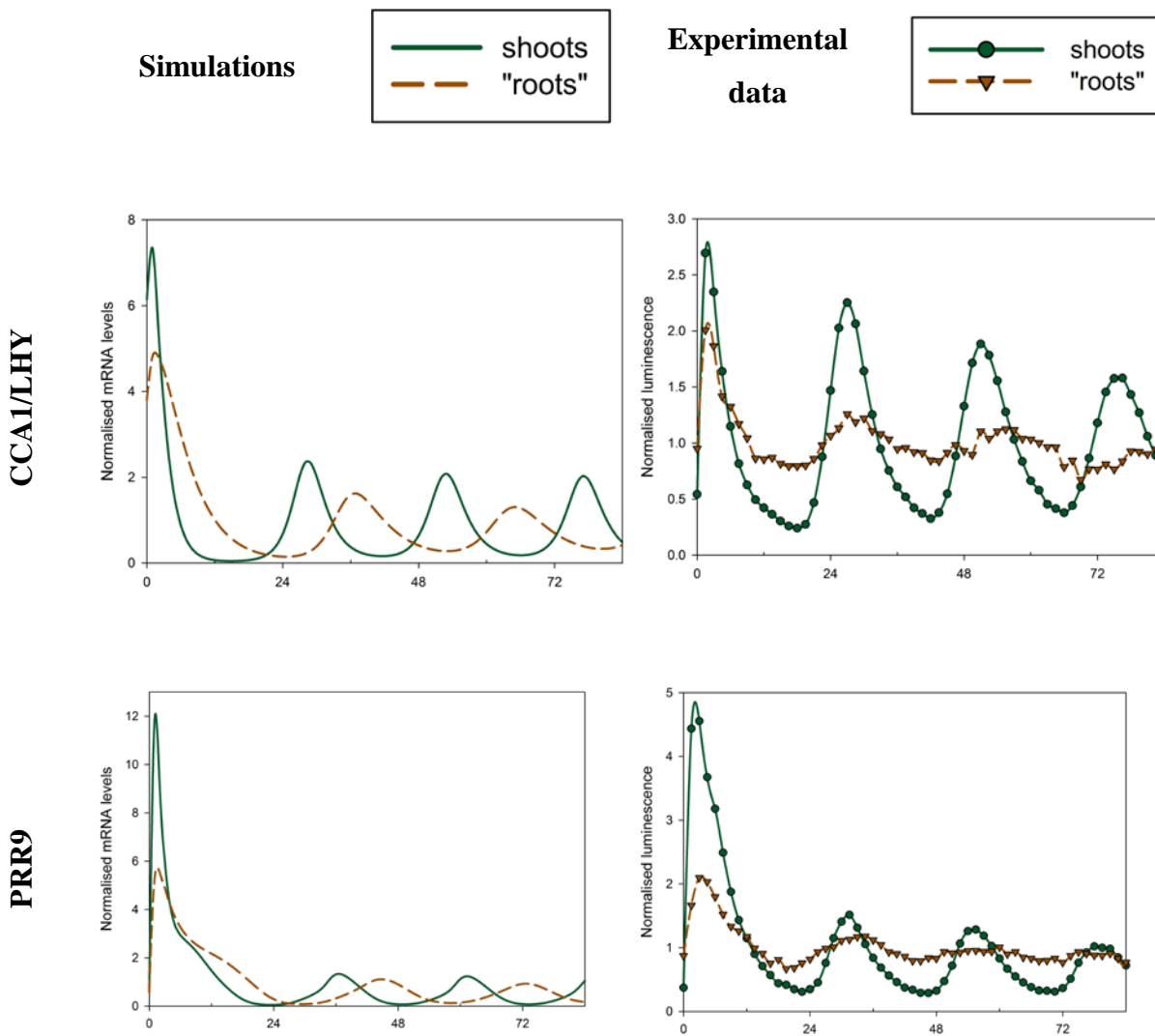
The L parameter was scanned with COPASI with 5 intervals on a linear scale between 0.2 and 1 (i.e. L takes the different values of 0.2, 0.4, 0.6, 0.8 and 1). Simulations for *LHY/CCA1* (A) and *GI* (B).

With $L=0.4$ the FRP of simulated mRNA levels were 3 h longer compared to the FRP with $L=1$; this is quantitatively similar to the differences observed between shoot and root clocks data under LL with imaging (Figure 7.7) (. There was a shift between the two first

⁷ there is also a function that simulates the smooth transition between L and D

peaks in LL, at least for *CCA1* and *PRR9* (Figure 7.7.A&B). This was only transient and possibly due to relatively high initial values used for the simulations (i.e. shoot values). The periods were estimated between ZT48 and ZT144 (i.e. 4 days in LL when the rhythms were more stable) using BRASS (data not shown).

Interestingly, compared to the amplitudes under LL when $L=1$, the amplitudes under LL when $L=0.4$ were similar for morning genes but much lower for evening genes. This is also consistent with experimental data (Figure 4.4) and could explain why some rhythms were harder to detect in roots under constant conditions (e.g. *TOC1*).



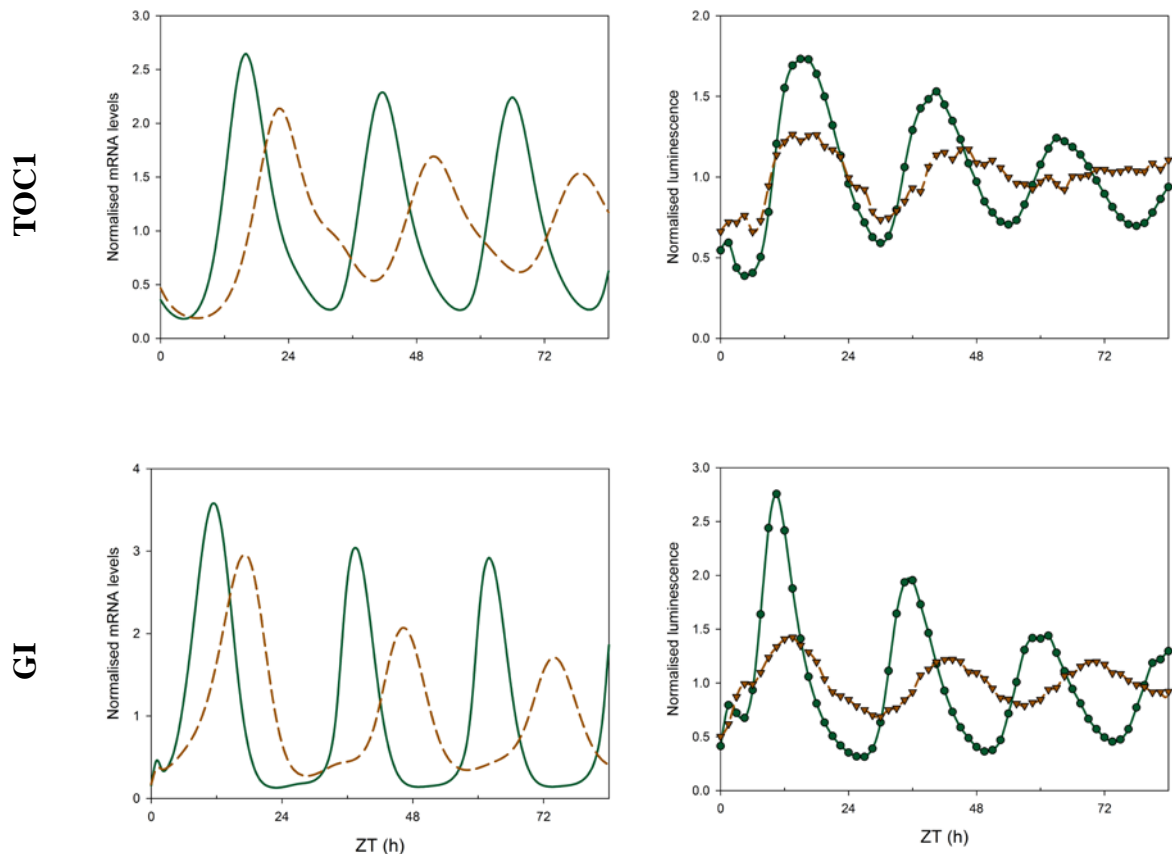


Figure 7.6: Simulations of clock genes mRNA levels in shoots and “roots” under LL using the P2012 model with different light intensities

Simulations (left, smooth lines) are compared to experimental data (right, lines with symbols). The simulations with default parameters of the P2012 model are labelled shoots. The other simulations (labelled “roots”) use the same set of parameters as shoots except light amplitude set to 0.4 (instead of 1). Experimental data are from Figure 4.3 (first 84 h in LL from shoots and dark-grown roots); these are averages (SEM are not shown here for clarity) except for *CCA1* and *TOC1* root data for which only one rhythmic set of data is presented here. Simulations and experimental data were normalised with the average of the corresponding time-course over the 84 h in LL. A, B, C and D: *CCA1*, *PRR9*, *TOC1* and *GI* mRNA levels respectively.

This lower level of light ($L=0.4$) could also simulate lower amplitude for all clock genes under LD; some of the simulations are shown in Figure 7.8. The amplitudes were halved in “roots” compared to shoots, especially for *CCA1* and *PRR9* (Figure 7.8. A&B); the reduction in amplitude was bigger than this for *TOC1* but less for *GI* (Figure 7.8.C&D). These differences are similar to experimental data (Figure 7.8). As for simulations in LL, the rhythms were quickly stabilised after a ~48 h transition at the start of the simulation.

Thus the low light intensity perceived by dark-grown roots compared to the higher light perceived by the shoots could be sufficient to explain the two main differences between their clocks: different FRP under LL and lower amplitudes in roots under diurnal cycles.

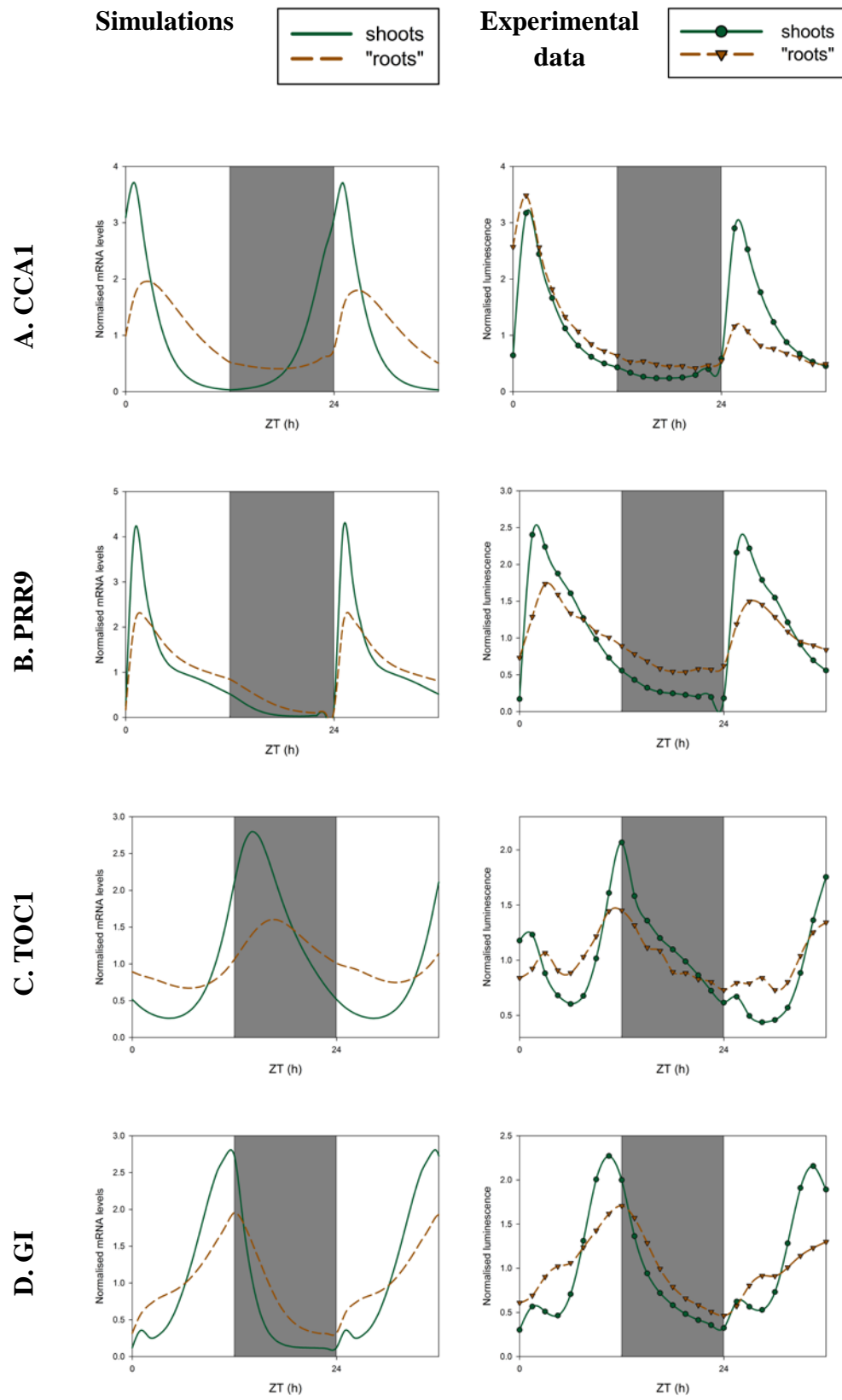


Figure 7.7: Simulations of clock genes mRNA levels in shoots and “roots” under LD using the P2012 model with different light intensities

Same simulations as in Figure 7.7 but under LD. Simulations (left, smooth lines) are compared to experimental data (right, lines with symbols). The simulations with default parameters of the P2012 model are labelled shoots. The other simulations (labelled “roots”) use the same set of parameters as shoots except light amplitude set to 0.4 (instead of 1). Experimental data are from Figure 4.3 (36 h in LD from shoots and dark-grown roots); these are averages (SEM are not shown here for clarity). Simulations and experimental data were normalised with the average of the corresponding time-course over the 36 h in LD. A, B, C and D: *CCA1*, *PRR9*, *TOC1* and *GI* mRNA levels respectively.

7.5 Entrainment of the root clock and longer FRPs in light-grown roots compared to shoots can be simulated after optimising P2012 model parameters

The previous section showed that changing only one parameter of the P2012 model (the light amplitude) can simulate the low amplitude and the long FRP of clock genes observed in the root clock under LD and LL respectively. Indeed dark-grown roots can perceive light channelled by tissues exposed to light (chapter 5). But the clock of light-grown roots, which are exposed to the same light intensity as shoots, also has a longer FRP in LL compared to the shoot clock. One possible explanation would be that the light signalling pathway is different in the two organs; for instance the levels of light perceived by roots might be buffered, so that the effective levels (reaching the core clock) would be similar regardless of the actual light intensity (e.g. the one perceived by shoots). This would be surprising. In addition, the amplitude of some clock genes in the roots (e.g. *GI*) depends on the light intensity they are exposed to: the higher the light intensity, the higher the amplitude (chapter 4 and 5). Therefore the root clock can distinguish different light intensities. Thus other parameters than the light amplitude may differ in the root clock in order to explain differences with the shoot clock, such as different FRPs under LL.

Changing parameters related to the inhibition of evening genes by LHY/CCA1 could give a longer FRP under LL, with $L=1$ (sections 7.2 and 7.3). For instance in section 7.3 a longer FRP could be simulated by increasing only one parameter of the P2010 model: $g5$. This parameter was the constant of *TOC1* inhibition by LHY/CCA1, which is still represented by $g5$ in the P2012 model (cf. Figure 1.4.C and equation 9 in section 2.5). But increasing $g5$ value up to 100 fold had almost no effect on the FRP under LL in this later

model (simulations not shown). Since CCA1 and LHY were thought to be unable to inhibit gene expression in roots (James *et al.*, 2008), other parameters could be affected in this organ: namely g15, g16 and g6 (cf. Figure 1.4.C and equation 10-12 in section 2.5). They represent all the other constant of inhibition by LHY/CCA1 in the P2012 model. g15 is the equivalent of g15 in the P2010 model and represents the inhibition constant of *GI*, whereas g16 and g6 represent the inhibition constants of *ELF3* and *LUX/ELF4*, respectively, by LHY/CCA1. All these evening components contain EE in their promoter, so they might not be inhibited by LHY/CCA1 in the roots. However, scanning these parameters individually with COPASI (with changes up to 100 fold) did not lengthen the FRP under LL either (simulations not shown). On the contrary, increasing some of these parameter values tended to shorten the FRP.

Then the same parameters were reduced up to 10 fold, each one being scanned individually. Decreasing g5 and g15 values tended to shorten the FRP under LL, whereas decreasing g6 and g16 lengthened the FRP (simulations not shown). Although a decrease in these values would simulate more inhibition of the corresponding genes by LHY/CCA1 (which was not suggested by experiments done by James *et al.*, 2008), it is conceivable that the morning genes may affect evening genes differentially. For instance, CCA1 and LHY proteins might inhibit only some of these genes (e.g. *ELF3/4* or *LUX*) through binding to their EE, resulting in a longer FRP, without binding to other gene promoters (e.g. *TOC1* and *GI*). This could be compatible with the EMSA results previously published (James *et al.*, 2008) since this assay was not gene-specific. In other words, there might be some binding of CCA1 and LHY proteins to EE in roots, but less than in shoots (hence harder to detect) and with more affinity to some promoters. In addition, more or less binding of CCA1 or LHY to EE does not need to imply more or less inhibition of the corresponding gene; in general, binding to gene promoters can also activate expression. In order to test this idea, SBSI was used to search a broader space of parameters. The simulations mentioned in the previous paragraph only tested one parameter a time. But changing two or more parameters simultaneously could have more complex effects on the clock (e.g. not just additive effects).

Not only the 4 parameters mentioned above (i.e. g5, g6, g15 and g16) were used for the following optimisation process, but also g1 and g8 (cf. Figure 1.4.C and equations 7 and 8 in section 2.5). These two parameters were chosen for several reasons. First, the skeleton

photoperiod experiments presented in chapter 5 (Figure 5.7) suggested that *CCA1* and *PRR9* may be respectively less and more repressed during the evening in the roots compared to shoots; this might be simulated by increasing the value of $g1$ (inhibition constant of *LHY/CCA1* by the PRRs) and decreasing the value of $g8$ (inhibition constant of *PRR9* by the EC) respectively. Interestingly, scanning these two parameters individually in that way (i.e. increasing $g1$ or decreasing $g8$) lengthened the FRP under LL (simulations not shown). Second, a lower inhibition of *LHY/CCA1* by the PRRs (especially by the later expressed ones such as *TOC1*) may allow *CCA1* mRNA levels to rise and peak earlier, contrary to the simulations presented in Figure 7.8.A where it peaked too late in the simulated roots. Indeed the profiles of *CCA1* mRNA levels should be very similar in shoots and roots (apart from the amplitude that is lower in roots). Third, increasing the value of $g8$ could contribute to some uncoupling between morning and evening genes observed in roots under LL. This uncoupling was thought to be achieved by a lack of evening genes inhibition by *LHY/CCA1* and to result in arrhythmia of evening genes under LL (James *et al.*, 2008). Although these results were not confirmed by the more recent work presented in this thesis, different FRPs were observed between morning and evening genes at the mRNA level (Figure 4.4) and suggest less coupling - if any at all - between morning and evening loops in roots under LL.

A parameter optimisation was run using the L2012 model and light-grown root data in LL, namely the imaging data of *CCA1*, *PRR9*, *GI* and *TOC1* presented in Figure 4.2. The six parameters mentioned above ($g1$, $g5$, $g6$, $g8$, $g15$ and $g16$) were chosen for the optimisation process, starting from their initial (default) values and allowing up to 10 fold changes. As in section 7.3, the optimisation algorithm was the PGA. Two cost functions were used: the FFT (with a target of 28 h) and the χ^2 cost functions. The best set of parameters (after 400 generations) is presented in Table 7.3. It gave a longer FRP in LL (simulations not shown). But the simulated levels of *GI* and *CCA1* were then much higher in “roots” compared to shoots, contrary to experimental data (e.g. Figure 4.4) which showed the opposite (higher mRNA levels in shoots compared to roots). This was probably because $g1$ and $g15$ were too high (7.8 and 10 time their default value respectively): it simulated much lower inhibition of *CCA1* and *GI* respectively (compared to the default values of $g1$ and $g15$), resulting in higher mRNA levels in these simulations (“roots”) compared to shoots. The simulations previously done with COPASI (mentioned earlier) showed that increasing individually $g1$ and $g15$ respectively lengthen and shorten the FRP.

When both values were increased by the optimisation process - done here with SBSI (Table 7.3), the resulting FRP was longer (this was constrained by the FFT cost function). This was good enough to reduce the overall cost, but does not mean it was the best solution. Indeed the process could be stuck in local optima. Besides, the number of generations may not have been enough to give a better solution.

Table 7.3: Optimal sets of parameters related to inhibition constants in roots

A combination of six parameters (first column) of the P2012 model, related to inhibition constants, was optimised with SBSI. Three optimisation processes attempted to fit root clock data. The initial (default) parameter values are presented in the second column (shoots). The third and fourth columns (labelled “roots” [*10 (LL)]” and “roots” [*2 (LL)]”) were the best sets obtained when parameters could increase or decrease up to 10 or 2 fold respectively; these two optimisation processes attempted to fit light-grown root clock data under LL. The last column (labelled “roots” [*10 (DD)]”) was the best set obtained when parameters could increase or decrease up to 10 fold; this last optimisation process attempted to fit dark-grown root clock data under DD. Simulations using the “*2(LL)” set are show in Figure 7.9. The values of g1, g15 and g16 (in bold) were consistently increased in these optimisation processes compared to their default values

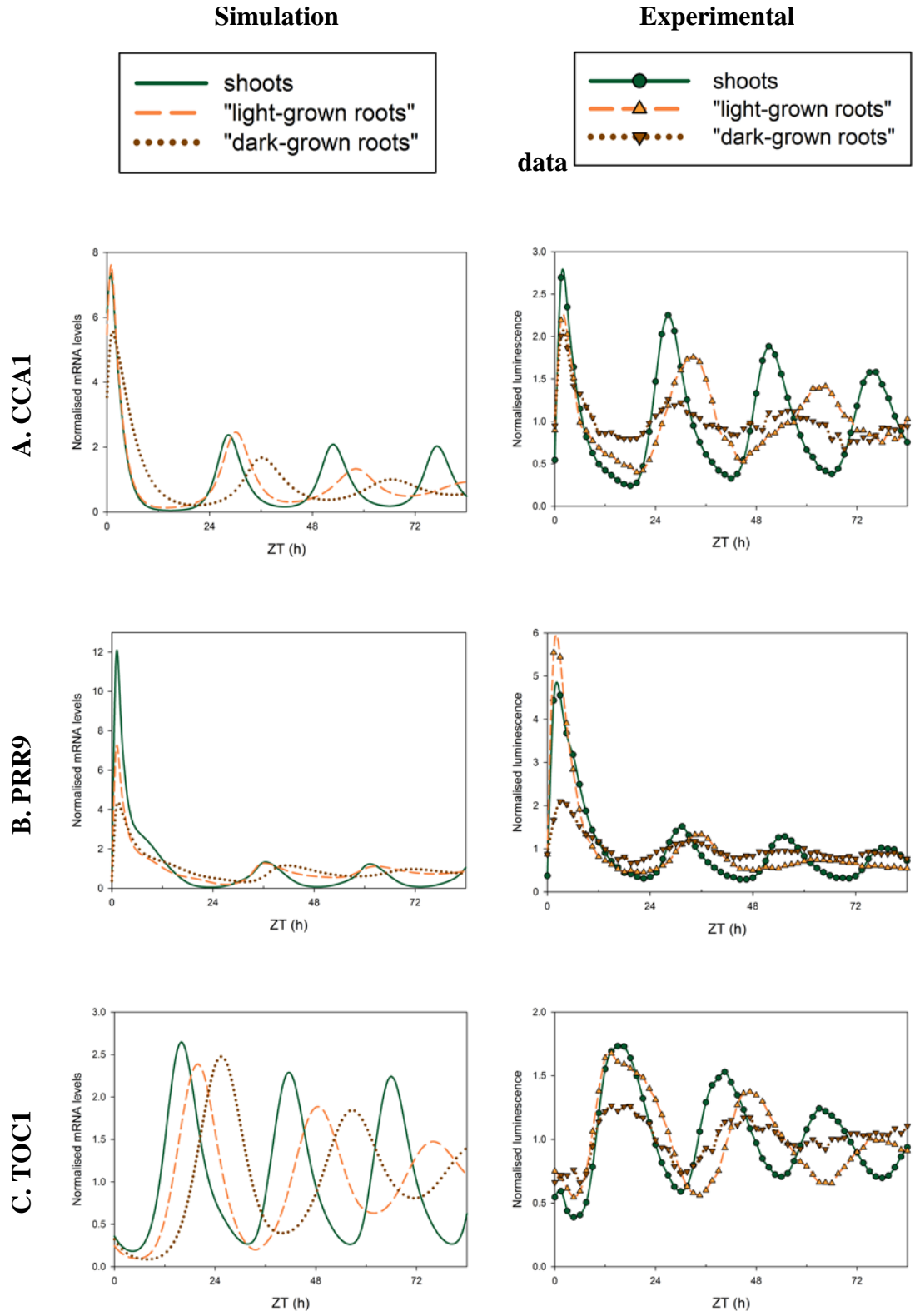
	shoots	“roots” [*10 (LL)]”	“roots” [*2 (LL)]”	“roots” [*10 (DD)]
g1	0.100	0.789	0.200	0.225
g5	0.150	0.131	0.118	0.064
g6	0.300	0.409	0.103	1.608
g8	0.010	0.003	0.020	0.021
g15	0.400	4.000	0.798	3.171
g16	0.300	2.446	0.600	3.000

In order to avoid such high values of parameters, the same optimisation process was repeated but with a reduced parameter space: the 6 parameters could increase or decrease up to two fold only. The best set of parameters (after 1000 generations) is presented in Table 7.3. It also gave a longer FRP in LL; simulations in LL were run with this optimal set (Figure 7.9). In this case the mRNA levels of clock genes were closer to their default values, except for GI that remains higher. The damping rate under LL was also higher compared to the default rate, for all the genes presented here (the simulations for shoots gave very few – if any at all – damping after the second day in LL). However, damping of clock gene expression was also observed experimentally, for both shoots and roots.

Figure 7.9 present actually three sets of simulations for each gene: 1) the default values (representing shoots), 2) the simulations with the “*2(LL)” set of parameters (with 6 modified parameters presented in Table 7.3) and 3) the simulations with the same set as 2) but with a lower light intensity (value of L halved⁸). The latter attempted to simulate dark-grown roots. As we have seen earlier, the FRP under LL should be similar in light and dark-grown roots. At least both FRP should be longer than the shoot FRP in LL. Figure 7.9 shows it was the case. However, the FRP was too long for these “simulated dark-grown roots”. Indeed it should be rather shorter than longer compared to the FRP in light-grown roots (chapter 4 and 5). But interestingly, this set of parameters gives a ~24 h period under LD, whether L=1 (“light-grown roots”) or L=0.5 (“dark-grown roots”), and with lower amplitudes when L=0.5 (simulations not shown). Simulations were also carried out under DD with the same set of parameters (simulations not shown). But all the genes dampened very quickly and their mRNA levels became completely flat after less than 2 or 3 cycles in DD. This was in contrast with experimental data where rhythms are sustained longer in DD (Figure 4.5 and 4.6). Therefore this set of parameter could not simulate root data in all conditions tested experimentally.

Another optimisation job was run under DD, as in section 7.3, but with the P2012 model. In that section, although the optimisation process used DD data, the optimal set also gave a longer FRP under LL and a 24 h period under LD. Compared to section 7.3, more root data were used in the following optimisation: not only *CCA1* and *PRR7*, but also *GI* and *PRR9* imaging data under DD (Figure 4.5). The same optimisation algorithm (PGA) and two cost functions were used: FFT (with a target of 29 h) and χ^2 . The 6 parameters presented in Table 7.3 were optimised, allowing up to 10 fold increase or decrease. The cost hardly decreased after 1000 generations and the process was stopped. Nevertheless the optimal set of parameters (Table 7.3, “roots” [*10 (DD)]) was used for simulations (not shown). It did not fit data any better than the “*2(LL)” set discussed earlier. For instance the “*10 (DD)” set did not give any sustained rhythms under LL.

⁸ a small parameter scan of “L” showed that with these new “g parameter set” L=0.5 gave a better fit than L=0.4 used previously



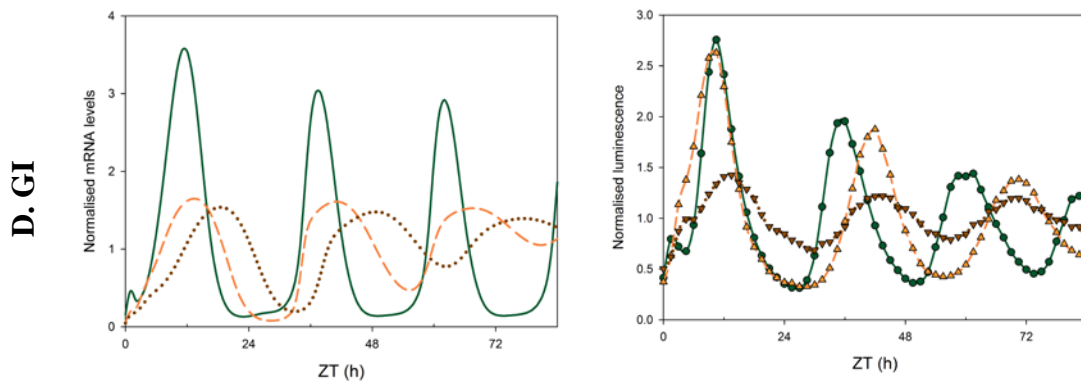


Figure 7.8: Simulations of clock genes mRNA levels in shoots and “roots” under LL after modifying parameters related to inhibition constants

Simulations (left, smooth lines) are compared to experimental data (right, lines with symbols). The simulations with default parameters of the P2012 model are labelled “shoot”. The other simulations (labelled “light-grown roots” and “dark-grown roots”) use the “*2(LL)” set of parameters presented in Table 7.3 but with different light intensities ($L=1$ for light-grown roots and $L=0.5$ for dark-grown roots). Experimental data are from Figure 4.3 (first 84 h in LL from shoots and dark-grown roots); these are averages (SEM are not shown here for clarity). Simulations and experimental data were normalised with the average of the corresponding time-course over the 84 h in LL. A, B, C and D A, B, C and D: *LHY/CCA1*, *PRR9*, *TOC1* and *GI* mRNA levels respectively.

The optimal sets of parameters presented in this section could fit qualitatively some root clock data in specific conditions: in LD and either LL or DD. A similar trend could be observed in the values of 3 parameters presented in Table 7.3: g_1 , g_{15} and g_{16} were always increased in the optimal sets. The increase in the value of g_1 would be consistent with the root data for *CCA1* under skeleton photoperiods: it simulated a lower inhibition of *LHY/CCA1* by the PRRs, which could explain the lower inhibition observed before dusk. The increase in g_{15} and g_{16} values simulated a lower inhibition of *GI* and *ELF3* by morning genes. This is not only consistent with a possible lack of binding of *LHY/CCA1* proteins to EE. It would also explain the shoulder of *GI* observed in roots (instead of the dawn peak observed in shoots; cf. Figure A.6 in Appendix). In addition, a higher value of g_{16} lowers the amplitudes of clock genes under LL (simulations not shown); this might explain why the possible rhythmic expression of some genes, such as *ELF3*, was hardly detected in roots. Indeed, the mRNA levels of *ELF3* were scored arrhythmic in our microarray data (Sullivan et al, unpublished). Interestingly, the values of g_{15} and g_{16} tended to their maximum levels in each optimisation process (Table 7.3).

The choice of parameters optimised in this section was partly based on experimental data, notably the lack of inhibition of LHY/CCA1 to EE. It was also motivated by previous optimisations using similar parameters in the previous models (sections 7.2 and 7.3): the optimal sets gave qualitative fits to root data in several – but not all - light conditions. Some optimisations attempted to fit root data under DD. However, more recent results showed that shoot and root clock data are similar under DD. The main differences between the two clocks are observed under LD and LL. In the following section, attempts to simulate these differences while keeping the similarities under DD are discussed.

7.6 Differences in light inputs could explain most differences observed between shoot and root clocks under LD and LL

The optimisation processes under LL presented in the previous section did not give any set of parameters that fit root data under DD. These experimental data are similar to the shoot clock data under DD (Figure 4.5 and 4.6). Notably both clocks have a similar long FRP under these conditions. Therefore the parameters of the model might be the same in shoots and roots under DD. It is only when light is present that obvious differences can be observed between shoots and roots (i.e. under LL and LD). Some parameters must be organ-specific in order to explain these differences. Changing only the light intensity could explain these differences in dark-grown roots (section 7.4), and would be consistent with the low light levels perceived by these roots. However, the clock of light-grown roots also has a longer FRP compared to the shoot clock. Thus, other parameters are probably organ-specific, allowing a long FRP in roots in any condition.

Light affects the expression of several clock genes and proteins, and this is translated into many “light-related parameters” in the P2012 model. What I will call the “light-related parameters” hereafter are the parameters that appear in the equations of the P2012 model together with the “L” parameters (cf. Figure 1.4.C and equations 13-19 in section 2.5); these parameters are always multiplied by “L”. It means they have no effect under DD (when $L=0$). The “light-related parameters” could be divided in two categories: those that always appear with “ c_p ”⁹, and those that do not. The latter comprises only 5 parameters

⁹ c_p is the concentration of the light-sensitive protein P, used in the model for the acute light activation of *PRR9*, *LHY/CCA1* and *GI*

which will be used for the following optimisation process: $m1$, $p1$, $p12$, $p15$ and $p24$. The former (the “ c_p related parameters”) must have almost no effect under LL since c_p tends quickly to 0 under LL, but they contribute to the entrainment of the clock under LD. That is why the “ c_p related parameters” were not included in the following optimisation process run under LL.

Some of the “light-related parameters” might be organ-specific. Light may affect gene expression differentially in shoots and roots: compared to DD, different combinations of light inputs may shorten the FRP under LL in shoots but not in roots (chapter 4). The question is: which of these parameters could be different in roots? The parameters chosen for previous optimisations were modified “a posteriori”, because each of them were suspected to be different in roots given our experimental data. In this section the idea is to optimise “a priori” the “light-related parameters” mentioned above ($m1$, $p1$, $p12$, $p15$ and $p24$). There is no direct evidence that any of these specific parameters might be organ-specific. But modifying them would not affect the behaviour of clock components under DD (consistent with the similarities between shoot and root clock under these conditions) and should allow entrainment under LD (since the “ c_p related parameters” and the “dark related parameters”¹⁰ would be unchanged). An optimisation process that tries to fit the clock data of light-grown roots, especially their longer FRP, can be used to constrain these “light-related parameters”. If such an optimal set of parameters could be found, it may also give a lower amplitude under LD (and possibly a similar FRP under LL) when the light amplitude is reduced.

An optimisation process was run under LL in order to fit data of light-grown roots (*CCA1*, *PRR9*, *TOC1* and *GI*, as in the previous section). The default values of the P2012 model were used at the start (with $L=1$). All the 5 “light-related parameters” mentioned above ($m1$, $p1$, $p12$, $p15$ and $p24$) were optimised. Their value could increase up to two fold, or decrease. Two optimisation algorithms were used simultaneously: the PGA (used previously) together with the Particle Swarm Optimisation (PGO, described in section 2.5). Both FFT and χ^2 cost functions were used, with a target period of 28 h. The population size and the maximum number of generation were both set to 1000. The optimal set of parameters resulting from this process is presented in Table 7.4.

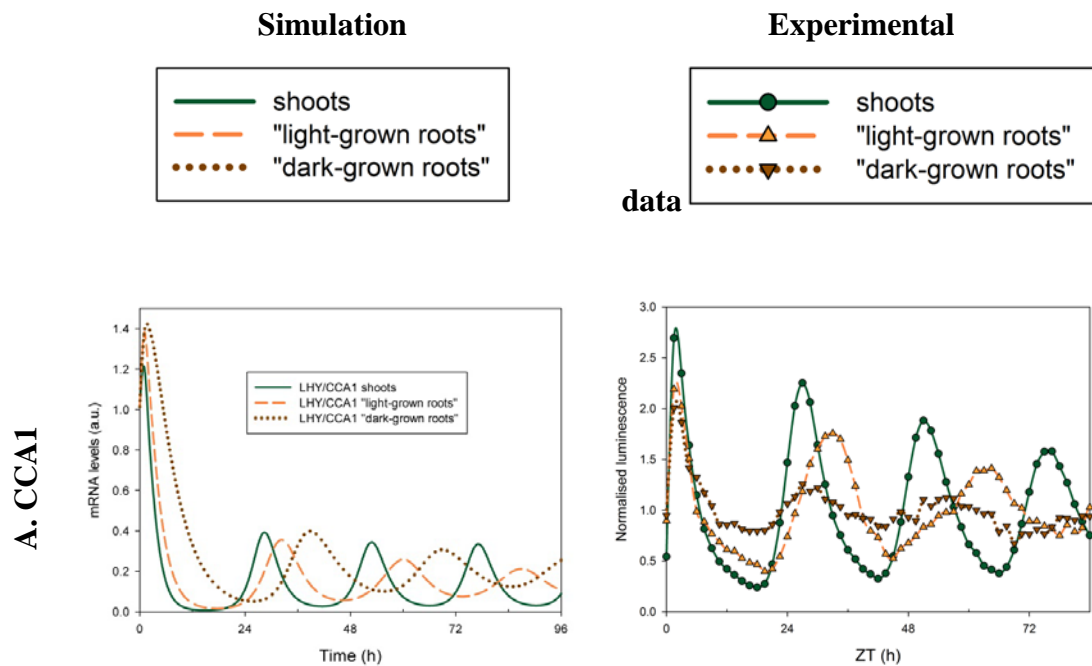
¹⁰ by “dark-related parameters” I mean the parameters that appear in the equations of the P2012 model together with the “D” parameters

Table 7.4: Optimal set of “light-related parameters” for the root clock

The 5 parameters presented in the first column are related to light inputs in the P2012 model. Their default values are in the second column. They were optimised with SBSI to fit the data of light-grown roots under LL. The optimised values are in the last column

	default (h^{-1})	optimal (h^{-1})
m1	0.54	0.37
p1	0.13	1.46E-05
p12	3.40	6.80
p15	3.00	0.23
p24	10.00	13.67

Simulations were run under LL (Figure 7.10) and LD (Figure 7.11) with the optimal set presented in Table 7.4. Both Figures show 3 simulations for each gene expression: 1) the default values (representing shoots), 2) the simulations with the optimal set of parameters which represent “light-grown roots”, and 3) the simulations with the same set as 2) but with a lower light intensity (value of L halved); the latter attempted to simulate “dark-grown roots”. All the simulations presented in Figure 7.10 and 7.11 were circadian: the periods were 24 h under LD and longer under LL (Table 7.5).



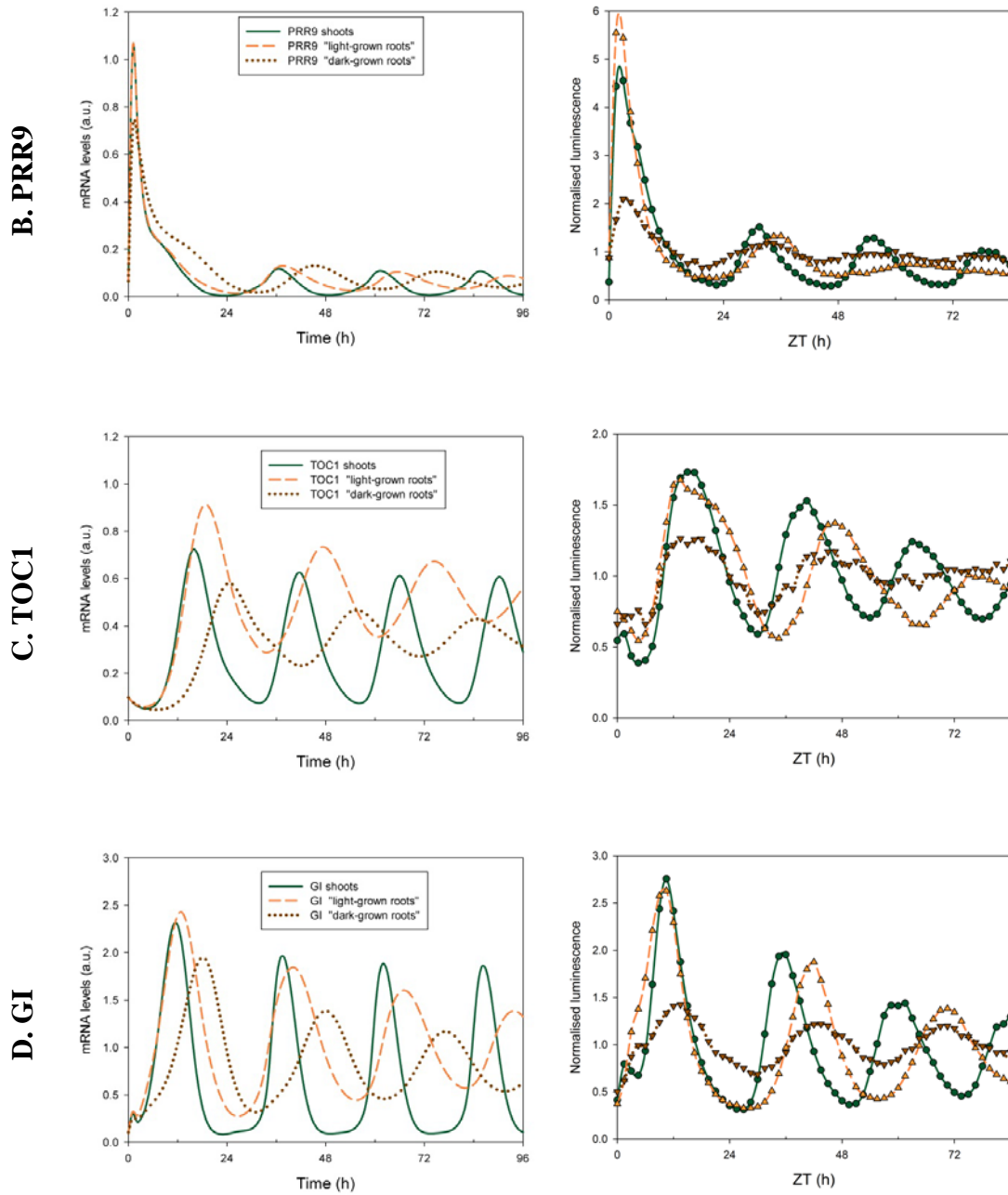
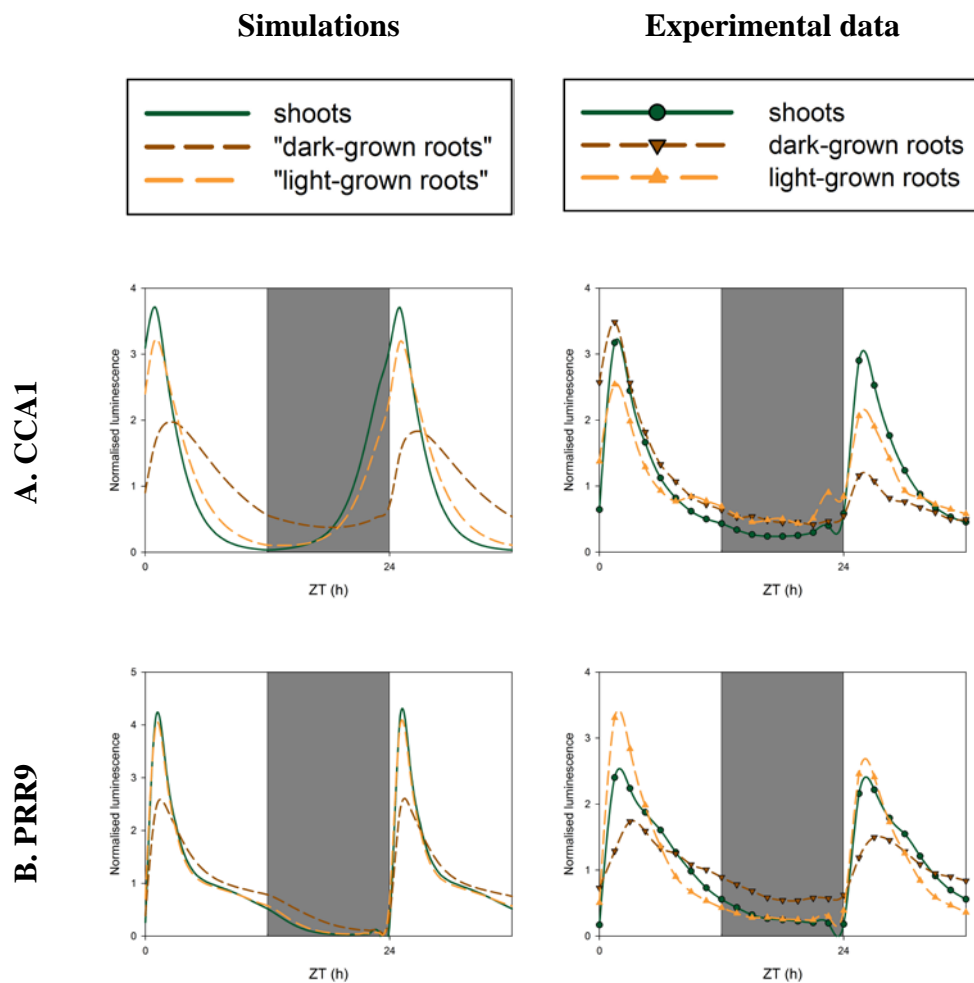


Figure 7.9: Simulations of clock genes mRNA levels in shoots, “dark-grown roots” and “light-grown roots” under LL after modifying parameters related to light inputs

Simulations (left, smooth lines) are compared to experimental data (right, lines with symbols). The simulations with default parameters of the P2012 model are labelled “shoot”. The other simulations (labelled “light-grown roots” and “dark-grown roots”) use the “optimal” set of parameters presented in Table 7.5 but with different light intensities ($L=1$ for light-grown roots and $L=0.5$ for dark-grown roots). Experimental data are from Figure 4.3 (first 84 h in LL from shoots and dark-grown roots); these are averages (SEM are not shown here for clarity). Experimental data were normalised with the average of the corresponding time-course over the 84 h in LL. A, B, C and D A, B, C and D: LHY/CCA1, PRR9, TOC1 and GI mRNA levels respectively.

Under LL, the simulations of clock genes in roots all gave a longer period compared to shoots (Table 7.5). The periods were on average 2.6 h longer in “light-grown roots” compared to shoots, which is consistent with imaging data. They were even longer in “dark-grown roots” (~29.4 h) although experimental data showed they should not be longer than in “light-grown roots”. But apart from this discrepancy, most simulations had a good qualitative fit with experiments. All mRNA levels were damping under LL (Figure 7.10). Interestingly, their amplitude were similar in shoots and “roots” for morning genes (Figure 7.10 A&C), but they were lower in roots for evening genes (Figure 7.10 B&D). In addition, these evening genes had even lower amplitude in “dark-grown roots”, whereas their expression was higher in “light-grown roots”. This is consistent with experimental data and could explain why the rhythms of evening genes were harder to detect in dark-grown roots compared to light-grown roots or shoots under LL.



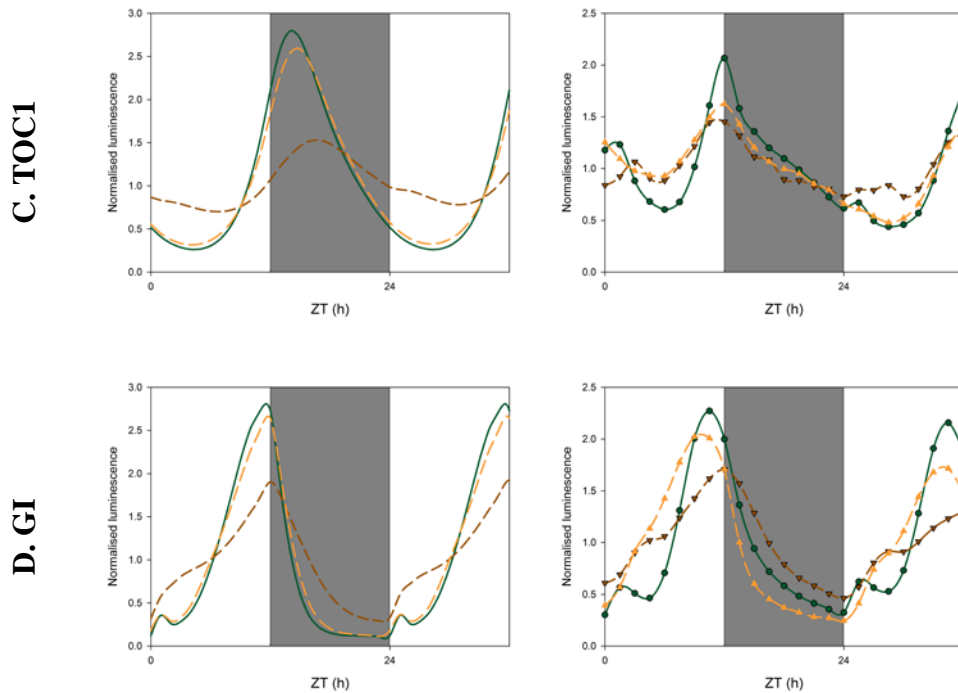


Figure 7.11: Simulations of clock genes mRNA levels in shoots, “dark-grown roots” and “light-grown roots” under LD using the P2012 model after modifying parameters related to light inputs

Same simulations as in Figure 7.10 but under LD. Simulations (left, smooth lines) are compared to experimental data (right, lines with symbols). The other simulations (labelled “light-grown roots” and “dark-grown roots”) use the “optimal” set of parameters presented in Table 7.5 but with different light intensities ($L=1$ for light-grown roots and $L=0.5$ for dark-grown roots). Experimental data are from Figure 4.3 (36 h in LD from shoots and roots); these are averages (SEM are not shown here for clarity). Simulations and experimental data were normalised with the average of the corresponding time-course over the 36 h in LD. A, B, C and D: *CCA1*, *PRR9*, *TOC1* and *GI* mRNA levels respectively.

Under LD, the simulations for shoots and “light-grown roots” were almost superimposable (Figure 7.11). This is surprising given that 5 parameters are very different between the two sets. However, when a sixth parameter was changed (namely the light amplitude that was halved) to simulate the “dark-grown roots”, the simulated profiles differed markedly. The main difference was lower amplitude, which is consistent with “dark-grown roots” data. The shapes of the oscillations also differed between these “dark-grown roots” and shoots, especially for *GI*. In that case, the dawn peak of *GI* observed in shoots was replaced by a shoulder in roots. Again this is consistent with imaging data (Figure 7.11.D). This could be due to lower levels of LHY/CCA1 proteins (resulting from their lower mRNA levels) which would reduce the inhibition of *GI* synthesis. However, the simulation of *LHY/CCA1* mRNA peak only 3h after dawn in the “dark-grown roots” (Figure 7.11.A), which is not

observed experimentally. But more importantly, all the simulated rhythms presented in Figure 7.11 had a 24 h period (Table 7.5).

Table 7.5: Period estimate of simulated rhythms in shoots and “roots” under LL and LD using the P2012 model

The periods of simulated rhythms from Figure 7.10 and 7.11 were estimated with BRASS (in hours); the periods for different mRNA were then averaged for each time course; SD: Standard Deviation. The default values (labelled shoots) are from the P2012 model. The other parameter sets are the “optimal set” presented in Table 7.5 with L=1 (“light-grown roots”) or L=0.5 (“dark-grown roots”).

	LL			LD		
	shoots	"light-grown roots"	"dark-grown roots"	shoots	"light-grown roots"	"dark-grown roots"
GI	24.39	27.16	29.47	24.04	24.06	24.16
LHY/CCA1	24.25	26.67	29.07	24.01	24.02	24.00
PRR9	24.44	27.20	29.59	24.11	24.14	24.11
TOC1	24.26	26.90	29.36	24.02	24.02	23.99
average	24.34	26.98	29.37	24.05	24.06	24.07
SD	0.09	0.25	0.22	0.05	0.06	0.08

Among the optimised parameters, p_1 changed most dramatically (from 0.13 h⁻¹ to ~0; Table 7.5). p_1 is the constant of CCA1/LHY activation by light. The lower its value, the less activation. The other important change of parameter concerned p_{15} (Table 7.5). Its reduction in the optimisation process indicates that COP1 may be less degraded by light in roots compared to shoots. These “predictions” could be tested experimentally by measuring the effects of light on the synthesis and degradation of the corresponding proteins.

Optimising 5 parameters directly related to light inputs to the clock could simulate most differences observed between shoot and root clocks under LD and LL. These parameters have no influence under DD. Therefore simulations with this new set would give very similar results in shoots and “roots” under DD (not shown), which is consistent with experimental RT-qPCR data. However, these simulations would not be identical if different initial states are taken into account. Indeed, if shoots and “roots” (especially “dark-grown roots”) are simulated in LD before release in DD, their “initial states” (e.g. levels of proteins) when DD starts would be different. This could influence the results.

7.7 Conclusion

In this chapter several “shoot clock” mathematical models were used and some of their parameters modified in order to try and fit the root clock data. Newer versions of these models were used once available. In the meantime, more experimental data were produced and guided different parameter optimisation processes.

Modifying manually 3 parameters of the L2006 model could simulate a major difference between shoot and root clock under LL: a 2 h longer FRP in roots compared to shoots. Two of these parameters were increased in accordance with other experimental data: LHY protein did not seem to bind to EE and therefore might not inhibit gene expression in roots (James *et al.*, 2008). The same modified set of parameters simulated higher levels of *TOC1* mRNA with much lower amplitude in roots compared to shoots. This already indicated that *TOC1* might be circadian in roots, but its rhythm could be harder to detect experimentally. But the number of data fitted was very limited and the manual process very time-consuming.

The P2010 and P2012 models were later used to optimise similar parameters, based on the same idea: there may be less inhibition of clock genes by LHY in roots. But more recent data were used for these optimisation processes (e.g. evening genes were actually circadian in roots too), and these optimisations were mainly done in an automatic way, using SBSI. A broader space of parameter could then be searched, and more data could be simultaneously fitted. For instance, a longer FRP could also be achieved by modifying just a few parameters. Interestingly, the Michaelis-Menten constants that corresponded to inhibitions by LHY/CCA1 tended to increase in these automatic processes although they were also allowed to decrease. These increases are consistent with a lack of inhibition of evening genes by LHY/CCA1 in roots. But with the P2012 model, only some of these constants were increased, which indicate that LHY/CCA1 may actually bind to some EE and inhibit gene expression in roots. It would be useful to test this idea experimentally with ChIP assays. This method could give more specific results than the EMSA carried out in James *et al.* (2008). For instance it could indicate whether LHY/CCA1 have different affinities for different clock gene promoters. More generally, this kind of data would be very useful in guiding the modelling process.

The best fits to root data were obtained with optimised sets of parameters related to light. Indeed changing only the light amplitude could explain most of the data from dark-grown roots, with lower amplitudes under LD and longer FRP in LL compared to the shoot clock. This parameter change was motivated by a more recent discovery: dark-grown roots can perceive low levels of light channelled from exposed tissues and therefore be directly entrained by LD cycles (chapter 5). But simulating low light could not explain data from light-grown roots: when roots are exposed to the same light intensity as shoots, their FRP is still longer in roots. A last parameter optimisation was carried out with more “light-related parameters” and gave interesting results. Changing several light inputs to the clock can simulate a longer FRP for both light- and dark-grown roots. The parameter set found could also explain entrainment under LD cycles, with lower amplitudes when roots are dark-grown. And the clock behaviour would be similar in shoots and roots under DD, consistent with experimental data. However, the FRP should be similar in light- and dark-grown roots under LL, if not shorter in the latter case.

In general, the results obtained with sets of parameters optimised in a specific condition (e.g. simulations in LL) could be validated in some but not all other condition(s) (e.g. simulations in LD but not in DD). Some discrepancies could be clarified with more experiments, which could better constrain the model and its parameters. Nevertheless, the ideas – if not predictions – suggested by this theoretical work could be tested experimentally and might help us to better understand the root clock.

8 General discussion

The work presented in this thesis confirmed that shoot and root circadian systems are different in *Arabidopsis*. However, these differences revealed here, mainly using imaging, were not exactly the same as those reported by James *et al.* (2008) using different techniques. In addition, my work shows that both clocks also have more similarities than James and colleagues suggested.

8.1 Shoot and root circadian systems: same structure but different inputs?

A system is characterised by its structure, i.e. its components and their interactions (wiring), and may be subjected to different inputs. This section will discuss plant circadian systems at the cellular level, assuming that all the cells of an organ have the same clock.

8.1.1 Components

Many of the components of the shoot clock have been identified by screening of seedlings to select those with a circadian phenotype. The role of these components in the clock machinery were then confirmed and refined with other studies, including reverse genetics. There is no highthroughput technique allowing the identification of clock genes in roots. Nevertheless, clocks of different plant cells are believed to be similar, sharing many components but with possible biochemical differences (Harmer, 2009).

The root circadian clock was recently shown to be a simplified version of the shoot clock, with only the morning loop running in the root clock under constant conditions. A feedback loop between LHY/CCA1 and PRR7/9 would form this loop. My work confirmed with imaging that these four genes are rhythmic under various diurnal and constant conditions (chapters 4 and 5). A preliminary study on the *cca1-11/lhy-21* double mutant showed that rhythms seem to be affected in a similar way in shoots and roots of this mutant compared to the WT: the acrophases of *CCR2* expression were earlier in LD, the FRPs under LL were shortened and the rhythms dampened rapidly in both organs (chapter

6). *PRR7* and *PRR9* were proposed to form a loop with *CCA1* and *LHY*, and the *prr7/9* double mutant had a very long FRP in shoots, over 30 h (Farre *et al.*, 2005; Salome and McClung, 2005a). *PRR7* and *PRR9* are expressed rhythmically in roots as well as in shoots. This was shown with RT-qPCR and confirmed with imaging in various conditions (James *et al.* 2008, chapters 4 and 5). A long FRP was observed in the roots of the *prr7/9* double mutant as well as in shoots (James *et al.*, 2008; Sullivan et al, unpublished). Together these results suggest that *PRR7* and *PRR9* also play a role in the root clock. However evening genes such as *TOC1* and *GI* regained rhythmicity in the roots of the *prr7/9* double mutant (James *et al.*, 2008). This already indicated that the root clock involved more than just the morning loop. The rhythmicity observed in the *cca1-11/lhy-21* double mutant also suggests that the root clock contains more than one loop (chapter 6). The existence of several feedback loops in the root clock as well as in the shoot clock are supported by the rhythmicity of evening clock genes in most (if not all) conditions tested in this thesis.

GI rhythms were detected in roots in all the condition tested, whether roots were light- or dark-grown: LD and constant conditions (LL and DD) following different entrainment, e.g. different photoperiods and T cycles. *GI* was also rhythmic under DD and temperature cycles. In addition, preliminary data show that both shoot and root clocks are strongly perturbed in the *gi-201* mutant under LL (Sullivan et al, unpublished). Therefore *GI* is probably a component of the root clock. The role of *TOC1* in the root clock was less clear because of its weak rhythms in dark-grown roots (chapter 3 and 4). However *TOC1* rhythms were detected in roots at least once in each condition tested (LD, LL and DD) with RT-qPCR and imaging. *TOC1* expression levels were higher in light-grown roots compared to dark-grown roots, so that in the former case rhythms were detected easily under LD and LL. In addition, the preliminary studies on the *toc1* mutant indicated that *TOC1* plays a role in the root clock: indeed its mutation led to shorter FRP in roots under LL compared to the WT. Although these experiments on the *toc1-4* mutant need to be repeated, they were carried out in two conditions (light- and dark-grown roots) and with similar results. Taken together all these data suggest that *TOC1* is a component of the root clock, although its rhythm is weaker compared to other components such as *CCA1* or *GI*.

In the current model of the “plant” circadian clock, other key players are included and rhythmic at the transcript level, for example *ELF3*, *ELF4* and *LUX* (Pokhilko *et al.*, 2012).

In our recent microarray *ELF4* and *LUX* mRNA levels were scored rhythmic under LL in roots, but *ELF3* was not (Sullivan *et al.*, unpublished). This was only one set of data, so it is possible that *ELF3* rhythms were present but too weak to be detected. In the P2012 model, *NI* may represent *PRR5* which is rhythmic at the transcript level in shoots but not in roots (Sullivan *et al.*, unpublished). As for *ELF3*, *PRR5* may be truly arrhythmic in roots or a low amplitude rhythm may not have been detected. More studies would be required to conclude that the evening genes mentioned above are part of the root clock. However there may be one piece of indirect evidence that *ELF3* could play a role in the root clock, although *ELF3* was not scored rhythmic in our microarray. Takase and colleagues studied water dynamics in roots and showed that it displayed circadian rhythms under LL and DD; however the circadian oscillation in water dynamics was obscured in the roots of the *elf3* mutant under LL (Takase *et al.*, 2011). More generally the study of other single and multiple mutants in roots and their effects on circadian rhythms could be useful to confirm the possible role of corresponding genes as components of the root clock.

Other genes are involved in the shoot clock, such as *CHE* and *RVE8* (Nagel and Kay, 2012). Although *CHE* transcript levels were not oscillating in roots in our microarray, *RVE8* was expressed rhythmically in roots under LL, and with a longer FRP compared to shoots (Sullivan *et al.* unpublished). Interestingly the same microarray showed that several photoreceptors were expressed in dark-grown roots, and amongst them *PHYB* was scored rhythmic. This suggests that not only many core clock components may be shared in both organs, but also some components involved in the light input pathway.

More mRNA and imaging data from roots have been produced during the last few years. However little is known about other levels of regulation in the root clock. At the protein level, the expression pattern of LHY and TOC1 were analysed in roots over 3 days under LL: only LHY seemed to be circadian in roots (James *et al.*, 2008). This could be consistent with the lower amplitude of *TOC1* rhythm compared to *LHY* at the mRNA level (chapter 4). Rhythms at the transcript level do not necessarily feed through to rhythms at the protein level. For instance in plants carrying the *CAB2:LUC* fusion, the levels of the LUC protein were relatively constant although *LUC* mRNA levels were oscillating (Millar *et al.*, 1992). Conversely, rhythms at the protein level do not necessarily require the corresponding mRNA to be expressed rhythmically. For instance *ZTL* mRNA is not circadian in shoots but its protein level is circadian regulated in this organ and plays a role

in the shoot clock (Mas *et al.*, 2003; Kim *et al.*, 2007). It would be interesting to know whether the same is true for ZTL expression in roots. More generally the study of clock protein levels in roots would be informative.

All these evening components were not only rhythmic in roots under LL, their FRPs in roots were longer compared to shoots and comparable with the FRP of morning components in roots, suggesting they could be part of the same oscillator. Alternatively they might be driven by the same oscillator. The role of the putative clock components in roots needs to be confirmed, e.g. by studying their protein levels and their interactions and by investigating the effects of mutations on the root clock.

8.1.2 Wiring

Even if the same components are present in shoot and root clock, their functions may differ in these two organs. For instance an EMSA assay revealed the presence of EE-binding complex containing LHY in shoots but not in roots (James *et al.*, 2008). This indicated that morning and evening loops might be uncoupled in roots, and the authors suggested that this mechanism could explain fewer genes expressed rhythmically in roots compared to shoots. For instance several genes containing EEs in their promoter were not scored rhythmic by James *et al.* (2008). However the more recent results presented in this thesis showed that *TOC1*, *GI* and *CCR2* – all EE-containing genes – were actually circadian in roots although their rhythms were weaker than in shoots. Besides the FRP in LL of these EE-containing genes were comparable to the FRP of morning genes, such as *CCA1* and *LHY*. These new results suggest that morning and evening loops are coupled in roots as they are in shoots, but this is not necessarily in contradiction with the EMSA results of James *et al.*: coupling between loops might be achieved by different mechanisms in roots.

In fact, the possible lack of binding of LHY to EE might explain other features of the root clock. In shoots the binding of CCA1 and LHY proteins to EE promoter sequences was correlated to repression of evening-expressed genes (Harmer, 2009). Therefore less binding to the promoter of an EE-containing gene may lead to less repression of this gene, and consequently weaker rhythms – if any at all. For instance in roots CCA1 and LHY proteins may have less affinity to EE, or their levels were too low, so that their binding may have been missed in the EMSA assay performed by James *et al.* (2008). This would

reconcile older and more recent root data: coupling between the morning and evening loops, and also coupling between morning transcription factors and output genes containing the EE would exist in roots but they would be weaker than in shoots. Consequently the EE-containing genes would have lower amplitude rhythms or they would be arrhythmic in roots.

O'Neill and colleagues suggested that LHY/CCA1 heterodimer has a higher affinity for the EE than either homodimer. In addition LHY binding to EE was enhanced by casein kinase 2-mediated phosphorylation (O'Neill *et al.*, 2011b). If these in vitro results were reproducible in vivo, it would suggest that a lower binding to EE might be due to a lack of interaction between CCA1 and LHY and/or a lack of phosphorylation of LHY. Interestingly the casein kinase 2 (CK2) is involved in the pace of the clock. In the shoots of a *ck2* mutant a reduced level of CK2 activity and CCA1 phosphorylation correlated with the period lengthening of various output rhythms and clock gene expression (Lu *et al.*, 2011). In addition, the longer FRP in roots under LL could be simulated in all the models tested by reducing the inhibition of one or more EE-containing genes by LHY/CCA1 (Figure 7.1, 7.4 and 7.9), and with these change of parameter morning and evening genes were still coupled in LD and LL. Taken together these results suggest that the longer FRP in roots may be explained by lower affinity of LHY or CCA1 protein for EE sequences, resulting in less repression of evening genes, and this lower affinity might be due to reduced phosphorylation of CCA1 and LHY in roots compared to shoots. Alternatively, the lower levels of *CCA1* and *LHY* mRNA may result in lower levels of their protein in roots compared to shoots, which might also explain less binding to the EE and therefore less inhibition of clock gene expression by LHY/CCA1 in roots compared to shoots. It would be very interesting to investigate experimentally the post-translational modifications of CCA1 and LHY in roots, and their possible effect on their binding to EE.

The profile of *GI* expression differs in shoots and roots under LD. James *et al.* showed that *GI* mRNA peak was broader in roots compared to shoots. This could also be observed in several experiments with imaging (e.g. in Figure 4.7). In shoots under LD, *GI* peaks at dusk but also at dawn to a lesser extent. In the P2012 model the dawn peak of *GI* can be explained by the acute light activation of *GI* transcription at dawn followed by its repression by LHY/CCA1. This peak of *GI* at dawn could be observed in shoots with imaging because of the better temporal resolution compared to most of our RT-qPCR

experiments. However, only a shoulder could be observed at dawn for *GI* expression in roots. This would be consistent with a reduced inhibition of *GI* expression by LHY/CCA1 (see Figure A.6 in appendix). Interestingly the value of g_{15} , which represents the constant for inhibition of *GI* expression by LHY/CCA1 in the P2012 model, was consistently increased in several optimisation processes, although the value of g_{15} was allowed to decrease in these automated processes (Table 7.3). On the contrary, the value of g_5 , i.e. the constant for inhibition of *TOC1* expression by LHY/CCA1, was less changed and in fact decreased in the same parameter optimisation processes. This would be consistent with the small peak of *TOC1* observed at dawn in roots (e.g. in Figure 4.2). Therefore a few differences in the wiring of shoot and root clock might explain different FRPs but also different expression profiles in these two organs.

Thus many core clock components seem to be shared between shoots and roots. These components might have similar interaction in both organs, although the strength of these connections may differ in shoots and roots. Changing the parameters related to the coupling between morning and evening genes in several shoot clock models could simulate the possibly different wiring in the root clock and fit qualitatively data under specific conditions: LD, LL and DD (chapter 7). However none of these parameter optimisation processes could give a set of parameters that fit root data in all three conditions. Other parameters of the clock model may be organ-specific. A genome-wide identification of protein–protein and protein-DNA interactions would provide more insight to the root clock structure.

8.1.3 Inputs

What is surely organ-specific in the plant circadian system is the different light inputs that shoots and dark-grown roots receive. The main differences between shoot and root clocks are their FRP under LL and their amplitude under LD: these are respectively longer and lower in roots compared to shoots. Interestingly these two features could be simulated with the P2012 model by changing only one parameter: the light intensity (L). Indeed reducing L could lower the amplitudes of clock genes under LD and lengthen their FRP under LL (Figure 7.7 and 7.8). These simulations were motivated by at least three facts:

- dark-grown roots can perceive low light via channelling from exposed tissues (Sun *et al.*, 2005);

- some photoreceptors are expressed in roots (Toth *et al.*, 2001) (Sullivan *et al.*, unpublished) and could be functional (Costigan *et al.*, 2011);
- the root clock can be directly entrained by very low light levels (chapter 5).

However, simulating low light intensity delayed the phase of *CCA1* (Figure 7.8), which was not observed experimentally in dark-grown roots. In addition experiments showed that the FRP was longer not only in dark-grown roots, but also in light-grown roots compared to shoots, shoots and light-grown roots being exposed to the same light-intensity (chapter 4). Therefore the different light conditions experienced by shoots and roots cannot solely explain the differences between their clocks. Nevertheless, shoot and root clocks were more similar in DD than in any condition with illumination. This suggests that at least some differences between the two clocks may be related to light. Although differences between shoot and root circadian systems might reside within the structure of their core clock (i.e. different components or different interactions as discussed earlier), other parts of the circadian network could be organ-specific, such as light input pathways.

Light can differentially regulate gene expression in different organs of *Arabidopsis* and rice, including roots (Jiao *et al.*, 2007). In *Arabidopsis* seedlings, light regulated the transcriptomes of cotyledons, hypocotyls and roots in a similar way, but with little overlap (~1%) between the light-regulated genes in these three organs (Jiao *et al.*, 2007). The authors suggested that different signalling cascades could be involved in different organs and cell types, although the same photoreceptors seemed to be shared between organs. The idea of different cascades was supported by the overrepresentation of specific promoter motifs of light-regulated genes in roots and leaves, some of these motifs being organ-specific (Jiao *et al.*, 2005).

Both blue and red light could entrain the shoot and root clocks (Figure 4.7). Under LL with blue or red light, the FRP was shortened in shoots compared to DD. But blue light alone did not significantly shorten the FRP in roots compared to DD, whereas red light did (Figure 4.8). *ZTL* is a blue light photoreceptor closely linked to core clock components (Mas *et al.*, 2003; Kim *et al.*, 2007). The *ztl-105* mutation did not lengthen the FRP in roots as much as in shoots compared to the WT under a combination of blue and red light (Figure 6.3). These two experiments, with monochromatic light or with the *ztl-105* mutant, were only done once and need to be repeated before drawing any conclusions, but taken

together their results indicate that *ZTL* might be less functional in roots compared to shoots. However other blue light photoreceptors such as *CRY1* and *2* are expressed in dark-grown roots (Sullivan *et al.*, unpublished) and might be functional in roots. In dark-grown roots all blue light photoreceptor may be less active because less blue light can reach the roots (via channelling or penetration through the soil) compared to red light (Sun *et al.*, 2005; Tester and Morris, 1987). The effect of the *ztl* mutation on the root clock should be further investigated under blue or red light separately in roots.

On the other hand, red light photoreceptors might be more active in dark-grown roots. Red and far red light could reach dark-grown roots more easily than blue light, via better penetration through soil or piping from the aerial tissues (Sun *et al.*, 2005; Tester and Morris, 1987). In addition, *PHYA* and *PHYB* were expressed in dark-grown roots (Sullivan *et al.*, unpublished) and *PHYB* mRNA was scored rhythmic under LL. The *PHYA* promoter was even found rhythmic in excised roots under DD, although rhythms were quickly dampened (Hall *et al.*, 2001). This suggests that some photoreceptors could be involved in the root circadian system, most likely in its input pathways. Furthermore putative phyA-induced motifs were overrepresented in light-induced genes in both cotyledons and roots of light-grown seedlings (Jiao *et al.*, 2005). Interestingly *PHYA* is a photoreceptor that is sensitive to very low levels of red light; therefore it would be the most obvious candidate for photoreception in dark-grown roots.

As mentioned in chapter 1, the effects of light on the circadian system can be found at many levels, from the photoreceptors to the core clock components. The light input pathways might be organ-specific because of different amounts of photoreceptors or their different functions in roots compared to shoots. This would need to be tested, for instance by investigating the possible effects of photoreceptor mutations on the root clock. Some other differences might be downstream of these photoreceptors and at different levels of regulation. Although the promoter activities of clock and output genes in roots were all similarly affected by light, i.e. increased levels of expression and amplitude (chapter 4), the mRNA levels of clock genes seemed to be differentially regulated by light in roots. For instance in light-grown roots compared to dark-grown roots, the levels of *GI* mRNA were higher, whereas *CCA1* transcript levels seemed to be reduced. The lower levels of *CCA1* transcripts in roots exposed to light were consistent with its known degradation by light in shoots (Yakir *et al.*, 2007). Taken together, this indicates post-transcriptional regulation by

light in roots, and this level of regulation could affect differentially clock gene expression in this organ. This might be true in dark-grown roots, although the levels of light would be much lower compared to shoots. The quality of light perceived by these two organs is probably different too; this will be further discussed in the next section.

Plant cells were thought to have very similar clocks, partly because the different rhythms observed within a plant were different outputs generated by different cells (Harmer 2009). The root clock appeared to be an exception, because not only output rhythms but also core clock gene expression differed markedly in this organ compared to shoots. My work suggests that core clocks are probably more similar in shoots and roots than previously thought. Many components are likely shared, and their interaction has not been shown to differ dramatically in roots compared to shoots. However the light inputs to shoots and roots are obviously different, and could explain most differences observed between the two organs, such as the longer FRPs and lower amplitudes observed in roots compared to shoots. These differences could be simulated with the P2012 model by changing parameters related to light inputs (chapter 7); with these new parameters, the long FRP observed in both dark- and light-grown roots under LL could be reproduced without affecting entrainment under LD cycles. The parameters of the P2012 model should be further optimised to better fit the behaviour of the root clock. Once validated, a model with new parameter values could give predictions directly testable experimentally.

8.2 Plant circadian systems and their inputs at different levels of organisation

The previous section assumed that the circadian clocks are identical within the same organ. However, evidence suggests differences between the clocks of different tissues, as discussed in chapter 1. This section will discuss the plant circadian systems and their inputs at different levels of organisation, from intracellular levels to the whole plant and its environment.

8.2.1 Intracellular networks and microenvironment

A circadian system can be considered at the subcellular level where it is represented by a complex network between clock components and other signalling pathways. Many efforts have contributed to a better understanding of this network in plants during the last decades, and experimental approaches were combined with mathematical modelling to reproduce the dynamics of the system.

All the ODE models of the “plant” circadian clock published so far have been based on seedling data and assume that the core oscillator was identical in every cell. They focused on the TTFLs between clock genes and progressively integrated more components and their interactions in an increasingly complex network with many levels of regulation, including post-transcriptional and post-translational modifications. These models could explain more and more data from wild-type plants and mutants under various environmental conditions and have provided predictions that were verified experimentally.

Although these models were all based on the TTFLs in shoots, they were used to reproduce other aspects of the circadian system. For instance the parameters of the L2005b and L2006 models were optimised to simulate the interaction of the clock with cADPR and sucrose respectively (Dodd *et al.*, 2007; Dalchau *et al.*, 2011). Integrating such interactions, and more generally other regulatory networks into future versions of the circadian system will probably help to explain more data and better understand plant physiology. More complex models may also help to distinguish the circadian systems of different tissues and their different inputs. For instance most differences between the shoot and root clocks could be simulated by changing a few parameters of the P2012 model (chapter 7). These parameters were all related to light inputs and some of them were not present in the previous versions of the ODE models.

The effects of light on the clock machinery are now better integrated in the ODE model. In the P2012 model light affect many components at several levels of regulation (transcriptional, post-transcriptional and post-translational). However, the detail input pathway remains unclear. For instance, the acute light activation of gene transcription has been modelled by an unknown protein P since 2005. In addition, none of the ODE models has distinguished light qualities yet, although multiple light signalling pathways are required for correct biological timing in *Arabidopsis* (Dalchau *et al.*, 2010). Nevertheless,

light intensity can be modified in the P2012 model and this was useful to simulate the low light intensity perceived by dark-grown roots, which could reproduce several aspect of the root clock behaviour (chapter 7).

Light is a complex parameter that can have a huge range of values in terms of quantity and also quality; even a combination of only 2 monochromatic lights could take an infinite number of values, e.g. in terms of blue/red ratio. Light quantity can vary greatly over space in a single organism. This is obvious when comparing two organs: the differences between the light perceived by aerial tissues and dark-grown roots of a single plant are evident. Even within the same organ, such as a leaf, different light irradiances can be observed. Interestingly different light intensities perceived by different tissues has been suggested to be a possible cause of different FRP in leaves. For instance the longer period of stomatal conductance rhythms compared to photosynthesis in the *ztl1* mutant were correlated to the lower light intensity perceived by stomata compared to photosynthetic cells (Dodd *et al.*, 2004).

Furthermore the light quantity and quality might well vary in different cells, and even in different organelles, partly because of different fibre optic properties of different cells, but also because light would have to cross different physical (e.g. membranes) and chemical (e.g. pigments) barriers where light might be diffracted or absorbed. Therefore it is conceivable that with the same light source for an organism, the light quantity and quality may vary greatly between tissues, cells and organelles. This may highlight the interest of using monochromatic light; yet the different light intensities reaching different part of an organism need to be considered.

Many parameters vary in the microenvironment of a plant cell, and some of them may affect the clock. For instance solutes such as calcium and sucrose can affect clock gene expression (Haydon *et al.*, 2011) and their concentrations probably vary between cells or tissues. Any difference in inputs might contribute to different dynamics in the circadian system of different cells and tissues.

8.2.2 Tissue specificity in roots under constant light

As discussed in chapter 1, the specificity of circadian clocks has been observed in various plant tissues the last decade, mainly in leaf tissues under LL. In seedling roots, different patterns of CCA1:LUC⁺ activity were recently observed in different tissues (Fukuda *et al.*,

2012). The authors showed with imaging that the phase of *CCA1* expression varied within the root tissue, and they also observed arrhythmic regions under constant conditions. Such information could have been missed in my work because the analyses presented in this thesis were done at the whole organ level. Some of my data could be reanalysed by distinguishing different areas in the roots, but most of the time the roots were entangled which would make such analysis difficult. Indeed many areas contained different regions from different roots. In addition, the root signal was usually low at the organ level so it would be even harder to detect in different root tissues. This is partly because my plants were usually dark-grown on a medium without sucrose, so the root signal was certainly lower compared to Fukuda *et al.* (2012) who used sucrose and light-grown roots. In addition, I usually imaged several plates at a time when the roots were light-grown: the signal was then high enough at the organ level but may be too low for more detailed spatial analysis. Nevertheless our imaging system could (and indeed should) be used to study the clock in different regions of the roots. This possibility has not been exploited yet.

The results of Fukuda *et al.* (2012), and more generally the tissue specificity of plant circadian clocks, raise several questions about the root clock. First the rhythms observed at the organ level may reflect the oscillations of certain root cells or tissues only, the others being arrhythmic. It was only observed for *CCA1* expression in roots, but may be true for other genes as well. For example, *PRR3* is mainly expressed in the vasculature in leaves and its role in the shoot clock may be restricted to this tissue (Para *et al.*, 2007). If clock genes are not expressed in all the root cells, this might contribute to their lower amplitude observed in the whole organ. And if some clock-controlled genes are expressed in roots with different phases in different tissues or cells, this may not only contribute to lower amplitudes and broader peaks observed at the organ level, but could also result in apparent arrhythmia in roots. In fact, many less genes are expressed rhythmically in roots compared to shoots under LL (James *et al.*, 2008; Sullivan *et al.*, unpublished). One can wonder if there are more arrhythmic transcripts in roots compared to shoots, or if (some of) these are expressed at different phases and/or with different FRPs in different root tissues. Imaging clock gene expression in roots with a high spatial resolution could provide answers to these questions.

Within a plant with dark-grown roots, the range of light intensities reaching cells and molecules could be expected to be broader in roots than in shoots. For example the top of

the root would be closer to the light source and receive a considerable amount of light via piping or light penetration/leakage, whereas the bottom of the roots would perceive much less light. If Aschoff's rules are valid at the cellular level, this would lead to a broader range of FRP in roots compared to shoots, which would result in broader peaks or arrhythmia under LL when the whole roots are considered (i.e. when the heterogeneous rhythms are pooled together), and that can indeed be observed for several clock genes (chapter 4). Interestingly, when the roots were light-grown, the rhythms were more robust and the peaks of clock gene expression were sharper compared to dark-grown roots (Figure 4.2). Again this would be consistent with Aschoff's rules because all the tissues of light-grown roots were exposed to the same light intensity, contrary to the tissues of dark-grown roots.

The differences between tissues discussed so far in this section considered rhythms under LL. In such conditions the rhythms are not entrained by a zeitgeber and so can become desynchronised. The tissues of the same organs were pooled together in the experiments presented in this thesis, and therefore some cell or tissue specific information has probably been lost. Nevertheless, some consistent differences remained between the shoot and root circadian systems, under LL and LD, as discussed below.

8.2.3 Organ specificity and autonomy in different conditions

The organ specificity of the plant circadian system was first investigated with plants grown in hydroponic culture and by using RT-qPCR mainly (hydroponic system) and then with plants grown on plates (imaging system). Two main differences between shoot and root clocks could be observed with both systems: longer FRPs of clock gene expression under LL and lower amplitudes of oscillations under LD in roots compared to shoots. There were some discrepancies between the results obtained with these two systems, such as longer FRPs observed with imaging experiments compared to RT-qPCR experiments. This was probably due to the lower light intensity used for imaging (chapter 4). However, there were other differences between the environmental conditions used for imaging and RT-qPCR experiments. Some of these differences, and their possible effects on clock functions, are discussed below.

A major difference between the hydroponic and imaging systems was the light quality. Plants grown in hydroponic culture were exposed to white light, whereas most of the imaging experiments were carried out with a combination of blue and red light, which could be considered as an extremely simplified version of white light. However other wavelengths of the white light spectrum can play a role in the circadian system. For instance FR light can profoundly alter rhythmic gene expression in seedlings (Wenden *et al.*, 2011). This range of the light spectrum seems particularly relevant for roots since FR light is probably the main light source for underground plant tissues (Sun *et al.*, 2005; Sun *et al.*, 2003). Therefore the effects of FR light should be studied on the root clock and this could be done with imaging.

At the other end of the visible light spectrum, UV light can also affect rhythms. Several clock genes were shown to respond to low-intensity UV-B radiation ($1 \mu\text{mol.m}^{-2}.\text{s}^{-1}$), which seems to contribute to entrainment of the shoot clock (Feher *et al.*, 2011). Although UV-B light is present in the white spectrum, it can hardly be channelled by light tissues (or penetrate through the soil) so this range of light did probably not affect the clocks of our dark-grown roots. However, the exposure of roots to high white light (and therefore significant amounts of UV-B) could explain some differences between our results and those of Thain *et al.* (2000, 2002) regarding the expression of *CHS* in roots. *CHS* is a key enzyme involved in the production of photoprotective pigments. Its expression cannot be detected in dark-grown roots (James *et al.*, 2008). It could not be detected under $60 \mu\text{mol.m}^{-2}.\text{s}^{-1}$ of white light either, but it was expressed rhythmically in roots exposed to higher light intensities ($150\text{-}250 \mu\text{mol.m}^{-2}.\text{s}^{-1}$) (Thain *et al.*, 2000 and 2002). It is possible that *CHS* was induced by UV-B but only above a certain threshold in the studies of Thain *et al.* Moreover *CHS* expression rose before dawn in roots under white light. This would suggest that the root circadian system is flexible: it might control the rhythmic production of “sunscreens” only if necessary.

There may be other gene expressions that could be circadian-controlled in roots depending on the environmental conditions, such as the nitrate transporter *NRT2.1*. This gene was expressed rhythmically in the roots of plants grown hydroponically under LL (James *et al.*, 2008). However, I could not detect any rhythm in the luminescence of *NRT2.1:LUC* (data not shown). Note that the concentration of nutrients, including nitrates, is much higher in the $\frac{1}{2}$ MS medium used for the imaging system compared to our hydroponic solution.

Therefore the expression of *NRT2.1* was probably inhibited by the high level of nitrate present in the ½ MS medium, which would be consistent with the results of Girin *et al.* (2010a). Gutierrez *et al.* (Gutierrez *et al.*, 2008) suggested that N status could serve as an input for the circadian clock: pulses of organic and inorganic N could shift the phase of *CCA1* expression, and this clock gene is a central regulator of nitrogen (N) metabolism. It would be very interesting to further investigate the circadian regulation of nitrate transporters on different media. This may illustrate the importance of non-photic signals for the generation of circadian outputs in roots.

There was at least one other obvious difference between hydroponic and imaging environmental conditions. Roots of plants grown in hydroponic system were submerged in water. Oxygen has a very low solubility in water, and low levels of oxygen have been correlated to stress in plants. To escape this stress caused by low-O₂ plants can alter their architecture, metabolism and elongation growth (Bailey-Serres and Voesenek, 2008). On the contrary, the roots of plants grown on vertical plates were mainly growing on the surface of the medium, i.e. exposed to air where the concentration of O₂ is ~ 20%. Therefore the plants grown on plate and in hydroponic cultures were probably in different physiological states.

The environmental conditions for imaging and RT-qPCR experiments were different at several levels: the light quality and quantity, the nutrient concentrations, oxygen availability for roots. Yet major differences in terms of periods and amplitudes of clock gene expression between the shoot and root clocks could be observed with both settings. This demonstrates that at least some aspects of the root circadian clock are robust to environmental variations. Other aspects seem to be more flexible, such as the light-dependent expression of *CHS* and the nitrate-dependent expression of *NRT2.1* in roots. More output genes should be studied in roots under different conditions. This would provide further insight into the physiological relevance of the root clock.

The flexibility and organ specificity of the plant circadian clock was also supported by experiments under artificial diurnal conditions, such as T cycles, skeleton photoperiod, and conflicting LD cycles (chapter 5). The latter also suggested that the root clock is preferably entrained by direct absorption of light rather than signals from the shoots. Together with

the “decapitation experiment” (chapter 5), these experiments indicate that the clock is probably organ autonomous. For instance *GI* and *CCR2* were expressed rhythmically in excised roots under diurnal and constant conditions. The clocks of root tissues may be coupled more strongly to external LD cycles than to intercellular signalling, consistent with previous studies (Thain *et al.*, 2000; Wenden *et al.*, 2012). The autonomy of circadian systems in dark-grown roots under LD cycles is possible because their clock is very sensitive to entrainment by low light/dark cycles, with a light intensity that would be comparable to the light levels channelled by exposed tissues. A possible coupling between the clocks of tissues and organs cannot be ruled out, but it needs to be proven. The idea of intercellular coupling between different clocks of plant seems plausible, and may well occur in certain conditions. It could contribute to the synchronisation between different tissue functions. However, this synchronisation may be achieved faster by a direct entrainment of all the plant cells (even in roots) by external cues.

In natural conditions, light but also temperature are obvious zeitbebers for both shoot and root clocks. Temperature changes certainly have complex effects on living organisms and on their clock in particular. For instance cyclic changes in temperature can entrain the clock of diverse species, including *Arabidopsis thaliana*. But the pace of these clocks is little affected by steady-state temperature, a phenomenon known as temperature compensation which is a fundamental property of circadian rhythms. The shoot clock is temperature compensated, so the root clock may be as well: that would need to be verified experimentally. This thesis presented a preliminary study on temperature as a zeitgeber. The root clock could be entrained by HC 20/12 °C cycles under DD, after the plants were entrained by LD cycles at constant temperature. Although HC cycles were in antiphase with the previous LD cycles, clock and output genes were rapidly entrained by temperature cycles: it took only 2-3 transient days for the clock to be in phase with the HC cycles.

The mechanism of entrainment by temperature is still poorly understood. The temperature-dependent alternative splicing of several clock components probably contribute to entrainment. Indeed dynamic changes in alternatively spliced transcripts were recently correlated to temperature transitions; this was mainly shown in shoots but also in roots (James *et al.*, 2012). Rhythmic changes of about 8 °C between days and night are realistic in temperate regions. However temperature changes are buffered underground (Walter *et al.*, 2009). Therefore it would be interesting to further study the effects of temperature on the root clock with less variation between “days” and “nights”. Such study may be done in

the near future, possibly under LL or DD in order to dissect the effects of light and temperature as entraining agents. However organisms experience both LD and temperature cycles simultaneously in nature.

8.2.4 Plants in complex environments

In natural conditions, many parameters vary simultaneously and some of them can affect circadian systems. The most obvious are light and temperature cycles. These two zeitgebers have been shown to act synergistically to entrain behavioural and molecular rhythms of *Drosophila* (Yoshii *et al.*, 2009). The authors compared the effects of LD cycles and/or temperature cycles behavioural rhythms and showed that the rhythms were more robust under the combination of LD and temperature cycles, with enhanced amplitude of *Timeless*, a core clock component in *Drosophila*. Similarly, a combination of light and temperature cycles may result in stronger rhythms in plants and might reveal more rhythmicity in roots. This needs to be tested. Other parameters, such as water and nutrient availability can fluctuate in the environment, and may have an effect on circadian rhythms in plants as discussed earlier.

Little is known about how the circadian system contributes to diurnal rhythms in plants under natural conditions (Izawa, 2012). However plants have evolved under natural diurnal conditions that are much more complex than laboratory conditions. Izawa and colleagues studied the rhythms of WT and *OsGI* mutant rice grown in the field. Although the transcriptome data differed markedly between WT and mutant, flowering time and yields were comparable (Izawa, 2012). Studies on animal also revealed that known “clock genes” had less effect on circadian rhythms under more natural conditions compared to laboratory conditions (Gattermann *et al.*, 2008; Daan *et al.*, 2011; Vanin *et al.*, 2012). This suggests that clock components may not have the same role under different environments, an idea that was also mentioned by Izawa regarding plant rhythms (Izawa, 2012).

Other striking differences between circadian rhythms observed in laboratory and in more natural conditions were reported for several animals including the fruit fly (Gattermann *et al.*, 2008; Daan *et al.*, 2011; Vanin *et al.*, 2012). The activity of *Drosophila* was dramatically different outdoors compared to laboratory conditions using LD cycles (Vanin *et al.*, 2012). The authors questioned key assumptions about circadian behaviour that were based on laboratory studies, for instance the presumed crepuscular activity of flies. When

the same strains of flies were subjected to more complex variations in their environment, they were predominantly diurnal, with a major peak of activity in the afternoon that was not observed under LD cycles. Vanin and colleagues also conclude that temperature is the critical variable for predicting circadian behaviour in flies. The importance of temperature for plant circadian rhythms may also have been overlooked in the past decades.

Interestingly several of the new observations made outdoors with *Drosophila* could be reproduced indoors when light and temperature settings in the lab mimicked the natural variation of these two parameters, with e.g. twilights and gradual changes in temperature (Vanin *et al.*, 2012). Similarly circadian rhythms of *Arabidopsis* could be studied in the lab with more realistic conditions. Natural conditions would include other varying parameters than light and temperature. However “realistic” conditions are not necessarily natural: studying the clock of crop plants under greenhouse conditions could be very realistic.

In my work, all the plants were grown on media without sucrose, many experiments were done with dark-grown roots, and some of them were carried out under diurnal cycles. This is a first (and modest) step towards realistic environment. The “realism” should go further, at least varying both light and temperature using gradients. This would certainly provide new information about rhythms in plants.

8.2.5 Concluding remarks

Circadian rhythms are by definition rhythms with a sustained period of about 24 h under constant conditions. Therefore one cannot know whether a rhythm is circadian until it is studied under constant condition. That is why many experiments presented in this thesis were done in LL or DD. Indeed the study of the root circadian clock has a short history compared to that of shoots, and it was not clear which component were circadian in roots, especially the ones that are core clock components in shoots. My work suggests that the clock structure is similar in both organs, at least in the conditions tested. The difference between the plant circadian systems may be mainly related to different inputs. The relatively simple inputs used in laboratory conditions should be adjusted to simulate more realistic environments, at least in terms of light and temperature, to understand the effects of these two major parameters and their interaction on plant rhythms. These may reveal different mechanisms of the plant clocks compared to more simple conditions. In turn,

these clocks may generate different outputs to adapt their physiology to their environment. The adaptive advantage conferred by the circadian clock has only been demonstrated in shoots so far. However a plant needs both shoots and roots to function properly. It is likely that the root clock plays a role in the synchronisation of physiological processes between shoots and roots, and possibly the anticipation of environmental changes, therefore contributing to the plant fitness. The physiological relevance of the root clock needs to be investigated and overt rhythms should be explored in roots, together with shoot rhythms.

Appendix

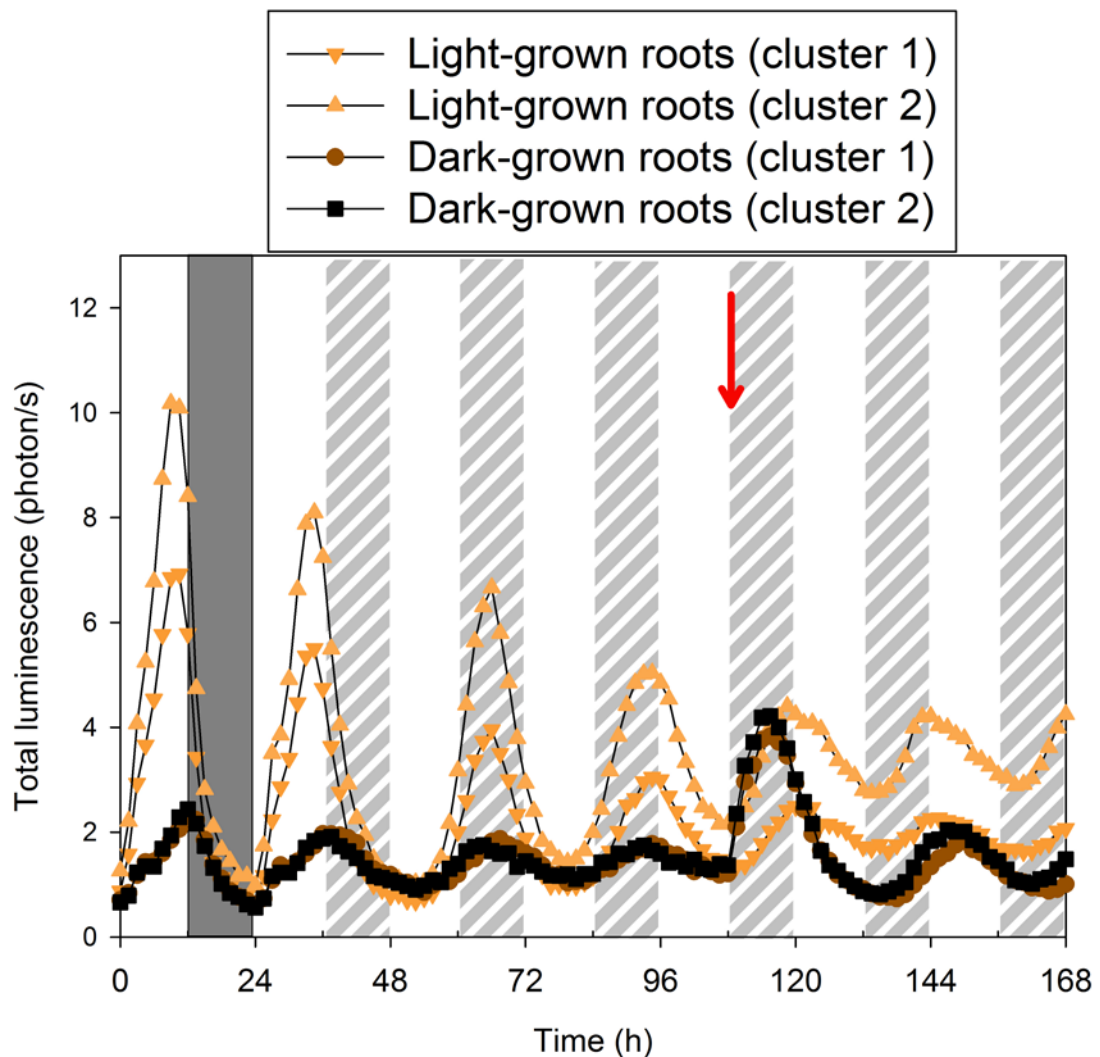


Figure A.1: GI total luminescence in light- and dark-grown roots under LD and LL.

Plants were entrained for 3-4 weeks in LD (12/12) before release in LL. For half of the plants, roots were light-grown (i.e. exposed to the same light/dark conditions as shoots); for the other half roots were dark-grown. The promoter activity of GI was monitored in roots and shoots over the last day in LD (ZT0 = dawn) and in LL. From ZT108 (red arrows), dark-grown roots were exposed to light (i.e. put in the same conditions as shoots and light-grown roots). Bars in the backgrounds represent days or subjective days (white bars), night (dark grey bars) and subjective night (hatched bars). 2 clusters of 2-3 plants (organs) from 2 independent experiments are presented for each condition. These raw data and others were then normalised, averaged and used for Figure 4.2.

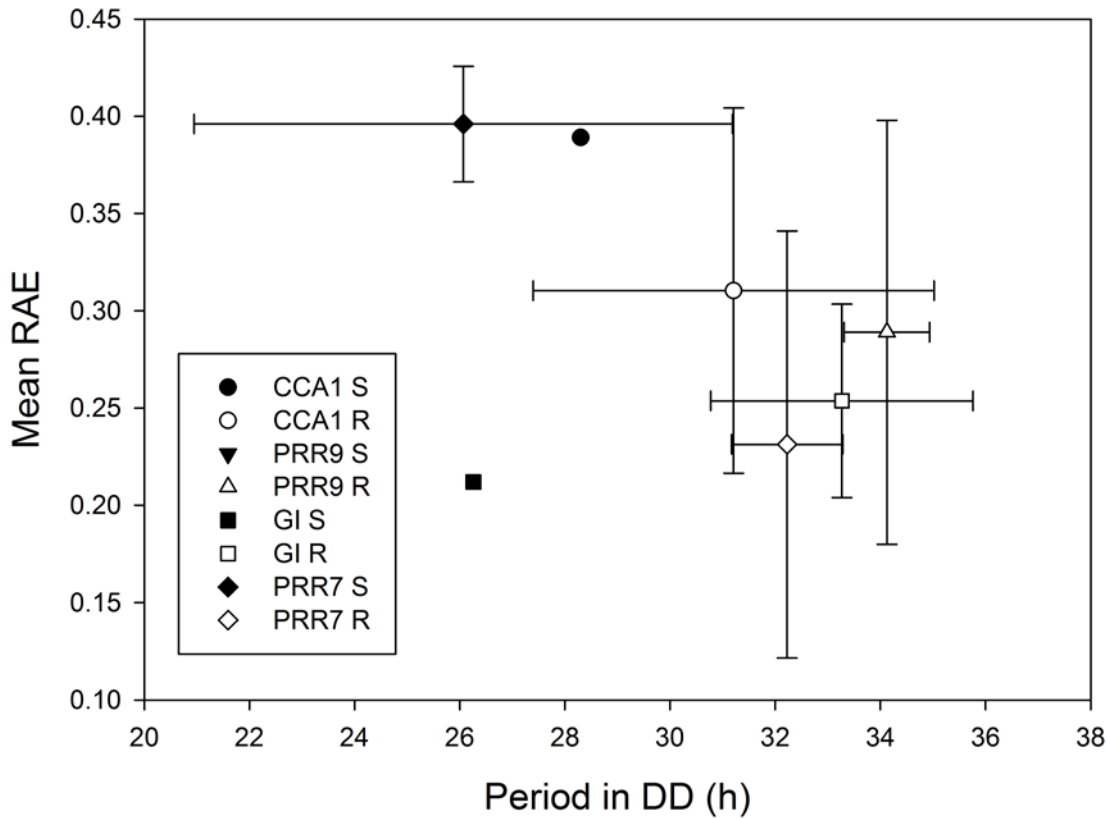


Figure A.2: LUC rhythms are less robust in shoots compared to roots under DD

The periods of data presented in Figure 4.5 (A-D) were estimated with BRASS using the same 84h window for all time-courses, i.e. the whole period under DD except the first 24 h. In roots, all the time-courses were scored rhythmic (bars represent standard errors for 2-4 independent experiments), whereas in shoots, 2 time-courses were scored rhythmic for PRR7, only 1 for CCA1 and GI (hence no error bars) and none for PRR9.

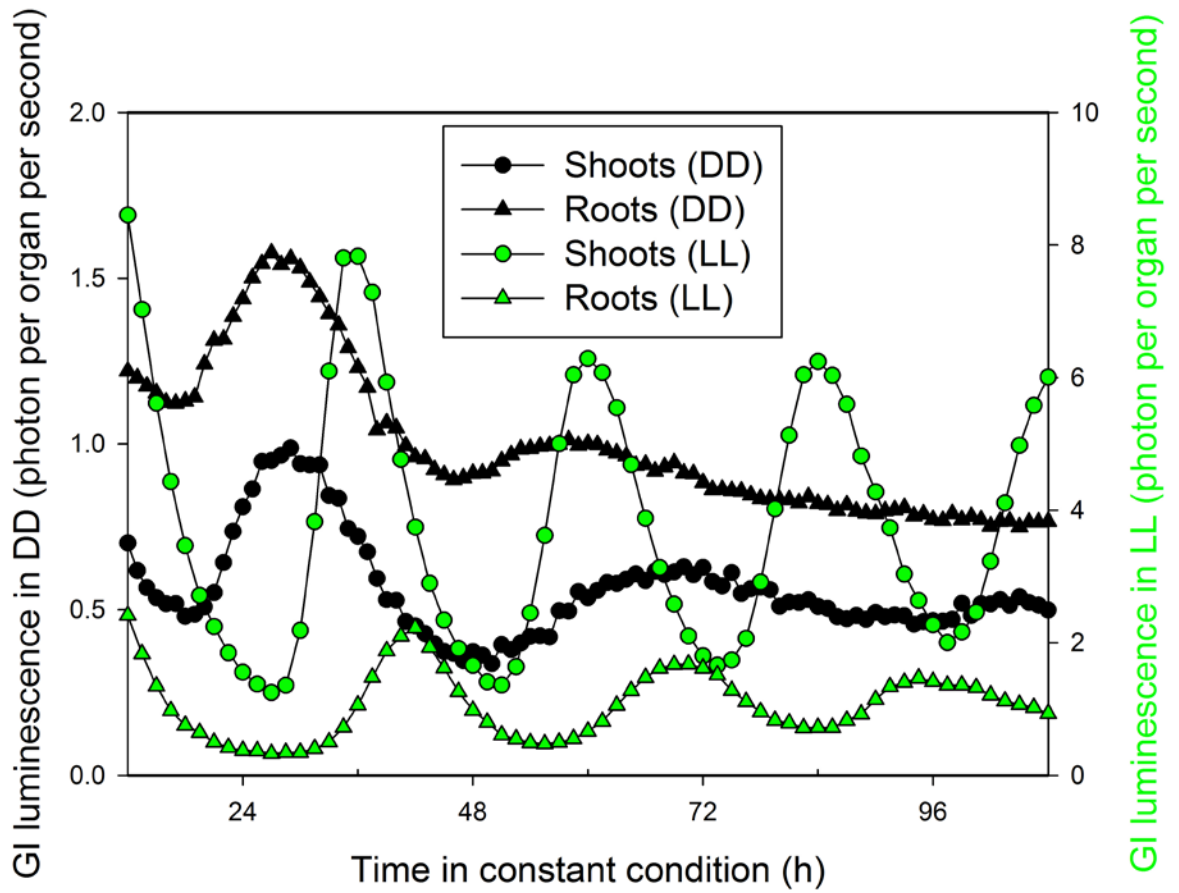


Figure A.3: GI:LUC signals are much lower in DD compared to LL

Shoot and root raw data from 2 individual time-courses, 1 used for Figure 4.5 (DD) and 1 for Figure 4.2 (LL). Note the different scales for DD and LL

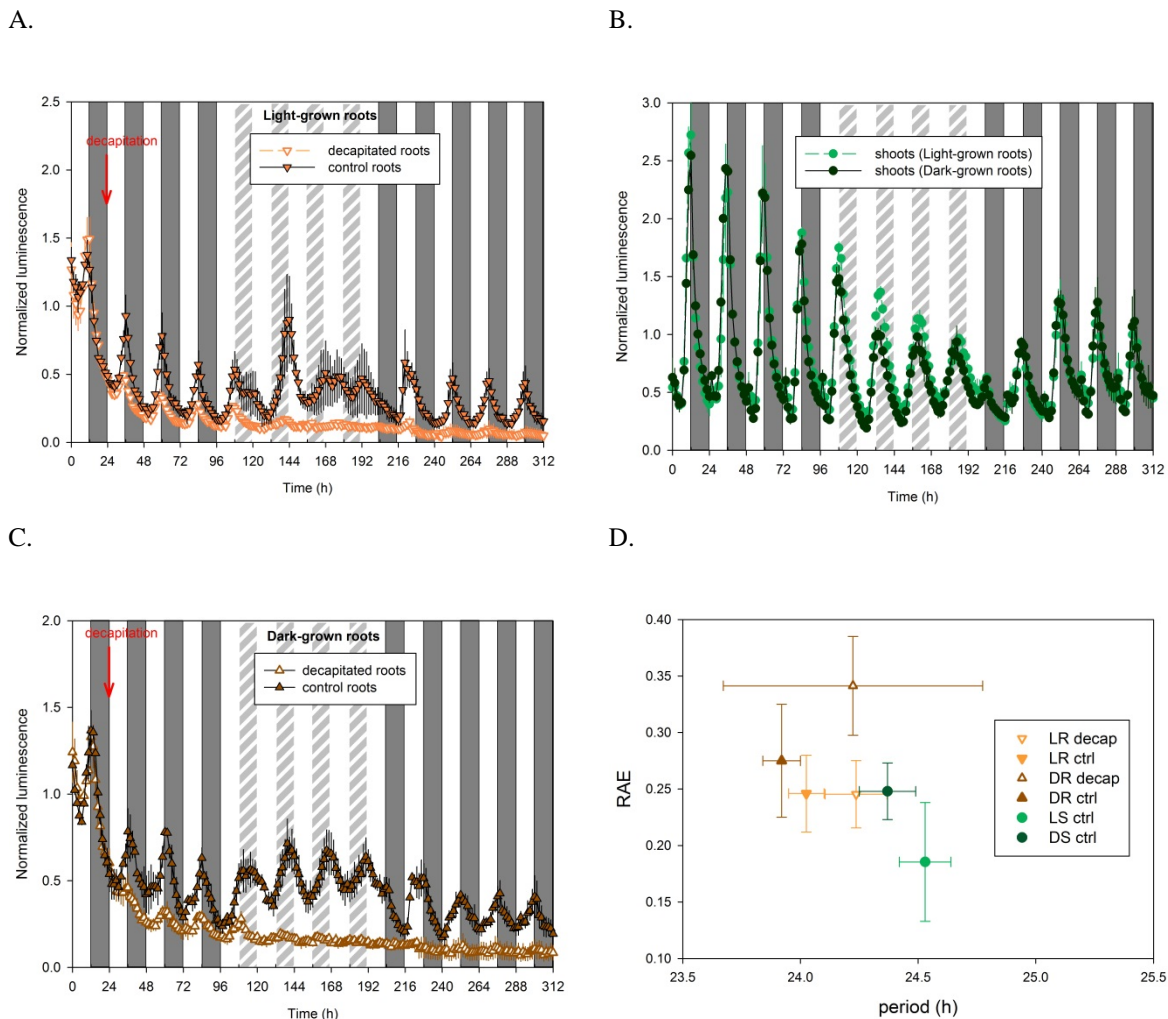


Figure A.4: LD cycles can directly entrain *CCR2* expression in roots

Plants with the *CCR2:LUC+* reporter were entrained 3-4 weeks in LD (white light) before imaging (blue and red light); roots were light- or dark-grown. Plants were imaged for 24h in LD. Then half of them were decapitated before dawn (at ZT24, indicated by the red arrows) and all the plants were transferred to LD and LL cycles (A-C)

A-C: Bioluminescence over time of light-grown roots (A), shoots (B) and dark-grown roots (C). Grey bar represents D cycles, white and light grey hatched bars represent L and subjective L respectively, and dark grey hatched bars represent subjective nights. Data were normalised with the mean luminescence of the first LD cycle (before decapitation, A-C) Error bars are SEM for 2 clusters of 2-3 plants (organs) from 2 independent experiments.

D: Circadian period estimates of data presented in A-C in LD using BRASS for roots and shoots.

Symbols and colours used in Figure C-F are the same as in Figure G and H for clarity. Shoots and roots are represented by circles and triangles respectively. For each graph the lighter colours represents organs of plants with light-grown roots, whereas darker colours represents organs of plants with dark-grown roots. The

open symbols represent decapitated plants.

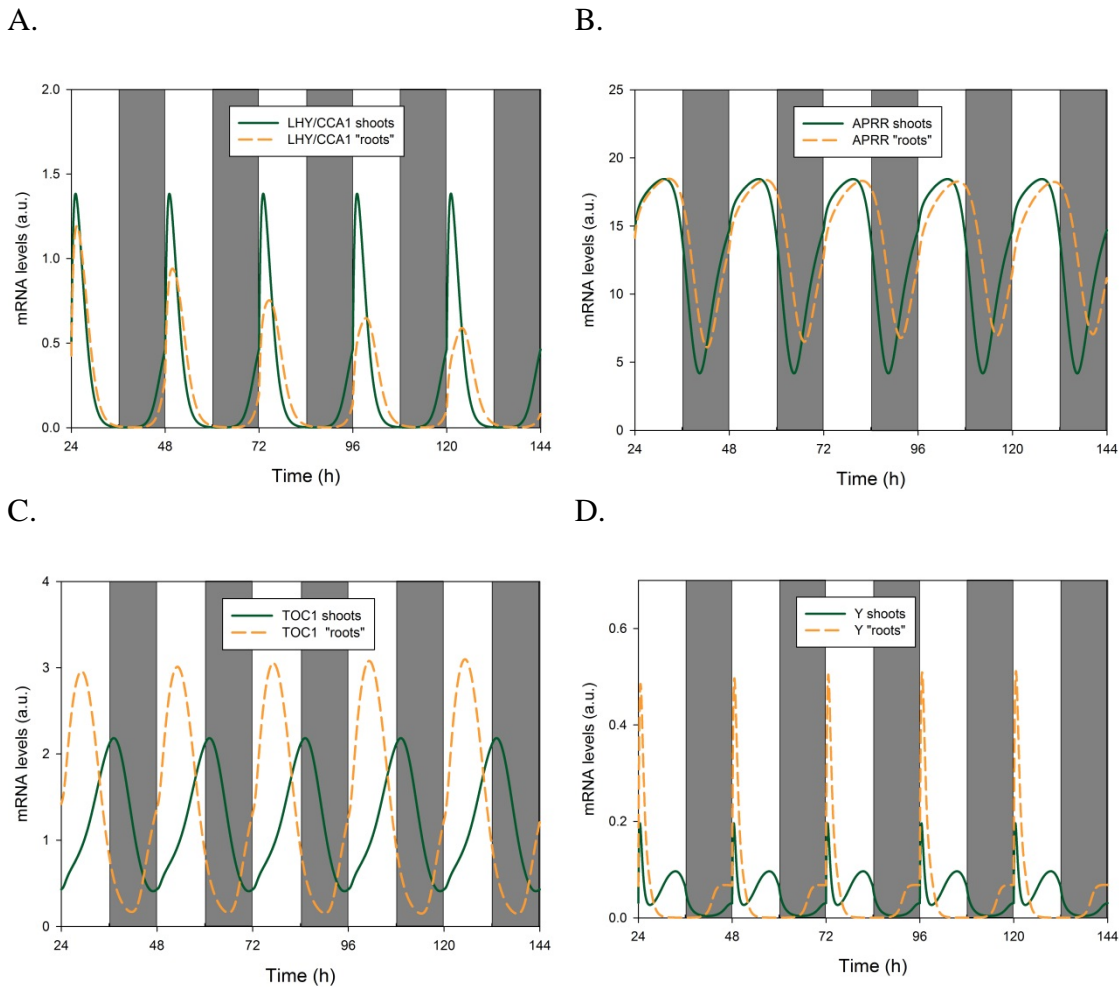
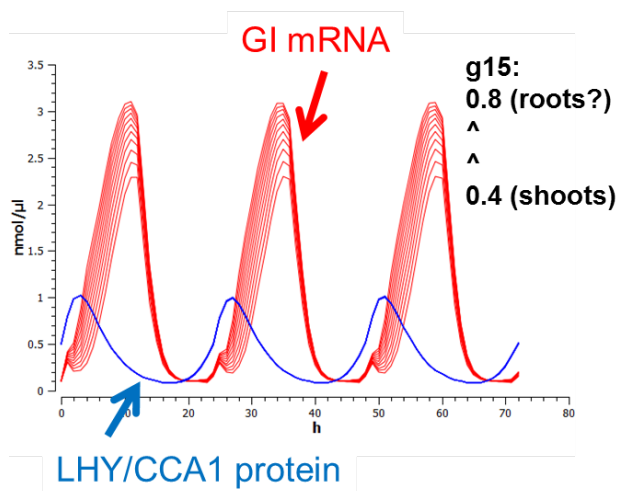


Figure A.5: Simulations of clock genes mRNA levels in shoots and “roots” under LD (12/12) using the L2006 model

The simulations with default parameters of the L2006 model represent seedling data in LD and are labelled shoots (green solid lines). The other simulations attempt to fit the root clock data obtained with dark-grown roots in LD (12/12); they are labelled “roots” (orange dashes). For the “roots” simulations, the “20(g3g6)0.01g4” set of parameters (presented in fig. 7.1 C&D) was used: the default set of parameters of the L2006 models were used, except g3 and g6 (both increased 1000 or 20 fold respectively) and g4 (decreased 100 fold).

A-D: Simulations of *LHY/CCA1* (A), *APRR* (B), *TOC1* (C) and *Y* (D) mRNA levels.

A.



B.

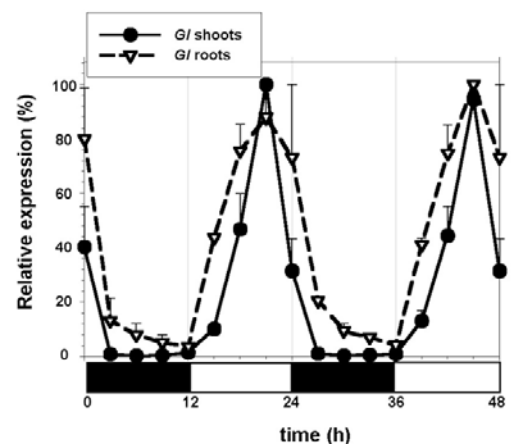


Figure A.6: Increasing the parameter g_{15} in the P2012 model removes the dawn peak of GI mRNA and broaden its dusk peak.

A. Simulation using the P2012 model. The parameter g_{15} was scanned with COPASI for values between 0.4 (default value for the shoot model) and 0.8. Increasing g_{15} simulates less inhibition of *G_I* mRNA synthesis by LHY/CCA1 protein. This results in a broader and higher peak of *G_I* expression (red lines); the lower and higher lines represent simulations for $g_{15} = 0.4$ and $g_{15} = 0.8$ respectively. The modification of g_{15} does not affect the level of LHY/CCA1 protein (blue line).

B. Experimental data from James *et al.* (2008). Relative levels of *G_I* transcripts in shoots and roots under LD.

References

- Abraham,U., Granada,A.E., Westermarck,P.O., Heine,M., Kramer,A., and Herzog,H. (2010). Coupling governs entrainment range of circadian clocks. *Molecular Systems Biology* 6.
- Adams,S. and Carre,I.A. (2011). Downstream of the plant circadian clock: output pathways for the control of physiology and development. *Essays in Biochemistry: Chronobiology* 49, 53-69.
- Adrian Troncoso-Ponce,M. and Mas,P. (2012). Newly Described Components and Regulatory Mechanisms of Circadian Clock Function in *Arabidopsis thaliana*. *Molecular Plant* 5, 545-553.
- Alabadi,D., Oyama,T., Yanovsky,M.J., Harmon,F.G., Mas,P., and Kay,S.A. (2001). Reciprocal regulation between TOC1 and LHY/CCA1 within the *Arabidopsis* circadian clock. *Science* 293, 880-883.
- Alabadi,D., Yanovsky,M.J., Mas,P., Harmer,S.L., and Kay,S.A. (2002). Critical role for CCA1 and LHY in maintaining circadian rhythmicity in *Arabidopsis*. *Current Biology* 12, 757-761.
- Allada,R. and Chung,B.Y. (2010). Circadian Organization of Behavior and Physiology in *Drosophila*. *Annual Review of Physiology* 72, 605-624.
- Andres,F. and Coupland,G. (2012). The genetic basis of flowering responses to seasonal cues. *Nature Reviews Genetics* 13, 627-639.
- Aschoff,J. (1960). Exogenous and Endogenous Components in Circadian Rhythms. *Cold Spring Harbor Symposia on Quantitative Biology* 25, 11-28.
- Ay,A. and Arnosti,D.N. (2011). Mathematical modeling of gene expression: a guide for the perplexed biologist. *Critical Reviews in Biochemistry and Molecular Biology* 46, 137-151.
- Bailey-Serres,J. and Voesenek,L. (2008). Flooding stress: Acclimations and genetic diversity.
- Baker,C.L., Loros,J.J., and Dunlap,J.C. (2012). The circadian clock of *Neurospora crassa*. *Fems Microbiology Reviews* 36, 95-110.
- Baudry,A., Ito,S., Song,Y.H., Strait,A.A., Kiba,T., Lu,S., Henriques,R., Pruneda-Paz,J.L., Chua,N.H., Tobin,E.M., Kay,S.A., and Imaizumi,T. (2010). F-Box Proteins FKF1 and LKP2 Act in Concert with ZEITLUPE to Control *Arabidopsis* Clock Progression. *Plant Cell* 22, 606-622.
- Beersma,D.G.M. (2005). Why and how do we model circadian rhythms? *Journal of Biological Rhythms* 20, 304-313.

Bell-Pedersen,D., Cassone,V.M., Earnest,D.J., Golden,S.S., Hardin,P.E., Thomas,T.L., and Zoran,M.J. (2005). Circadian rhythms from multiple oscillators: Lessons from diverse organisms. *Nature Reviews Genetics* 6, 544-556.

Bischoff,F., Millar,A.J., Kay,S.A., and Furuya,M. (1997). Phytochrome-induced intercellular signalling activates cab:luciferase gene expression. *Plant Journal* 12, 839-849.

Blasing,O.E., Gibon,Y., Gunther,M., Hohne,M., Morcuende,R., Osuna,D., Thimm,O., Usadel,B., Scheible,W.R., and Stitt,M. (2005). Sugars and circadian regulation make major contributions to the global regulation of diurnal gene expression in *Arabidopsis*. *Plant Cell* 17, 3257-3281.

Bunning,E. (1932). On the inheritance of daily periodicity in *Phaseolus* leaves. *Jahrbuch fur Wissenschaftliche Botanik* 77, 283-320.

Bunning,E.R.W.I. (1931). Untersuchungen uber die autonomen tagesperiodischen Bewegungen der Primar-blatter von *Phaseolus multiflorus*. *Jahrb Wiss Bot* 75, 439-480.

Carre,I.A. and Kim,J.Y. (2002). MYB transcription factors in the *Arabidopsis* circadian clock. *Journal of Experimental Botany* 53, 1551-1557.

Christie,J.M. and Briggs,W.R. (2001). Blue light sensing in higher plants. *Journal of Biological Chemistry* 276, 11457-11460.

Costigan,S.E., Warnasooriya,S.N., Humphries,B.A., and Montgomery,B.L. (2011). Root-Localized Phytochrome Chromophore Synthesis Is Required for Photoregulation of Root Elongation and Impacts Root Sensitivity to Jasmonic Acid in *Arabidopsis*. *Plant Physiology* 157, 1138-1150.

Covington,M.F., Panda,S., Liu,X.L., Strayer,C.A., Wagner,D.R., and Kay,S.A. (2001). ELF3 modulates resetting of the circadian clock in *Arabidopsis*. *Plant Cell* 13, 1305-1315.

Cumming,B.G. and Wagner,E. (1968). Rhythmic Processes in Plants. *Annual Review of Plant Physiology* 19, 381-&.

Daan,S., Spoelstra,K., Albrecht,U., Schmutz,I., Daan,M., Daan,B., Rienks,F., Poletaeva,I., Dell'Omo,G., Vyssotski,A., and Lipp,H.P. (2011). Lab Mice in the Field: Unorthodox Daily Activity and Effects of a Dysfunctional Circadian Clock Allele. *Journal of Biological Rhythms* 26, 118-129.

Dai,S., Wei,X., Pei,L., Thompson,R.L., Liu,Y., Heard,J.E., Ruff,T.G., and Beachy,R.N. (2011). Brother of Lux Arrhythmo Is A Component of the *Arabidopsis* Circadian Clock. *Plant Cell* 23, 961-972.

Dalchau,N., Baek,S.J., Briggs,H.M., Robertson,F.C., Dodd,A.N., Gardner,M.J., Stancombe,M.A., Haydon,M.J., Stan,G.B., Goncalves,J.M., and Webb,A.A. (2011). The circadian oscillator gene GIGANTEA mediates a long-term response of the *Arabidopsis thaliana* circadian clock to sucrose. *Proceedings of the National Academy of Sciences of the United States of America* 108, 5104-5109.

- Dalchau,N., Hubbard,K.E., Robertson,F.C., Hotta,C.T., Briggs,H.M., Stan,G.B., Goncalves,J.M., and Webb,A.A. (2010). Correct biological timing in Arabidopsis requires multiple light-signaling pathways. *Proceedings of the National Academy of Sciences of the United States of America* *107*, 13171-13176.
- de Ruijter,N.C.A., Verhees,J., van Leeuwen,W., and van der Krol,A.R. (2003). Evaluation and comparison of the GUS, LUC and GFP reporter system for gene expression studies in plants. *Plant Biology* *5*, 103-115.
- DeCoursey,P.J. (2004a). Overview of biological timing from unicells to Humans. In *Chronobiology - Biological timekeeping*, J.C.Dunlap, J.J.Loros, and P.J.DeCoursey, eds.
- DeCoursey,P.J. (2004b). The behavioral ecology and evolution of biological timing systems. In *Chronobiology - Biological timekeeping*, J.C.Dunlap, J.J.Loros, and P.J.DeCoursey, eds.
- Devlin,P.F. and Kay,S.A. (2001). Circadian photoperception. *Annual Review of Physiology* *63*, 677-694.
- Dixon,L.E., Knox,K., Kozma-Bognar,L., Southern,M.M., Pokhilko,A., and Millar,A.J. (2011). Temporal Repression of Core Circadian Genes Is Mediated through EARLY FLOWERING 3 in Arabidopsis. *Current Biology* *21*, 120-125.
- Dodd,A.N., Parkinson,K., and Webb,A.A.R. (2004). Independent circadian regulation of assimilation and stomatal conductance in the *ztl-1* mutant of Arabidopsis. *New Phytologist* *162*, 63-70.
- Dodd,A.N., Salathia,N., Hall,A., Kevei,E., Toth,R., Nagy,F., Hibberd,J.M., Millar,A.J., and Webb,A.A.R. (2005). Plant circadian clocks increase photosynthesis, growth, survival, and competitive advantage. *Science* *309*, 630-633.
- Dodd,A.N., Gardner,M.J., Hotta,C.T., Hubbard,K.E., Dalchau,N., Love,J., Assie,J.M., Robertson,F.C., Jakobsen,M.K., Goncalves,J., Sanders,D., and Webb,A.A. (2007). The Arabidopsis circadian clock incorporates a cADPR-based feedback loop. *Science* *318*, 1789-1792.
- Doyle,M.R., Davis,S.J., Bastow,R.M., McWatters,H.G., Kozma-Bognar,L., Nagy,F., Millar,A.J., and Amasino,R.M. (2002). The ELF4 gene controls circadian rhythms and flowering time in Arabidopsis thaliana. *Nature* *419*, 74-77.
- Dunlap,J.C. (1999). Molecular bases for circadian clocks. *Cell* *96*, 271-290.
- Edwards,K.D., Akman,O.E., Knox,K., Lumsden,P.J., Thomson,A.W., Brown,P.E., Pokhilko,A., Kozma-Bognar,L., Nagy,F., Rand,D.A., and Millar,A.J. (2010). Quantitative analysis of regulatory flexibility under changing environmental conditions. *Molecular Systems Biology* *6*.
- Eriksson,M.E. and Webb,A.A. (2011). Plant cell responses to cold are all about timing. *Current Opinion in Plant Biology* *14*, 731-737.

Farre,E. (2012). The regulation of plant growth by the circadian clock. *Plant Biology* 14, 401-410.

Farre,E.M., Harmer,S.L., Harmon,F.G., Yanovsky,M.J., and Kay,S.A. (2005). Overlapping and distinct roles of PRR7 and PRR9 in the Arabidopsis circadian clock. *Current Biology* 15, 47-54.

Faure,S., Turner,A.S., Gruszka,D., Christodoulou,V., Davis,S.J., von Korff,M., and Laurie,D.A. (2012). Mutation at the circadian clock gene EARLY MATURITY 8 adapts domesticated barley (*Hordeum vulgare*) to short growing seasons. *Proceedings of the National Academy of Sciences of the United States of America* 109, 8328-8333.

Feher,B., Kozma-Bognar,L., Kevei,E., Hajdu,A., Binkert,M., Davis,S.J., Schaefer,E., Ulm,R., and Nagy,F. (2011). Functional interaction of the circadian clock and UV RESISTANCE LOCUS 8-controlled UV-B signaling pathways in *Arabidopsis thaliana*. *Plant Journal* 67, 37-48.

Fowler,S., Lee,K., Onouchi,H., Samach,A., Richardson,K., Coupland,G., and Putterill,J. (1999). GIGANTEA: a circadian clock-controlled gene that regulates photoperiodic flowering in *Arabidopsis* and encodes a protein with several possible membrane-spanning domains. *Embo Journal* 18, 4679-4688.

Fukuda,H., Ukai,K., and Oyama,T. (2012). Self-arrangement of cellular circadian rhythms through phase-resetting in plant roots. *Physical Review* e 86.

Gattermann,R., Johnston,R.E., Yigit,N., Fritzsche,P., Larimer,S., Oezkurt,S., Neumann,K., Song,Z., Colak,E., Johnston,J., and McPhee,M. (2008). Golden hamsters are nocturnal in captivity but diurnal in nature. *Biology Letters* 4, 253-255.

Gendron,J.M., Pruneda-Paz,J.L., Doherty,C.J., Gross,A.M., Kang,S.E., and Kay,S.A. (2012). Arabidopsis circadian clock protein, TOC1, is a DNA-binding transcription factor. *Proceedings of the National Academy of Sciences of the United States of America* 109, 3167-3172.

Girin,T., El Kafafi,E.S., Widiez,T., Erban,A., Hubberten,H.M., Kopka,J., Hoefgen,R., Gojon,A., and Lepetit,M. (2010a). Identification of Arabidopsis Mutants Impaired in the Systemic Regulation of Root Nitrate Uptake by the Nitrogen Status of the Plant. *Plant Physiology* 153, 1250-1260.

Girin,T., El-Kafafi,E.S., Widiez,T., Erban,A., Hubberten,H.M., Kopka,J., Hoefgen,R., Gojon,A., and Lepetit,M. (2010b). Identification of Arabidopsis Mutants Impaired in the Systemic Regulation of Root Nitrate Uptake by the Nitrogen Status of the Plant. *Plant Physiology* 153, 1250-1260.

Goodspeed,D., Chehab,E.W., Min-Venditti,A., Braam,J., and Covington,M.F. (2012). Arabidopsis synchronizes jasmonate-mediated defense with insect circadian behavior. *Proceedings of the National Academy of Sciences of the United States of America* 109, 4674-4677.

Green,R.M., Tingay,S., Wang,Z.Y., and Tobin,E.M. (2002). Circadian rhythms confer a higher level of fitness to Arabidopsis plants. *Plant Physiology* 129, 576-584.

- Guerriero,M.L., Pokhilko,A., Fernandez,A.P., Halliday,K.J., Millar,A.J., and Hillston,J. (2012). Stochastic properties of the plant circadian clock. *Journal of the Royal Society Interface* 9, 744-756.
- Gutierrez,R.A., Stokes,T.L., Thum,K., Xu,X., Obertello,M., Katari,M.S., Tanurdzic,M., Dean,A., Nero,D.C., McClung,C., and Coruzzi,G.M. (2008). Systems approach identifies an organic nitrogen-responsive gene network that is regulated by the master clock control gene CCA1. *Proceedings of the National Academy of Sciences of the United States of America* 105, 4939-4944.
- Hall,A., Kozma-Bognar,L., Bastow,R.M., Nagy,F., and Millar,A.J. (2002). Distinct regulation of CAB and PHYB gene expression by similar circadian clocks. *Plant Journal* 32, 529-537.
- Hall,A., Kozma-Bognar,L., Toth,R., Nagy,F., and Millar,A.J. (2001). Conditional circadian regulation of PHYTOCHROME A gene expression. *Plant Physiology* 127, 1808-1818.
- Hall,A. and Brown,P. (2007). Monitoring circadian rhythms in *Arabidopsis thaliana* using luciferase reporter genes. *Methods in molecular biology (Clifton, N. J.)* 362, 143-152.
- Harmer,S.L., Hogenesch,L.B., Straume,M., Chang,H.S., Han,B., Zhu,T., Wang,X., Kreps,J.A., and Kay,S.A. (2000). Orchestrated transcription of key pathways in *Arabidopsis* by the circadian clock. *Science* 290, 2110-2113.
- Harmer,S.L. and Kay,S.A. (2005). Positive and negative factors confer phase-specific circadian regulation of transcription in *Arabidopsis*. *Plant Cell* 17, 1926-1940.
- Harmer,S.L. (2009). The Circadian System in Higher Plants. *Annual Review of Plant Biology* 60, 357-377.
- Haydon,M.J., Bell,L.J., and Webb,A.A. (2011). Interactions between plant circadian clocks and solute transport. *Journal of Experimental Botany* 62, 2333-2348.
- Hazen,S.P., Schultz,T.F., Pruneda-Paz,J.L., Borevitz,J.O., Ecker,J.R., and Kay,S.A. (2005). LUX ARRHYTHMO encodes a Myb domain protein essential for circadian rhythms. *Proceedings of the National Academy of Sciences of the United States of America* 102, 10387-10392.
- Helfer,A., Nusinow,D.A., Chow,B.Y., Gehrke,A.R., Bulyk,M.L., and Kay,S.A. (2011). LUX ARRHYTHMO Encodes a Nighttime Repressor of Circadian Gene Expression in the *Arabidopsis* Core Clock. *Current Biology* 21, 126-133.
- Herrero,E. and Davis,S.J. (2012). Time for a Nuclear Meeting: Protein Trafficking and Chromatin Dynamics Intersect in the Plant Circadian System. *Molecular Plant* 5, 554-565.
- Hicks,K.A., Millar,A.J., Carre,I.A., Somers,D.E., Straume,M., MeeksWagner,D.R., and Kay,S.A. (1996). Conditional circadian dysfunction of the *Arabidopsis* early-flowering 3 mutant. *Science* 274, 790-792.
- Hogenesch,J.B. and Ueda,H.R. (2011). Understanding systems-level properties: timely stories from the study of clocks. *Nature Reviews Genetics* 12, 407-416.

Hotta,C.T., Gardner,M.J., Hubbard,K.E., Baek,S.J., Dalchau,N., Suhita,D., Dodd,A.N., and Webb,A.A. (2007). Modulation of environmental responses of plants by circadian clocks. *Plant Cell and Environment* 30, 333-349.

Hotta,C.T., Xu,X., Xie,Q., Dodd,A.N., Johnson,C.H., and Webb,A.A. (2008). Are there multiple circadian clocks in plants? *Plant signaling & behavior* 3, 342-344.

Huang,W., Perez-Garcia,P., Pokhilko,A., Millar,A., Antoshechkin,I., Riechmann,J., and Mas,P. (2012). Mapping the Core of the Arabidopsis Circadian Clock Defines the Network Structure of the Oscillator. *Science* 336, 75-79.

Ito,S., Nakamichi,N., Matsushika,A., Fujimori,T., Yamashino,T., and Mizuno,T. (2005). Molecular dissection of the promoter of the light-induced and circadian-controlled APRR9 gene encoding a clock-associated component of Arabidopsis thaliana. *Bioscience Biotechnology and Biochemistry* 69, 382-390.

Izawa,T. (2012). Physiological significance of the plant circadian clock in natural field conditions. *Plant Cell and Environment* 35, 1729-1741.

James,A.B., Monreal,J.A., Nimmo,G.A., Kelly,C.L., Herzyk,P., Jenkins,G.I., and Nimmo,H.G. (2008). The Circadian Clock in Arabidopsis Roots Is a Simplified Slave Version of the Clock in Shoots. *Science* 322, 1832-1835.

James,A.B., Syed,N.H., Bordage,S., Marshall,J., Nimmo,G.A., Jenkins,G.I., Herzyk,P., Brown,J.W., and Nimmo,H.G. (2012). Alternative Splicing Mediates Responses of the Arabidopsis Circadian Clock to Temperature Changes. *Plant Cell* 24, 961-981.

Jander,G. (2012). Timely plant defenses protect against caterpillar herbivory. *Proceedings of the National Academy of Sciences of the United States of America* 109, 4343-4344.

Janzen,D.H. (1976). Why Bamboos Wait So Long to Flower. *Annual Review of Ecology and Systematics* 7, 347-391.

Jiao,Y.L., Ma,L.G., Strickland,E., and Deng,X.W. (2005). Conservation and divergence of light-regulated genome expression patterns during seedling development in rice and Arabidopsis. *Plant Cell* 17, 3239-3256.

Jiao,Y., Lau,O.S., and Deng,X.W. (2007). Light-regulated transcriptional networks in higher plants. *Nature Reviews Genetics* 8, 217-230.

Johnson,C.H., Elliott,J., Foster,R., Honma,K., and Kronauer,R. (2004). Fundamental properties of circadian rhythms. In *Chronobiology - Biological timekeeping*, J.C.Dunlap, J.J.Loros, and P.J.DeCoursey, eds.

Johnson,C.H., Elliott,J.A., and Foster,R. (2003). Entrainment of circadian programs. *Chronobiology International* 20, 741-774.

Johnson,C.H., Stewart,P.L., and Egli,M. (2011). The Cyanobacterial Circadian System: From Biophysics to Bioevolution.

- Kerwin,R.E., Jimenez-Gomez,J.M., Fulop,D., Harmer,S.L., Maloof,J.N., and Kliebenstein,D.J. (2011). Network Quantitative Trait Loci Mapping of Circadian Clock Outputs Identifies Metabolic Pathway-to-Clock Linkages in Arabidopsis. *Plant Cell* 23, 471-485.
- Kevei,E., Gyula,P., Hall,A., Kozma-Bognar,L., Kim,W.Y., Eriksson,M.E., Toth,R., Hanano,S., Feher,B., Southern,M.M., Bastow,R.M., Viczian,A., Hibberd,V., Davis,S.J., Somers,D.E., Nagy,F., and Millar,A.J. (2006). Forward genetic analysis of the circadian clock separates the multiple functions of ZEITLUPE. *Plant Physiology* 140, 933-945.
- Kikis,E.A., Khanna,R., and Quail,P.H. (2005). ELF4 is a phytochrome-regulated component of a negative feedback loop involving the central oscillator components CCA1 and LHY. *Plant Journal* 44, 300-313.
- Kim,J., Kim,Y., Yeom,M., Kim,J.H., and Nam,H.G. (2008). FIONA1 is essential for regulating period length in the Arabidopsis circadian clock. *Plant Cell* 20, 307-319.
- Kim,J.Y., Song,H.R., Taylor,B.L., and Carre,I.A. (2003a). Light-regulated translation mediates gated induction of the Arabidopsis clock protein LHY. *Embo Journal* 22, 935-944.
- Kim,W.Y., Geng,R.S., and Somers,D.E. (2003b). Circadian phase-specific degradation of the F-box protein ZTL is mediated by the proteasome. *Proceedings of the National Academy of Sciences of the United States of America* 100, 4933-4938.
- Kim,W.Y., Fujiwara,S., Suh,S.S., Kim,J., Kim,Y., Han,L., David,K., Putterill,J., Nam,H.G., and Somers,D.E. (2007). ZEITLUPE is a circadian photoreceptor stabilized by GIGANTEA in blue light. *Nature* 449, 356-+.
- Kolmos,E., Nowak,M., Werner,M., Fischer,K., Schwarz,G., Mathews,S., Schoof,H., Nagy,F., Bujnicki,J.M., and Davis,S.J. (2009). Integrating ELF4 into the circadian system through combined structural and functional studies. *Hfsp Journal* 3, 350-366.
- Koukkari,W.L. and Sothorn,R.B. (2006a). 1. The study of biological rhythms. In *Introducing Biological Rhythms*.
- Koukkari,W.L. and Sothorn,R.B. (2006b). 2. General features of rhythms: terminology and characteristics. In *Introducing Biological Rhythms*.
- Koukkari,W.L. and Sothorn,R.B. (2006c). 8. Natural resources and agriculture. In *Introducing Biological Rhythms*.
- Kozma-Bognar,L. and Kaldi,K. (2008). Synchronization of the Fungal and the Plant Circadian Clock by Light. *Chembiochem* 9, 2565-2573.
- Lee,J.S. (2010). Stomatal Opening Mechanism of CAM Plants. *Journal of Plant Biology* 53, 19-23.
- Legnaioli,T., Cuevas,J., and Mas,P. (2009). TOC1 functions as a molecular switch connecting the circadian clock with plant responses to drought. *Embo Journal* 28, 3745-3757.

- Levi,F., Okyar,A., Dulong,S., Innominato,P.F., and Clairambault,J. (2010). Circadian Timing in Cancer Treatments. *Annual Review of Pharmacology and Toxicology* 50, 377-421.
- Liu,Y., Mellow,M., Loros,J.J., and Dunlap,J.C. (1998). How temperature changes reset a circadian oscillator. *Science* 281, 825-829.
- Locke,J.C.W., Millar,A.J., and Turner,M.S. (2005a). Modelling genetic networks with noisy and varied experimental data: the circadian clock in *Arabidopsis thaliana*. *Journal of Theoretical Biology* 234, 383-393.
- Locke,J.C., Kozma-Bognar,L., Gould,P.D., Feher,B., Kevei,E., Nagy,F., Turner,M.S., Hall,A., and Millar,A.J. (2006). Experimental validation of a predicted feedback loop in the multi-oscillator clock of *Arabidopsis thaliana*. *Molecular Systems Biology* 2.
- Locke,J.C., Southern,M.M., Kozma-Bognar,L., Hibberd,V., Brown,P.E., Turner,M.S., and Millar,A.J. (2005b). Extension of a genetic network model by iterative experimentation and mathematical analysis. *Molecular Systems Biology* 1.
- Lu,S.X., Liu,H., Knowles,S.M., Li,J., Ma,L., Tobin,E.M., and Lin,C. (2011). A Role for Protein Kinase Casein Kinase2 alpha-Subunits in the *Arabidopsis* Circadian Clock. *Plant Physiology* 157, 1537-1545.
- Lu,S.X. and Tobin,E.M. (2011). Chromatin remodeling and the circadian clock: Jumonji C-domain containing proteins. *Plant signaling & behavior* 6, 810-814.
- Martinez-Garcia,J.F., Huq,E., and Quail,P.H. (2000). Direct targeting of light signals to a promoter element-bound transcription factor. *Science* 288, 859-863.
- Mas,P., Kim,W.Y., Somers,D.E., and Kay,S.A. (2003). Targeted degradation of TOC1 by ZTL modulates circadian function in *Arabidopsis thaliana*. *Nature* 426, 567-570.
- Matsushika,A., Makino,S., Kojima,M., Yamashino,T., and Mizuno,T. (2002). The APRR1/TOC1 quintet implicated in circadian rhythms of *Arabidopsis thaliana*: II. Characterization with CCA1-overexpressing plants. *Plant and Cell Physiology* 43, 118-122.
- McClung,C. (2011). The Genetics of Plant Clocks. *Genetics of Circadian Rhythms* 74, 105-139.
- McClung,C. and Kay,S.A. (1994). *Circadian Rhythms in Arabidopsis thaliana*. Cold Spring Harbor Monograph Series; *Arabidopsis* 615-637.
- McClung,C.R. (2006). Plant circadian rhythms. *Plant Cell* 18, 792-803.
- McWatters,H.G., Kolmos,E., Hall,A., Doyle,M.R., Amasino,R.M., Gyula,P., Nagy,F., Millar,A.J., and Davis,S.J. (2007). ELF4 is required for oscillatory properties of the circadian clock. *Plant Physiology* 144, 391-401.
- Michael,T.P. and McClung,C.R. (2003). Enhancer trapping reveals widespread circadian clock transcriptional control in *Arabidopsis*. *Plant Physiology* 132, 629-639.

- Michael,T.P., Salome,P.A., and McClung,C.R. (2003). Two *Arabidopsis* circadian oscillators can be distinguished by differential temperature sensitivity. *Proceedings of the National Academy of Sciences of the United States of America* *100*, 6878-6883.
- Michael,T.P., Mockler,T.C., Breton,G., McEntee,C., Byer,A., Trout,J.D., Hazen,S.P., Shen,R., Priest,H.D., Sullivan,C.M., Givan,S.A., Yanovsky,M., Hong,F., Kay,S.A., and Chory,J. (2008). Network discovery pipeline elucidates conserved time-of-day-specific cis-regulatory modules. *Plos Genetics* *4*.
- Millar,A.J. (2003). Suite of photoreceptors entrains the plant circadian clock. *Journal of Biological Rhythms* *18*, 217-226.
- Millar,A.J., Carre,I.A., Strayer,C.A., Chua,N.H., and Kay,S.A. (1995a). Circadian Clock Mutants in *Arabidopsis* Identified by Luciferase Imaging. *Science* *267*, 1161-1163.
- Millar,A.J. and Kay,S.A. (1991). Circadian Control of Cab Gene-Transcription and Messenger-Rna Accumulation in *Arabidopsis*. *Plant Cell* *3*, 541-550.
- Millar,A.J., Short,S.R., Chua,N.H., and Kay,S.A. (1992). A Novel Circadian Phenotype Based on Firefly Luciferase Expression in Transgenic Plants. *Plant Cell* *4*, 1075-1087.
- Millar,A.J., Straume,M., Chory,J., Chua,N.H., and Kay,S.A. (1995b). The Regulation of Circadian Period by Phototransduction Pathways in *Arabidopsis*. *Science* *267*, 1163-1166.
- Miller,R.P., Martinson,K.B., Sothorn,R.B., Durgan,B.R., and Gunsolus,J.L. (2003). Circadian response of annual weeds in a natural setting to high and low application rates of four herbicides with different modes of action. *Chronobiology International* *20*, 299-324.
- Mizoguchi,T., Wheatley,K., Hanzawa,Y., Wright,L., Mizoguchi,M., Song,H.R., Carre,I.A., and Coupland,G. (2002). LHY and CCA1 are partially redundant genes required to maintain circadian rhythms in *Arabidopsis*. *Developmental Cell* *2*, 629-641.
- Nagel,D.H. and Kay,S.A. (2012). Complexity in the Wiring and Regulation of Plant Circadian Networks. *Current Biology* *22*, R648-R657.
- Nagoshi,E., Saini,C., Bauer,C., Laroche,T., Naef,F., and Schibler,U. (2004). Circadian gene expression in individual fibroblasts: Cell-autonomous and self-sustained oscillators pass time to daughter cells. *Cell* *119*, 693-705.
- Nagy,F., Kay,S.A., and Chua,N.H. (1988). A Circadian Clock Regulates Transcription of the Wheat Cab-1 Gene. *Genes & Development* *2*, 376-382.
- Nakajima,M., Imai,K., Ito,H., Nishiwaki,T., Murayama,Y., Iwasaki,H., Oyarna,T., and Kondo,T. (2005). Reconstitution of circadian oscillation of cyanobacterial KaiC phosphorylation in vitro. *Science* *308*, 414-415.
- Nakamichi,N., Kita,M., Ito,S., Yamashino,T., and Mizuno,T. (2005). Pseudo-Response Regulators, Prr9, Prr7 and Prr5, Together Play Essential Roles Close to the Circadian Clock of *Arabidopsis Thaliana*. *Plant and Cell Physiology* *46*, 686-698.

Nakamichi,N., Matsushika,A., Yamashino,T., and Mizuno,T. (2003). Cell autonomous circadian waves of the APRR1/TOC1 quintet in an established cell line of *Arabidopsis thaliana*. *Plant and Cell Physiology* 44, 360-365.

Nakamichi,N. (2011). Molecular Mechanisms Underlying the *Arabidopsis* Circadian Clock. *Plant and Cell Physiology* 52, 1709-1718.

Nakamichi,N., Kiba,T., Henriques,R., Mizuno,T., Chua,N.H., and Sakakibara,H. (2010). Pseudo-Response Regulators 9, 7, and 5 Are Transcriptional Repressors in the *Arabidopsis* Circadian Clock. *Plant Cell* 22, 594-605.

Nelson,D.C., Lasswell,J., Rogg,L.E., Cohen,M.A., and Bartel,B. (2000). FKF1, a clock-controlled gene that regulates the transition to flowering in *Arabidopsis*. *Cell* 101, 331-340.

Nozue,K., Covington,M.F., Duek,P.D., Lorrain,S., Fankhauser,C., Harmer,S.L., and Maloof,J.N. (2007). Rhythmic growth explained by coincidence between internal and external cues. *Nature* 448, 358-U11.

Nusinow,D.A., Helfer,A., Hamilton,E.E., King,J.J., Imaizumi,T., Schultz,T.F., Farre,E.M., and Kay,S.A. (2011). The ELF4-ELF3-LUX complex links the circadian clock to diurnal control of hypocotyl growth. *Nature* 475, 398-U161.

O'Neill,J.S., van Ooijen,G., Dixon,L.E., Troein,C., Corellou,F., Bouget,F.Y., Reddy,A.B., and Millar,A.J. (2011a). Circadian rhythms persist without transcription in a eukaryote. *Nature* 469, 554-558.

O'Neill,J.S. and Reddy,A.B. (2011). Circadian clocks in human red blood cells. *Nature* 469, 498-U70.

O'Neill,J.S., van Ooijen,G., Le Bihan,T., and Millar,A.J. (2011b). Circadian Clock Parameter Measurement: Characterization of Clock Transcription Factors Using Surface Plasmon Resonance. *Journal of Biological Rhythms* 26, 91-98.

Ow,D.W., Wood,K., V, Deluca,M., De Wet,J.R., Helinski,D.R., and Howell,S.H. (1986). Transient and Stable Expression of the Firefly Luciferase Gene in Plant Cells and Transgenic Plants. *Science (Washington D C)* 234, 856-859.

Palmer, J. D. *The Living Clock. The Orchestrator of Biological Rhythms.* 2002.

Ref Type: Generic

Panda,S., Antoch,M.P., Miller,B.H., Su,A.I., Schook,A.B., Straume,M., Schultz,P.G., Kay,S.A., Takahashi,J.S., and Hogenesch,J.B. (2002). Coordinated transcription of key pathways in the mouse by the circadian clock. *Cell* 109, 307-320.

Para,A., Farre,E.M., Imaizumi,T., Pruneda-Paz,J.L., Harmon,F.G., and Kay,S.A. (2007). PRR3 is a vascular regulator of TOC1 stability in the *Arabidopsis* circadian clock. *Plant Cell* 19, 3462-3473.

- Park,D.H., Somers,D.E., Kim,Y.S., Choy,Y.H., Lim,H.K., Soh,M.S., Kim,H.J., Kay,S.A., and Nam,H.G. (1999). Control of circadian rhythms and photoperiodic flowering by the Arabidopsis GIGANTEA gene. *Science* 285, 1579-1582.
- Perales,M. and Mas,P. (2007). A functional link between rhythmic changes in chromatin structure and the Arabidopsis biological clock. *Plant Cell* 19, 2111-2123.
- Pfeuty,B., Thommen,Q., Corellou,F., Djouani-Tahri,E.B., Bouget,F.Y., and Lefranc,M. (2012). Circadian clocks in changing weather and seasons: Lessons from the picoalga *Ostreococcus tauri*. *Bioessays* 34, 781-790.
- Pittendrigh,C.S. (1993). Temporal Organization - Reflections of A Darwinian Clock-Watcher. *Annual Review of Physiology* 55, 16-54.
- Poggio,G.F. and Viernstein,L.J. (1964). Time Series Analysis of Impulse Sequences of Thalamic Somatic Sensory Neurons. *Journal of Neurophysiology* 27, 517-&.
- Pokhilko,A., Fernandez,A.P., Edwards,K.D., Southern,M.M., Halliday,K.J., and Millar,A.J. (2012). The clock gene circuit in Arabidopsis includes a repressilator with additional feedback loops. *Molecular Systems Biology* 8.
- Pokhilko,A., Hodge,S.K., Stratford,K., Knox,K., Edwards,K.D., Thomson,A.W., Mizuno,T., and Millar,A.J. (2010). Data assimilation constrains new connections and components in a complex, eukaryotic circadian clock model. *Molecular Systems Biology* 6.
- Pruneda-Paz,J.L., Breton,G., Para,A., and Kay,S.A. (2009). A Functional Genomics Approach Reveals CHE as a Component of the Arabidopsis Circadian Clock. *Science* 323, 1481-1485.
- Pruneda-Paz,J.L. and Kay,S.A. (2010). An expanding universe of circadian networks in higher plants. *Trends in Plant Science* 15, 259-265.
- Rand,D.A., Shulgin,B.V., Salazar,J.D., and Millar,A.J. (2006). Uncovering the design principles analysis of flexibility of circadian clocks: Mathematical and evolutionary goals. *Journal of Theoretical Biology* 238, 616-635.
- Rapp,P.E. (1987). Why Are So Many Biological-Systems Periodic. *Progress in Neurobiology* 29, 261-273.
- Rawat,R., Schwartz,J., Jones,M.A., Sairanen,I., Cheng,Y., Andersson,C.R., Zhao,Y., Ljung,K., and Harmer,S.L. (2009). REVEILLE1, a Myb-like transcription factor, integrates the circadian clock and auxin pathways. *Proceedings of the National Academy of Sciences of the United States of America* 106, 16883-16888.
- Rawat,R., Takahashi,N., Hsu,P.Y., Jones,M.A., Schwartz,J., Salemi,M.R., Phinney,B.S., and Harmer,S.L. (2011). Reveille8 and Pseudo-Response Regulator5 Form A Negative Feedback Loop Within the Arabidopsis Circadian Clock. *Plos Genetics* 7.

Rensing,L. and Ruoff,P. (2002). Temperature effect on entrainment, phase shifting, and amplitude of circadian clocks and its molecular bases. *Chronobiology International* 19, 807-864.

Richards,J. and Gumz,M.L. (2012). Advances in understanding the peripheral circadian clocks. *Faseb Journal* 26, 3602-3613.

Rikin,A., Stjohn,J.B., Wergin,W.P., and Anderson,J.D. (1984). Rhythmical Changes in the Sensitivity of Cotton Seedlings to Herbicides. *Plant Physiology* 76, 297-300.

Robertson,F.C., Skeffington,A.W., Gardner,M.J., and Webb,A.A. (2009). Interactions between circadian and hormonal signalling in plants. *Plant Molecular Biology* 69, 419-427.

Roden,L.C., Song,H.R., Jackson,S., Morris,K., and Carre,I.A. (2002). Floral responses to photoperiod are correlated with the timing of rhythmic expression relative to dawn and dusk in *Arabidopsis*. *Proceedings of the National Academy of Sciences of the United States of America* 99, 13313-13318.

Roenneberg,T., Daan,S., and Mellow,M. (2003). The art of entrainment. *Journal of Biological Rhythms* 18, 183-194.

Roenneberg,T., Chua,E.J., Bernardo,R., and Mendoza,E. (2008). Modelling biological rhythms. *Current Biology* 18, R826-R835.

Ruts,T., Matsubara,S., Wiese-Klinkenberg,A., and Walter,A. (2012a). Diel patterns of leaf and root growth: endogenous rhythmicity or environmental response? *Journal of Experimental Botany* 63, 3339-3351.

Ruts,T., Matsubara,S., Wiese-Klinkenberg,A., and Walter,A. (2012b). Aberrant temporal growth pattern and morphology of root and shoot caused by a defective circadian clock in *Arabidopsis thaliana*. *Plant Journal* 72, 154-161.

Sai,J. and Johnson,C.H. (1999). Different circadian oscillators control Ca²⁺ fluxes and *Lhcb* gene expression. *Proceedings of the National Academy of Sciences of the United States of America* 96, 11659-11663.

Salome,P.A. and McClung,C.R. (2005a). Pseudo-Response Regulator 7 and 9 Are Partially Redundant Genes Essential for the Temperature Responsiveness of the *Arabidopsis* Circadian Clock. *Plant Cell* 17, 791-803.

Salome,P.A. and McClung,C.R. (2005b). What makes the *Arabidopsis* clock tick on time? A review on entrainment. *Plant Cell and Environment* 28, 21-38.

Santamaria,M., Thomson,C.J., Read,N.D., and Loake,G.J. (2001). The promoter of a basic PR1-like gene, *AtPRB1*, from *Arabidopsis* establishes an organ-specific expression pattern and responsiveness to ethylene and methyl jasmonate. *Plant Molecular Biology* 47, 641-652.

Schultz,T.F., Kiyosue,T., Yanovsky,M., Wada,M., and Kay,S.A. (2001). A role for LKP2 in the circadian clock of *Arabidopsis*. *Plant Cell* 13, 2659-2670.

- Seung,D., Risopatron,J.P.M., Jones,B.J., and Marc,J. (2012). Circadian clock-dependent gating in ABA signalling networks. *Protoplasma* 249, 445-457.
- Somers,D.E., Devlin,P.F., and Kay,S.A. (1998a). Phytochromes and cryptochromes in the entrainment of the Arabidopsis circadian clock. *Science* 282, 1488-1490.
- Somers,D.E., Kim,W.Y., and Geng,R.S. (2004). The F-box protein ZEITLUPE confers dosage-dependent control on the circadian clock, photomorphogenesis, and flowering time. *Plant Cell* 16, 769-782.
- Somers,D.E., Webb,A.A.R., Pearson,M., and Kay,S.A. (1998b). The short-period mutant, *toc1-1*, alters circadian clock regulation of multiple outputs throughout development in Arabidopsis thaliana. *Development* 125, 485-494.
- Somerville,C. and Koornneef,M. (2002). Timeline - A fortunate choice: the history of Arabidopsis as a model plant. *Nature Reviews Genetics* 3, 883-889.
- Southern,M.M. and Millar,A.J. (2005). Circadian genetics in the model higher plant, Arabidopsis thaliana. *Circadian Rhythms* 393, 23-35.
- Staiger,D. and Green,R. (2011). RNA-based regulation in the plant circadian clock. *Trends in Plant Science* 16, 517-523.
- Sullivan,S., Jenkins,G.I., and Nimmo,H.G. (2004). Roots, cycles and leaves. Expression of the phosphoenolpyruvate carboxylase kinase gene family in soybean. *Plant Physiology* 135, 2078-2087.
- Sulzman,F.M., Ellman,D., Fuller,C.A., Moorede,M.C., and Wassmer,G. (1984). Neurospora Circadian-Rhythms in Space - A Reexamination of the Endogenous-Exogenous Question. *Science* 225, 232-234.
- Sun,Q., Yoda,K., and Suzuki,H. (2005). Internal axial light conduction in the stems and roots of herbaceous plants. *Journal of Experimental Botany* 56, 191-203.
- Sun,Q., Yoda,K., Suzuki,M., and Suzuki,H. (2003). Vascular tissue in the stem and roots of woody plants can conduct light. *Journal of Experimental Botany* 54, 1627-1635.
- Sweeney,B.M. and Hastings,J.W. (1960). Effects of Temperature Upon Diurnal Rhythms. *Cold Spring Harbor Symposia on Quantitative Biology* 25, 87-104.
- Takase,T., Ishikawa,H., Murakami,H., Kikuchi,J., Sato-Nara,K., and Suzuki,H. (2011). The Circadian Clock Modulates Water Dynamics and Aquaporin Expression in Arabidopsis Roots. *Plant and Cell Physiology* 52, 373-383.
- Tester,M. and Morris,C. (1987). The Penetration of Light Through Soil. *Plant Cell and Environment* 10, 281-286.
- Thain,S.C., Hall,A., and Millar,A.J. (2000). Functional independence of circadian clocks that regulate giant gene expression. *Current Biology* 10, 951-956.

Thain,S.C., Murtas,G., Lynn,J.R., McGrath,R.B., and Millar,A.J. (2002). The circadian clock that controls gene expression in *Arabidopsis* is tissue specific. *Plant Physiology* *130*, 102-110.

Thommen,Q., Pfeuty,B., Corellou,F., Bouget,F.Y., and Lefranc,M. (2012). Robust and flexible response of the *Ostreococcus tauri* circadian clock to light/dark cycles of varying photoperiod. *Febs Journal* *279*, 3432-3448.

Toth,R., Kevei,E., Hall,A., Millar,A.J., Nagy,F., and Kozma-Bognar,L. (2001). Circadian clock-regulated expression of phytochrome and cryptochrome genes in *Arabidopsis*. *Plant Physiology* *127*, 1607-1616.

Van Loon,L.C. (1985). Pathogenesis-Related Proteins. *Plant Molecular Biology* *4*, 111-116.

Vanin,S., Bhutani,S., Montelli,S., Menegazzi,P., Green,E.W., Pegoraro,M., Sandrelli,F., Costa,R., and Kyriacou,C.P. (2012). Unexpected features of *Drosophila* circadian behavioural rhythms under natural conditions. *Nature* *484*, 371-U108.

Walter,A., Silk,W.K., and Schurr,U. (2009). Environmental Effects on Spatial and Temporal Patterns of Leaf and Root Growth. *Annual Review of Plant Biology* *60*, 279-304.

Wang,L., Fujiwara,S., and Somers,D.E. (2010). PRR5 regulates phosphorylation, nuclear import and subnuclear localization of TOC1 in the *Arabidopsis* circadian clock. *Embo Journal* *29*, 1903-1915.

Wang,W., Barnaby,J.Y., Tada,Y., Li,H., Toer,M., Caldelari,D., Lee,D.u., Fu,X.D., and Dong,X. (2011a). Timing of plant immune responses by a central circadian regulator. *Nature* *470*, 110-U126.

Wang,Y., Wu,J.F., Nakamichi,N., Sakakibara,H., Nam,H.G., and Wu,S.H. (2011b). Light-Regulated Wd1 and Pseudo-Response Regulator9 Form A Positive Feedback Regulatory Loop in the *Arabidopsis* Circadian Clock. *Plant Cell* *23*, 486-498.

Wang,Z.Y. and Tobin,E.M. (1998). Constitutive expression of the CIRCADIAN CLOCK ASSOCIATED 1 (CCA1) gene disrupts circadian rhythms and suppresses its own expression. *Cell* *93*, 1207-1217.

Welsh,D.K. and Kay,S.A. (2005). Bioluminescence imaging in living organisms. *Current Opinion in Biotechnology* *16*, 73-78.

Wenden,B., Kozma-Bognar,L., Edwards,K.D., Hall,A.J., Locke,J.C., and Millar,A.J. (2011). Light inputs shape the *Arabidopsis* circadian system. *Plant Journal* *66*, 480-491.

Wenden,B., Toner,D.L., Hodge,S.K., Grima,R., and Millar,A.J. (2012). Spontaneous spatiotemporal waves of gene expression from biological clocks in the leaf. *Proceedings of the National Academy of Sciences of the United States of America* *109*, 6757-6762.

Wilkins,M.B. and Holowins,A.W. (1965). Occurrence of An Endogenous Circadian Rhythm in A Plant Tissue Culture. *Plant Physiology* *40*, 907-&.

- Yakir,E., Hassidim,M., Melamed-Book,N., Hilman,D., Kron,I., and Green,R.M. (2011). Cell autonomous and cell-type specific circadian rhythms in Arabidopsis. *Plant Journal* 68, 520-531.
- Yakir,E., Hilman,D., Hassidim,M., and Green,R.M. (2007). Circadian Clock Associated1 Transcript Stability and the Entrainment of the Circadian Clock in Arabidopsis. *Plant Physiology* 145, 925-932.
- Yakir,E., Hilman,D., Kron,I., Hassidim,M., Melamed-Book,N., and Green,R.M. (2009). Posttranslational Regulation of CIRCADIAN CLOCK ASSOCIATED1 in the Circadian Oscillator of Arabidopsis. *Plant Physiology* 150, 844-857.
- Yerushalmi,S., Yakir,E., and Green,R.M. (2011). Circadian clocks and adaptation in Arabidopsis. *Molecular Ecology* 20, 1155-1165.
- Yoshii,T., Vanin,S., Costa,R., and Helfrich-Foerster,C. (2009). Synergic Entrainment of Drosophila's Circadian Clock by Light and Temperature. *Journal of Biological Rhythms* 24, 452-464.
- Yu,J.W., Rubio,V., Lee,N.Y., Bai,S., Lee,S.Y., Kim,S.S., Liu,L., Zhang,Y., Irigoyen,M.L., Sullivan,J.A., Zhang,Y., Lee,I., Xie,Q., Paek,N.C., and Deng,X.W. (2008). COP1 and ELF3 Control Circadian Function and Photoperiodic Flowering by Regulating GI Stability. *Molecular Cell* 32, 617-630.
- Zakhrabekova,S., Gough,S.P., Braumann,I., Muller,A.H., Lundqvist,J., Ahmann,K., Dockter,C., Matyszczyk,I., Kurowska,M., Druka,A., Waugh,R., Graner,A., Stein,N., Steuernagel,B., Lundqvist,U., and Hansson,M. (2012). Induced mutations in circadian clock regulator Mat-a facilitated short-season adaptation and range extension in cultivated barley. *Proceedings of the National Academy of Sciences of the United States of America* 109, 4326-4331.
- Zeilinger,M.N., Farre,E.M., Taylor,S.R., Kay,S.A., and Doyle,F.J. (2006). A novel computational model of the circadian clock in Arabidopsis that incorporates PRR7 and PRR9. *Molecular Systems Biology* 2.